

## Preface

This publication is a result of the 15th TRACE conference „Tree Rings in Archaeology, Climatology and Ecology” organized by the University of Silesia, Silesian Botanical Garden, University of Wrocław, Forest Research Institute and Białowieża National Park. The conference was held on May 11th – 15th, 2016 in Białowieża, Poland, in the heart of the Białowieża Forest, the last natural forest in the European Lowlands, a UNESCO World Heritage Site and Biosphere Reserve.

TRACE is an initiative of the ‘Association for Tree-Ring Research’ (ATR) and seeks to strengthen the networking and scientific exchange of scientists and students involved in the study of tree rings. The annual conference provides a scientific platform for young scientists to present and discuss new discoveries and approaches in tree-ring science.

146 scientists working on tree-ring related topics participated in the conference coming from 24 countries: Austria, Belarus, Belgium, Bulgaria, China, Czech Republic, France, Germany, Greece, Hungary, India, Italy, Kenya, Kosovo, Romania, Russia, Slovakia, Slovenia, Spain, Sweden, Switzerland, United Kingdom, United States and Poland. The participants enjoyed 54 oral presentations and 79 posters divided into six thematic sessions: “Archaeology”, “Climate-Growth Relationships”, “Dendroclimatology”, “Dendroecology”, “Isotopes in Dendrochronology” and “Wood Anatomy and Methods”.

After review, 11 short papers are published in this volume, giving an overview of the wide spectrum of different fields covered at TRACE 2016. We would like to thank the authors for contributing to this TRACE volume, and the reviewers for their valuable comments on the manuscripts.

During the conference three keynote presentations were given by Dieter Eckstein (“Dendrochronology - looking back on amazing 50 years of its recent past”), Kurt Nicolussi (“Tree rings, glacier variability and climate in the Alps – the long-term view”) and Ewa Zin (“Białowieża Forest - disturbance history and forest dynamics in past and ongoing scientific research”). Two short pre-conference courses were organized on “Basic Wood Anatomy” (by Paweł Kojs, Ireneusz Malik and Magdalena Opała) and “Detecting and Dating Growth Disturbances” (by Tomasz Zielonka and Elżbieta Muter). The participants had also the opportunity to enjoy the pre-conference excursion around the Podlasie Region, NE Poland (organized by Piotr Owczarek) and the mid-conference field trip to magnificent forests of the Strictly Protected Area of the Białowieża National Park (organized by Ewa Zin).

We thank all keynote speakers, short-course teachers and excursion guides for their contribution. The organizers of the conference also wish to acknowledge financial support from the sponsors of TRACE 2016: Hotel Białowieski Conference, Wellness & SPA (Poland), Haglöf (Sweden), Leading National Research Centre (KNOW): Centre for Polar Studies, University of Silesia (Poland), Regent Instruments Inc. (Canada), Technical School of Forestry in Białowieża (Poland) and Wejmutka – Białowieża Biodiversity Academy (Poland).

We would finally like to thank all participants of TRACE 2016 for bringing your results and brilliant tree-ring ideas to Poland and hope you’ll keep good memories of your spring visit in the homeland of European wood bison.

Małgorzata Wistuba  
Anna Cedro  
Ireneusz Malik  
Gerhard Helle  
Holger Gärtner



# CONTENTS

## SECTION 1 CLIMATOLOGY

- Kaczka R.J., Janecka K. & P. Guzik:** 06  
The influence of climate on the growth of Oriental plane *Platanus orientalis* L. in two divergent habitats
- Kaczka R.J., Janecka K., Hulist A. & B. Spyt:** 13  
Linking the growth/climate response of daily resolution with annual ring formation of Norway spruce in the Tatra Mountains
- Kaczka R.J., Spyt B., Janecka K. & R. Musiol:** 23  
The Blue Intensity proxy for >400 years growing season temperature reconstruction from the Tatra Mountains
- Opala-Owczarek M., Niedźwiedz T., Rahmonov O. & P.Owczarek:** 31  
Millennia-long dendroclimatic records from the Pamir-Alay Mountains (Tajikistan)  
- perspectives and limitations
- Tiwari A., Ze-Xin F. & Z. Zhe-Kun:** 39  
Spring season (March-May) precipitation signal of *Ephedra intermedia* (a perennial shrub) in the Trans-Himalayan dry valley (central Himalaya)
- Hartl-Meier, C., Schneider L. & J. Esper:** 46  
Site-specific temperature response to seven major volcanic eruptions over the last millennium
- Hochreuther P., Wernicke J., Grießinger J. & A. Bräuning:** 54  
On the influence of autocorrelation on the significance of wavelet spectral peaks
- Konter O., Büntgen U., Carrer M. & J. Esper:** 59  
Testing for climate signal age effects at two treeline sites in the European Alps and Tatra Mountains

## SECTION 2 ECOLOGY

- Cedro A. & B. Cedro:** 68  
Frost rings in the service tree populations in Poland
- Rutkiewicz P., Malik I., Wistuba M. & D. Gawior:** 75  
Tree-ring reductions among Norway spruce in relation to air pollution and a human morbidity  
- examples from southern Poland
- Klippel L., Krusic P.J., Hartl-Meier C., Trouet V. & J. Esper:** 81  
High-elevation inter-site differences in Mount Smolikas tree-ring width data
- He M.H., Yang B., Bräuning A. & S.Y. Kang:** 88  
Tree-ring reductions among Norway spruce in relation to air pollution and a human morbidity  
– examples from southern Poland

## SECTION 3 GEOMORPHOLOGY

- Franek M., Wistuba M. & I. Malik:** 96  
Dendrochronological record of terrain subsidence caused by underground mining (Silesian Upland)

- Gawior D., Malik I., Wistuba M., Tie Y., Michałowicz P., Jiang J. & P. Rutkiewicz:** 104  
The impact of earthquakes on radial growth and wood anatomy, examples from Western Carpathians, Poland and Wenchuan, China
- Łuszczynska K., Wistuba M. & I. Malik:** 112  
Landslide activity and its triggering factors reconstructed from tree-ring eccentricity in Norway spruce (Western Carpathians, Czech Republic)

#### **SECTION 4 ISOTOPES**

- Bräuning A., Volland F. & A.D. Pucha:** 120  
Stable oxygen isotope series in tropical trees – how much is enough to represent a robust signal?
- Foroozan Z., Pourtahmasi K. & A. Bräuning:** 126  
Climatic signals in stable carbon isotope ratios of juniper tree rings in northern Iran

## **SECTION 1**

### **CLIMATOLOGY**

# The influence of climate on the growth of Oriental plane *Platanus orientalis* L. in two divergent habitats

R.J. Kaczka, K. Janecka & P. Guzik

Faculty of Earth Sciences, University of Silesia in Katowice, Sosnowiec, Poland  
E-mail: ryszard.kaczka@us.edu.pl

## Introduction

Tree rings are commonly used climatic (Fritts 1976) and hydro-climatic (Case & MacDonald 2003) proxies of temperature, precipitation, drought, water stage, river discharge etc. The strength and comprehensiveness of the signal depend on the species, habitat and human impact (Fritts 1976). Oriental plane *Platanus orientalis* L. is a relatively large, fast-growing, long-living deciduous tree growing in a wide variety of soils but it prefers the riverine habitats. It is tolerant of drought, air-pollution and various mechanical disturbances, although it cannot grow in shaded site. *P. orientalis* presents the wide distribution range, from the eastern Mediterranean and middle-east to south-east Siberia, constituting a vital element of the riparian ecosystems (Zogaris et al. 2009, Zaimis et al. 2010, Mucina et al. 2016) and potential for silviculture purposes (Aravanopoulos 2010). Although the other species or hybrids from *Platanaceae* family were investigated using dendrochronological methods (e.g. Cedro, Nowak 2006), there is lack of the tree-ring studies of that particular species (e.g., no entries in ITRDB or EUFORGEN databases). The aim of the study was to test the possibility of establishing the coherent tree-ring width chronology of *P. orientalis* and to identify the environmental factors that control the growth of the oriental plane in river valley. The studies were conducted at the northern foothills of Mount Olympus in the Orlias River Valley (Fig. 1). The plane in the valley creates scarce forest covering riverbank of braided river channel and slopes of small hills made of loose sediments. Two distinguished habitats can be recognized within small area: i) the relatively humid site on the riverbank and ii) dry site on the slope (Fig. 2).

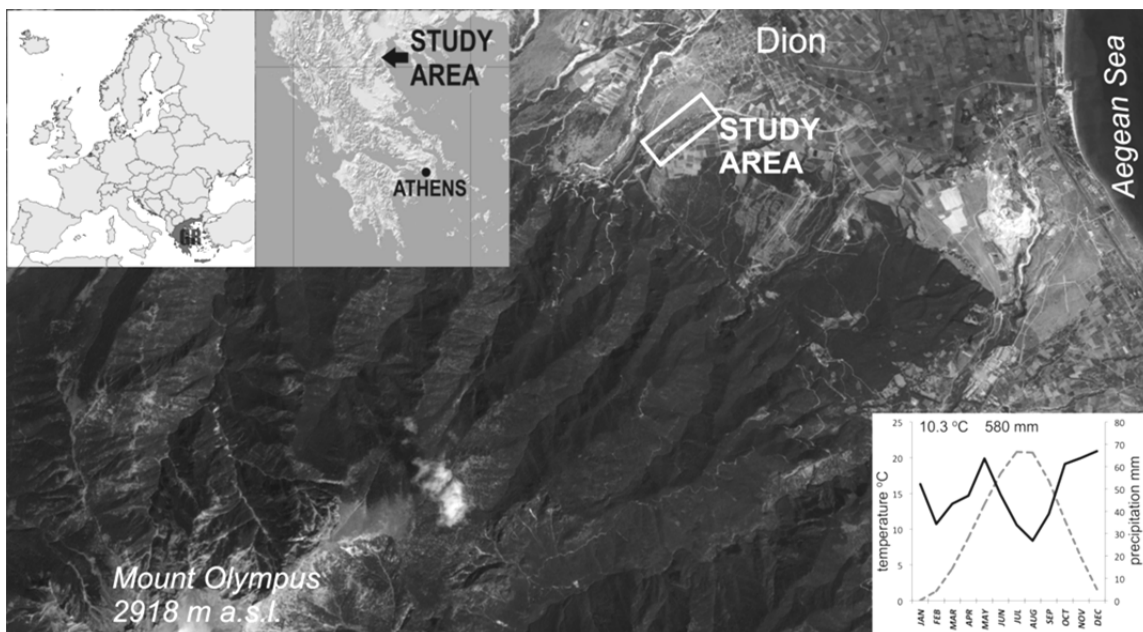


Figure 1: Location of the study site – the Orlias River Valley (elevation 170 m a.s.l.) at the foothills of Mount Olympus, Dion Region, Greece. The climate diagram based on the data derived from CRU TS3.24 (Harris et al. 2013).

The records of water stage or discharge of the Orlias River are not available. However, the field observations and studies of the regional characteristics of precipitation (Katsoulis & Kambetidis 1989) suggest that the river channel is dry during the summer and may be flooded during spring (due to melting snow/high precipitation) and winter (rainfalls).

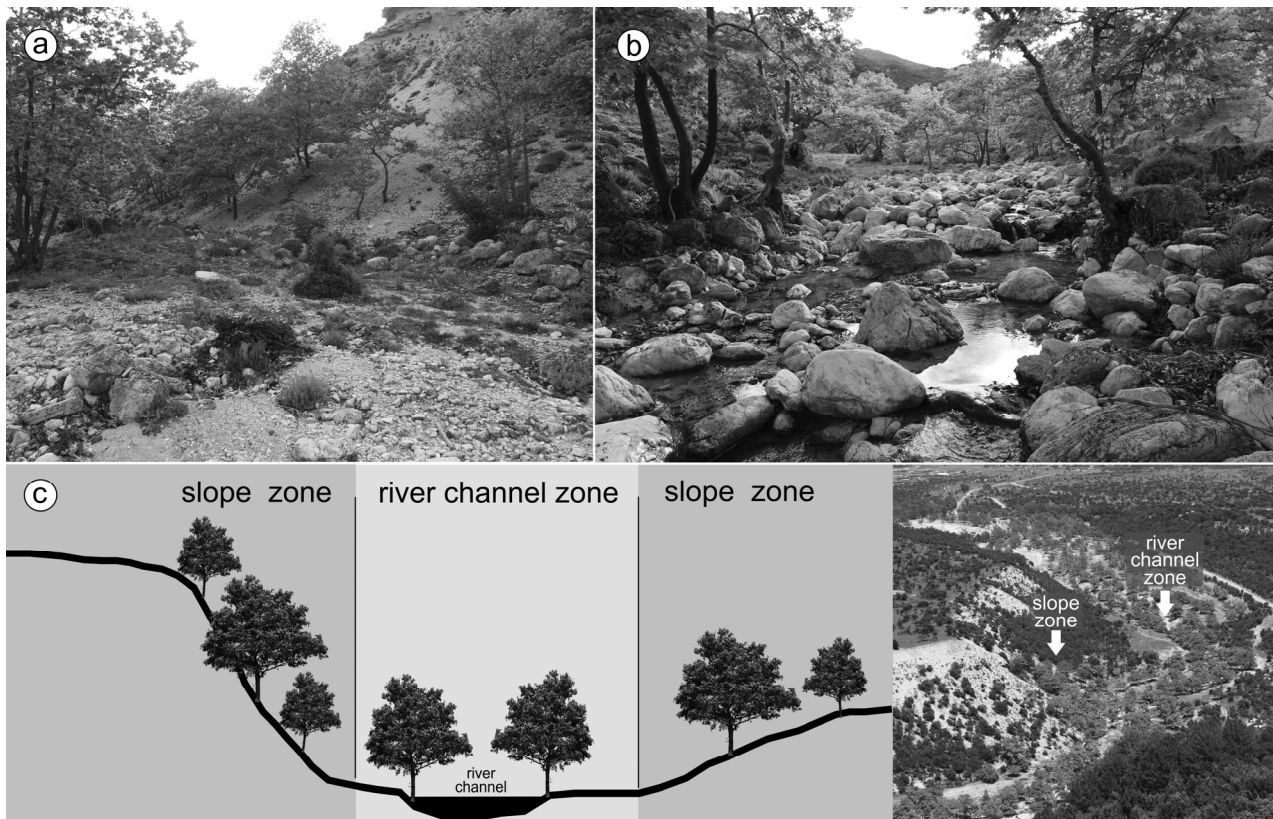


Figure 2: The Oriental plane growing in two contrasting habitats: (a) the dry slopes of the hill, (b) the riverbank providing water for most of the year (see also Zaimis et al. 2010). (c) The sampling was conducted to capture the difference between site conditions: slope zone (SLZ) and river channel zone (RCZ).

## Materials and methods

The core samples were extracted from 118 trees: 75 from river channel zone (RCZ) and 43 from slope zone (SLZ). The samples were dried, mounted on wooden supports and sanded to prepare the surface providing a clear picture of ring boundaries. The samples were scanned in a high-resolution image (2400 DPI) using a flatbed scanner. Tree-ring width (TRW) measurements were obtained with CooRecorder 8.0 software provided by Cybis Elektronik & Data AB (Larsson 2013). The well-defined and well-visible ring boundaries allowed to use this technique, however, the verification of the measurements often required the wood examination under a microscope. The quality and synchronicity of measurement series were tested using the visual (CDendro software; Larsson 2013) and statistical (Cofecha software; Holmes 1983) cross-dating. Two TRW chronologies were established with the use of ARSTAN software (Cook 1985). The standard chronologies were computed applying the 40-years (~mean length of series) cubic smoothing splines with a 50% frequency-response cutoff at 40 years (SPLs; Cook & Peters, 1981) detrending. Additionally the adaptive power transformation and Keith-Briffa Rbar-weighted method of variance stabilization (Osborn et al. 1997) were used. Signal strength of the chronologies was evaluated by calculating the inter-series correlation (Rbar) and the Expressed Population Signal (EPS) statistics (Wigley et al. 1984). The dendroclimatic analyses were conducted using temperature and precipitation gridded data derived from E-OBS 14.0 (Haylock et al. 2008) and self-calibrating Palmer Drought Severity Index derived from CRU scPDSI 3.24 (van der Schrier et al. 2013,

Osborn et al. 2016). The growth-climate response was assessed by calculating bootstrap correlation coefficient relying on the random sampling with replacement 10K times between standard TRW chronologies and climate data for common 1965 – 2013 period using DendroCorr 3.2 software (Hulst et al. 2016). To identify the main climate drivers, the growth-climate response analyses were calculated for previous and current year monthly (from January to December) and seasonal (66 combinations between January and December) averages of climate data representing grid box: 40.00 - 40.25° N and 22.25 - 22.50° E.

## Results

The lengths of chronologies are almost equal (49 and 51 years), although two of sampled trees at SLZ site are considerable older (85 and 117 years). Also the average growth rate is similar for RCZ and SLZ (1.52 mm, SD=0.93 and 1.79 mm, SD=0.88, respectively). Trees representing two studied cohorts exhibit comparable mean sensitivity (0.296 and 0.288, respectively). Both RCZ and SLZ standard chronologies show high statistical parameters of Rbar (0.60 and 0.41, respectively) and EPS (0.99 and 0.96, respectively). Most of the singular series show similar year-to-year variation and longer-term changes (Fig. 3). The typical age-trend is present in most of the trees from both zones. The rings in years 1973 and 1988 are particularly narrow following by wide rings in the 1991-1992 period. Although the distance between sites is not larger than 100 m the chronologies correlate at relatively low level ( $r = 0.70$ ,  $p=0.01$ ). The similarity diminishes considerably after 2005 when RCZ chronology exhibits the increase of the ring widths whereas the SLZ chronology remains at the same level. These findings are confirmed by the results of the 15-years running correlation (Fig. 4). Both chronologies response only to precipitation, both temperature and scPDSI do not show any statistically significant correlations (Fig. 5).

The standard chronology composed by trees growing on the riverbank (RCZ) correlates with precipitation of April-June and April-July periods in the similar way ( $r=0.350$  and  $r=0.347$ , respectively). Slightly higher correlations were obtained for the shorter periods of May-June ( $r=0.355$ ) and May-July ( $r=0.351$ ). The chronology built based on the trees growing on the slope of the river valley (SLZ) correlates negatively with precipitation of March of current year ( $r=-0.450$ ) and February-March season ( $r=-0.415$ ). The chronology responds also negatively to the precipitation averaged over longer period: January-March ( $r=-0.429$ ) and January-April ( $r=-0.401$ ). In contrast, the average precipitation calculated over 8 different seasons from April to August and even September shows significant positive correlations (from  $r=0.387$  to  $r=0.615$  for May-September and May-June, respectively,  $p=0.01$ ) (Fig. 5) with the SLZ chronology.

The results of the spatial correlations reveal that in both cases (March and May-June), the planes growing in the Orlia River Valley are mainly influenced by precipitation restricted to the north and eastern Greece (Fig. 6). Our two studied chronologies, representing adjoining but different habitats, reveal similar correlation with May-June precipitation although the strength of the signal differs (SLZ:  $r=0.615$ , RCZ:  $r=0.355$ ). The planes growing in the riparian forest, at the riverbank have better access to the ground water during the year. Therefore, they are less exposed to droughts and show weaker link with precipitation. The trees growing on the slope and well-drained soil are more susceptible to lack of water, and consequently they reveal stronger correlation with precipitation. The pattern shows that precipitation is the main source of water in both zones. The channel flow, resulted from snow melting at higher parts of the Orlia River catchment, probably provides water only during the early spring. The late spring and summer rainfall in the Olympus Range does not provide enough suitable discharge to significantly discriminate the growth conditions of the two analysed sites. The precipitation during typical period of flooding in Greece occurring in September-January period (Diakakis et al. 2012) is not recorded by studied trees.

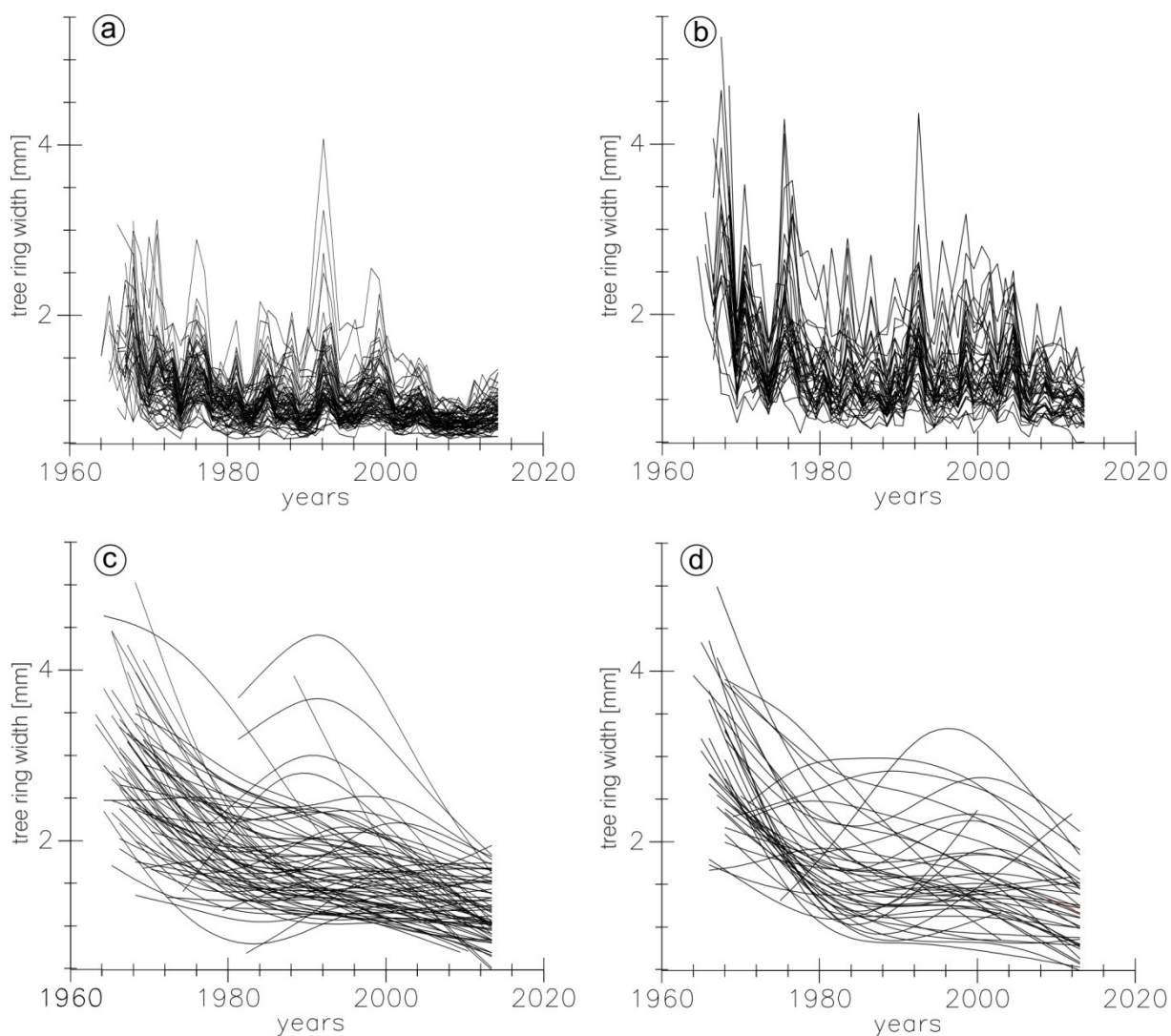


Figure 3: The spaghetti plots of (a) 75 TRW series from RCZ site and (b) 43 TRW series from SLZ site. The 40 years smoothing spline trend lines calculated for each (c) RCZ and (d) SLZ TRW series.

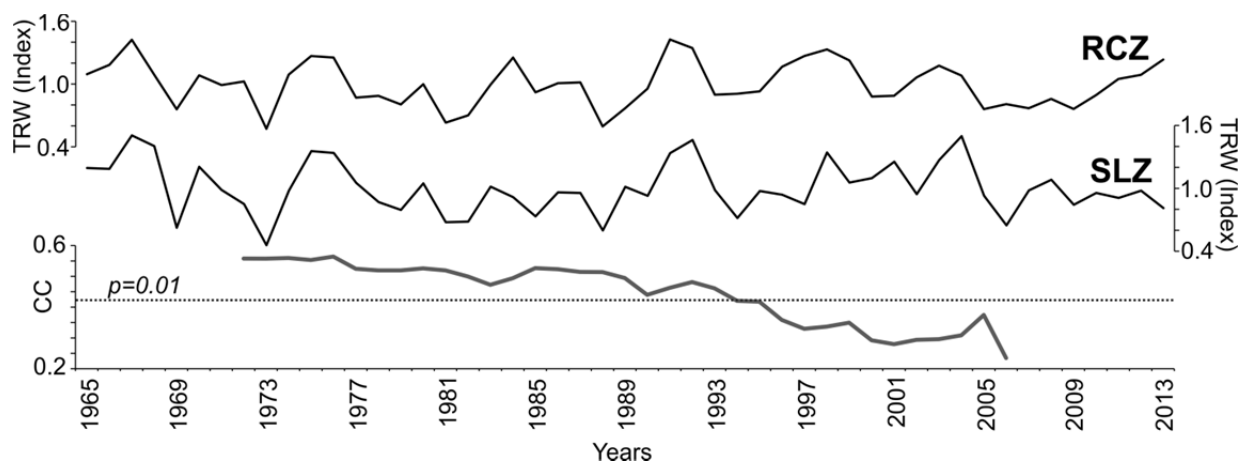


Figure 4: Standard TRW chronologies representing the planes from river channel zone (RCZ) and slope zone (SLZ) truncated at < 5 series (black lines). The 15-years running correlation (below grey bold line) (CC) shows a significant divergence after 1995.

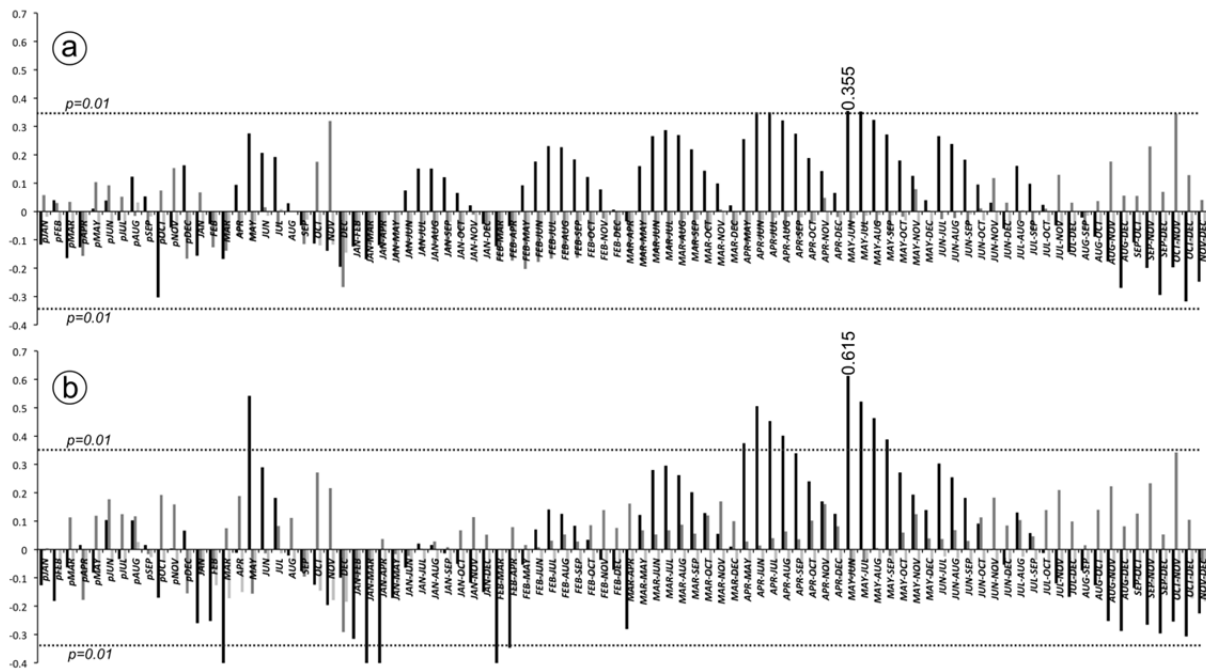


Figure 5: The bootstrap correlation coefficient between RCZ (a), SLZ (b) TRW standard chronologies and climate data (temperature, precipitation and scPDSI indicated by dark grey, black and light grey colors, respectively) calculated over 1965 – 2013 common period.

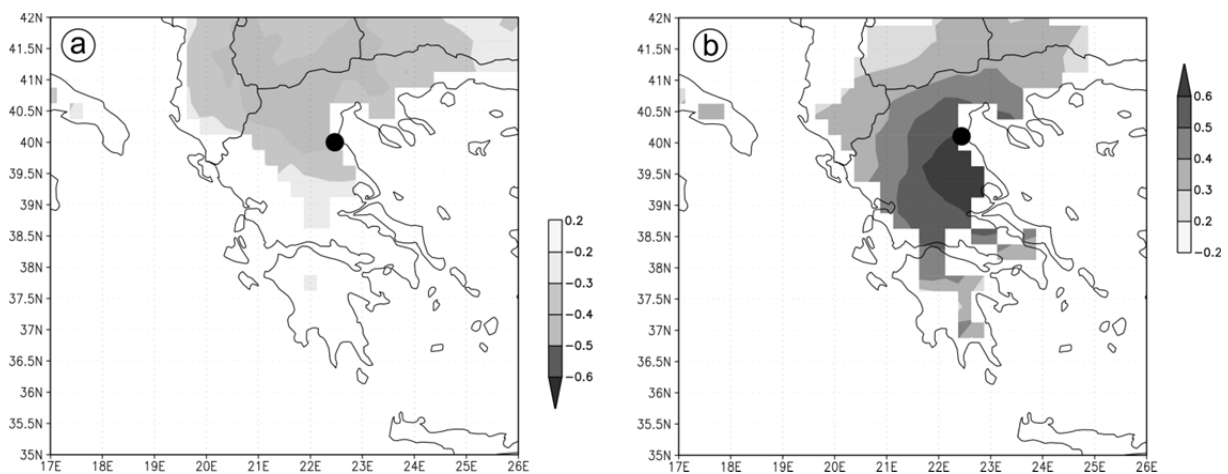


Figure 6: The spatial field correlations calculated for TRW standard chronology of SLZ site and gridded (a) March and (b) May precipitation throughout the 1965 – 2013 common period, the black dot indicates the sample site.

## Conclusions

The Oriental plane *Platanus orientalis* L. is suitable species for tree-ring studies. The example of our two chronologies from the Orlias River Valley in Greece demonstrates that Oriental plane has a potential for dendroclimatological and dendrohydrological analyses. Although the built chronologies are relatively short (49 and 50 years), findings of the older trees (85 and 117 years) confirm the potential of establishing much longer chronologies.

The investigation of two contrasting sites (in the terms of water availability) revealed that:

- a) the established chronologies show comprehensive characteristics (Rbar, EPS),
- b) the growth of trees in both zones is mainly driven by precipitation of late spring – early summer (May-June),
- c) the temperature and scPDSI have not significant influence on the growth of the plane trees,
- d) the strength of the precipitation signal depends on the location of the site. The chronology representing slope site shows stronger correlation with precipitation than the one representing riverbank (May-June  $r=0.615$  vs.  $0.355$ , respectively),
- e) the planes growing at the riverbank have contact with groundwater, therefore, trees are less likely to suffer from droughts. The water availability on the slope is much lower hence the growth of plane is mainly dependent on precipitation.

## References

- Aravanopoulos, F.A. (2010): Breeding of fast growing forest tree species for biomass production in Greece. *Biomass and bioenergy* 34(11): 1531-1537
- Case, R.A., MacDonald G.M. (2003): Tree Ring Reconstructions of Streamflow for Three Canadian Prairie Rivers. *American Water Resources Association* 39(3): 703-716.
- Cook, E.R. (1985): A time series analysis approach to tree-ring standardization. Ph.D. Thesis, University of Arizona, Tucson. 171 pp.
- Cook, E.R., Peters, K. (1981): The smoothing spline: A new approach to standardizing forest interior tree-ring width series for dendroclimatic studies. *Tree-Ring Bulletin* 41: 45–53.
- Cedro, A., Nowak, G. (2006): Effects of climatic conditions on annual tree ring growth of the *Platanus x hispanica* "Acerifolia" under urban conditions of Szczecin. *Dendrobiology* 55: 11-17.
- Diakakis, M., Mavroulis, S., Deligiannakis, G. (2012): Floods in Greece, a statistical and spatial approach. *Natural hazards* 62(2): 485-500.
- Fritts, H. C. (1976): Tree rings and climate, Academic, San Diego, California. 567 pp.
- Harris I., Jones P.D., Osborn T.J., Lister D.H. (2013): Updated high resolution grids of monthly climatic observations—the CRU TS3. 10 Dataset. *International Journal of Climatology* 34: 623-642.
- Haylock, M.R., Hofstra, N., Klein Tank, A M.G., Klok, E.J., Jones, P.D., New, M. (2008): A European daily high-resolution gridded data set of surface temperature and precipitation for 1950–2006. *Journal of Geophysical Research: Atmospheres*, 113 (D20).
- Holmes, R.L. (1983): Computer-assisted quality control in tree-ring dating and measurements. *Tree-Ring Bulletin*, 43: 69-78.
- Hulist, A., Janecka, K., Kaczka, R.J. (2016): DendroCorr the simple and powerful software to calculate the growth/climate response In: Hevia, A., Sánchez-Salguero, R., Linares, J. C., Olano, J. M., Camarero, J. J., Gutiérrez, E., Helle, G., Gärtner, H. (ed.): TRACE - Tree Rings in Archaeology, Climatology and Ecology, Volume 14. *Scientific Technical Report* 16/04, GFZ German Research Centre for Geosciences. doi: 10.2312/GFZ.b103-16042. 44-49.
- Katsoulis, B.D., Kambetzidis, H D. (1989): Analysis of the long-term precipitation series at Athens, Greece. *Climatic change*, 14(3): 263-290.
- Larsson, L., (2013): CooRecorder and Cdendro programs of the CooRecorder/Cdendro package version 7.8. <http://www.cybis.se/forfun/dendro/>
- Mucina, L., Bültmann, H., Dierßen, K., Theurillat, J. P., Raus, T., Čarni, A., Chytrý, M. (2016): Vegetation of Europe: Hierarchical floristic classification system of vascular plant, bryophyte, lichen, and algal communities. *Applied Vegetation Science* 19(S1): 3-264.
- Osborn, T.J., K.R. Briffa and P.D. Jones. (1997): Adjusting variance for sample-size in tree-ring chronologies and other regional-mean time-series. *Dendrochronologia* 15: 89–99.

- Osborn, T.J., Barichivich, J., Harris, I., van der Schrier G., Jones P.D. (2016): Monitoring global drought using the self-calibrating Palmer Drought Severity Index [in "State of the Climate in 2015"]. *Bulletin of the American Meteorological Society*, 97: 32-36.
- van der Schrier G., Barichivich J., Briffa K.R., Jones P.D. (2013): A scPDSI-based global data set of dry and wet spells for 1901-2009. *Journal of Geophysical Research: Atmospheres* 118: 4025-4048.
- Wigley, T.M., Briffa, K.R., Jones, P.D. (1984): On the average value of correlated time series, with applications in dendroclimatology and hydrometeorology. *Journal of climate and Applied Meteorology*, 23(2): 201-213.
- Zaimes, G.N., Iakovoglou, V., Emmanouloudis, D., Gounaridis, D. (2010): Riparian areas of Greece: their definition and characteristics. *Journal of Engineering Science and Technology Review* 3(1): 176-183.
- Zogaris, S., Chatzinikolaou, Y., Dimopoulos, P. (2009): Assessing environmental degradation of montane riparian zones in Greece. *Journal of Environmental Biology* 30: 719–726.

# Linking the growth/climate response of daily resolution with annual ring formation of Norway spruce in the Tatra Mountains

R.J. Kaczka<sup>1</sup>, K. Janecka<sup>1</sup>, A. Hulist<sup>2</sup> & B. Spyt<sup>1</sup>

<sup>1</sup>Faculty of Earth Sciences, University of Silesia in Katowice, Sosnowiec, Poland

<sup>2</sup>Faculty of Mathematics, Physics and Chemistry, University of Silesia in Katowice, Poland  
e-mail: ryszard.kaczka@us.edu.pl

## Introduction

In dendrochronology the standard procedure of identifying growth/climate responses relies on calculating the statistical relationship between time series of tree-ring measurements like tree-ring width (TRW), maximum wood density (MXD), composition of stable isotopes and time series of climate data e.g. temperature, precipitation averaged over monthly or seasonal intervals (Fritts 1976, Cook & Kairiukstis 1990). Monthly averaged climate data has been commonly used in climate/growth calculations, since the very first (Douglas 1920, Huber 1943, Schulman 1953) to most modern (Büntgen et al. 2016, Dũthorn et al. 2016, Esper et al. 2016, Grießinger et al. 2016) dendroclimatological studies. Nevertheless, monthly aggregation of climate data is poorly related to the phenological calendar and the cycle of tree growth. A novel approach was proposed by Beck et al. (2013) who criticised the use of monthly aggregated climate data and designed a procedure implemented in the CLIMTREG software, which allows calculating climate/growth correlations based on daily climate data. To do so, moving windows of increasing length (21-121 days) with mean daily temperatures and daily precipitation sums are correlated to annual tree ring measurements like TRW or MXD within a time period from previous year July to October of the current year of ring formation in order to find the most appropriate aggregation period. The proposed method was successfully employed to studies of climate influence on the Scots pine growth in NE Germany (Liang et al. 2013) and southern Sweden (Pritzkowa et al. 2014), Oaks in SE-Britain (Sanders et al. 2014), hydraulic parameters of xylem of Norway spruce in the Italian Alps (Castagneri et al. 2015) and drought influence on various tree species in Germany (Beck 2011). The introduction of the use of daily climate intervals can help to broaden the knowledge about the development of annual rings (Beck et al. 2013).

The process of cell formation, fundamental for the final size and character of the annual ring is synchronised with the summer solstice, the time of the longest photoperiod, and not necessarily related to the period of highest temperatures (Rossi et al. 2006, 2007). However, the onset and length of the xylogenesis of conifer species in cold environments strongly depends on the thermal conditions. Phenological studies of sites from America and Europe link the beginning of cambium activity with the threshold of daily temperature reaching 4-5°C, which occurs in most studied locations at the beginning of May (Deslauriers et al. 2008).

Dendroclimatic studies conducted in standard manner (comparing the tree-ring width and monthly intervals of climate data) for similar locations reveal high correlations between TRW and temperature of June and July (*Larix decidua* in the Italian Alps; Carrer & Urbinati 2004), July and August (*Pinus cembra* in the Italian Alps; Carrer & Urbinati 2004), July-August (*Pinus sylvestris* in Finland; Dũthorn et al. 2016). TRW chronologies from high elevations in the Alps usually show highest response to temperatures of the June-August interval, whereas in the Carpathians, depending on the coniferous species, correlations are highest for June-July or July-August (Büntgen et al. 2007, Kaczka et al. 2016). All these studies demonstrate the temporal pattern of growth/climate response, which somehow fits poorly to the monthly division of growing season. This raises the questions whether the use of daily data and calculation monthly-independent intervals will result in a better picture of growth/climate response and if the knowledge about timing of annual ring development can improve the understanding of how the climate signal is recorded?

Therefore we aim at testing the potential of improving the results of growth/climate response by using intervals based on daily instead of monthly data and linking the outcomes with information about intra-annual xylem development.

### Materials and methods

The study site is located in the Tatra Mountains in the subalpine spruce forest at the elevation of ~1500 m a.s.l. (Fig. 1). The local climate is characterized by average annual temperature reaching +2.5 °C and total sum of annual precipitation equals 1660 mm (Hala Gašienicowa meteostation 1520 m a.s.l., 1946-2004 CE). 64 Norway spruce samples were collected using an increment borer 5.15 mm in diameter. The cores were prepared in a standard way (dried, mounted on wooden laths and sanded) to obtain the surface offering a clear picture of ring boundaries. The samples were scanned using a flatbed scanner in a 2400 DPI resolution. Tree-ring widths were measured with CooRecorder 8.0 software provided by Cybis Elektronik & Data AB (Larsson 2013). The quality of the measurements and synchronicity of series were tested using the visual (CDendro software, Larsson 2013) and statistical (Cofecha software, Holmes 1983) cross-dating.

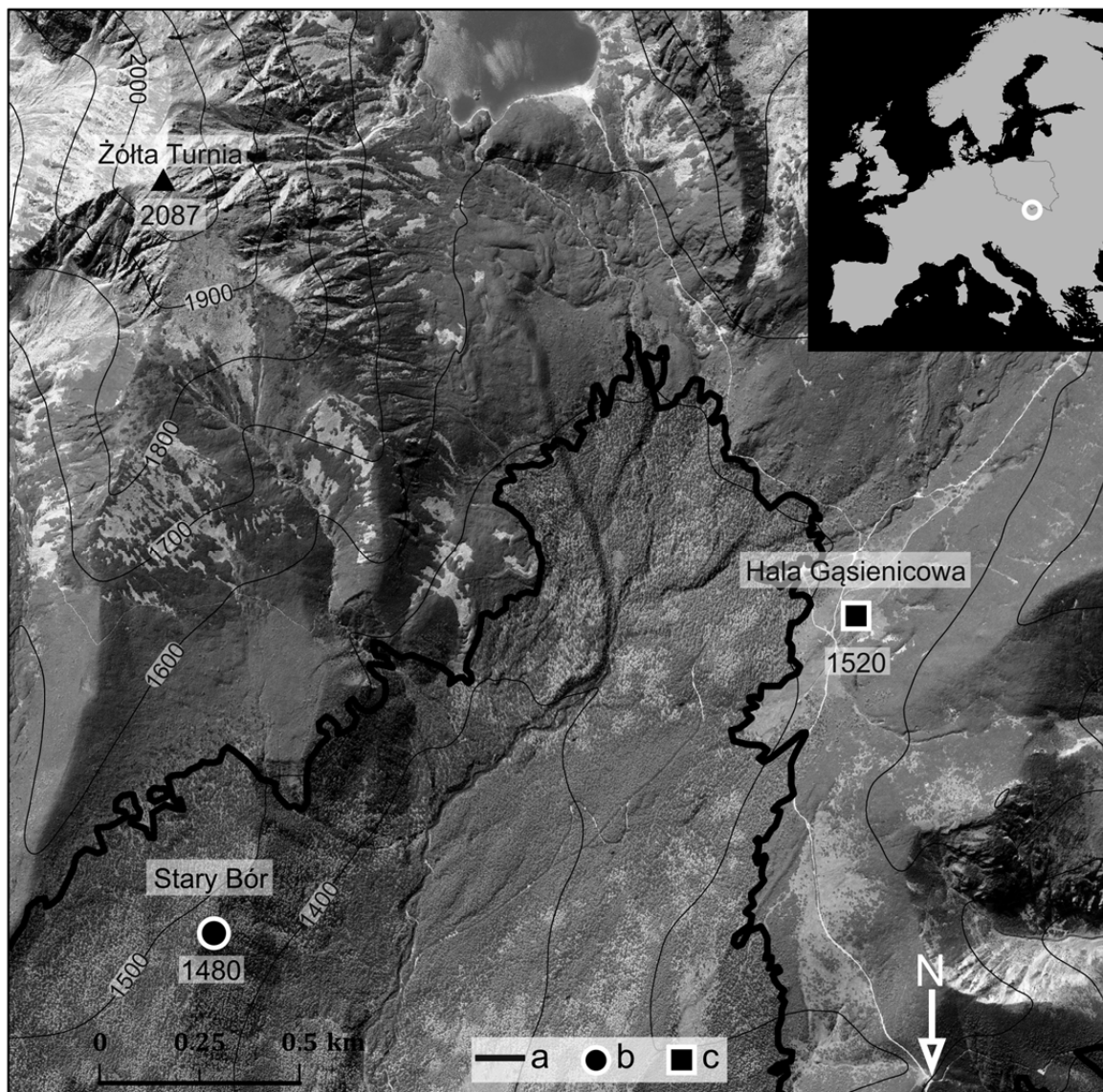


Figure 1: Location of the study site: a) timberline, b) Stary Bór sampling site, c) Hala Gašienicowa meteostation.

The tree-ring width chronology was established using ARSTAN software (Cook 1985). The raw measurements were power transformed to stabilize the variance and detrended using 120-year (~60% of the mean length of series) cubic smoothing splines with a 50% frequency-response cutoff at 120 years (SPLs; Cook & Peters 1981). Additionally, the Keith-Briffa rbar-weighted method of variance stabilization (Osborn et al. 1997) was applied. The chronologies coherency and signal strength were evaluated by calculating the inter-series correlation (Rbar) and the Expressed Population Signal (EPS) statistics (Wigley et al. 1984).

The dendroclimatic analyses were conducted using instrumental daily temperature from Hala Gąsienicowa meteostation covering the 1927 – 2012 CE, Zakopane meteostation (860 m a.s.l.) 1950 – 2012 CE and gridded daily data for 1950 – 2012 CE derived from E-OBS 14.0 grid (Haylock et al. 2008). Hala Gąsienicowa meteostation is located at the elevation of 1520 m a.s.l. and well represents the timberline conditions of the northern part of the Tatras, whereas Zakopane meteostation is located at the foothills of the Tatras. The growth/climate response for monthly intervals (data from Hala Gąsienicowa meteostation, 1927-2012 CE) was determined using DendroCorr 3.2 software (Hulist et al. 2016) by calculating bootstrap correlation coefficients which rely on random sampling with replacement 10K times between standard TRW chronologies and climate data over the common period 1927 – 2012. One of the main features of DendroCorr 3.2 is the possibility to calculate correlations between dendrochronological and daily climatic data. Afterwards the software identifies the exact time interval within a year for which the highest correlations occur.

Algorithm steps for daily calculations are as follows (for this example, assume that data is available for years 1950-2012, number of years  $L=63$ ):

1. List date ranges within a year. The average temperature is computed over intervals from 1 to 365 days and the number of possibilities is equal to

$$S = \sum_{i=1}^N i = \frac{1}{2}N(N + 1)$$

where  $N$  is number of days. For 365 days (29<sup>th</sup> of February is discarded in all cases) there are 66795 distinct date ranges.

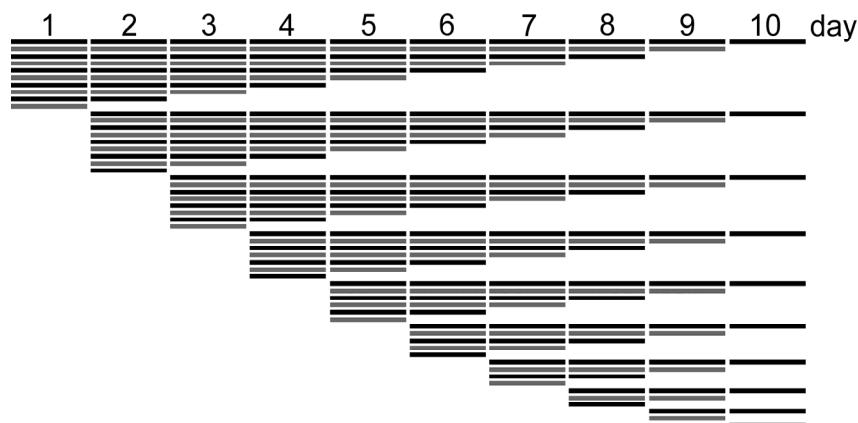


Figure 2: The example of the intervals over which the average temperature is calculated within the period of 10 days producing 55 intervals. The same principles are applied for the entire year which results in 66795 intervals ranging from 1 day to 365 days.

2. Take the first range out of  $S$  date ranges:  $r_1 = \text{January } 01^{\text{st}} - \text{December } 31^{\text{th}}$ .
  - a. Average all daily values in range  $r_1$  for year 1950 to obtain  $a_1$ .
  - b. Repeat step 2a for all following years 1951-2012 to obtain averaged values  $a_1 - a_L$ .

3. Correlate dendrochronological data for years 1950-2012 with a1-aL sequence to obtain a correlation coefficient cr1.
4. Repeat steps 2-3 for all date ranges  $r_S$  to obtain S distinct values of correlation.
5. Plot c1-crS points on a 2-dimensional 365x365 diagram where X-axis represents starting day and Y-axis - ending day (as a 1-365 number). Set points' color as red for a positive correlation or blue for negative correlation. Set color opacity to be equal to the absolute value of the correlation coefficient (0 for transparent, 1 for opaque).

Step 2 requires S averaging operations for one year, therefore there are S×L averaging operations for all L years. In order to calculate averaged values, each day data has to be read from memory several times. Total number of reads is given by the formula:

$$K = \sum_{i=1}^N i(N - i + 1) = \frac{1}{6}N(N + 1)(N + 2)$$

If N = 365 then K = 8 171 255. Using Welford's Method (Knuth 1998) for computing Rolling Average, K can be reduced to only S access operations, which significantly reduces the time needed to accomplish step 2.

In step 3, Pearson Correlation Coefficient (PCC) is computed S times, i.e. once for each date range resulting in one point on the diagram (step 5).

Computational complexity for both averaging and computing PCC is O(n), therefore the algorithm scales linearly depending on the number of years L. Total number of operations for averaging and correlating is therefore:

$$T = SL + S = S(L + 1)$$

In this study  $T = 66795 \times (63 + 1) = 4\,274\,880$ .

The analyses of xylogenesis were performed on wood micro-cores (1.2–2.4 mm in diameter) collected around four Norway spruce stems growing at the same site as the rest of sampled trees. The sampling was performed in weekly intervals from May to October 2005. The micro-cores were processed following the procedure described by Deslauriers et al. (2003) and Rossi et al. (2006).

## Results

### *The intra-annual analyses*

The intra-annual growth of Norway spruce in the timberline ecotone of the Tatra Mountains follows the same pattern as other conifers from mountain/cold environments of Europe. Figure 3 shows the cycle of the cambium activity, formation of new tracheids, lignification and accumulation of mature cells during one growing season in the year 2005. The cambium activity started in mid-May when the number of cells rose from average 4 (1.4SD) to 6 (1.9SD) and continued growing to maximum number of 8 (0.8SD), which occurred, in the first week of July. One month later the number of cambial cells decreased to 5 (1.1SD) and remained at this level to the end of the growing season. The first new tracheids (in the enlargement phase) appeared at the end of May and reached the maximum number between June 21<sup>st</sup> and June 28<sup>th</sup> (172 - 179 DOY). The last new xylem cells were produced by cambium at the end of August but the maximum of ring development in terms of number of new cells took place in the second half of June and first weeks of July (165 – 200 DOY). The new tracheids expanded, the cell walls were thickened due to the lignification mainly during the second half of July and August. The first mature cell was identified in the samples in mid-July and at the end of September the ring was composed by 22 (7.5SD) cells and fully mature.

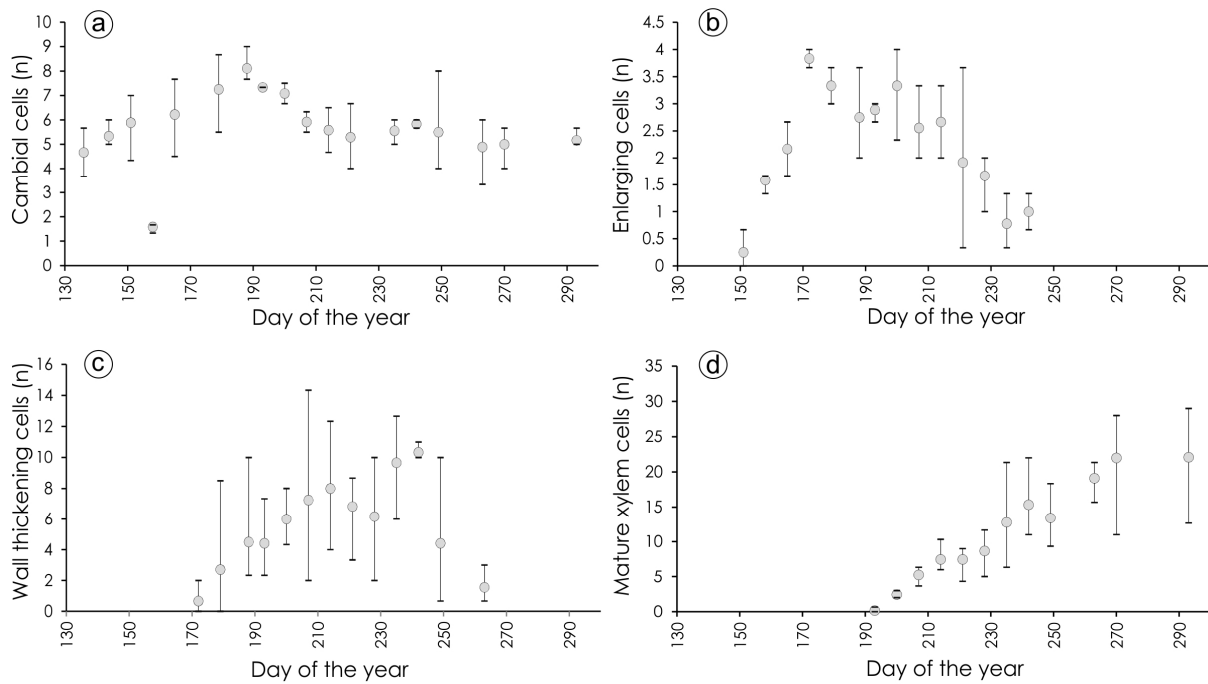


Figure 3: Number of cells: a) in the cambial zone; b) in radial enlargement; c) in secondary wall thickening and lignification; d) mature xylem cells during 2005.

#### Tree-ring width chronology

The chronology was built using 64 trees representing the age ranging from 74 to 285 years. The mean length of series and the average growth rate equal 186 years and 0.86 mm, respectively. Most of the series show similar longer-term trends in a negative exponential form, typical for the age-trend. The chronology was truncated at a minimum sample replication of five series and covers the period 1771 – 2012 (Fig. 4). The standard chronology shows high statistical parameters of  $R_{bar}$  and EPS (0.63 and 0.96, respectively).

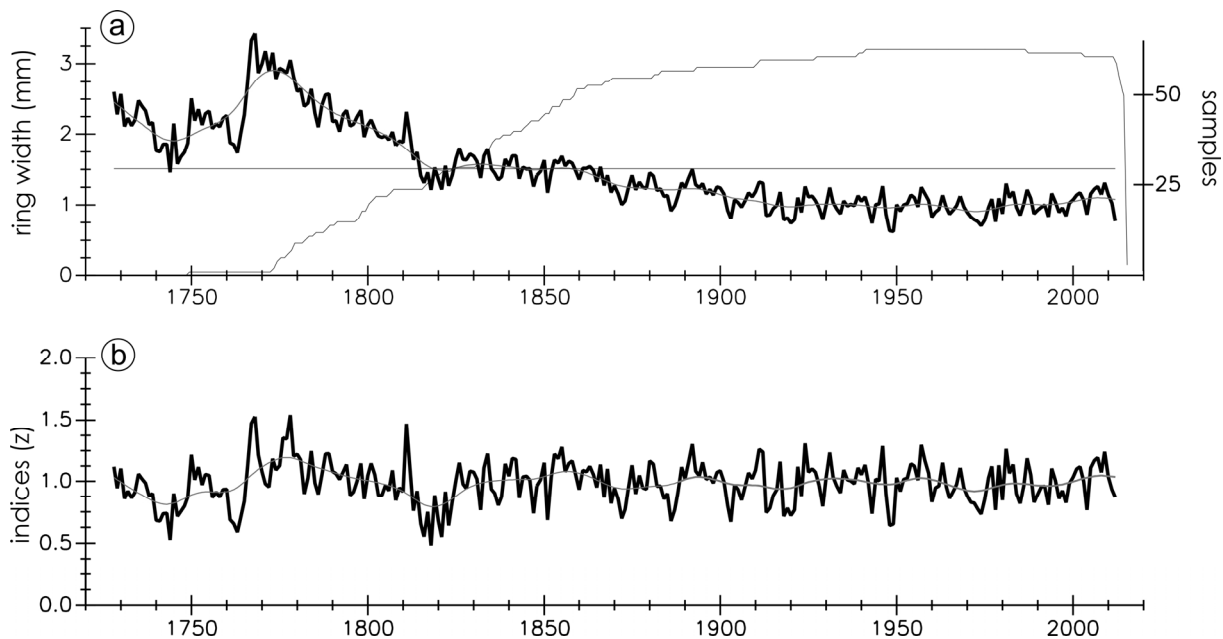


Figure 4: Raw (a) and standard (b) chronologies.

### The growth/climate response calculated using monthly intervals

The correlation between TRW spruce standard chronology and climate data derived from Hala Gąsienicowa meteorostation was first calculated against 18 monthly averages, starting from May of the year preceding ring formation to October of the actual year of ring-formation and some multi-months intervals (so-called seasons). The analyses reveal that radial growth of the studied trees is affected at statistically significant level ( $p=0.01$ ) by temperature of three monthly intervals and five seasons (Fig. 5). The response to temperature of previous year October ( $r=0.39$ ) can be explained by a direct positive effect of the level of reserves accumulated during warm autumn in the year preceding ring formation. However, the temperatures of the two consequent summer months June ( $r=0.38$ ) and July ( $r=0.47$ ) show stronger influence. The results of growth/climate response obtained for intervals representing the summer or whole warm season are even higher (Fig. 5). The temperature of June-July season displays the highest impact on ring widths of studied trees ( $r=0.54$ ). The correlations for other seasons covering late spring/ early summer (May-July) and summer period (June-August, July-August) are also statically significant ( $r= 0.46, 0.44, r=0.33$ , respectively). The chronology responses also to temperature of late summer/early autumn (July-September,  $r=0.36$ ) and whole growing season (April-September,  $r=0.36$ ).

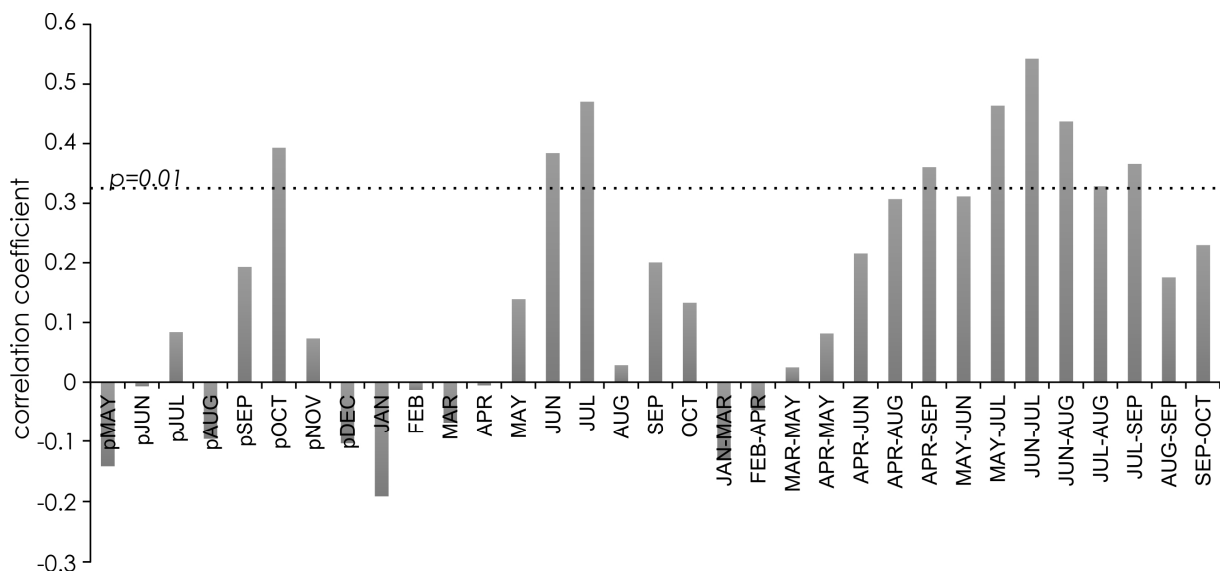


Figure 5: The bootstrap correlation coefficients calculated between standard chronology and monthly intervals of temperature data from Hala Gąsienicowa meteorostation.

### The growth/climate response calculated for daily intervals

To test if narrowing down the time window over which the average of air temperature is calculated would influence the result of growth/climate response, correlations were calculated between developed standard chronology and climate data using DendroCorr 3.2 (Hulst et al. 2016). The procedure was performed for three sets of daily climate data: i) instrumental data from Zakopane meteorostation (1950-2012), ii) daily gridded data E-OBS 14.0 (1950-2012), and iii) instrumental data from Hala Gąsienicowa meteorostation (1927-2012) as a closest one to the sampling site (2.2 km) and longest available series (Fig. 6). The highest correlation ( $r=0.68$ ) was obtained for the temperature averaged over 32 days period from the beginning of June 14<sup>th</sup> (165 DOY) to July 15<sup>th</sup> (196 DOY) and measured at Hala Gąsienicowa meteorostation. For Zakopane meteorostation slightly different period: June 9<sup>th</sup> (160 DOY) to July 19<sup>th</sup> (200 DOY) was indicated as providing the best results ( $r=0.60$ ). The results for intervals calculated based on gridded data E-OBS 14.0 are lower in terms of the value of correlation ( $r=0.58$ ) but in terms of indicated interval they are very similar to the results yielded using instrumental data: June 14<sup>th</sup> (165 DOY) to July 19<sup>th</sup> (200 DOY). Detailed examination of the results calculated for Hala Gąsienicowa reveals more than 10K statistically significant values of correlations for various intervals from 117 to 318 DOY. Generally this time

window corresponds with the time frame (91 to 273 DAY) of statistically significant results derived from monthly climate data. On the one hand such results support the use of monthly averaged data but on the other hand demonstrate how the employment of daily-based intervals can improve the accuracy of computed growth/climate response and provide higher correlations.

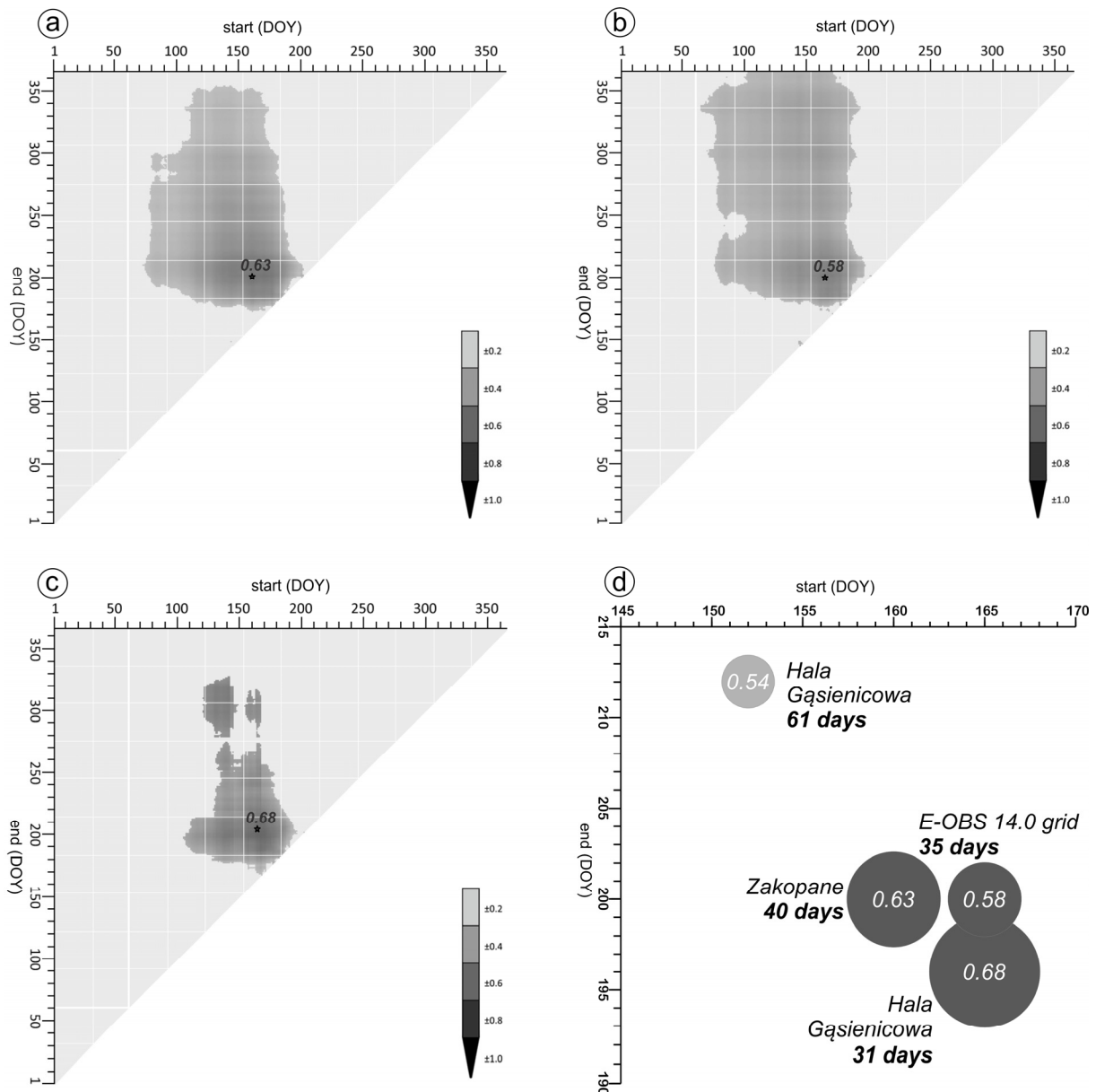


Figure 6: The visual outcome of the DendroCorr in the mode of the bootstrap correlation coefficient (only statistically significant values shown), calculated for different intervals using daily data from: (a) Zakopane meteorostation (1950-2012), (b) grid (1951-2012), c) Hala Gąsienicowa meteorostation (1927-2012). The X-axis and Y-axis indicate the beginning and the end of the particular interval, black star designates the interval of the highest correlation. (d) The comparison of the three daily-based (dark grey) and one monthly (light grey) based intervals used to compute growth/climate response shows the meaningful difference between this two kind of climate data. TRW chronology correlates the best with temperature calculated over 31-days interval (165-196 DOY).

### The xylogenesis perspective

The detailed picture of growth/climate response obtained as a result of employment of daily data agrees with the knowledge about intra-annual ring development for Norway spruce in the subalpine

zone. The example from 2005 shows that the period of the emergence of most of the new cells and its enlargement occurred in the second half of June and first weeks of July (165 – 201 DOY). That process and the following phases defining both the number and the diameter of the cells is crucial for the size of the ring - the main parameter used in dendrochronology. The studied spruces follow the pattern, described by Rossi et al. (2006, 2007) of maximum rate of tracheids production centred on summer solstice (172 DOY). The environmental conditions, especially temperatures directly before and during this period, strongly influence the efficiency of the process and the size of the annual ring. Therefore, the thermal conditions of that period are clearly recorded in ring widths. The highest correlation between TRW and temperature was identified for the interval 165 - 196 DOY, very similar to preliminary results of cambium activity and including the summer solstice almost in the middle of that period. The other processes of the intra-annual ring development (lignification, cell wall thickening) change the features of the tracheids but do not influence their size and number. Therefore, they are rather recorded in the other parameters of the ring such as MXD, BI etc. The traditional approach of using monthly data results in including the time before and after the period of most intensive cell production, here: period of 152 - 212 DOY instead of 165 - 196 DOY. This can be one of the main reasons for the difference in the strength of the obtained results of correlations (0.68 for 165 – 196 DOY period and 0.54 for 152 – 212 DOY period).

### Summary

1. The analyses of various temporally scaled growth/climate responses of TRW chronology of Norway spruce from the subalpine zone in the Polish Tatras allow concluding that narrowing down the time window over which the average temperature is calculated provides a better picture of climate influence on ring formation.
2. The new procedure of computing averages for all possible intervals of length between 1 and 365 days, calculating bootstrap correlations and automatic selection of the highest results now implemented in DendroCorr 3.2 proves to be an efficient and fast way to test the growth/climate response in more detailed temporal scale.
3. Linking the knowledge about xylogenesis and the results of growth/climate response performed in detailed temporal scale helps to understand the process of recording the temperature in the width of the ring.
4. The time-window for which the climatic conditions are recorded by TRW is rather shorter and does not follow the monthly division of a year, so the highest correlation obtained from traditionally performed growth/climate response (time window: June-July,  $r=0.54$ ) is only partially reflected in results of daily-based analyses (time window June 14<sup>th</sup> – July 15<sup>th</sup>,  $r=0.69$ ).

### Acknowledgement

We would like to thank Sergio Rossi, Annie Deslauriers, Tommaso Anfodillo, Hubert Morin for their help in understanding the processes of intra-annual development of xylem and making the lab available to perform the wood anatomy analyses. The research was funded by National Science Centre, based on the decision DEC-2013/11/B/ST10/04764 as a part of the project The application of Blue Intensity as a new proxy for dendrochronological research of climate change in Europe.

### References

- Beck, W. (2011): Impact of drought and heat on tree and stand vitality—results of the study commissioned by the Federal Ministry of Food, Agriculture and Consumer Protection. In: Maaten-Theunissen M, Spiecker H, Gärtner H, Helle G, Heinrich I (ed.) (2011): TRACE - Tree Rings in Archaeology, Climatology and Ecology, Volume 9. Scientific Technical Report STR 11/07, GFZ German Research Centre for Geosciences. Potsdam, 20 - 27.

- Beck, W., Sanders, T. G., Pofahl, U. (2013): CLIMTREG: detecting temporal changes in climate–growth reactions—a computer program using intra-annual daily and yearly moving time intervals of variable width. *Dendrochronologia*, 31(3): 232-241.
- Büntgen, U., Frank, D. C., Kaczka, R. J., Verstege, A., Zwijacz-Kozica, T., Esper, J. (2007): Growth responses to climate in a multi-species tree-ring network in the Western Carpathian Tatra Mountains, Poland and Slovakia. *Tree Physiology*, 27(5): 689-702.
- Büntgen, U., Myglan, V.S., Ljungqvist, F.C., McCormick, M., Di Cosmo, N., Sigl, M., Jungclaus, J., Wagner, S., Krusic, P.J., Esper, J., Kaplan, J.O., de Vaan, M.A.C., Luterbacher, J., Wacker, L., Tegel, W., Kirilyanov, A.V. (2016): Cooling and societal change during the Late Antique Little Ice Age from 536 to around 660 AD. *Nature Geoscience*.
- Carrer, M., Urbinati, C. (2004): Age-dependent tree ring growth responses to climate of *Larix decidua* and *Pinus cembra* in the Italian Alps. *Ecology*, 85(3): 730-740.
- Castagneri, D., Petit, G., Carrer, M. (2015): Divergent climate response on hydraulic-related xylem anatomical traits of *Picea abies* along a 900-m altitudinal gradient. *Tree Physiology* 35: 1378-1387.
- Cook, E.R., Peters, K. (1981): The smoothing spline: A new approach to standardizing forest interior tree-ring width series for dendroclimatic studies. *Tree-Ring Bull.* 41: 45–53.
- Cook, E.R. (1985): A time series analysis approach to tree-ring standardization. Ph.D. Thesis, University of Arizona, Tucson. 171 pp.
- Cook, E. R., Kairiukstis, L. A. (Eds.). (1990): Methods of dendrochronology: applications in the environmental sciences. Springer Science & Business Media.
- Deslauriers, A., Morin, H., Bégin, Y. (2003): Cellular phenology of annual ring formation of *Abies balsamea* in the Québec boreal forest (Canada). *Canadian Journal of Forest Research* 33: 190–200.
- Deslauriers, A., Rossi, S., Anfodillo, T., Saracino, A. (2008): Cambial phenology, wood formation and temperature thresholds in two contrasting years at high altitude in southern Italy. *Tree Physiology*, 28(6): 863-871.
- Douglass, A. E. (1920): Evidence of climatic effects in the annual rings of trees. *Ecology*, 1(1): 24-32.
- Düthorn, E., Schneider, L., Günther, B., Gläser, S., Esper, J. (2016): Ecological and climatological signals in tree-ring width and density chronologies along a latitudinal boreal transect. *Scandinavian Journal of Forest Research*: 1-8.
- Esper, J., Krusic, P.J., Ljungqvist, F.C., Luterbacher, J., Carrer, M., Cook, E., Davii, N.K., Hartl-Meier, C., Kirilyanov, A., Konter, I.O., Myglan, V., Timonen, M., Treydte, K., Trouet, V., Villalba, R., Yang, B., Büntgen, U. (2016): Ranking of tree-ring based temperature reconstructions of the past millennium. *Quaternary Science Reviews*, 145: 134-151.
- Fritts, H. C. (1976): Tree rings and climate. *Scientific American*, 226: 92-100.
- Grießinger, J., Bräuning, A., Helle, G., Hochreuther, P., Schleser, G. (2016): Late Holocene relative humidity history on the southeastern Tibetan plateau inferred from a tree-ring  $\delta^{18}O$  record: Recent decrease and conditions during the last 1500 years. *Quaternary International*. <http://dx.doi.org/10.1016/j.quaint.2016.02.011>
- Haylock, M. R., Hofstra, N., Klein Tank, A. M. G., Klok, E. J., Jones, P. D., New, M. (2008): A European daily high-resolution gridded data set of surface temperature and precipitation for 1950–2006. *Journal of Geophysical Research: Atmospheres*, 113(D20).
- Holmes, R.L. (1983): Computer-assisted quality control in tree-ring dating and measurements. *Tree-Ring Bulletin*, 43: 69-78.
- Huber, B. (1943): Über die Sicherheit jahringchronologischer Datierung. *Holz als Roh- und Werkstoff*, 6(10): 263–268.

- Hulist, A., Janecka, K., Kaczka, R.J. (2016): DendroCorr the simple and powerful software to calculate the growth/climate response. In: Hevia, A., Sánchez-Salguero, R., Linares, J. C., Olano, J. M., Camarero, J. J., Gutiérrez, E., Helle, G., Gärtner, H. (ed.): TRACE - Tree Rings in Archaeology, Climatology and Ecology, Volume 14. Scientific Technical Report 16/04, GFZ German Research Centre for Geosciences. doi: 10.2312/GFZ.b103-16042. 44-49.
- Kaczka, R. J., Spyt, B., Janecka, K., Niedźwiedz, T., Bednarz, Z. (2016): Climate reconstruction from tree-rings in the Tatra Mountains. In *Flood Risk in the Upper Vistula Basin* (pp. 209-229). Springer International Publishing.
- Knuth, D.E. (1998): The Art of Computer Programming, volume 2: Seminumerical Algorithms, 3rd edn., p. 232. Boston: Addison-Wesley.
- Larsson, L., (2013): CooRecorder and Cdendro programs of the CooRecorder/Cdendro package version 7.8. <http://www.cybis.se/forfun/dendro/>
- Liang, W., Heinrich, I., Simard, S., Helle, G., Liñán, I. D., Heinken, T. (2013): Climate signals derived from cell anatomy of Scots pine in NE Germany. *Tree physiology*, 33(8): 833-844.
- Osborn, T.J., Briffa K.R., Jones P.D. (1997): Adjusting variance for sample-size in tree-ring chronologies and other regional-mean time-series. *Dendrochronologia* 15: 89–99.
- Pritzkow, C., Heinrich, I., Grudd, H., Helle, G. (2014): Relationship between wood anatomy, tree-ring widths and wood density of *Pinus sylvestris* L. and climate at high latitudes in northern Sweden. *Dendrochronologia*, 32(4): 295-302.
- Rossi, S., Deslauriers, A., Anfodillo, T., Morin, H., Saracino, A., Motta, R. Borghetti, M. (2006): Conifers in cold environments synchronize maximum growth rate of tree-ring formation with day length. *New Phytologist*, 170, 301– 310.
- Rossi, S., Deslauriers, A., Anfodillo, T. Carraro, V. (2007): Evidence of threshold temperatures for xylogenesis in conifers at high altitudes. *Oecologia*, 152, 1–12.
- Sanders, T. G., Pitman, R., Broadmeadow, M. S. (2014): Species-specific climate response of oaks (*Quercus* spp.) under identical environmental conditions. *iForest-Biogeosciences and Forestry*, 7(2): 61.
- Schulman, E. (1953): Tree-ring evidence for climatic changes. [in]: Shapley H. (ed.) Climatic Change. Harvard University Press: Cambridge, 209-219.
- Wigley, T.M., Briffa, K.R., Jones, P.D. (1984): On the average value of correlated time series, with applications in dendroclimatology and hydrometeorology. *Journal of climate and Applied Meteorology*, 23(2): 201-213.

# The Blue Intensity proxy for >400 years growing season temperature reconstruction from the Tatra Mountains

R.J. Kaczka<sup>1</sup>, B. Spyt<sup>1</sup>, K. Janecka<sup>1</sup> & R. Musioł<sup>2</sup>

<sup>1</sup>Faculty of Earth Sciences, University of Silesia in Katowice, Sosnowiec

<sup>2</sup>Institute of Chemistry, University of Silesia in Katowice, Katowice

E-mail: ryszard.kaczka@us.edu.pl

## Introduction

Tree rings comprise valuable paleoclimate information in annual resolution (Fritts 1976). Although ring widths (TRW) have been the most commonly applied tree-ring parameter, various others are explored as a climate proxy (Björklund et al. 2014). For instance, in cool environment maximum latewood density (MXD) has proven to be a superior proxy that provides strong paleoclimatic signal, pretty often stronger than ring widths (Sheppard et al. 1996, González & Eckstein 2003, Wilson & Luckman 2003, Campbell et al. 2007). Therefore, MXD has often been used to reconstruct summer temperature in cold regions (Esper et al. 2012, Björklund et al. 2013, Briffa et al. 2013). The Blue Intensity (BI) is a proxy capturing similar signal but the procedure of sample preparation and BI measuring is much less time-consuming and inexpensive in comparison with MXD. It has been presented that Blue Intensity (here BI of latewood) is strongly correlated with MXD and it has been suggested to be a potential surrogate for MXD (McCarroll et al. 2002, Campbell et al. 2007, Campbell et al. 2011). Nevertheless, recently BI is more often used as an independent proxy (Björklund et al. 2014, Rydval et al. 2014) also to develop paleoclimate reconstructions (Trachsel et al. 2012, Young et al. 2012, McCarroll et al. 2013, Dolgova 2016). The objectives of the research were to test: i) the use of BI measured on Norway spruce (*Picea abies* (L.) Karst) as a proxy of climate, and ii) the possibility to use BI to develop the temperature reconstruction of substantial length for the northern part of the Tatra Mountains (Fig. 1).

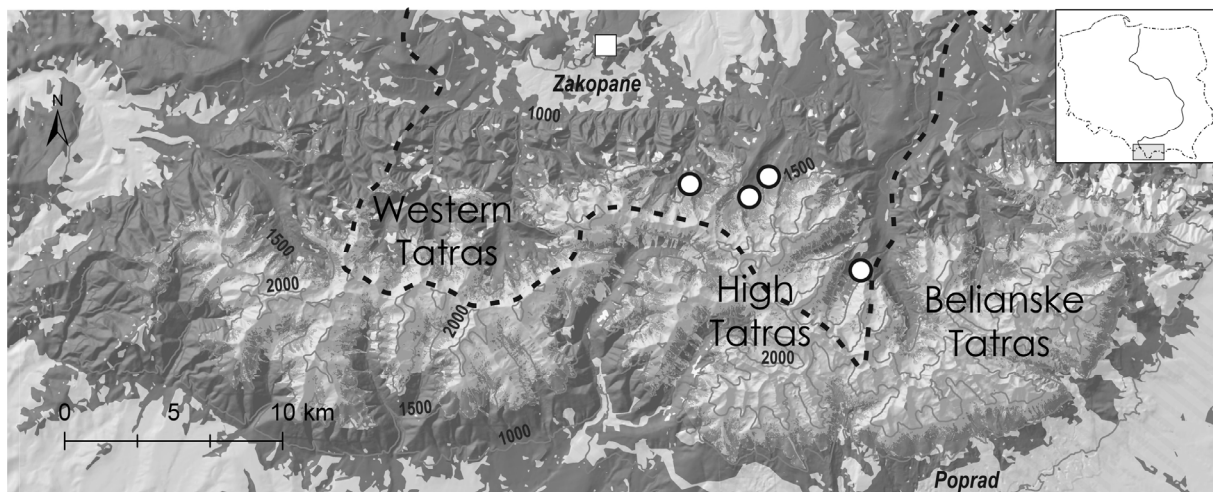


Figure 1: The geographical settings: sampling sites of Norway spruce growing in the subalpine forest (white dot), and location of Zakopane meteorological station (rectangle).

## Materials and methods

Samples were selected from the collection of cores from three sites representing the natural Norway spruce stands of the subalpine forest near the timberline in the Tatra Mountains, Poland (Fig. 1). The cores were collected using increment borer and prepared for TRW and BI measurements. The non-structural compounds (e.g. resin, tannins, oils, gums) were extracted for

48 hours in soxhlet extractor in boiling acetone. The samples were dried, glued into wooden laths and sanded to prepare flat surface providing clear picture of annual rings. The first step of sample selection further subjected to analyses was mainly orientated at eliminating samples with unnatural wood colour (due to decay, presence of compression wood, etc.) The selected cores were scanned in darkroom conditions with a 2400 – 4800 DPI resolution, in RGB mode employing the flatbed scanner. The scanner was colour calibrated (ICC) utilized the IT8 Calibration Target (IT8.7/2) printed on Kodak Professional Endura paper with software SilverFast 8.4 LaserSoft Imaging Incorporated. Whole procedure resulted in high-resolution RGB images recording the natural colours of wood. Both TRW and BI were measured using the standard and Colour Intensity modes of CooRecorder 8.0 software provided by Cybis Elektronik & Data AB (Larsson 2013). The settings were adjusted to measure only BI of latewood, consequently only one collector of a rather small frame was used (width (w)/ offset (f)/ deepness (d) = 100/2/100, all in pixels and 50% dark latewood) (see Rydval et al. 2014). The visual cross-dating (CDendro software, Larsson 2013) was performed to verify the synchronicity of measurement series, detect errors and missing rings. The results were furthermore assessed by statistical analyses of TRW and BI series using Cofecha software (Holmes 1983). The final set of measurements from 63 trees were selected as the outcome of this evaluation. The standard chronologies for both proxies were established with the use of the same procedure employing ARSTAN software (Cook 1985). The series were detrended using 300-years cubic smoothing splines with a 50% frequency-response cutoff at 300 years (Cook & Peters 1981), and additionally the adaptive power transformation and Keith-Briffa Rbar-weighted method of variance stabilization (Osborn et al. 1997) were applied. Signal strength of the chronologies was assessed by calculating the inter-series correlation (Rbar) and the Expressed Population Signal (EPS) statistics (Wigley et al. 1984). The growth-climate relationships were calculated using bootstrap correlation coefficient relying on the random sampling with replacement 20K times using DendroCorr 3.2 software (Hulst et al. 2016). The instrumental and gridded temperature data were utilized. The average of climate data for the 49.00 - 49.50° N and 19.50 – 20.00° E region for the 1901-2015 period was computed from 0.5 degree CRU TS3.24, 24 (Harris et al. 2014). The instrumental measurements for the 1895-2015 period were obtained from Zakopane meteorological station, located at 860 m a.s.l., approximately 6 km from the sampling sites. The growth-climate responses were calculated for previous (from May to December) and recent year monthly (from January to October) and seasonal (10 combinations between January and December) intervals. The climate reconstruction was performed using the scaling method (Esper et al. 2005). The average values and standard deviations of a proxy (BI series) were brought to the equal level as the corresponding values of climate records (temperature) over an established common period (Esper et al. 2005). The half of the overlap period (1895 – 1955) was used as the calibration period. The model was checked against the climate data over the verification interval, the second half of the common period (1956 – 2015). The common measures used to assess the adequacy of statistical predictions (Fritts 1974, Cook et al. 1994) like the mean squared error of the estimate (MSE), reduction of error (RE), coefficient of efficiency (CE) and the squared correlation ( $r^2$ ) were employed here.

## Results

The mean length of the series reached 225 years with the age ranging from 425 to 65 years. The average TRW is rather low (0.69 mm, SD=0.33) and changes from 0.34 mm (SD=0.23) to 1.3 mm (SD=0.46), which is mainly related to the tree age (387 and 157 years, respectively). Whereas, the corresponding parameters for BI measurements are not age-dependended. The mean value of BI reaches 1.43 (SD=0.16). The mean sensitivity of the TRW proxy (0.221) is higher than BI proxy (0.066). The chronologies span from 1609 to 2015 after truncated at minimum replication < 5 series (Fig. 2). The Rbar statistics of the TRW and BI chronologies range from 0.63 to 0.59, respectively, whereas the values of EPS are equal (0.92) in both cases. The BI chronology

corresponds very well with the existing MXD chronology from the northern slopes of the Tatra Mts. (Büntgen et al. 2007). The comparison between BI and MXD chronologies performed for the common period (1709-2006) reveals high correlation ( $r=0.88$ ) and similar long-term trends.

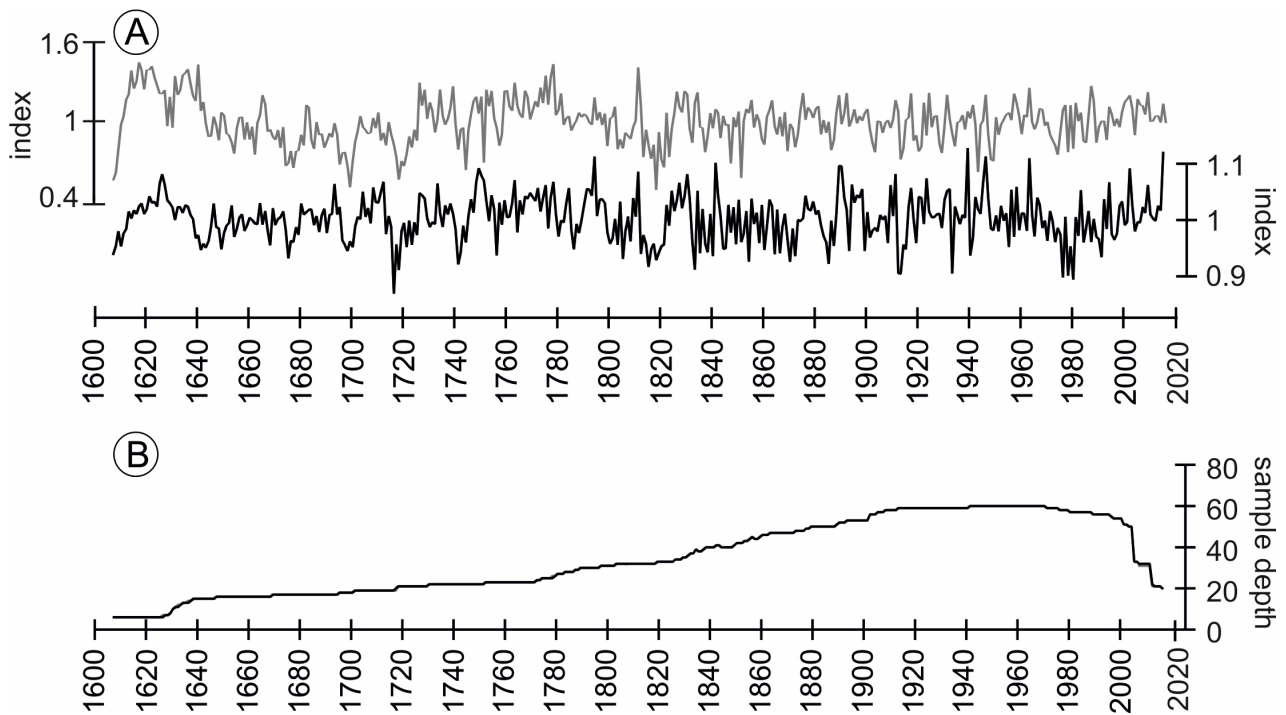


Figure 2: A - the standard TRW (grey) and BI (black) chronologies truncated at < 5 series, B - the distribution of the sample.

The BI and TRW chronologies correlate better with instrumental than gridded data (Fig. 3). The growth-climate response of TRW chronology reveals statistically significant ( $p=0.01$ ) influence of temperatures of several single months, among which the highest correlation values for the current year June and July ( $r=0.51$  and  $r=0.43$ , respectively), and lower for the previous year October ( $r=0.33$ ) are noticeable. Nevertheless, the strongest signal in TRW appears for the mean June-July temperature ( $r=0.58$ ). The mean temperatures of June-August ( $r=0.48$ ) and warm period April-October play a role in a tree growth, although the  $r$ -value for the latest period is lower. The BI chronology does not correlate with the temperature of year preceding ring formation. The monthly mean temperature of single months intervals between April and September influences the BI, with the highest values for July and August ( $r=0.41$  and  $r=0.48$ , respectively). All correlations between BI and mean temperature of months within April - September are significant. Among intervals May-September period is characterized by the highest value of correlation ( $r=0.60$ ), which is also the maximum value for the whole dendroclimatic analyses. The 31-years running correlation, calculated for the common period 1895-2015, shows a constantly significant correlation for May-September interval (Fig. 3). Due to this result we reconstructed mean monthly temperature of May-September interval using BI proxy (Fig. 4). The MXD chronology from the Tatra Mts. shows the similar climatic signal. The MXD correlated strongly with the April-September mean temperature ( $r=0.66$ ) (Büntgen et al. 2007). Although the formation of latewood, especially the cell wall thickening including lignification of the latewood cells are the latest stages of annual ring development (Wodzicki 1971, Gindl et al. 2000, Deslauriers et al. 2003), both BI and MXD register temperature of much wider period spanning from spring to autumn.

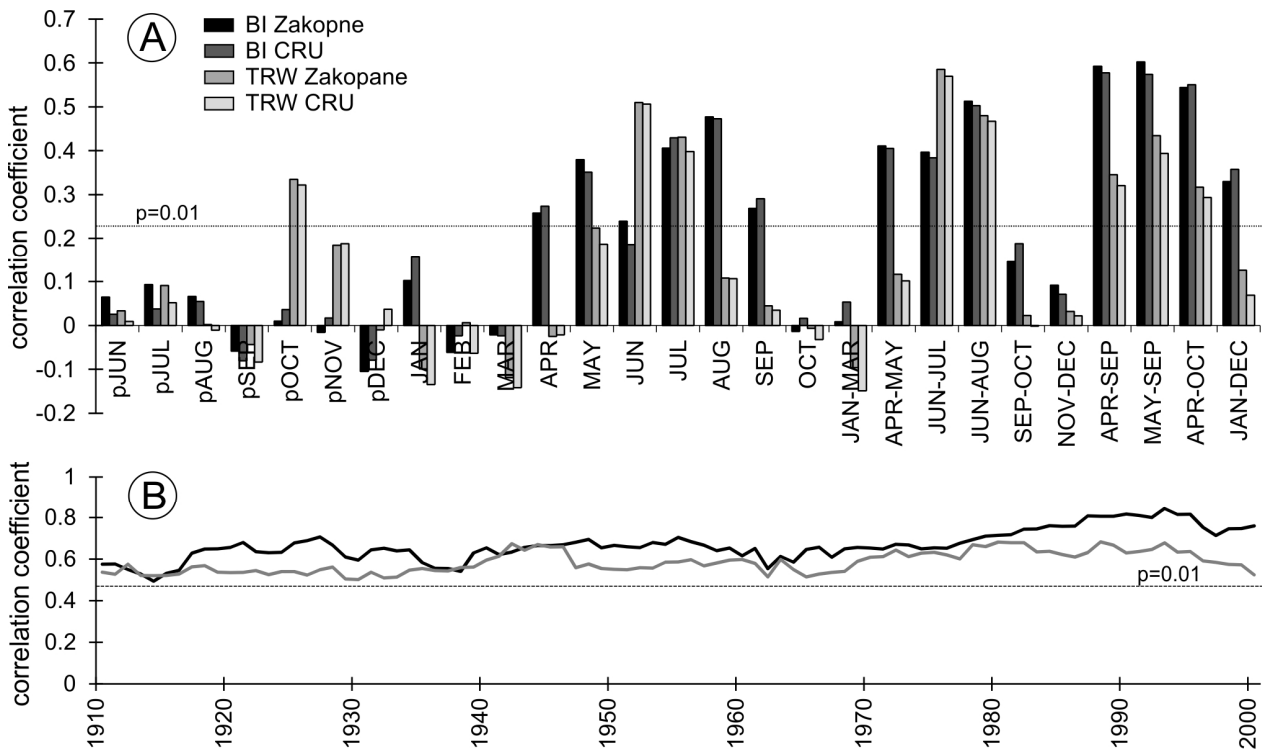


Figure 3: The growth-climate response: A - the bootstrap correlation coefficient between standard TRW and BI chronologies and monthly intervals of temperature data from Zakopane meteorological station and gridded data (CRU TS3.24); B - the running correlations between TRW (grey line) and BI (black line) chronologies and periods characterized by the highest correlations (June-July and May-September, respectively).

The common 1895-2015 period was split in two roughly equal periods (60 and 61 years) to perform the calibration and verification procedure. The calibration of May-September temperature/BI model for the 1895-1954 period is at the same level like for the whole period ( $r^2=0.43$  and  $r^2=0.43$ , respectively) and standard error of the estimates reaches  $MSE=0.54$ . The verification was performed based on the 1955-2015 period. The results of the statistics such squared correlation ( $r^2=0.50$ ), standard error of the estimates ( $MSE=0.42$ ), reduction of error ( $RE=0.17$ ), coefficient of efficiency ( $CE=0.46$ ) signify that the employed model has reconstructing skills.

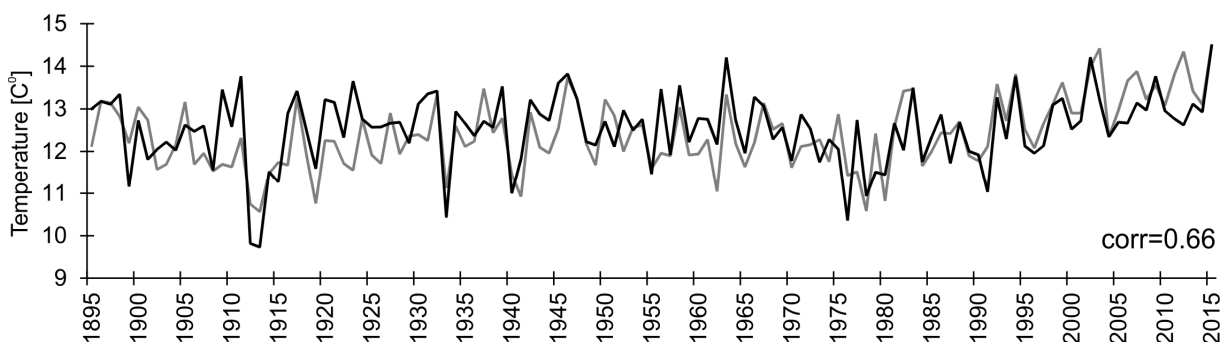


Figure 4: The comparison of the BI standard chronology (black) and selected May-September temperature (grey) over common period of 1895 – 2015.

The BI chronology and the reconstruction of May-September temperature capture very well several short-term cooling events and also longer trends (Fig. 5). Two of them are very pronounced: the cold period of 1640-1700 associated with the Late Maunder Minimum (Eddy 1976), and the cooling at the beginning of the 1800s related with the Dalton Minimum intensifying by the major activity of the Tambora volcano in 1815 (Crowley 2000, Robock 2000). The recent rise of the temperature is

particularly evident after cold period of 1976-1980. The similar changes are present in TRW-based summer temperature reconstructions (Büntgen et al. 2015, Kaczka et al. 2016). The results of the spatial correlation computed over the whole Europe reveal strong connection with South-East Europe especially with the whole range of the Carpathian arc and part of the Dinaric Mountains (Fig. 6).

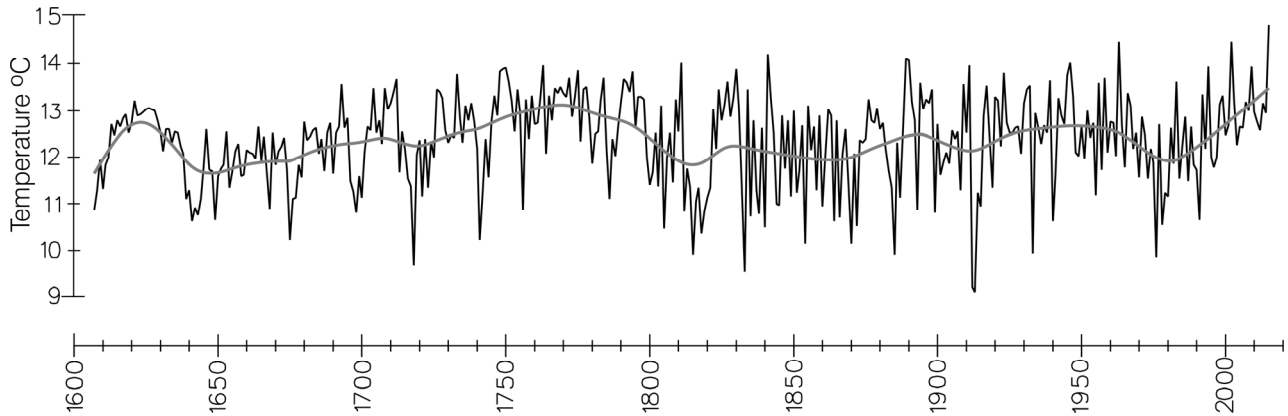


Figure 5: The reconstruction of warm season temperature (May-September) for the Tatra Mountains based on latewood BI proxy.

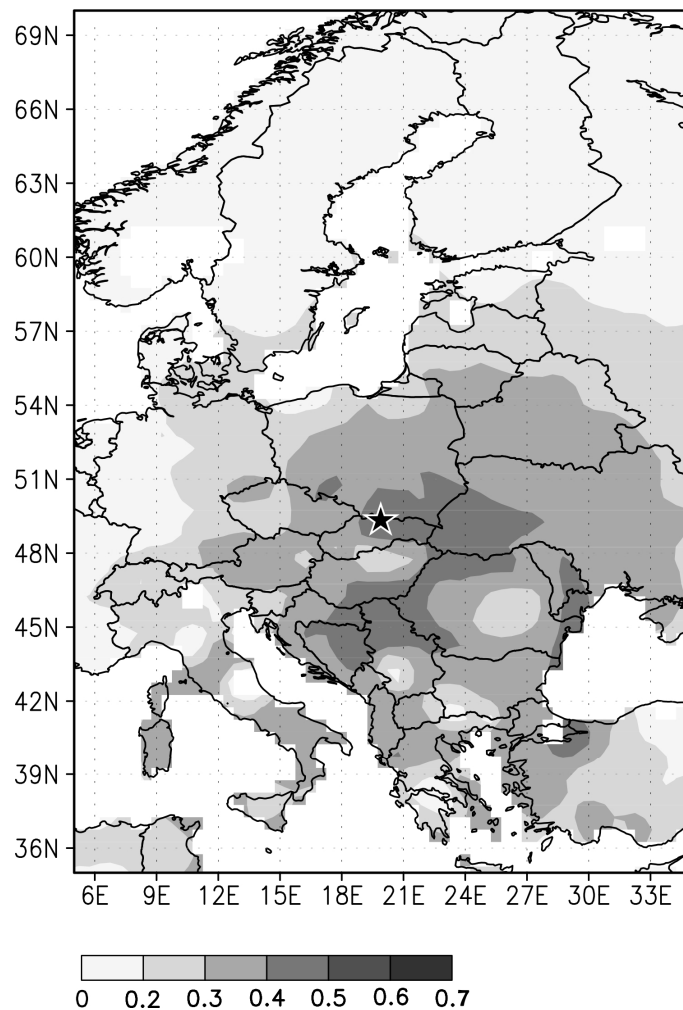


Figure 6: The spatial field correlations of the BI standard chronology against gridded (CPC GHCN/CAMS t2) May-September temperature throughout the 1948 – 2015 period. The black star indicates the site location.

## Summary

The first attempt to reconstruct temperature using Blue Intensity measurements of Norway spruce proved the potential of that proxy. The BI chronology is sensitive to temperature of longer season (May–September) and correlates stronger ( $r=0.60$ ) than tree-ring width. Even more in comparison with TRW, the BI reveals more stable over time the growth-temperature relationship. The reconstruction shows short events of cooling among which several are related to volcanic eruptions (Laki 1783, Tambora 1815, Katmai 1912). The long-term changes are depicted, cold periods of the Little Ice Age (Late Maunder Minimum and Dalton Minimum) and recent climate warming.

## Acknowledgement

The research was funded by National Science Centre, based on the decision DEC-2013/11/B/ST10/04764 as a part of the project *The application of Blue Intensity as a new proxy for dendrochronological research of climate change in Europe*.

## References

- Björklund, J., Gunnarson, B., Krusic, P., Grudd, H., Josefsson, T., Östlund, L. Linderholm, W. (2013): Advances towards improved low-frequency tree-ring reconstructions, using an updated *Pinus sylvestris* L. MXD network from the Scandinavian Mountains. *Theoretical and Applied Climatology* 113(3): 697–710.
- Björklund, J., Gunnarson, B., Seftigen, K., Esper, J., Linderholm, H.W. (2014): Blue intensity and density from northern Fennoscandian tree rings, exploring the potential to improve summer temperature reconstructions with earlywood information. *Climate of the Past* 10(2): 877-885.
- Briffa, K.R., Melvin, T.M., Osborn, T.J., Hantemirov, R.M., Kirilyanov, A.V., Mazepa, V.S., Shiyatov, S.G., Esper, J. (2013): Reassessing the evidence for tree-growth and inferred temperature change during the Common Era in Yamalia, Northwest Siberia. *Quaternary Science Reviews* 72:83–107.
- Büntgen, U., Frank, D.C., Kaczka, R.J., Verstege, A., Zwijacz-Kozica, T., Esper, J. (2007): Growth responses to climate in a multi-species tree-ring network in the Western Carpathian Tatra Mountains, Poland and Slovakia. *Tree Physiology* 27(5): 689-702.
- Büntgen, U., Trnka, M., Krusic, P. J., Kyncl, T., Kyncl, J., Luterbacher, J., Zorita, E., Ljungqvist, F.Ch., Auer, I., Konter, O., Schneider, L., Tegel, W., Štěpánek, P., Brönnimann, S., Hellmann, L., Nievergelt, D., Esper, J. (2015): Tree-ring amplification of the early Nineteenth-Century summer cooling in Central Europe. *Journal of Climate* 28(13): 5272-5288.
- Campbell, R., McCarroll, D., Loader, N.J., Grudd, H., Robertson, I., Jalkanen, R. (2007): Blue intensity in *Pinus sylvestris* tree-rings: developing a new palaeoclimate proxy. *The Holocene* 17(6): 821-828.
- Campbell R., McCarroll D., Robertson I., Loader N.J., Grudd H., Gunnarson B. 2011. Blue intensity in *Pinus sylvestris* tree rings: a manual for a new palaeoclimate proxy. *Tree-Ring Research* 67(2): 127-134.
- Cook, E.R., Peters, K. (1981): The smoothing spline: a new approach to standardizing forest interior tree-ring width series for dendroclimatic studies. *Tree-ring bulletin*.
- Cook, E.R. (1985): A time series analysis approach to tree ring standardization (dendrochronology, forestry, dendroclimatology, autoregressive process). University of Arizona, pp. 171
- Cook, E.R., Briffa, K.R., Jones, P.D. (1994): Spatial regression methods in dendroclimatology: a review and comparison of two techniques. *International Journal of Climatology* 14(4): 379-402.
- Crowley, T.J. (2000): Causes of climate change over the past 1000 years. *Science* 289(5477): 270-277.
- Deslauriers, A., Morin, H., Begin, Y. (2003): Cellular phenology of annual ring formation of *Abies balsamea* in the Quebec boreal forest (Canada). *Canadian Journal of Forest Research* 33(2): 190-200.

- Dolgora, E. (2016): June–September temperature reconstruction in the Northern Caucasus based on blue intensity data. *Dendrochronologia* 39: 17-23.
- Eddy, J.A. (1976): The maunder minimum. *Science* 192(4245): 1189-1202.
- Esper, J., Frank, D.C., Wilson R.J., Briffa K.R. (2005). Effect of scaling and regression on reconstructed temperature amplitude for the past millennium. *Geophysical Research Letters* 32(7).
- Esper J., Büntgen, U., Timonen, M., Frank, D.C. (2012): Variability and extremes of northern Scandinavian summer temperatures over the past two millennia. *Global and Planetary Change* 88-89:1-9.
- Fritts, H. C. (1976): *Tree rings and climate*, Academic, San Diego, California. 567 pp.
- Gindl, W., Grabner, M., Wimmer, R. (2000): The influence of temperature on latewood lignin content in treeline Norway spruce compared with maximum density and ring width. *Trees Structure and Function* 14: 409–414.
- González, I.G., Eckstein, D. (2003): Climatic signal of earlywood vessels of oak on a maritime site. *Tree Physiology* 23(7): 497-504.
- Harris, I.P.D.J., Jones, P.D., Osborn, T.J., Lister, D.H. (2014): Updated high-resolution grids of monthly climatic observations—the CRU TS3. 10 Dataset. *International Journal of Climatology* 34(3): 623-642.
- Holmes, R.L. (1983): Computer-assisted quality control in tree-ring dating and measurement. *Tree-ring bulletin* 43(1): 69-78.
- Hulist, A., Janecka, K., Kaczka, R.J. (2016): DendroCorr—a simple and powerful software to calculate the growth\ climate response. [in:] Hevia, A., Sánchez-Salguero, R., Linares, J.C., Olano, J.M., Camarero, J.J., Gutiérrez, E., Helle, G., Gärtner, H. (eds.) *TRACE - Tree Rings in Archaeology, Climatology and Ecology*, Volume 14. Scientific Technical Report 16/04, GFZ German Research Centre for Geosciences. 44-49.
- Kaczka, R.J., Spyt, B., Janecka, K., Niedźwiedz, T., Bednarz, Z. (2016): Climate Reconstruction from Tree-Rings in the Tatra Mountains. [in] Kundzewicz, Z., Stoffel, M., Niedźwiedz, T., Wyżga, B. (eds.) *Flood Risk in the Upper Vistula Basin*. GeoPlanet: Earth and Planetary Sciences 209-229
- Larsson, L.A. (2013): *CooRecorder&CDendro* program. Cybis Elektronik & Data AB. Version 7.6
- McCarroll, D., Pettigrew, E., Luckman, A., Guibal, F., Edouard, J.L. (2002): Blue reflectance provides a surrogate for latewood density of high-latitude pine tree rings. *Arctic, Antarctic, and Alpine Research* 450-453.
- McCarroll, D., Loader, N.J., Jalkanen, R., Gagen, M.H., Grudd, H., Gunnarson, B.E., Kirchhefer, A.J., Friedrich, M., Linderholm, H.W., Lindhol, M., Boettger, T., Los, S.O., Remmele, S., Kononov, R.M., Yamazaki, Y.H., Young, G.H.F., Zorita, E. (2013): A 1200-year multiproxy record of tree growth and summer temperature at the northern pine forest limit of Europe. *The Holocene* 23(4): 471-484.
- Osborn, T.J., Biffa, K.R., Jones, P.D. (1997): Adjusting variance for sample-size in tree-ring chronologies and other regional-mean timeseries. *Dendrochronologia* 15: 89-99.
- Robock, A. (2000): Volcanic eruptions and climate. *Reviews of Geophysics* 38 (2): 191-219.
- Rydval, M., Larsson, L.Å., McGlynn, L., Gunnarson, B.E., Loader, N.J., Young, G.H., Wilson, R. (2014): Blue intensity for dendroclimatology: should we have the blues? Experiments from Scotland. *Dendrochronologia* 32(3): 191-204.
- Sheppard, P.R., Graumlich, L.J., Conkey, L.E. (1996): Reflected-light image analysis of conifer tree rings for reconstructing climate. *The Holocene* 6(1): 62-68.

- Trachsel, M., Kamenik, C., Grosjean, M., McCarroll, D., Moberg, A., Brázdil, R., Büntgen, U., Dobrovolný, P., Esper, J., Frank, D.C., Friedrich, M., Glaser, R., Larocque-Tobler, I., Nicolussi, K., Riemann, D. (2012): Multi-archive summer temperature reconstruction for the European Alps, AD 1053–1996. *Quaternary Science Reviews* 46: 66-79.
- Wigley, T.M., Briffa, K.R., Jones, P.D. (1984): On the average value of correlated time series, with applications in dendroclimatology and hydrometeorology. *Journal of climate and Applied Meteorology* 23(2): 201-213.
- Wilson, R., Luckman, B. (2003): Dendroclimatic reconstruction of maximum summer temperatures from upper treeline sites in Interior British Columbia, Canada. *The Holocen* 13(6):851-861.
- Wodzicki T.J. (1971): Mechanism of xylem differentiation in *Pinus silvestris* L. *Journal of Experimental Botany* 22: 670–687.
- Young, G.H., McCarroll, D., Loader, N.J., Gagen, M.H., Kirchhefer, A.J., Demmler, J.C. (2012): Changes in atmospheric circulation and the Arctic Oscillation preserved within a millennial length reconstruction of summer cloud cover from northern Fennoscandia. *Climate dynamics* 39(1-2): 495-507.

# Millennia-long dendroclimatic records from the Pamir-Alay Mountains (Tajikistan) - perspectives and limitations

M. Opała-Owczarek<sup>1</sup>, T. Niedźwiedź<sup>1</sup>, O. Rahmonov<sup>1</sup> & P. Owczarek<sup>2</sup>

<sup>1</sup>University of Silesia in Katowice, Faculty of Earth Sciences, Bedzinska 60, 41-200 Sosnowiec, Poland

<sup>2</sup>University of Wrocław, Institute of Geography and Regional Development, Pl. Uniwersytecki 1, 50-137 Wrocław, Poland  
E-mail: magdalena.opala@us.edu.pl

## Introduction

To improve our understanding of past climate variability over the globe, the development of new tree-ring climate proxies is crucial. Millennial long records are especially important, as they are quite rare, despite the significant progress in high resolution paleoclimatology made in the last decade (Jones et al. 2009, Esper et al. 2016). One of the best sources of high-resolution paleoclimatic information are tree rings. Dendroclimatological studies from High Asia are of special interest due to immense potential for developing millennia long climate records. However, the response of trees to climate can show high spatial variability which is often not completely understood. Furthermore, despite the fact that a number of tree-ring studies have been carried out in the Himalayas (e.g. Cook et al. 2003, Yadav et al. 2011, Krusic et al. 2015), Karakoram (e.g. Esper et al. 2002, Ahmed et al. 2010), Tien Shan (e.g. Esper et al. 2002) and Tibetan Plateau (e.g. Bräuning et al. 2001, Gou et al. 2014), the Pamirs region remains a research gap. The dendroclimatological potential of the Pamir-Alay region was recently investigated by Opała et al. (2013, 2016, 2017) and Seim et al. (2016). The lack of tree-ring records from Pamir Mountains was due to several reasons, among which restricted access caused by Civil war operations, logistical difficulties, and the scattered spatial distribution of old-growth forest ecosystems should be mentioned.

In this study we investigate tree-ring material from the semi-arid high mountain area of Pamir-Alay to assess its potential for the reconstruction of climatic changes over the last millennium. We also address limitations of dendroclimatological research in Tajikistan, which are connected with high-seismicity of the whole Pamirs region and human activity.

## Materials and methods

### *Studied sites and wood material*

The study area is located in the western Pamir mountain system (Fig. 1A) in Central Asia. The study area has a typical high-mountain relief characterized by steep slopes (Fig. 1B) and deep valleys shaped by glacial processes. The highest parts of the mountains are glaciated. The western Pamir-Alay, surrounded by the Kyzyl-Kum desert plains, has a typical arid continental climate. The mean annual total precipitation is 271.3 mm, and mean annual air temperature is 6.6°C (Iskanderkul Meteorological Station). The most important plant community is formed by *Juniperus semiglobosa* and *Juniperus seravschanica* with a significant participation of shrubs and dwarf shrubs of the genera *Rosa*, *Berberis*, *Ephedra*, *Sorbus* and *Cerasus* (Rahmonov et al. 2016). During the field investigations in 2014 and 2015 about 500 samples of living and relict juniper wood were collected from different sites in western Tajikistan. Investigated sites are located within the elevation transect starting from 2000 m a.s.l. up to the near timberline sites above 3000 m a.s.l. In order to analyse if climatic responses differ among sites, samples were taken from all aspects. Additionally, we collected wood from historical buildings, from a village located in the upper part of the Zarafshan river catchment.

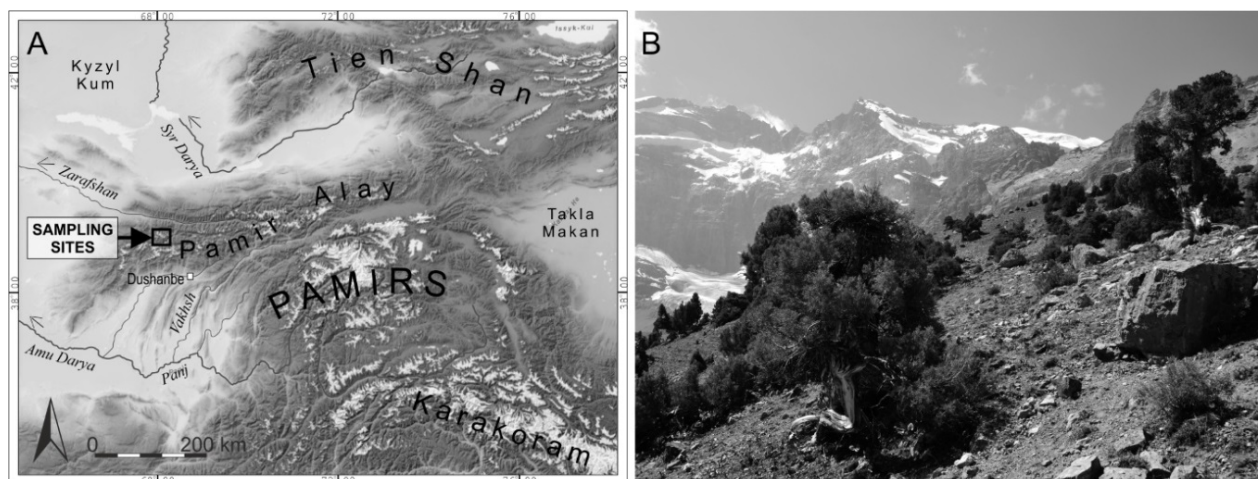


Figure 1: (A) Location of the study area, (B) Examples of old-growth *Juniperus* trees from the western Pamir-Alay.

## Methods

Standard 5 mm increment cores were collected from living trees and historical material and taken to the laboratory for processing. Samples were analysed using standard dendrochronological techniques (Stokes & Smiley 1996). Ring widths were measured with a system for automatic recognition of tree rings WinDENDRO (WinDENDRO 2006). Additionally, juniper samples with very narrow rings were re-measured with an optically magnified, stitched image from the system ATRICS based on a high resolution digital video camera attached to a high quality binocular (Levanič 2007). To remove or reduce non-climatic influences, measured ring-width series were detrended with negative exponential curves using ARSTAN software. The individual index series were combined into chronologies by calculating a bi-weight robust means. Cluster analysis was used as technique for grouping the RES site chronologies based on the similarity degree.

For identification of dendroclimatic signal correlation analysis between tree-ring widths and climatic factors was calculated on a 'dendroclimatic year' (from June of the previous growing season to August of the current growing season) (Cook & Kairiukstis 1990). Meteorological data (temperature and precipitation) from weather station Anzob Pass (3373 m a.s.l.) was used in the analysis.

The Pamir region seismicity was received for the period 1900-2014 from available on-line seismic catalogues (ANSS ComCat 2016, Storchak et al. 2013). The earthquakes, which were taken into account in this study, have occurred in a radius within c.200 km of the sampling place.

## Results and discussion

### *Perspectives: tree-ring chronology development*

The general descriptive statistics of eight developed tree-ring width chronologies along with their sample depths are shown in table 1 and figure 2. Data from two sites were already analysed and presented by Opała et al. 2017. The other six newly constructed chronologies allow for more comprehensive dendrochronological and dendroclimatological analysis for different altitudes. All chronologies exceed 200 years and the longest ones were developed for the highest locations (site 01, 02 and 03).

The oldest tree, found at the Kulikalon glacier site, is 1311 year old. However, this specimen is not included into the local chronology due to poor correlation with the respective master series. In addition to our recent findings, there is much greater potential for developing long-term tree-ring chronologies based on surrounding trees and other sites, which will be the subject of further study during the next Pamir expedition. Preliminary studies also indicated a great potential of historical wood from this region. Dating of wood samples revealed that historical wood comes from different time periods (Fig. 2). These materials are especially important for the development of millennial

chronologies. Part of timber samples were dated back to the period of 11<sup>th</sup>-13<sup>th</sup> centuries, thus it will be possible to improve the statistical properties of the early part of the living trees' regional chronology.

*Table 1: Characteristics of juniper tree-ring chronologies from eight sites in the Pamir-Alay Mountains, Tajikistan. TRW = tree ring width*

Code	Name	Elevation (m a.s.l.)	No of cores*	Span (length)	Mean segment length	Correlation with master chronology	Mean TRW
01	Kulikalon timberline	3000	17	1005-2014 (1010)	428	.517	0.33
02	Kulikalon glacier	2900	15	1117-2015 (899)	610	.493	0.29
03	Kulikalon plateau	2800	20	900-2014 (1115)	583	.485	0.29
04	Kulikuczurak	2550	17	1597-2014 (418)	205	.560	0.66
05	Isputa	2500	15	1770-2014 (245)	134	.549	1.01
06	Base camp	2300	20	1796-2014 (218)	124	.536	0.98
07	Iguroz	2250	20	1795-2014 (219)	103	.598	1.47
08	Archa Maydan	2200	15	1345-2015 (670)	418	.520	0.49

\*Number of cores which were included to the site chronology

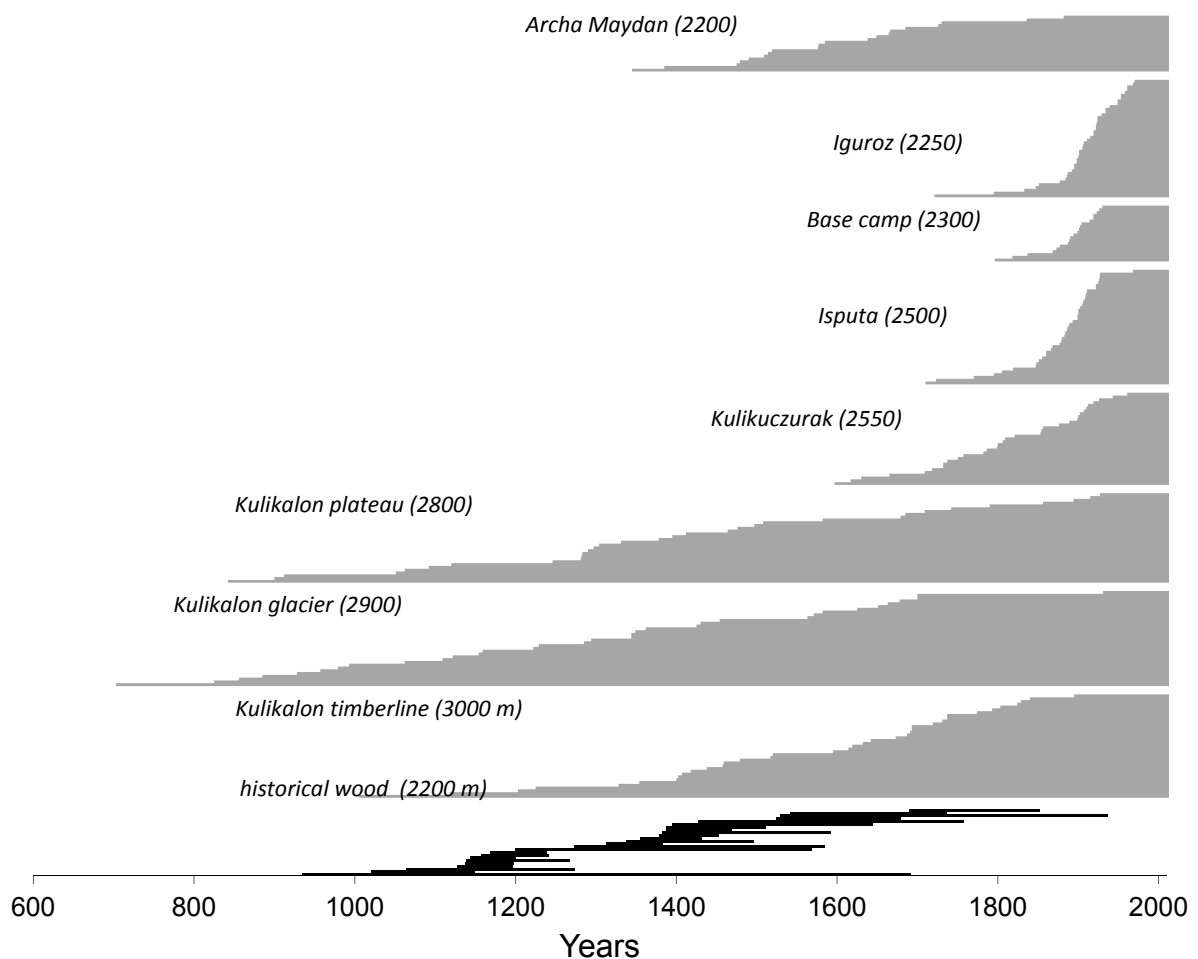


*Figure 2: Bar graph showing the time spans covered by the individual measurement series ordered by sites.*

Cluster analysis of chronologies using the growth index as variables showed the degree of similarity among site chronologies (Fig. 3). The chronologies of trees from the highest located sites (Kulikalon 01, 02 and 03) were the most similar to each other. Also the similarity between

chronologies from sites: Iguroz, Base Camp, and Kulikuczurak was relatively high. The chronologies from Isputa and Archa Maydan sites were least similar to chronologies from the remaining sites.

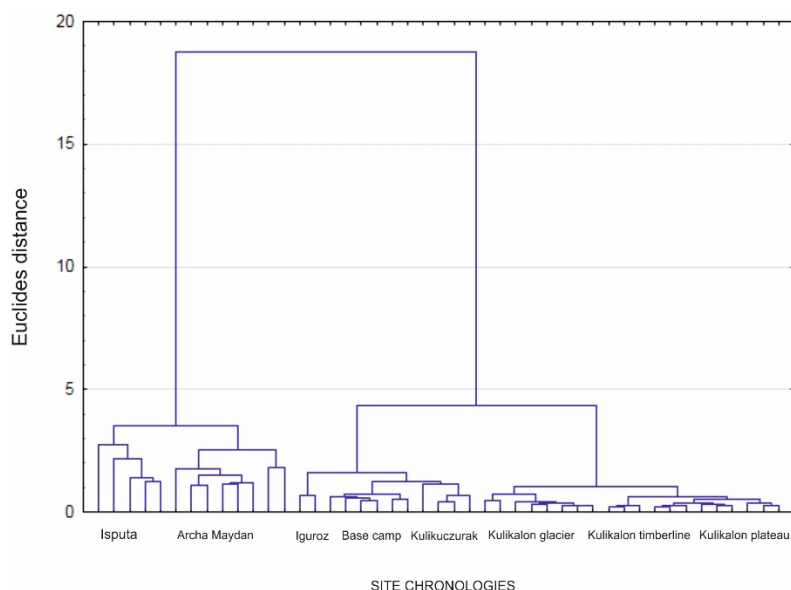


Figure 3: Hierarchical clustering dendrogram of tree-ring chronologies from eight sampling sites over the common period 1900-2014.

#### *Perspectives: climatic signals*

In general, trees from the Pamir-Alay did not contain a strong temperature signal, however tree rings from site 02 revealed significant correlations with June and July-August temperatures. In most months the correlations to temperatures were not statistically significant (Tab. 2). The ring-width chronologies were generally positively correlated to winter precipitation and cold month temperatures, especially at the highest elevations (Tab. 3). Very strong correlations were observed between DJF temperatures and the Kulikalon plateau tree-ring width chronology ( $r=0.78$ ). Hence, moisture availability is the major determinant of tree growth, while temperature plays an indirect role in tree growth by modulating the soil moisture via snowmelt and evaporation (Opala et al. 2017). At the lower locations, summer precipitation and summer temperature seem to be the most important factors determining ring formation. The effect of temperature is inverse, indicating drought stress as growth-limiting factor, since high temperatures during June and July can cause soil moisture deficit. At all sites, significant positive relationships were observed with annual precipitation.

Table 2: Correlation coefficients between site tree-ring-width chronologies and the mean temperature from previous June to current August and for different seasons during period 1946-1993. Bold indicate values at the 95% confidence level.

Site	pJun	pJul	pAug	pSep	pOct	pNov	pDec	Jan	Feb	Mar	Apr	May	Jun	Jul	Aug	DJF	pJ-Aug
01	0,22	-0,06	0,20	-0,22	-0,06	<b>0,41</b>	-0,11	-0,24	-0,13	0,24	0,07	0,05	<b>0,35</b>	0,07	0,13	0,12	0,18
02	0,17	0,01	0,20	-0,14	0,06	<b>0,40</b>	-0,12	-0,16	-0,13	-0,01	0,13	0,25	0,25	<b>0,38</b>	<b>0,32</b>	<b>0,42</b>	<b>0,43</b>
03	0,25	0,29	0,20	0,07	0,06	<b>0,32</b>	<b>0,34</b>	0,06	-0,17	0,08	0,02	0,14	0,20	0,17	0,15	0,20	0,23
04	0,24	-0,21	-0,03	<b>-0,45</b>	0,09	0,02	<b>0,35</b>	-0,13	-0,05	-0,16	0,12	0,22	0,27	-0,08	0,19	0,06	0,20
05	0,03	-0,10	0,07	-0,07	-0,02	-0,03	<b>0,34</b>	0,09	0,21	-0,06	0,00	0,17	-0,01	0,05	0,17	0,13	0,14
06	-0,08	-0,27	-0,10	-0,12	0,06	<b>-0,32</b>	<b>0,41</b>	-0,05	-0,03	0,14	-0,01	-0,08	-0,16	<b>-0,30</b>	0,06	-0,15	-0,17
07	0,10	-0,18	-0,10	-0,19	-0,02	-0,19	<b>0,47</b>	0,10	0,01	-0,03	-0,13	-0,19	<b>-0,30</b>	<b>-0,34</b>	-0,05	-0,28	-0,29
08	0,07	<b>-0,38</b>	-0,11	-0,05	0,05	0,11	<b>0,35</b>	-0,01	0,14	-0,06	-0,01	0,04	0,00	-0,12	-0,03	-0,10	-0,02

Table 3: Correlation coefficients between site tree-ring-width chronologies and the precipitation totals from previous June to current August and for different seasons during period 1946-1993. Bold indicate values at the 95% confidence level.

Site	pJun	pJul	pAug	pSep	pOct	pNov	pDec	Jan	Feb	Mar	Apr	May	Jun	Jul	Aug	DJF	pJ-Aug
01	0,03	0,23	0,02	<b>0,46</b>	<b>0,33</b>	<b>0,31</b>	<b>0,58</b>	<b>0,62</b>	<b>0,49</b>	<b>0,32</b>	0,22	0,22	0,05	0,10	-0,11	<b>0,71</b>	<b>0,62</b>
02	-0,02	0,09	0,00	0,20	0,11	0,21	<b>0,57</b>	<b>0,53</b>	<b>0,41</b>	<b>0,36</b>	-0,03	0,29	0,20	-0,12	-0,11	<b>0,63</b>	<b>0,45</b>
03	-0,09	0,09	0,08	<b>0,35</b>	0,20	<b>0,49</b>	<b>0,68</b>	<b>0,62</b>	<b>0,59</b>	<b>0,47</b>	0,28	<b>0,30</b>	0,07	0,04	0,02	<b>0,78</b>	<b>0,64</b>
04	0,05	0,14	-0,06	<b>0,50</b>	<b>0,36</b>	0,25	<b>0,45</b>	<b>0,41</b>	0,15	0,29	0,18	0,06	0,11	0,29	-0,07	<b>0,47</b>	<b>0,52</b>
05	<b>0,31</b>	0,05	-0,06	0,16	<b>0,30</b>	0,29	0,22	0,22	0,06	0,07	0,10	-0,06	0,19	0,16	-0,01	0,23	<b>0,33</b>
06	0,20	-0,10	-0,17	0,12	<b>0,33</b>	0,20	0,19	0,21	-0,08	0,11	0,26	0,10	<b>0,35</b>	<b>0,34</b>	0,07	0,15	<b>0,39</b>
07	0,14	-0,20	-0,13	0,19	0,20	0,20	0,13	0,22	0,05	0,05	0,29	0,10	<b>0,33</b>	<b>0,30</b>	0,06	0,18	<b>0,34</b>
08	<b>0,32</b>	0,13	-0,06	0,23	0,19	0,19	<b>0,31</b>	0,16	0,10	0,16	0,11	0,02	<b>0,31</b>	<b>0,31</b>	0,03	0,24	<b>0,39</b>

#### Limitations: earthquakes & mass movements

Seismic and neo-tectonics studies pointed out that the Pamir region moves northward *en-bloc* and collides with the Tien Shan, which is reflected by high seismicity along this frontal Pamir thrust system and the Main Alay thrust system (Schurr et al. 2014). Seismic shaking influenced growth anomalies in two of our study sites: Archa Maydan and Isputa. These perturbations occurred because the roots of the trees growing in the unstable area were disturbed by sliding and creeping during or shortly after the earthquake event (Owczarek et al. 2017). Hierarchical clustering dendrogram showed that these two sites are characterized by lower similarity to other sites. Also, climatic signals in the ring-width chronologies are weaker. Most of the analysed sequences showed periods of non-climatic reductions of growth and recovery within an individual tree-ring series during the 1900-2014 period (Fig. 4). However, the duration and intensity of these signals vary between individuals. These growth reductions can be recorded immediately after the earthquake or in the following year depending on the time of the event occurrence (before, during, or after the vegetation season). During the 20<sup>th</sup> century only few earthquake events that are well known from instrumental measurements could be identified in tree-ring data by growth suppressions, e.g.: 1923 and 1924 (of 6.5 M and 6.2 M), 1943 (6.3 M), 1949 (7.5 M), 1955 (5.7 M), and 1999 (5.2 M) (Owczarek et al. 2017). Assuming that the seismic events are an important factor influencing tree growth in unstable areas, and that such impact may mask climatic signal in the

tree-ring series, one must take such uncertainties into consideration when undertaking dendroclimatic reconstruction efforts.

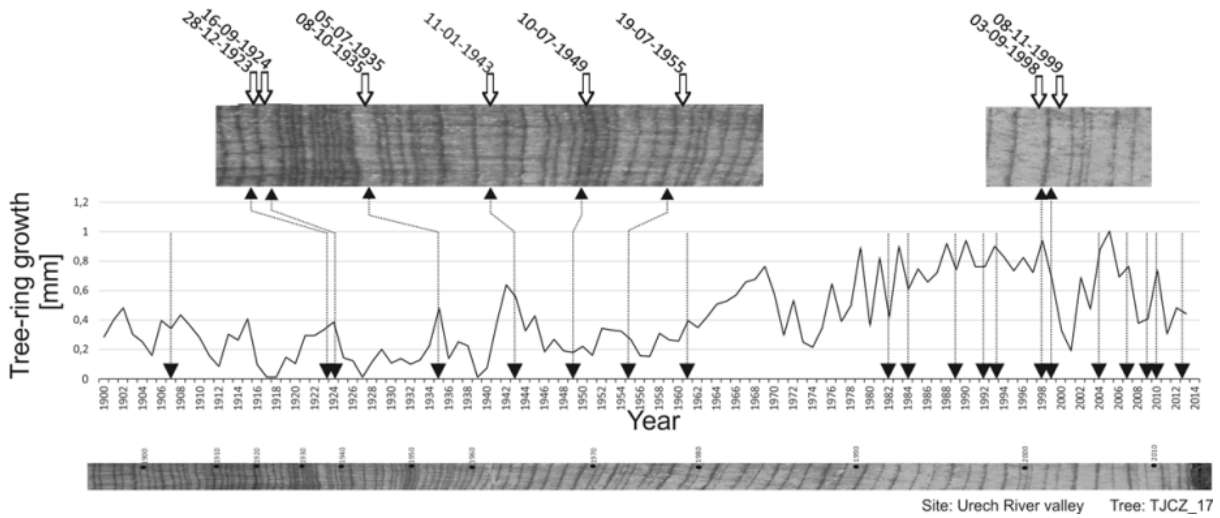


Figure 4: The impact of earthquakes found in an individual tree-ring sequence, visible as a growth suppression occurring in the year of the earthquake or in the first or second following years.

*Limitations: human impact*

Another limitation in the development of millennial-long chronologies is the impact of human activity. At the lower locations, close to the villages, the traces of wood harvesting like tree stumps or traces of cut branches can be found (Fig. 5 A). Obtaining pieces of living tree trunks with axes affect the course of the tree-ring sequences and cause inconsistencies of individual growth curves with the local tree-ring chronology. We found positive correlations between tree age and elevation (Fig. 5 B), indicating that the average tree age is increasing with elevation. This relationship is connected with timber harvesting in the vicinity of settlements, that lasts already for many centuries.

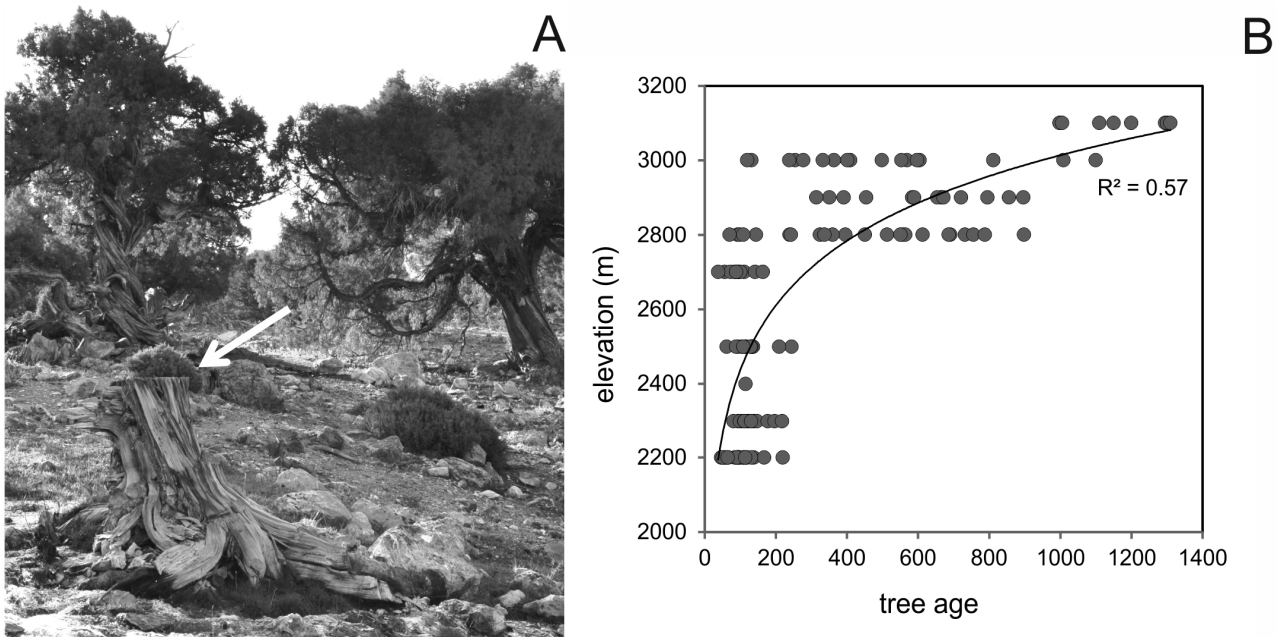


Figure 5: (A) Example of a snag resulting from wood harvesting, (B) Relation between the age of sampled juniper trees and altitude. The average tree age increased with altitude ( $R^2 = 0.57$ ).

## Conclusions

Our results demonstrated the great potential of Himalayan pencil juniper *Juniperus semiglobosa* ring-width data for developing multi centennial climate reconstructions for the Pamir-Alay region. The response of tree growth to climate shows that the collected material can serve as a valuable regional archive of past winter precipitation variations for the last 1000 years. Furthermore, the relict material can potentially improve the quality of the early part of these time series. Herein we also discuss the potential limitations for using juniper tree-ring width data from some sites. This is especially important for geologically unstable areas, where the possible impact of climate can be overshadowed by effects of earthquakes and mass movements on tree growth.

The newly developed proxy records can serve as important supplements for a regional tree-ring network in the Central Asia. Therefore, the tree-ring width data from our study will be available to the International Tree-Ring Data Bank for network analysis of pre-instrumental climate patterns in Central Asia. Future field campaigns in this region will enable the development of regional, dense networks of chronologies covering larger areas of the Pamir mountain system which are insufficiently investigated so far. The presented perspectives and limitations of dendroclimatological studies in Tajikistan indicate that it will be possible to bridge the research gap in the existing centuries long hydroclimatic reconstructions for Central Asia.

## Acknowledgements

This research was supported by the Polish National Science Centre (NCN) grant number 2013/09/B/ST10/00634.

## References

- Ahmed, M., Wahab, M., Khan, N., Zafar, M.U., Palmer, J., (2010): Tree-ring chronologies from upper Indus basin of Karakorum range, Pakistan. *Pakistan Journal of Botany* 42: 207–295.
- ANSS Comprehensive Earthquake Catalogue (ANSS ComCat), (2016): USGS Earthquake Hazards Program, online: <http://earthquake.usgs.gov/earthquakes/>
- Bräuning, A. (2001): Climate history of the Tibetan Plateau during the last 1000 years derived from a network of Juniper chronologies. *Dendrochronologia* 19 (1): 127-137.
- Cook, E.R., Kairiukstis, L.A. (1990): *Methods of Dendrochronology: Applications in the Environmental Science*. Kluwer Academic Publishers, Dordrecht, 1-394.
- Cook, E.R., Krusic, P.J., Jones, P.D. (2003): Dendroclimatic signals in long tree-ring chronologies from the Himalayas of Nepal. *International Journal of Climatology* 23(7): 707-732.
- Esper, J., Krusic, P.J., Ljungqvist, F.C., Luterbacher, J., Carrer, M., Cook, E., Davi, N.K., Hartl-Meier, C., Kirilyanov, A., Konter, O., Myglan, V., Timonen, M., Treydte, K., Trouet V., Villalba, R., Yang, B., Büntgen, U. (2016): Ranking of tree-ring based temperature reconstructions of the past millennium, *Quaternary Science Reviews* 145: 134-151.
- Esper, J., Schweingruber, F.H., Winiger, M. (2002): 1300 years of climatic history for Western Central Asia inferred from tree-ring. *Holocene* 12 (3): 267–277.
- Gou, X.H., Deng, Y., Chen, F.H. Yang, M., Gao, L., Nesje, A., Fang, K. (2014): Precipitation variations and possible forcing factors on the Northeastern Tibetan Plateau during the last millennium. *Quaternary Research* 81: 508–512.
- Jones, P.D., Briffa, K.R., Osborn, T.J., Lough, J.M., van Ommen, T.D., Vinther, B.M., Luterbacher, J., Wahl, E.R., Zwiars, F.W., Mann, M.E., Schmidt, G.A., Ammann, C.M., Buckley, B.M., Cobb, K.M., Esper, J., Goosse, H., Graham, N., Jansen, E., Kiefer, T., Kull, C., Küttel, M., Mosley-Thompson, E., Overpeck, J.T., Riedwy, N., Schulz, IM., Tudhope, A.W., Villalba, R., Wanner, H., Wolff, E., Xoplaki, E. (2009): High-resolution palaeoclimatology of the last millennium: a review of current status and future prospects. *The Holocene* 19(1): 3-49.

- Krusic, P.J., Cook, E.R., Dukpa, D., Putnam, A.E., Rupper, S., Schaefer, J. (2015): Six hundred thirty-eight years of summer temperature variability over the Bhutanese Himalaya. *Geophysical Research Letters* 42: 2988–2994.
- Levanič, T. (2007): ATRICS - A new system for image acquisition in dendrochronology. *Tree-Ring Research* 63 (2): 117–122.
- Opała, M., Niedźwiedź, T., Rahmonov, O. (2013): Dendrochronological potential of *Ephedra equisetina* from Zaravshan Mountains (Tajikistan) in climate change studies. *Contemporary Trends in Geoscience* 2: 48-52.
- Opała M., Niedźwiedź, T., Rahmonov, O., Małarzewski Ł., Owczarek, P. (2016): Dendroclimatic studies of *Juniperus* sp. along high elevation transect in the Pamir-Alay Mountains, Tajikistan. In: Villalba, R., Juñent, F.R. (eds.), AmeriDendro 2016 - Program & Abstracts, Mendoza, Argentina: 41.
- Opała, M., Niedźwiedź, T., Rahmonov, O., Owczarek, P., Małarzewski, Ł. (2017): Towards improving the Central Asian dendrochronological network - new data from Tajikistan, Pamir-Alay. *Dendrochronologia* 41: 10-23.
- Owczarek, P., Opała-Owczarek, M., Rahmonov, O., Mendecki, M. (2017): 100 years of earthquakes in the Pamir region as recorded in juniper wood: a case study of Tajikistan, *Journal of Asian Earth Sciences* 138: 173-185.
- Rahmonov, O., Niedźwiedź, T., Opała, M., Małarzewski, Ł., Owczarek, P. (2016): Landscape degradation and its effect on the soil-vegetation relations within juniper forest in the Fann mountains (western Pamir-Alay). In: Halada, L., Bača, A., Boltížiar, M. (eds). Landscape and Landscape Ecology. Proceedings of the 17th International Symposium on Landscape Ecology, 27-29 May 2015, Nitra, Slovakia, Slovak Academy of Sciences, Bratislava, 168-175.
- Schurr, B., Ratschbacher, L., Sippl, Ch., Gloaguen, R., Yuan, X., Mechie, J. (2014): Seismotectonics of the Pamir. *Tectonics* 33: 1501-1518.
- Seim, A., Tulyaganov, T., Omurova, G., Nikolyai, L., Botman, E., Linderholm, H.W. (2016): Dendroclimatological potential of three juniper species from the Turkestan range, northwestern Pamir-Alay Mountains, Uzbekistan. *Trees* 30 (3): 733–748.
- Stokes, M.A., Smiley, T.L. (1996): An Introduction to Tree-Ring Dating. University of Chicago, Chicago: 1–73.
- Storchak, D.A., Di Giacomo, D., Bondár, I., Engdahl, E.R., Harris, J., Lee W.H.K., Villaseñor, A., Bormann, P. (2013): Public Release of the ISC-GEM Global Instrumental Earthquake Catalogue (1900-2009). *Seismological Research Letters* 84: 810-815.
- WinDENDRO (2006): Manual. Regent Instrument INC, Quebec, Canada.
- Yadav, R.R., Braeuning, A., Singh J. (2011): Tree ring inferred summer temperature variations over the last millennium in western Himalaya, India. *Climate Dynamics* 36: 1545–1554.

# Spring season (March-May) precipitation signal of *Ephedra intermedia* (a perennial shrub) in the Trans-Himalayan dry valley (central Himalaya)

A. Tiwari<sup>1,2,3</sup>, F. Ze-Xin<sup>1</sup> & Z. Zhe-Kun<sup>1</sup>

<sup>1</sup> Key Laboratory of Tropical Forest Ecology, Xishuangbanna Tropical Botanical Garden, Chinese Academy of Sciences, Yunnan 666303, China

<sup>2</sup> University of Chinese Academy of Sciences, Beijing 100049, China

<sup>3</sup> Tri-Chandra Campus, Tribhuvan University, Ghantaghar, Kathmandu, Nepal  
E-mail: zhouzk@xtbg.ac.cn

## Introduction

Dendrochronological studies on shrubs and dwarf shrubs often provide more significant ecological implications compared to trees, because the former are also found in treeless extreme environments where trees cannot survive (Woodcock and Bradley 1994; Schweingruber and Dietz 2001; Forbes et al. 2010; Hallinger et al. 2010; Liang et al. 2012; Camarero et al. 2013). Such studies have broadened the scope of dendroclimatology beyond traditional dendrochronological research limited to trees. Hence there has been a growing interest for studies on climate-growth relationship of shrubs and dwarf shrubs in the recent years, particularly from the vegetation boundaries with treeless plant communities (Schmidt et al. 2006, Au and Tardif 2007, Xiao et al., 2007, Sass-Klaassen et al. 2008, Owczarek et al. 2013; Forbes et al. 2010; Hallinger et al. 2010; Liang et al. 2012; Camarero et al. 2013; Schweingruber et al. 2013; Zimowski et al. 2014; Opała and Niedźwiedź, 2014). Most of the studies are confined to arctic or subarctic shrub species. Despite some challenges related to shrub dendrochronology (e.g. sample preparation, highly fluctuating annual growth frequency, difficulty in cross-dating and limited age), shrubs and dwarf shrubs are reliable ecological indicators of climate change.

*Ephedra intermedia* is a perennial shrub (up to 1m height) commonly found at elevational range of 800-4600 m a.s.l., growing in grasslands, deserts, river valleys, flood plains, sandy beaches, cliffs and other dry, sandy or rocky places in arid areas (Ali and Qaiser 1987; Flora of China 1999; Fu et al. 2010). *E. intermedia* is reported from Afghanistan, China, India, Iran, Islamic Republic of; Kazakhstan; Kyrgyzstan; Mongolia; Nepal; Pakistan; Russian Federation, Tajikistan, Turkmenistan, Uzbekistan (Bell & Bachman 2011). It is usually associated with *Juniperus* and *Berberis*. Dendrochronological studies of the genus are very limited (Earl 2013; Opała and Niedźwiedź 2014). In this study we attempted to analyse the climate sensitivity of its growth patterns. Recent studies indicated that shrubs (e.g., *Hippophae rhamnoides*, *Juniperus pingii* var. *wilsonii* and *Rhododendron* spp., *Cassiope fastigiata*) recorded climatic signal in their growth rings similarly to timberline trees (Xiao et al. 2007; Liang and Eckstein 2009; Liang et al. 2009; Liang et al. 2012; Li et al. 2013; Liang et al. 2014).

## Materials and methods

### Study area

We carried out the study at Tukuche (28.70° N, 83.6° E, 2650 m a.s.l.) of Mustang district in the Trans-Himalayan zone of central Nepal (Fig 1a). Trans-Himalayan zone of central Nepal is located in the rain shadow of surrounding high mountains. Snow thaw is the main source of water for vegetation mainly during spring season (Aryal et al. 2012). The northern part of the Mustang lies in the Trans-Himalayan semi-arid dry zone, with the Tibetan-type highland being the driest zone of Nepal (Lomanthang: 200 mm annual rainfall) (Stainton 1972; Schickhoff 2005). The study site is located on the south-west slope of Kali Gandaki valley, representing semi-arid dry valley of

Tukuche as the transition zone between relatively moist western area of Kali Gandaki River and the eastern Tibetan-type semi-arid zone with low precipitation (Schikhoff 2005; Miede et al. 2015). The sites where samples were collected are located on a dry and rocky slope with very shallow soil depth (Fig. 1c). A meteorological station is located nearby (< 4 km) (Thakmarpha; 28.75° N, 83.7° E, 2566 m a.s.l.), with mean annual precipitation of 393 mm and mean annual temperature of 11.17 °C (1970-2013) (Fig. 1e).

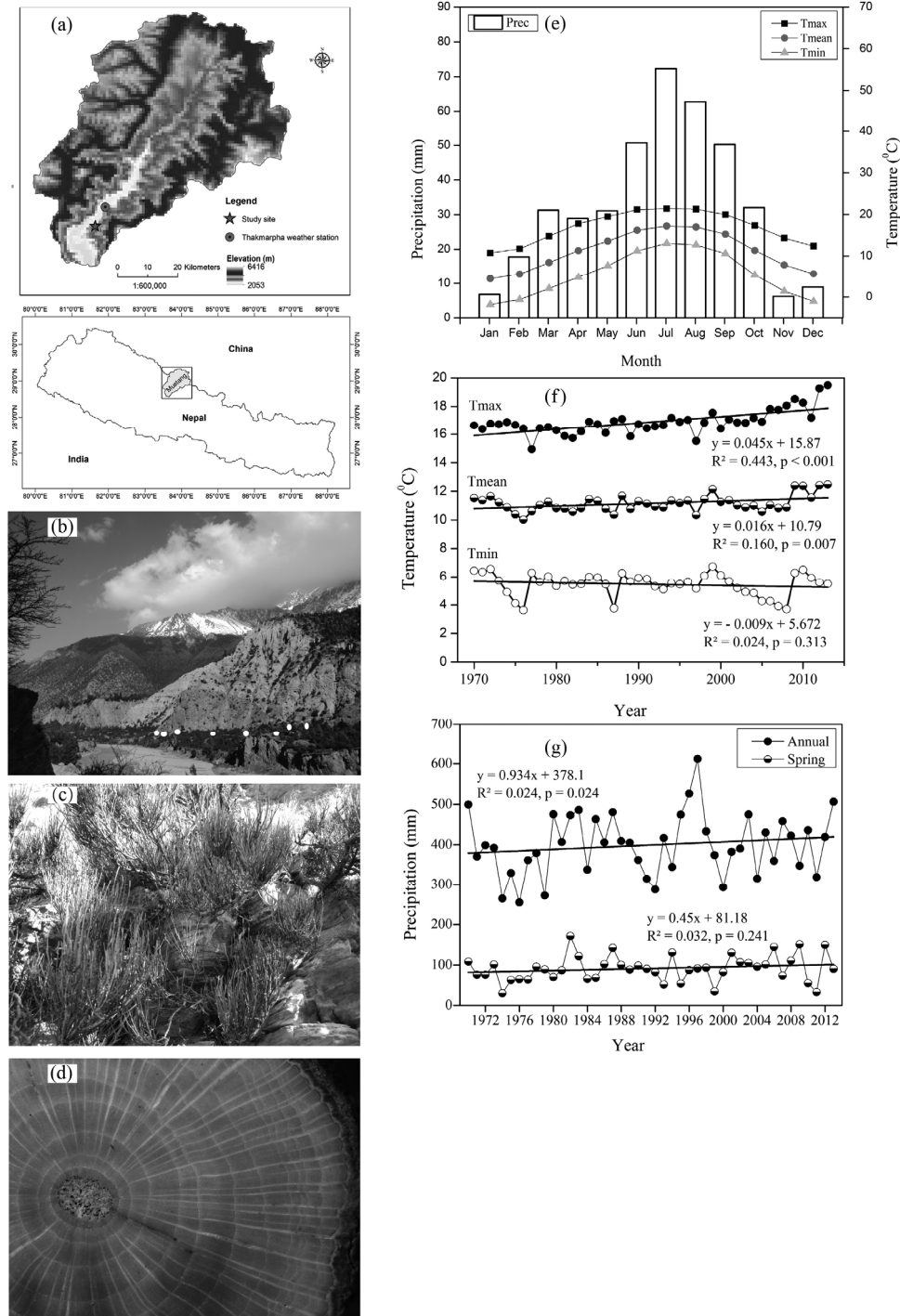


Fig. 1 Map of study area at Tukuche Mustang (a); sample collection points at the study site (b); *Ephedra intermedia* in the natural habitat (c); transverse section of *E. intermedia* disc after sanding (d); climate summary of Thakmarpha climate station (28.75° N, 83.7° E, 2566 m a.s.l.) (e); annual temperature trend of Thakmarpha (Mustang); maximum temperature (Tmax), mean temperature (Tmean) and minimum temperature (Tmin) (f); total annual precipitation and total spring season (March-May) precipitation trend for Thakmarpha (g).

### *Ring width measurement and crossdating*

From each individual shrub we collected single stem disc (basal). Stem discs were air dried, mounted on sample holders and sanded using progressively finer sandpaper according to standard methods (Fritts 1976). Ring widths were measured at a resolution of 0.01 mm with a LINTAB II measuring system (Rinntech, Germany). We adopted visual inspection for cross-dating the annual growth frequency (Stokes and Smiley 1968) with statistical tests (sign-test and *t*-test) using the software package TSAP-Win (Rinn 2003). Ring-width measurements were detrended with negative exponential curve using ARSTAN software (Cook 1985), and were used to explore climate-growth relationship.

### *Analysis of the climate-growth relationship*

The standard ring-width indices were correlated with monthly climatic variables (total precipitation, mean air temperature) from June of the previous growth year until October of the current growth year (Fritts 1976). Next, spring season (March-May) climate sensitivity was studied, given the previously identified sensitivity of tree in the region to spring moisture conditions (Kharal et al. 2014; Tiwari et al. 2016).

## **Results and discussion**

### *Climatic trend*

Southern part of Mustang (Thakmarpha) in Trans-Himalayan zone showed significant warming with a consistent increase of mean and maximum annual temperature during recent decades but without any significant trend in minimum temperatures (Fig. 1f). The region showed statistically no significant trend of annual, summer (June-September) and spring season (March-May) precipitation (Fig. 1g). Thakmarpha region is getting warmer and drier in the recent decades as indicated by co-occurring of warmer days and almost stable precipitation trend in the region. Further increasing of temperature in the semi-arid zone in the future (IPCC, 2013) may worsen the water stress to plants in the region.

### *Growth climate response*

We established standard ring-width chronology of 52 years using 26 stem radii from 13 stem discs. The mean growth rate of *Ephedra intermedia* from Thakmarpha was 0.19 mm per year (0.01-0.42±0.09 mm) which is lower than that of shrub samples from Tajikistan (Opala and Niedźwiedz 2014) and the growth of *Rhododendron* species (0.36 mm per year) from the Tibet (Liang and Eckstein 2009), and much wider than subarctic and arctic dwarf shrubs (0.01 mm – 0.1 mm per year) (Au and Tardif 2007; Owczarek 2009; Owczarek et al. 2013).

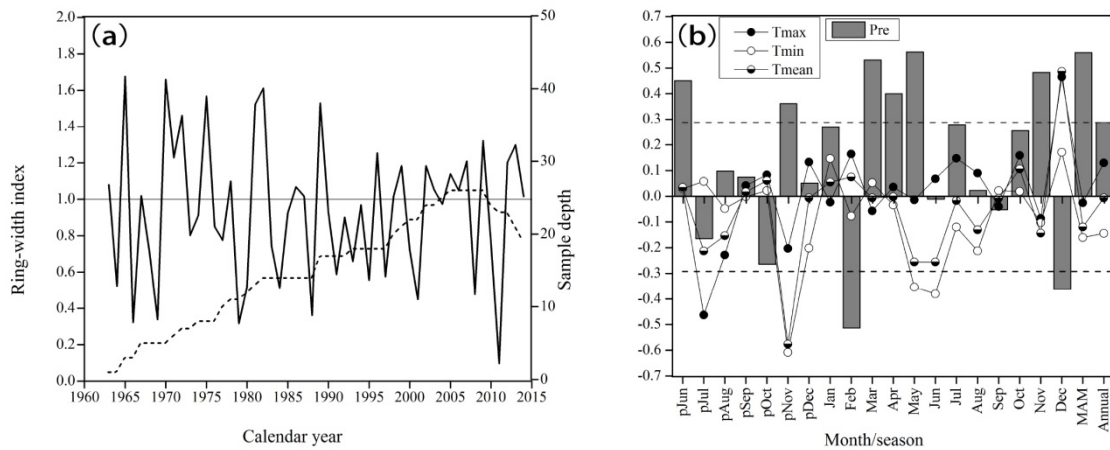


Fig. 2 Tree ring-width standard chronology of *E. intermedia* (a); Correlation coefficients between standard ring-width series and total monthly maximum (Tmax), mean (Tmean) and minimum temperature (Tmin) and total monthly precipitation of June in the previous year to December of the current year, spring season and annual climate, dashed horizontal lines indicate significant correlation at 95% confidence limit for a two-tailed test (b).

The constructed chronology spans the years 1950-2012. The mean correlation of analysed raw ring widths with the master series is 0.49, which represents the correlation between the shrubs and the strength of the common signal among the series. The relatively higher mean sensitivity was 0.581 (MS) and standard deviation 0.386 (SD), indicated greater climatic influence on growth (Cook and Kairiukstis 1990).

Table 1: Tree-ring chronology summary statistics.

Location	Elevation m asl	Chronology	Radii (stem disc)	Mean sensitivity	EPS	All series Rbar	1 <sup>st</sup> order AC
Tukucho	2550	52 years	26 (13)	0.581	0.624	0.250	0.062

(EPS: Expressed population signal; average over the full chronology length, AC: Autocorrelation)

The annual ring-width indices (radial growth) of *E. intermedia* showed a significant positive relationship with monthly precipitation during previous year's June ( $r = 0.45$ ,  $p < 0.05$ ), current year's March ( $r = 0.53$ ), April ( $r = 0.4$ ) May ( $r = 0.56$ ), November ( $r = 0.48$ ) and spring season (March-May) ( $r = 0.56$ ). However, the radial growth showed significant negative relation with the precipitation of February ( $r = -0.51$ ) and December ( $r = -0.36$ ) of the current growth year. The radial growth indicated significant negative correlation with Tmax of July of previous year ( $r = -0.47$ ), and positive correlation of December of current year ( $r = 0.45$ ), significant negative correlation ( $r = -0.58$ ) with November of previous year, and significant positive correlation ( $r = 0.47$ ) with December of the current year with the mean temperature (Tmean). However the minimum temperature (Tmin) showed significant negative correlation with previous year's November ( $r = -0.61$ ), current year's May ( $r = -0.36$ ) and June ( $r = -0.39$ ).

These results are in agreement with the previous finding of spring season (March-May) moisture sensitivity of *Abies spectabilis* from the nearby regions of the Trans-Himalaya of central Nepal (Kharal et al. 2014; Tiwari et al. 2016). However, we did not observe strong explainable influence of temperature on the radial growth of *E. intermedia*, which was observed as to have negative influence on the radial growth during the spring season (March-May) for both conifers (Kharal et al. 2014; Tiwari et al. 2016; Gaire et al. 2014) and broadleaved trees in the central Himalaya (Dawai et al. 2013; Liang et al. 2014; Gaire et al. 2016). It was also projected that the heat induced water deficit associated with high velocity of wind and increased evapotranspiration limit tree growth

(Fritts 1976; Cook et al. 2003; Gaire et al. 2014) and such water stress could pose productivity decline and growth reduction.

We infer that for *E. intermedia*, the highly reduced leaves in the form of needle and the relatively strong xerophytic characters (thick cuticle) might minimize the effect of transpiration and also decrease the influence of temperature on the radial growth. Contrary to our findings, the strong temperature sensitivity was found for *Ephedra equisetina* from Tajikistan (Opała and Niedźwiedź 2014), suggesting that the morphological and anatomical differences of root, leaf and stem should also be considered while interpreting climate-growth relationship of shrubs.

## Conclusion

This analysis provides an additional evidence of the usefulness of *Ephedra intermedia* for dendrochronological research. The spring season (March-May) precipitation was found to be critical for annual radial growth of *E. intermedia*, which is consistent with the tree radial growth response in the study area. This confirms that shrubs and dwarf shrubs could effectively record climate signal and that they could be reliable for exploring climate-growth relationships at the vegetation boundaries, devoid of trees. Further studies with more samples from different climatic conditions are required to better understand climate sensitivity and growth patterns of this shrub.

## Acknowledgements

We acknowledge Department of National Parks and Wildlife Reserve Government of Nepal and the Annapurna Conservation Area Project (ACAP, Nepal) for providing permission to carry out the field work.

## References

- Ali, S.I., Qaiser, M. (eds.) (1987): Flora of Pakistan. <http://www.efloras.org> (online since 2001).
- Aryal, A., Hipkins, J., Ji, W., Raubeinhimer, D., Brunton, D. (2012): Distribution and diet of brown bear in Annapurna Conservation Area, Nepal. *Ursus*. 23:231–236.
- Au, R., Tardif, J.C. (2007): Allometric relationships and dendroecology of the dwarf shrub *Dryas integrifolia* near Churchill, subarctic Manitoba. *Canadian Journal of Botany* 85, 585–597.
- Bell, A., Bachman, S. (2011): *Ephedra intermedia*. The IUCN Red List of Threatened Species 2011: e.T201664A9159437. <http://dx.doi.org/10.2305/IUCN.UK.2011.2.RLTS.T201664A9159437.en>.
- Camarero, J.J., Palacio, S., Montserrat-Marti, G. (2013): Contrasting seasonal overlaps between primary and secondary growth are linked to wood anatomy in Mediterranean sub-shrubs. *Plant Biology* 15:798–807.
- Cook, E.R. (1985): A time-series analysis approach to tree-ring standardization. Ph.D. Dissertation. The University of Arizona Press, Tucson.
- Cook, E.R., Kairiukstis, A. (1990): Methods of Dendrochronology: Applications in the Environmental Sciences. Kluwer Academic Press, Dordrecht.
- Cook, E.R., Krusic, P.J., Jones, P.D. (2003): Dendroclimatic signals in long tree-ring chronologies from the Himalayas of Nepal. *International Journal of Climatology* 23, 707e732.
- Dawadi, B., Liang, E., Tian, L., Devkota, L.P., Yao, T. (2013): Pre-monsoon precipitation signal in tree rings of timberline *Betula utilis* in the central Himalayas. *Quaternary International* 283:72–77. doi: 10.1016/j.quaint.2012.05.039.
- Earl, J.C. (ed.) (2013) The Gymnosperm Database <http://www.conifers.org/ep/Ephedraceae.php>.
- Flora of China [Internet]. *Ephedra przewalskii*, *Ephedra intermedia*. 1999 [cited 2016 Jun 3]. Available from: <http://foc.eflora.cn/volume.aspx?num=4>.
- Forbes, B.C., Fauria, M.M., Zetterberg, P. (2010): Russian Arctic warming and ‘greening’ is closely tracked by tundra shrub willows. *Global Change Biology* 16:1542–1554.

- Fritts, H.C., 1976. (Reprint, 2001) Tree rings and climate, Caldwell, New Jersey: The Blackburn Press.
- Fu, L., Yu, Y., Riedl, H. (1999): Ephedraceae. In Wu Zheng-yi and Peter H. Raven (eds.). *Flora of China, Volume 4*. Beijing: Science Press; St. Louis: Missouri Botanical Garden.
- Gaire, N.P., Koirala, M., Bhujju, D.R., Carrer, M. (2016): Site- and species-specific treeline responses to climatic variability in eastern Nepal Himalaya. *Dendrochronologia* 1–13. doi:10.1016/j.dendro.2016.03.001.
- Hallinger, M., Manthey, M., Wilmking, M. (2010): Establishing a missing link: warm summers and winter snow cover promote shrub expansion into alpine tundra in Scandinavia. *New Phytologist* 186:890–899.
- Kharal, D.K., Meilby, H., Rayamajhi, S., Bhujju, D., Thapa, U.K. (2014): Tree ring variability and climate response of *Abies spectabilis* along an elevation gradient in Mustang, Nepal. *Banko Janakari* 24, 3–13.
- Liang, E.Y., Eckstein, D. (2009) Dendrochronological potential of the alpine shrub *Rhododendron nivale* on the south-eastern Tibetan Plateau. *Annals of Botany* 104, 665–670.
- Liang, E., Shao, X., Xu, Y. (2009): Tree-ring evidence of recent abnormal warming on the southeast Tibetan Plateau. *Theor Appl Climatol* 98:9–18.
- Liang, E.Y., Lu, X., Ren, P., Li, X., Zhu, L., Eckstein, D. (2012): Annual increments of juniper dwarf shrubs above the tree line on the central Tibetan Plateau: a useful climatic proxy, *Annals of Botany* 109: 721–728.
- Liang, E., Dawadi, B., Pederson, N., Eckstein, D. (2014): Is the growth of birch at the upper timberline in the Himalayas limited by moisture or by temperature? *Ecology* 95, 140307191613003. doi:10.1890/13-1904.1.
- Li, Z., Liu, G., Fu, B., Zhang, Q., Ma, K., Pederson, N. (2013): The growth ring variations of alpine shrub *Rhododendron przewalskii* reflect regional climate signals in the alpine environment of Miyaluo Town in Western Sichuan Province, China. *Acta Ecologica Sinica* 33:23–31.
- Miehe, S., Miehe, G., Böhner, J., Bäumler, R., Ghimire, S.K., Bhattarai, K., Chaudhary, R.P., Subedi, M. (2015): 16. Vegetation Ecology.
- Opala, M., Niedźwiedz, T. (2014): Dendrochronological potential of *Ephedra equisetina* from Zaravshan Mountains ( Tajikistan ) in climate change studies 48–52. doi:10.2478/ctg-2014-0007.
- Owczarek, P. (2009) Dendrogeomorphological potential of Salicaceae from SW Spitsbergen, Svalbard. (In:) Kaczka, R., Malik, I., Owczarek, P., Gartner, H., Helle, G. & Heinrich, I. (eds.): TRACE –Tree Rings in Archaeology, Climatology and Ecology, Vol. 7. GFZ Potsdam. – Sci. Tech. Rep. STR 09/03, 181–186.
- Owczarek, P., Latocha, A., Wistuba, M., Malik, I. (2013): Reconstruction of modern debris flow activity in the arctic environment with the use of dwarf shrubs (south-western Spitsbergen) – a new dendrochronological approach, *Zeitschrift für Geomorphologie* Vol. 57 (2013), Suppl. 3, 075-095.
- Rinn, F. (2003): TSAP-Win: Time Series Analysis and Presentation for Dendrochronology and Related Applications. Version 0.55 User reference. Heidelberg, Germany (<http://www.rimatech.com>).
- Sass-Klaassen, U., Couralet, C., Sahle, Y., Sterck, F.J. (2008) Juniper from Ethiopia contains a large-scale precipitation signal. *International Journal of Plant Sciences* 169, 1057–1065.
- Schmidt, N.M., Baittinger, C., Forchhammer, M.C. (2006) Reconstructing century-long snow regimes using estimates of high arctic *Salix arctica* radial growth. *Arctic, Antarctic, and Alpine Research* 38: 257–262.
- Schweingruber, F.H., Dietz, H. (2001) Annual rings in the xylem of dwarf shrubs and perennial dicotyledonous herbs. *Dendrochronologia* 19:115–126.

- Schweingruber, F.H., Hellmann, L., Tegel, W., Braun, S., Nievergelt, D., Büntgen, U. (2013): Evaluating the wood anatomical and dendroecological potential of Arctic dwarf shrubs. *IAWA J* 34:485–497.
- Stainton, J.D.A. (1972): *Forests of Nepal*. New York.
- Stokes, M.A., Smiley, T.L. (1968): *An Introduction to Tree-Ring Dating*. The University of Chicago Press, Chicago. 63 p.
- Woodcock, H., Bradley, R.S. (1994) *Salix arctica* (Pall.): its potential for dendroclimatological studies in the High Arctic. *Dendrochronologia* 12:11–22.
- Schickhoff, U. (2005): The upper timberline in the Himalayas, Hindu Kush and Karakorum: a review of geographical and ecological aspects, in: *Mountain ecosystems: studies in treeline ecology*, edited by: Broll, G. and Keplin, B., Springer, Berlin, Germany, 275–354.
- Tiwari, A., Fan, Z.-X., Jump, A.S., Li, S.-F., Zhou, Z.-K. (2016): Gradual expansion of moisture sensitive *Abies spectabilis* forest in the Trans-Himalayan zone of central Nepal associated with climate change. *Dendrochronologia* 1–10. doi:10.1016/j.dendro.2016.01.006.
- Xiao, S., Xiao, H., Kobayashi, O., Liu, P. (2007): Dendroclimatological investigations of sea buckthorn (*Hippophae rhamnoides*) and reconstruction of the equilibrium line altitude of the July First Glacier in the Western Qilian mountains, northwestern China. *Tree-Ring Res* 63:15–26.
- Zimowski, M., Leuschner, H.H., Gärtner, H., Bergmeier, E. (2014): Age and diversity of Mediterranean dwarf shrublands: a dendrochronological approach along an altitudinal gradient on Crete. *Journal of Vegetation Science* 25:122–134.

# Site-specific temperature response to seven major volcanic eruptions over the last millennium

C. Hartl-Meier<sup>1</sup>, L. Schneider<sup>2</sup> & J. Esper<sup>1</sup>

<sup>1</sup> Department of Geography, Johannes Gutenberg-University, Mainz, Germany

<sup>2</sup> Department of Geography, Justus Liebig University, Gießen, Germany

E-mail: c.hartl-meier@geo.uni-mainz.de

## Introduction

Volcanic eruptions have major impact on our climate system. Through the injection of aerosols in the atmosphere, incoming solar radiation is scattered, resulting in a cooling of the earth's surface (Robock 2000). Climate model simulations for the past millennium implement ice core based volcanic forcing records (e.g. Crowley & Unterman 2013, Gao et al. 2008) to evaluate the cooling effect of volcanic eruptions (Schmidt et al. 2011). Even though a new ice-core based record was established by Sigl et al. (2015), there are still uncertainties regarding the timing and intensity of volcanic events and the subsequent temperature response. To illuminate discrepancies between volcanic forcing and reconstructed temperatures Schneider et al. (in prep.) established a new volcanic event history over the last millennium by detecting major eruptions in tree-ring derived hemispheric scale temperature reconstructions. However, volcanically induced temperature responses are more pronounced in high compared to mid latitudes (Esper et al. 2015), can also vary on local scale and are dependent on the event itself (Briffa et al. 1998). Knowledge about the spatial effects of specific eruptions is thus important for the implementation of volcanic forcing records into atmospheric circulation models, which simulate past climate but also project future climate conditions.

Here we analyse the site-specific temperature response to seven major volcanic events over the last millennium by using all millennium length temperature reconstructions of the Northern Hemisphere (Fig. 1) and test the dependence of cooling to geographical location.

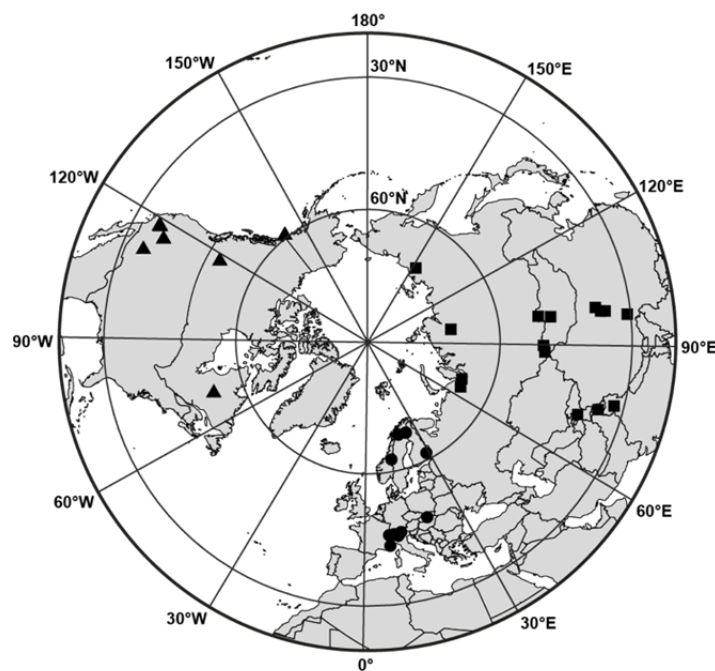


Figure 1: Location of the 36 millennium-length tree-ring based temperature reconstructions used in this study including 13 records in Europe (points), 15 in Asia (squares), and 8 in North America (triangles).

## Material and Methods

### *Tree-ring based temperature reconstructions*

We use all 36 existing tree-ring based temperature reconstructions from the Northern Hemisphere reaching back to AD 1000 (see Esper et al. 2016 for details). Thirteen records are located in Europe, 15 in Asia and eight in North America (Fig. 1, Table 1). All these records and the different characteristics of the underlying tree-ring data have been examined in-depth by Esper et al. (2016) (updates at: [www.blogs.uni-mainz.de/fb09climatology/reconranking](http://www.blogs.uni-mainz.de/fb09climatology/reconranking)). We herein use only the final temperature reconstructions from the original articles. This millennium-length dataset is a unique network as it enables the investigation of volcanic effects over the whole last millennium.

*Table 1: Millennium-length tree-ring based temperature reconstructions from the Northern Hemisphere. \* indicates MXD-based temperature reconstructions.*

<b>Continent</b>	<b>Record</b>	<b>Reference</b>	<b>Lat./Lon.</b>
<b>Europe</b>	Tornetraesk (MXD)*	Melvin et al. 2013	68.2N 19.5E
	Tornetraesk (TRW)	Melvin et al. 2013	68.2N 19.5E
	N-Scan*	Esper et al. 2012	67-69N 20-28E
	Finland	Helama et al. 2010	67-69N 20-28E
	Jämtland	Linderholm & Gunnarson 2005	63.2N 12-13E
	S-Finland*	Helama et al. 2014	61-62N 28-29E
	Tatra	Büntgen et al. 2013	48-49N 19-21E
	Swiss/Austrian Alps	Büntgen et al. 2005	46-47N 7-11E
	Central Alps	Büntgen et al. 2011	46-47N 10-12E
	Lauenen*	Schweingruber et al. 1988	46.4N 7.3E
	Lötschental*	Büntgen et al. 2006	46.3N 7.8E
	Alps (Larch)	Büntgen et al. 2009	45-47N 6-14E
	French Alps	Büntgen et al. 2012	44N 7.3E
<b>Asia</b>	Taimyr	Briffa et al. 2008	70-72N 95-105E
	Indigirka	Sidorova et al. 2006	70N 148E
	Yamal	Briffa et al. 2013	67-68N 69-71E
	Polar Ural*	Briffa et al. 2013	66.8N 65.6E
	Central Asia	Davi et al. 2015	51.1N 99.7E
	Mongun	Myglan et al. 2012a	50.3N 90E
	Dzhelo	Myglan et al. 2012b	50N 87.9E
	Mongolia	D'Arrigo et al. 2001	48.3N 98.9E
	Tien Shan	Esper et al. 2003	40N 71-72E
	Qilian	Zhang et al. 2014	38.7N 99.7E
	Wulan	Zhu et al. 2008	37N 98.7E
	Dulan	Liu et al. 2009	36N 98-99E
	Karakorum	Esper et al. 2002	35-36N 74-75E
	W-Himalaya	Yadav et al. 2011	32-33N 76-77E
Qamdo	Wang et al. 2014	31.1N 97.2E	
<b>N-America</b>	Gulf of Alaska	Wiles et al. 2014	58-61N 134-149W
	E-Canada	Gennaretti et al. 2014	54-55N 70-72W
	Icefield*	Luckman & Wilson 2005	51-53N 117-119W
	Great Basin	Salzer et al. 2014	37-40N 114-118W
	Crabtree	Graumlich 1993	36.5N 118.3W
	Boreal Plateau	Lloyd & Graumlich 1997	36.3N 118.5W
	Upper Wright	Lloyd & Graumlich 1997	36.3N 118.3W
	Southern Colorado	Salzer & Kipfmüller 2005	35.3N 111.7W

### Selection of volcanic events

The selection of volcanic events was performed according to the new volcanism reconstruction by Schneider et al. (in prep). This event history is based on a break detection algorithm applied to the three most recent Northern Hemisphere tree-ring based temperature reconstructions: Schneider et al. (2015), Stoffel et al. (2015) and Wilson et al. (2016). The intensity of the detected volcanic events varied among these temperature records but we here choose all events which rank within the top ten of all three records resulting in seven overlapping events: 1109, 1258, 1453, 1601, 1641, 1783 and 1816. All these events can be located to tropical latitudes except of the 1783 Laki (Iceland) eruption. Note that these events indicate the year with the strongest cooling which does not necessarily represent the year of the actual eruption (see Schneider et al. in prep).

### Temperature response to volcanic events

We calculated the temperature deviations for each of the above mentioned seven volcanic events with respect to the five pre-event years. This was done for each of the 36 temperature reconstructions separately. We then focus on the event year and the year following. Even though volcanic forcing can cause longer lasting cooling we refrain to consider other post-event years. Tree-ring width (TRW) can feign temporally extended cooling through biological memory effects which is not the case in maximum latewood data (MXD) (D'Arrigo et al. 2013, Esper et al. 2010, 2015); in this study only seven temperature reconstructions are based on MXD data (see Table 1) indicating that the absolute temperatures have to be interpreted with care. We assume, however, that the TRW-records are biased similarly, allowing the investigation of spatial patterns. We applied a linear regression model to test the relationship between temperature response and latitude.

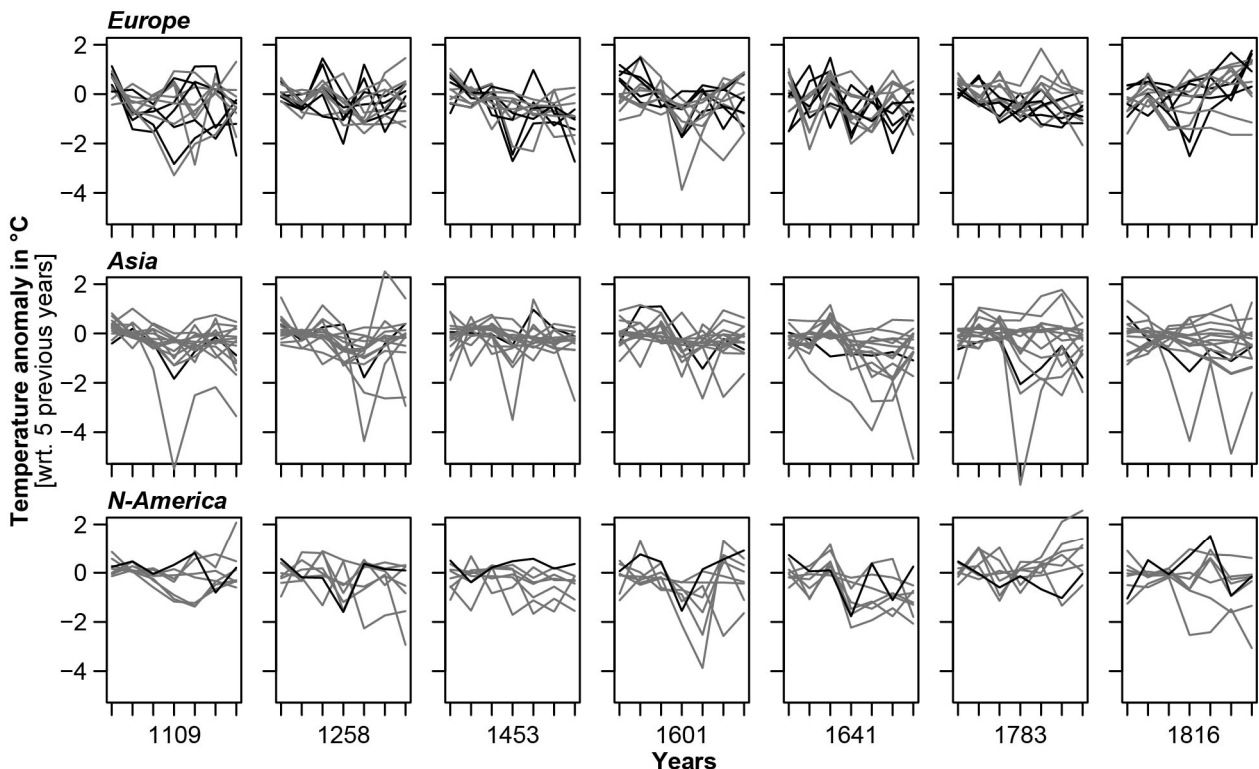


Figure 2: Temperature response in Europe, Asia and North-America to seven major volcanic cooling events. Temperature anomalies are calculated with respect to the 5 pre-event years. Grey lines refer to TRW and black lines to MXD-based temperature reconstructions.

## Results and Discussion

### *Temperature response to volcanic events*

The temperature response pattern to specific volcanic events varies considerable within a continent and also among the continents (Fig. 2). Interestingly, not only the TRW-based reconstructions (grey lines in Fig. 2) show a wide spread of temperature responses but also the MXD reconstructions (black lines in Fig. 2) show different responses. We expected a more pronounced and synchronous cooling in the MXD-based reconstructions as MXD contains clearer and less biased signals compared to TRW (D'Arrigo et al. 2013, Esper et al. 2010, 2015). Also, the timing of the maximum cooling differs among the sites. For example, the 1258 event caused cooling almost all-over Europe and North America during the event year, while in Asia maximum cooling occurred in 1259. The magnitude of cooling also strongly varies, the extra-tropical eruption in 1783 for example, caused only little cooling in Europe and North America but is quite pronounced in Asia, meaning that the location of the eruption itself influences the temperature response.

The temperature patterns also differ among the events, indicating that these seven volcanic eruptions caused different and site-specific temperature responses (Fig. 2 & 3). The spread of temperature responses is fairly high and some sites even show a warming. However, considering the overall temperature responses of all sites, each event caused cooling (Fig. 3). The overall strongest cooling can be detected for the 1641 event (median =  $-0.71^{\circ}\text{C}$ ) followed by the 1601 event (median =  $-0.63^{\circ}\text{C}$ ). Both events also show the strongest cooling in the following year. The most recent events of 1783 (median =  $-0.37^{\circ}\text{C}$ ) and 1816 (median =  $-0.23^{\circ}\text{C}$ ) caused least cooling and the following year even shows no extraordinary temperature deviations.

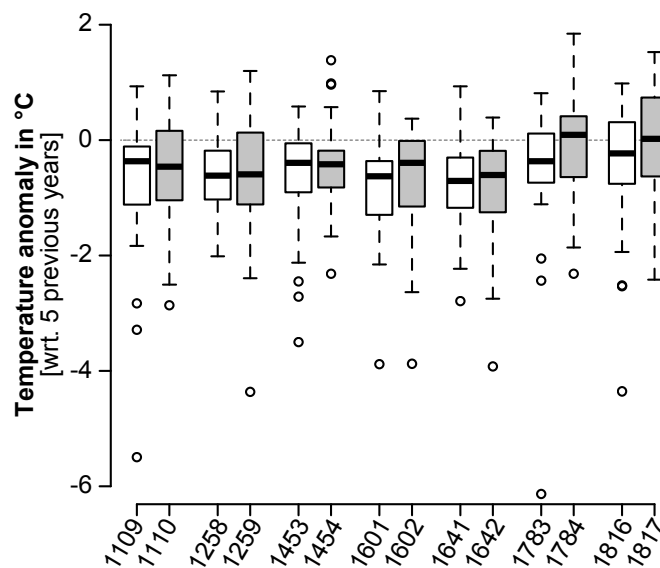


Figure 3: Comparison of the overall temperature response spread to seven major volcanic events.

### *Influence of geographical location*

As mentioned above the temperature responses vary considerable among the sites but also among the events. However, by plotting the temperature anomalies with latitude we can partly determine a relationship with latitude (Fig. 4). Esper et al. (2015) found a more pronounced cooling in high compared to mid latitudes. This finding was derived from a superposed epoch analysis, i.e. represents the mean over a couple of events. By observing this pattern for single events this relationship is only partly true. A significant correlation between latitude and the strength of cooling can be determined for the 1453, 1601 and 1783 event as well as the post-event years 1259 and

1784. However, the slopes of the regression models are – albeit not significant – for the most part negative, indicating that cooling is frequently strongest with increasing latitude. This is most pronounced in 1453 with a temperature decrease of  $-0.36^{\circ}\text{C}$  over  $10^{\circ}$  North as well as in 1783 with a cooling of  $-0.39^{\circ}\text{C}$  with  $10^{\circ}$  North. However, in 1783 this slope is especially caused through the extraordinary strong cooling ( $-6.14^{\circ}\text{C}$ ) of a reconstruction site in Asia (Yamal).

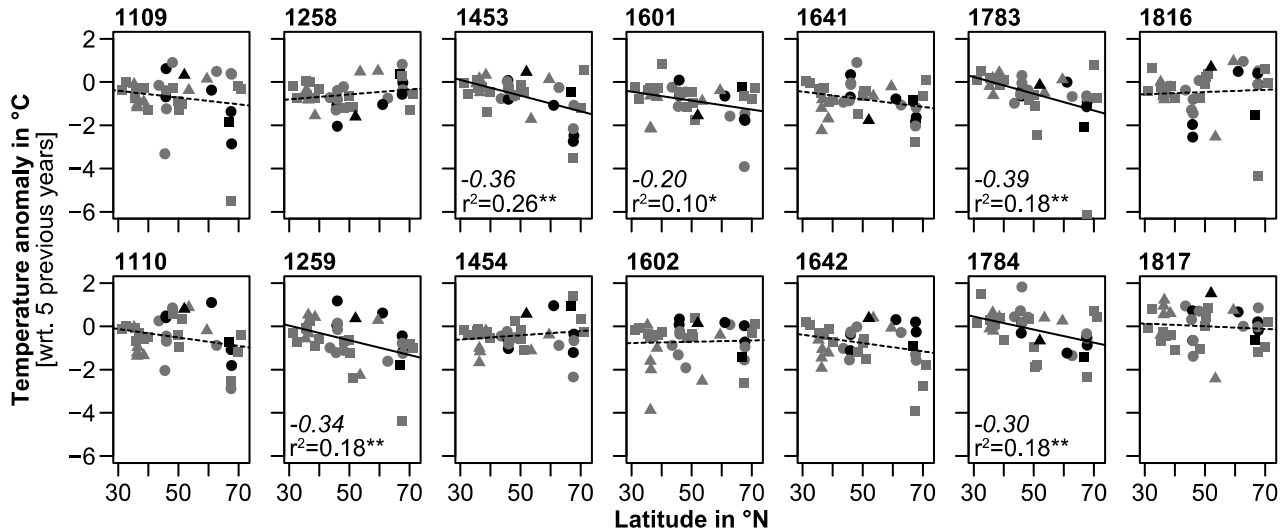


Figure 4: Temperature response in Europe (points), Asia (squares), and North America (triangles) to seven major volcanic events as a function of latitude. Upper panel shows temperature anomalies during the event year and lower panel for the respective following year (all wrt. to the 5 pre-event years). Grey symbols refer to TRW and black symbols to MXD based temperature reconstructions. Dashed lines represent non-significant and solid lines significant ( $* p < 0.05$ ,  $** p < 0.01$ ) linear fits. *Italic values indicate the slope of the regression model over  $10^{\circ}$  North.*

## Conclusion

Volcanically induced temperature responses can strongly vary in dependence to geographical location and differ among specific events. This is connected to the features of the volcanic eruption itself (location of the volcano, seasonal timing and strength of the eruption) but also to the atmospheric circulation patterns. In order to correctly represent volcanic forcing and the respective cooling in climate model simulations more research about the geographically varying cooling following different eruptions is needed. Ideally this has to be performed with MXD-based temperature reconstructions as MXD reflects more accurately the real temperature deviations than TRW (Anchukaitis et al. 2012, D'Arrigo et al. 2013, Esper et al. 2010, 2015). As only seven MXD-based reconstructions exist for the last millennium more effort has to be made for building up a denser millennium-length MXD-network. The site-specific temperature responses must be analysed in more detail to get a more accurate understanding of volcanically induced cooling.

## References

- Anchukaitis, K.J., Breitenmoser, P., Briffa K.R., Buchwal, A., Büntgen, U., Cook, E.R., D'Arrigo, R.D., Esper, J., Evans, M.N., Frank, D., Grudd, H., Gunnarson, B., Hughes, M.K., Kirilyanov, A.V., Körner, C., Krusic, P., Luckman, B., Melvin, T.M., Salzer, M.W., Shashkin, A.V., Timmreck, C., Vaganov, E.A., Wilson, R.J.S. (2012): Tree rings and volcanic cooling, *Nature Geoscience* 5: 836-837.
- Briffa, K. R., Jones, P. D., Schweingruber, F. H., Osborn, T. J. (1998): Influence of volcanic eruptions on Northern Hemisphere summer temperature over the past 600 years. *Nature* 393: 450-455.

- Briffa, K.R., Shishov, V.V., Melvin, T.M., Vaganov, E.A., Grudd, H., Hantemirov, R.M., Eronen, M., Naurzbaev, M.M. (2008): Trends in recent temperature and radial tree growth spanning 2000 years across northwest Eurasia. *Philosophical transactions of the Royal Society of London. Series B, Biological sciences* 363: 2269–2282.
- Briffa, K.R., Melvin, T.M., Osborn, T.J., Hantemirov, R.M., Kirilyanov, A.V., Mazepa, V.S., Shiyatov, S.G., Esper, J. (2013): Reassessing the evidence for tree-growth and inferred temperature change during the Common Era in Yamalia, Northwest Siberia. *Quaternary Science Reviews* 72: 83–107.
- Büntgen, U., Esper, J., Frank, D.C., Nicolussi, K., Schmidhalter, M. (2005): A 1052-year tree-ring proxy for Alpine summer temperatures. *Climate Dynamics* 25: 141–153.
- Büntgen, U., Frank, D.C., Nievergelt, D., Esper, J. (2006): Summer temperature variations in the European Alps, A.D. 755-2004. *Journal of Climate* 19: 5606–5623.
- Büntgen, U., Frank, D., Carrer, M., Urbinati, C., Esper, J. (2009): Improving Alpine summer temperature reconstructions by increasing sample size. *Trace* 7: 36–43.
- Büntgen, U., Tegel, W., Nicolussi, K., McCormick, M., Frank, D., Trouet, V., Kaplan, J.O., Herzig, F., Heussner, K.U., Wanner, H., Luterbacher, J., Esper, J. (2011): 2500 years of European climate variability and human susceptibility. *Science* 331: 578–582.
- Büntgen, U., Neuschwander, T., Frank, D., Esper, J. (2012): Fading temperature sensitivity of Alpine tree growth at its Mediterranean margin and associated effects on large-scale climate reconstructions. *Climate Change* 114: 651–666.
- Büntgen, U., Kyncl, T., Ginzler, C., Jacks, D.S., Esper, J., Tegel, W., Heussner, K.U., Kyncl, J. (2013): Filling the Eastern European gap in millennium-length temperature reconstructions. *Proceedings of the National Academy of Sciences* 110: 1773–1778.
- Crowley, T. J., Unterman, M. B. (2013): Technical details concerning development of a 1200 yr proxy index for global volcanism. *Earth System Science Data* 5(1): 187–197.
- D'Arrigo, R.D., Jacoby, G., Frank, D., Pederson, N., Cook, E.R., Buckley, B.M., Nachin, B., Mijiddorj, R., Dugarjav, C. (2001): 1738 years of Mongolian temperature variability inferred from a tree-ring width chronology of Siberian pine. *Geophysical Research Letters* 28: 543–546.
- D'Arrigo, R.D., Wilson, R., Anchukaitis, K.J. (2013): Volcanic cooling signal in tree-ring temperature reconstructions for the past millennium. *Journal of Geophysical Research* 118: 9000-9010.
- Davi, N. K., D'Arrigo, R. D., Jacoby, G. C., Cook, E. R., Anchukaitis, K. J., Nachin, B., Rao, M. P., Leland C. (2015): A long-term context (931–2005 C.E.) for rapid warming over Central Asia, *Quaternary Science Reviews* 121: 89–97.
- Esper, J., F. H. Schweingruber, and M. Winiger (2002): 1300 years of climatic history for Western Central Asia inferred from tree-rings, *The Holocene* 12(3): 267–277.
- Esper, J., Shiyatov, S.G., Mazepa, V.S., Wilson, R.J.S., Graybill, D.A., Funkhouser, G. (2003): Temperature-sensitive Tien Shan tree-ring chronologies show multi-centennial growth trends. *Climate Dynamics* 8: 699–706.
- Esper, J., Frank, D.C., Büntgen, U., Verstege, A., Hantemirov, R.M., Kirilyanov, A.V. (2010): Trends and uncertainties in Siberian indicators of 20th century warming. *Global Change Biology* 16: 386-398.
- Esper, J., Frank, D.C., Timonen, M., Zorita, E., Wilson, R.J.S., Luterbacher, J., Holzkämper, S., Fischer, N., Wagner, S., Nievergelt, D., Verstege, A., Büntgen U. (2012): Orbital forcing of tree-ring data. *Nature Climate Change* 2: 862–866.
- Esper, J., Schneider, L., Smerdon, J. E., Schöne, B. R., Büntgen, U. (2015): Signals and memory in tree-ring width and density data. *Dendrochronologia* 35: 62–70.
- Esper, J., Krusic, P. J., Ljungqvist, F. C., Luterbacher, J., Carrer, M., Cook, E. R., Davi, N. K., Hartl-Meier, C., Kirilyanov, A. V., Konter, O., Myglan, V. S., Timonen, M., Treydte, K., Trouet, V., Villalba, R., Yang, B., Büntgen, U. (2016): Ranking of tree-ring based temperature reconstructions of the past millennium, *Quaternary Science Reviews* 145: 134–151.

- Gao, C., Robock, A., Ammann C. M. (2008): Volcanic forcing of climate over the past 1500 years: An improved ice core-based index for climate models, *Journal of Geophysical Research* 113: D23111.
- Gennaretti, F., Arseneault, D., Nicault, A., Perreault, L., Bégin, Y. (2014): Volcano-induced regime shifts in millennial tree-ring chronologies from northeastern North America. *Proceedings of the National Academy of Sciences* 111: 10077–10082.
- Graumlich, L.J. (1993): A 1000-year record of temperature and precipitation in the Sierra Nevada. *Quaternary Research* 39: 249–255.
- Helama, S., Fauria, M.M., Mielikäinen, K., Timonen, M., Eronen, M. (2010): Sub-Milankovitch solar forcing of past climates: mid and late Holocene perspectives. *GSA Bulletin* 122: 1981–1988.
- Helama, S., Vartiainen, M., Holopainen, J., Mäkelä, H.M., Kolström, T., Meriläinen, J. (2014): A palaeotemperature record for the Finnish Lakeland based on microdensitometric variations in tree rings. *Geochronometria* 41: 265–277.
- Linderholm, H.W., Gunnarson, B.E. (2005): Summer temperature variability in central Scandinavia in the last 3600 years. *Geografiska Annaler A* 87: 231–241.
- Liu, Y., Z. An, H. W. Linderholm, D. Chen, H. Song, Q. Cai, J. Sun, and H. Tian (2009): Annual temperatures during the last 2485 years in the mid-eastern Tibetan Plateau inferred from tree rings. *Science in China Series D Earth Sciences* 52(3): 348–359.
- Lloyd, A.H., Graumlich, L.J. (1997): Holocene dynamics of treeline forests in the Sierra Nevada. *Ecology* 78: 1199–1210.
- Luckman, B.H., Wilson, R.J.S. (2005): Summer temperatures in the Canadian Rockies during the last millennium: a revised record. *Climate Dynamics* 24: 131–144.
- Melvin, T.M., Grudd, H., Briffa, K.R. (2013): Potential bias in ‘updating’ tree-ring chronologies using Regional Curve Standardization: re-processing the Torneträsk maximum-latewood-density data. *Holocene* 23: 364–373.
- Myglan, V.S., Oidupaa, O.C., Vaganov, E.A. (2012a): A 2367-year tree-ring chronology for the Altai-Sayan region (Mongun-Taiga Mountain Massif). *Archaeology Ethnology and Anthropology of Eurasia* 40: 76–83.
- Myglan, V.S., Zharnikova, O.A., Malysheva, N.V., Gerasimova, O.V., Vaganov, E.A., Sidorov, O.V. (2012b): Constructing the tree-ring chronology and reconstructing summertime air temperatures in southern Altai for the last 1500 years. *Geography and Natural Resources* 33: 200–207.
- Robock, A. (2000): Volcanic eruptions and climate. *Reviews of Geophysics* 38(2): 191–219.
- Salzer, M.W., Kipfmüller, K.F. (2005): Reconstructed temperature and precipitation on a millennial timescale from tree-rings in the southern Colorado Plateau, USA. *Climate Change* 70: 465–487.
- Salzer, M.W., Bunn, A.G., Graham, N.E., Hughes, M.K. (2014): Five millennia of paleotemperature from tree-rings in the Great Basin, USA. *Climate Dynamics* 42: 1517–1526
- Schmidt, G. A., Jungclaus, J. H., Ammann, C. M., Bard, E., Braconnot, P., Crowley, T. J., Delaygue, G., Joos, F., Krivova, N. A., Muscheler, R., Otto-Bliesner, B. L., Pongratz, J., Shindell, D. T., Solanki, S. K., Steinhilber, F., Vieira L. E. A. (2011): Climate forcing reconstructions for use in PMIP simulations of the last millennium (v1.0), *Geoscientific Model Development* 4(1): 33–45.
- Schneider, L., Smerdon, J. E., Büntgen, U., Wilson, R. J. S., Myglan, V. S., Kirilyanov, A. V., Esper, J. (2015): Revising midlatitude summer temperatures back to AD600 based on a wood density network. *Geophysical Research Letters* 42: 4556–4562.
- Schneider, L., Smerdon, J. E., Pretis, F., Hartl-Meier, C., Esper, J. (in prep): An alternative record of volcanism over the past millenium derived from reconstucted hemispheric summer temperatures.
- Schweingruber, F.H., Bartholin, T., Schär, E., Briffa, K.R. (1988): Radiodensitometric-dendroclimatological conifer chronologies from Lapland (Scandinavia) and the Alps (Switzerland). *Boreas* 17: 559–566.

- Sidorova, O.V., Naurzbaev, M.M., Vaganov, E.A. (2006): An integral estimation of tree-ring chronologies from subarctic regions of Eurasia. *Trace* 4: 84–91.
- Sigl, M., Winstrup, M., McConnell, J. R., Welten, K. C., Plunkett, G., Ludlow, F., Büntgen, U., Caffee, M., Chellman, N., Dahl-Jensen, D., Fischer, H., Kipfstuhl, S., Kostick, C., Maselli, O. J., Mekhaldi, F., Mulvaney, R., Muscheler, R., Pasteris, D. R., Pilcher, J. R., Salzer, M. W., Schüpbach, S., Steffensen, J. P., Vinther, B. M., Woodruff, T. E. (2015): Timing and climate forcing of volcanic eruptions for the past 2,500 years. *Nature* 523(7562): 543–549.
- Stoffel, M., Khodri, M., Corona, C., Guillet, S., Poulain, V., Bekki, S., Guiot, J., Luckman, B. H., Oppenheimer, C., Lebas, N., Beniston, M., Masson-Delmotte, V. (2015): Estimates of volcanic-induced cooling in the Northern Hemisphere over the past 1,500 years. *Nature Geoscience* 8, 784–791.
- Wang, J., Yang, B., Qin, C., Kang, S., He, M., Wang, Z. (2014): Tree-ring inferred annual mean temperature variations on the southeastern Tibetan Plateau during the last millennium and their relationships with the Atlantic Multidecadal Oscillation. *Climate Dynamics* 43: 627–640.
- Wiles, G.C., D'Arrigo, R.D., Barclay, D., Wilson, R.S., Jarvis, S.K., Vargo, L., Frank, D. (2014): Surface air temperature variability reconstructed with tree rings for the Gulf of Alaska over the past 1200 years. *Holocene* 24: 198–208.
- Wilson, R., Anchukaitis, K., Briffa, K. R., Büntgen, U., Cook, E., D'Arrigo, R., Davi, N., Esper, J., Frank, D., Gunnarson, B., Hegerl, G., Helama, S., Klesse, S., Krusic, P. J., Linderholm, H. W., Myglan, V., Osborn, T. J., Rydval, M., Schneider, L., Schurer, A., Wiles, G., Zhang, P., Zorita, E. (2016): Last millennium northern hemisphere summer temperatures from tree rings: Part I: The long term context. *Quaternary Science Reviews* 134: 1–18.
- Yadav, R.R., Braeuning, A., Singh, J. (2011): Tree ring inferred summer temperature variations over the last millennium in western Himalaya, India. *Climate Dynamics* 36: 1545–1554.
- Zhang, Y., X. Shao, Z.-Y. Yin, and Y. Wang (2014): Millennial minimum temperature variations in the Qilian Mountains, China: Evidence from tree rings, *Climate of the Past* 10(5): 1763–1778.
- Zhu, H., Y. Zheng, X. Shao, X. Liu, Y. Xu, and E. Liang (2008): Millennial temperature reconstruction based on tree-ring widths of Qilian juniper from Wulan, Qinghai Province, China. *Science Bulletin* 53(24): 3914–3920.

# On the influence of autocorrelation on the significance of wavelet spectral peaks

P. Hochreuther, J. Wernicke, J. Grießinger & A. Bräuning

<sup>1</sup>*Institute of Geography, FAU Erlangen-Nuremberg, Germany  
E-mail: philipp.hochreuther@fau.de*

## Introduction

Wavelet analysis of univariate time series is a useful tool in dendroclimatology, as it is able to unravel periodicities in the presence of noise (Torrence & Compo 1998). The comparative wavelet analysis, or wavelet coherence, improves this technique by offering the chance to compare the wavelet spectra of two time series, e.g. a tree-ring series and a climate variable (Sen and Kern 2016, Hochreuther et al., 2016). Discovering common (a-)periodic fluctuations, and thus common environmental forcing or changes of such relationships over the covered period, are just a few of the opportunities that set this method apart from classic power spectrum- and cross-spectral analysis (Grinsted et al. 2004, Cazelles et al. 2008). Nonetheless, both wavelet- and power spectrum analysis share common properties which have to be carefully considered when interpreting the results. One important factor influencing the spectra of time series is temporal autocorrelation: the higher the autocorrelation, the more will the spectrum tend to contain low-frequency power (Percival & Walden 1993, Figs. 1g/h and 2). This has important implications not only for the power spectrum-/wavelet analysis itself, but also for the respective coherence, since high power at certain frequencies/periods in one spectrum will result in elevated coherence, even if the other spectrum contains low power at these frequencies (Addison 2002). Since tree-ring proxies, especially ring-width, regularly show high first- and second-order autocorrelation, care should be taken when choosing the appropriate background spectrum for determining the significance of spectral peaks.

In this study, we evaluate the influence of autocorrelation on the wavelet power spectrum. We determine the average background spectrum of uncorrelated time series quantitatively, and compare it to spectra which bear significant amounts of first- to third-order autocorrelation. Based on these tests, we give recommendations for the choice of background spectra when determining significance levels in wavelet- and wavelet coherence analysis, based on the amount of autocorrelation in the tree-ring series. We apply our presumptions to a real-world ring-width series from Southeast Tibet to demonstrate how the results of frequency analysis depend on the applied framework parameters.

## Materials and methods

As real-world data usually contain variance portions in several high- or low frequencies that contain non-random environmental signals, we employ simulated time series of coloured noise (Allen and Smith 1996). White noise represents uncorrelated values with a flat power spectrum, as all possible frequencies have equal power on average, thus resembling the concept of white light (Fig. 1a-d). We simulate Gaussian white noise processes, defined by a mean of 0 and a variance of 1. Red noise contains a certain amount of autocorrelation, and is modelled in this study by a first-order autoregressive process (AR1) with AR coefficients of 0.5 and 0.9 using an autoregressive integrated moving average (ARIMA) simulation without the moving average (MA) component. In this manner, an AR coefficient of 0.5 induces a significant autocorrelation for  $t+1$  to  $t+3$ . The consequence is that the spectrum expresses a slope, indicating decreasing average power from low to high frequencies (Fig. 1e-h). We assume that any climatological or ecological effect on tree growth/stable isotope content does not influence the time series more than three years after the

current year. This may, of course, differ for singular extreme events, and if a different time resolution (e.g. dendrometer data) is used, this assumption is not valid and the respective parameters should be adjusted.

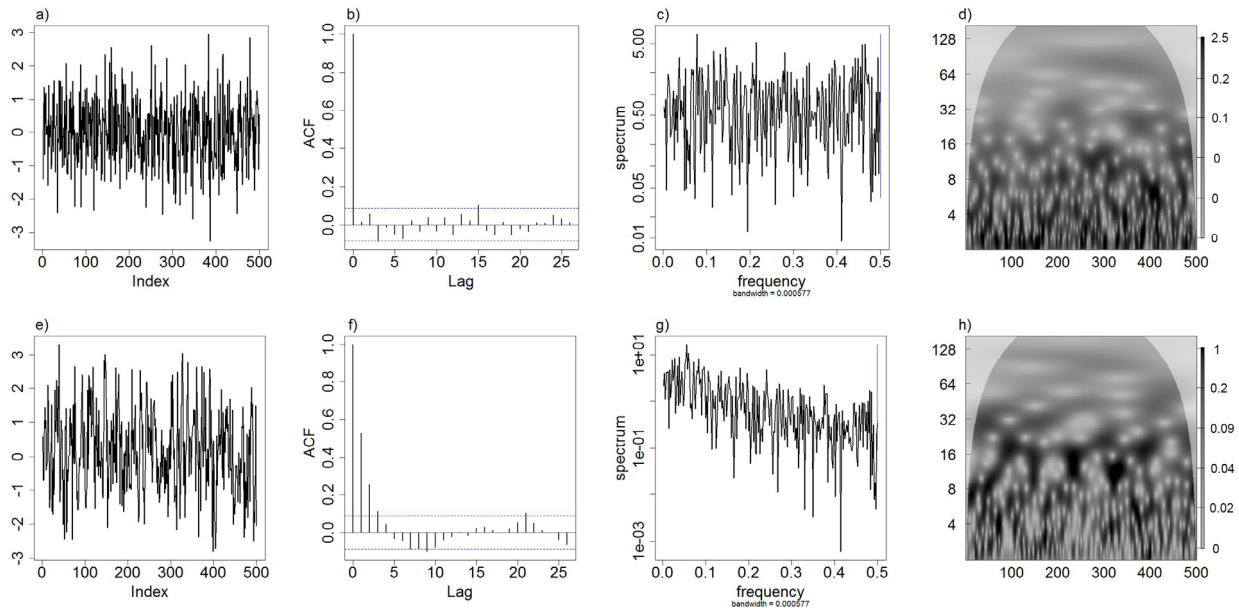


*Figure 1: Examples of simulated time series: a)-d) white noise process, with a) showing the raw series, b) its autocorrelation function (ACF), c) -power spectrum and d) wavelet transform. e)-h) the same for an example of a red noise process. Power spectra tapered with a bell-shaped cosine at the first and last 10% of the time series. In the wavelet plots, power ridges and significance contours were omitted.*

Each noise was modelled 1000 times, with a length of 250 data points/ time steps, as this number relates closely to the length of the real-world time series, and is close to the average length of all chronologies in the ITRDB which is 255 years (dataset as used in Breitenmoser et al. 2014). All calculations were carried out using R (R Core team 2012). A thousand repetitions were used since the WaveletComp package (Roesch & Schmidbauer 2014) employed for computation of the wavelet power spectra uses the same number for simulating series of background noise on which the significance calculations are based. Wavelet transformations for determination of average power values were computed for all modelled noise series, using the Morlet wavelet as the mother wavelet function.

The Galongla tree-ring width chronology employed for testing is composed of 39 trees of species *Larix griffithii* sampled in Bomi prefecture, Xizang Autonomous Region, China (Bräuning 2006, Hochreuther et al. 2016). The series entering the chronology were detrended with a regional growth curve beforehand (Esper et al. 2003). No variance-stabilizing procedures were applied.

### Simulation results and discussion

The wavelet spectrum of white noise, averaged over 1000 simulations over the whole time period, expresses high power in the high frequencies; the peak is at 2.38 years (Fig. 2a). This result can also be reproduced using the same time step for all simulations, and averaging at this point over all periods, e.g. an average of all periods at  $t = 250$ , as calculated by Torrence & Compo (1998). The power level is exponentially decreasing towards the low frequencies, approaching zero power at the end of the period length. Consequently, if the wavelet power spectrum of white noise is chosen as a background spectrum for the wavelet transform, the desired significance level is reached only at very high power levels for frequencies ranging between two and four years. The converse argument is that significance is easily reached at low-frequency fluctuations. This contrasts the assumption that white noise represents an equal background spectrum for all frequencies (Fig. 2e). This may be a result of the 'stretching' of the Morlet wavelet, resulting in better resolution and

higher power with the Heisenberg box (time-frequency box) becoming thinner and higher at high frequencies, but wider and lower at low frequencies (e.g. Cazelles et al. 2008).

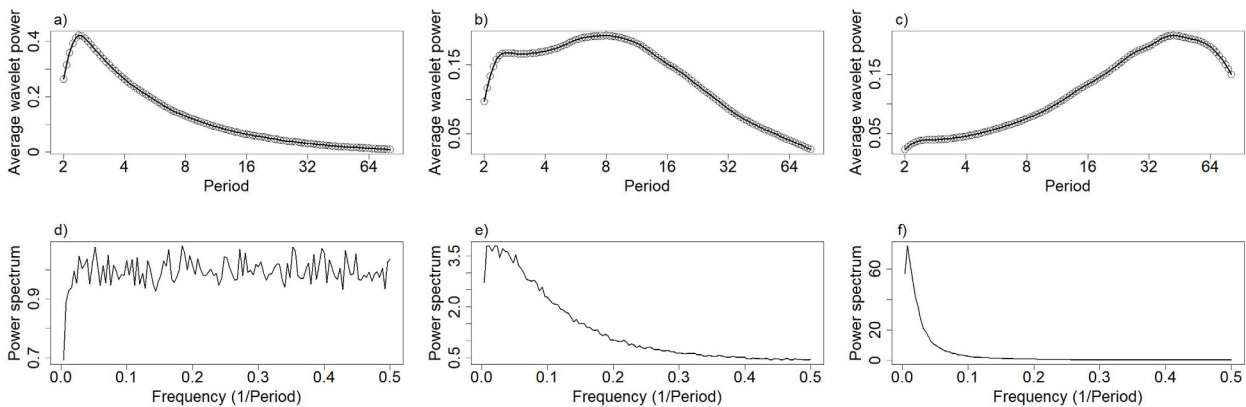


Figure 2: Wavelet power spectra (a-c) and Fourier power spectra (d-f), averaged over the wavelet transform of 1000 random white noise- (a) and red noise (b,c) processes, each containing 250 time steps. The AR1-coefficients for b) is 0.5, and 0.9 for c), respectively. Same prerequisites applied to the Fourier spectra (d-f), in a manner that the upper and lower graphs are spectral representations of the same dataset.

As the degree of autocorrelation increases, the maximum average power shifts from short periods/high frequencies towards longer periods/lower frequencies, with the maximum for AR1 = 0.5 at 8 years and for AR1 = 0.9 at 47 years. The average power simultaneously decreases, approaching 0.2 for both red noise wavelet power averages. Additionally, as the power maximum shifts through the period space, the average power of the background spectrum fluctuates in a narrow band between 0 and 0.2. This implies similar wavelet power spectra significances if those values for AR1 coefficients are chosen as background spectra for any time series.

### Application to real-world data

The Galongla tree-ring width chronology, detrended with a regional curve, is not strictly stationary over the whole covered period (Fig. 3a) and thus provides a good testing ground, as this is the case for many tree-ring based time series, and illustrates the capability of wavelet transform to deal with non-stationary time series.

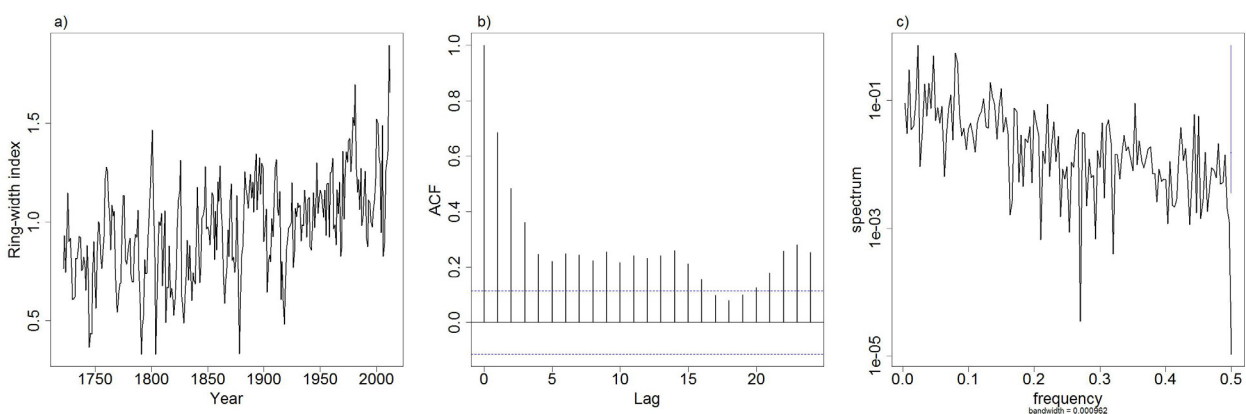


Figure 3: Characteristics of the Galongla ring-width chronology: a) rcs-detrended chronology, spanning from 1722 to 2012 with a minimum of 5 trees. b) ACF of the chronology, c) the power spectrum of the chronology.

The chronology is characterized by a strong temporal autocorrelation in the subsequent years (Fig. 3b). The growth conditions of the current year probably influence growth in the following year, in rare cases even the year after that, thus finding an appropriate AR model should be focused on the first and the second lagged year. The power spectrum (Fig. 3c) shows typical characteristics of a

moderate red noise spectrum (Fig. 2e), with strongest similarities compared to a spectrum with an AR1-coefficient of 0.7.

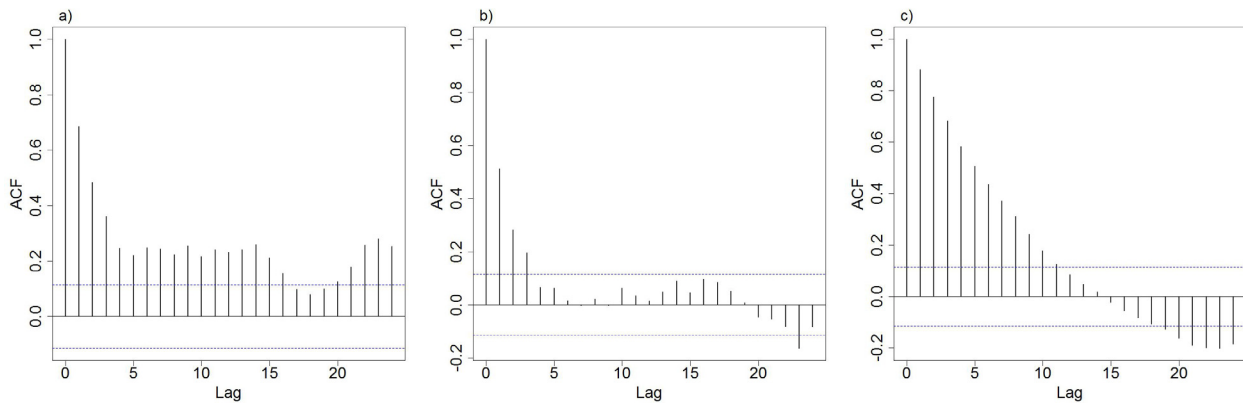


Figure 4: Comparison of the Galongla ring-width chronology ACF (a) with the ACF of 1000 simulations of red noise with AR1-coefficients of (b) 0.5 and (c) 0.9.

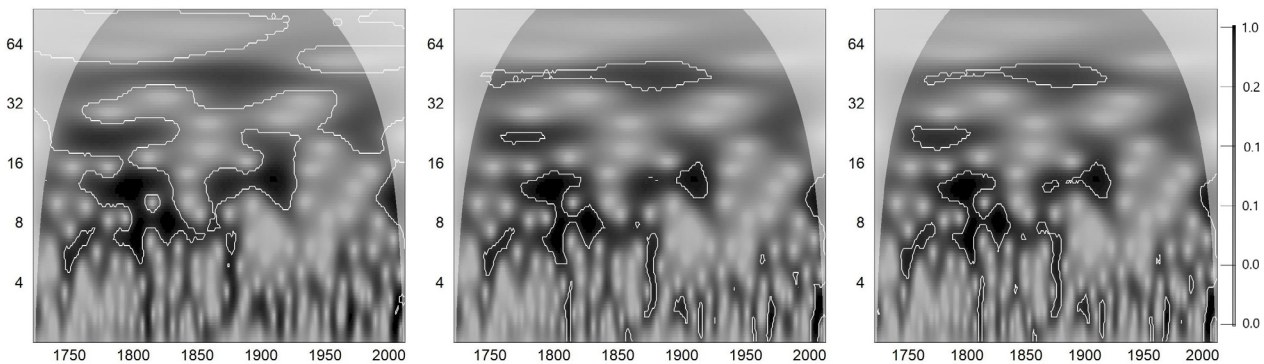


Figure 5: Wavelet transform of the Galongla ring-width chronology using different background spectra for computation of significance: a) white noise, b) red noise with AR1 = 0.5 and c) red noise with AR1 = 0.9. The average power between the two latter noise functions differs by maximum 0.08 per period, thus the wavelet power spectra look similar.

Comparing the wavelet transform of the Galongla chronology with different background spectra used to determine the 0.1 significance levels, it is evident that white noise practically eliminates all significance below 5 year periods. This fits our observation in Fig. 2a, where white noise produces highest values of wavelet spectra between two and four years, thus raising the values needed for passing significance levels. On the other hand, the significant periods increase with period length, culminating in a continuously significant band at approximately 45 years. The images representing two red noise spectra with AR1 = 0.5 and 0.9, respectively, including areas of significance, appear similar (Fig. 5b/c). This is probably the result of the narrow band in which the average wavelet power of the surrogate time series fluctuate, with the AR1 = 0.5 simulations reducing values below 16 years, and the AR1 = 0.9 simulations reducing the significance above 32 years, as indicated in Figs. 2b and 2c. Nonetheless, a significant area at a period of 45 years still appears in the two wavelet transforms with autocorrelated spectra, but only at a limited window in time. Thus, this period might still be meaningful, however its interpretation may strongly differ from the example with uncorrelated background spectra.

## Conclusion

For studies applying wavelet transform, we strongly recommend checking the univariate time series for autocorrelation before performing the actual analysis. This is also valid for wavelet coherence, in which case both time series should be examined. Using an ARIMA simulation with different AR coefficients is a fast and reliable way to determine an appropriate background spectrum for determining significance levels of the wavelet analysis. This is especially important if inference from tree-ring series on climate is to be evaluated, as inflated significance levels are not reliable and may lead to questionable conclusions.

## Acknowledgements

This work was supported by the German Research Foundation (DFG, project BR 1895/21-1) within the priority program 1372 TIP: Tibetan Plateau – Formation, Climate, Ecosystems.

## References

- Addison, P.S. (2002): *The illustrated wavelet transform handbook: Introductory theory and applications in science, engineering, medicine, and finance*. Bristol, UK, Philadelphia: Institute of Physics Pub.
- Allen, M.R., Smith, L.A. (1996): Monte Carlo SSA: Detecting irregular oscillations in the Presence of Colored Noise. *Journal of Climate* 9(12): 3373–3404.
- Bräuning, A. (2006): Tree-ring evidence of 'Little Ice Age' glacier advances in southern Tibet. *The Holocene* 16(3): 369–380.
- Breitenmoser, P., Brönnimann, S., Frank, D. (2014): Forward modelling of tree-ring width and comparison with a global network of tree-ring chronologies, *Clim. Past*, 10, 437–449, doi: 10.5194/cp-10-437-2014.
- Cazelles, B., Chavez, M., Berteaux, D., Menard, F., Vik, J.O., Jenouvrier, S., Stenseth, N.C. (2008): Wavelet analysis of ecological time series. *Oecologia* 156(2): 287–304.
- Esper, J., Cook, E.R., Krusic, P.J., Peters, K., Schweingruber, F.H. (2003): Tests of the RCS method for preserving low-frequency variability in long tree-ring chronologies. *Tree-ring research*(59(2)): 81–98.
- Grinsted, A., Moore, J. C., Jevrejeva, S. (2004): Application of the cross wavelet transform and wavelet coherence to geophysical time series, *Nonlin. Processes Geophys.*, 11, 561–566, doi: 10.5194/npg-11-561-2004.
- Hochreuther, P., Wernicke, J., Griesinger, J., Mölg, T., Zhu, H., Wang, L., Bräuning, A. (2016): Influence of the Indian Ocean Dipole on tree-ring  $\delta^{18}\text{O}$  of monsoonal Southeast Tibet. *Climatic Change* 137(1-2): 217–230.
- Percival, D.B., Walden, A.T. (1993): *Spectral Analysis for Physical Applications*. Cambridge: Cambridge University Press.
- R Core team (2012): *R: A language and environment for statistical computing*. Wien: R Foundation for Statistical Computing.
- Roesch, A., Schmidbauer, H. (2014): *WaveletComp: computational wavelet analysis: R package version 1.0*. <http://CRAN.R-project.org/package=WaveletComp>. Accessed 10 Nov 2016
- Sen, A. K., Kern, Z. (2016): Wavelet analysis of low-frequency variability in oak tree-ring chronologies from east Central Europe, *Open Geosciences*, 8, doi: 10.1515/geo-2016-0044.
- Torrence, C., Compo, G.P. (1998): A Practical Guide to Wavelet Analysis. *Bulletin of the American Meteorological Society* 79(1): 61–78.

# Testing for climate signal age effects at two treeline sites in the European Alps and Tatra Mountains

O. Konter<sup>1</sup>, U. Büntgen<sup>2,3,4</sup>, M. Carrer<sup>5</sup> & J. Esper<sup>1</sup>

<sup>1</sup>Department of Geography, Johannes Gutenberg University Mainz, Germany

<sup>2</sup>Swiss Federal Research Institute WSL, Birmensdorf, Switzerland

<sup>3</sup>Oeschger Centre for Climate Change Research, Bern, Switzerland

<sup>4</sup>Global Change Research Centre AS CR, Brno, Czech Republic

<sup>5</sup>Dipartimento TeSAF, Università degli Studi di Padova, Agripolis, Legnaro, PD, Italy

E-mail: o.konter@geo.uni-mainz.de

## Introduction

Age-related fluctuation in the sensitivity of tree-ring data to climate variability has been reported for different tree species, climatic zones and environmental envelopes (see Konter et al. 2016 for an overview). The resulting age-related growth-climate response patterns are, however, often inconsistent and different to compare. Some studies describe a stronger climate sensitivity of young trees (Rozas et al. 2009, Dorado Liñán et al. 2011, Konter et al. 2016) whereas others report stronger coherence between the growth of old trees and climatic parameters (Carrer & Urbinati 2004, Esper et al. 2008, Yu et al. 2008, Linares et al. 2013). Moreover, some authors consider these climate signal age effects (CSAE) negligible (Linderholm & Linderholm 2004, Esper et al. 2008, Dorado Liñán et al. 2011), while others find a significant impact on proxy calibration and the subsequent climate reconstructions (Carrer & Urbinati 2004, Rossi et al. 2008, Yu et al. 2008, Rozas et al. 2009, Linares et al. 2013). Any straightforward comparison of the impact of CSAE suffers from idiosyncratic differences of the existing study designs, including different tree species, geographical locations, environmental conditions, age class categories, and a combination thereof (Konter et al. 2016).

Here, we analyze CSAE at two upper treeline sites in the European Alps and the Tatra Mountains. This newly developed dataset incorporates temperature-sensitive tree-ring width (TRW) series of *Larix decidua* Mill. and *Pinus cembra* L. from the southern Swiss Alps and the northern Slovakian Tatra Mountains. Age-related trends in climate sensitivity are assessed by fitting linear regression models to the seasonal temperature correlations of the individual trees. This approach enables the assessment of CSAE and associated trends particularly focusing on the role of species and geographical origins.

## Material and methods

### *Study design and chronology development*

The Valais Alps in southern Switzerland and the High Tatra Mts in northern Slovakia provide the environmental settings for tree growth of the temperature-sensitive conifers: larch and pine. For this analysis we aggregated previously published 317 series of *Larix decidua* Mill. and 314 series of *Pinus cembra* L. from the Alps (Hartl-Meier et al. 2016), as well as 163 and 155 series from the Tatras, respectively (Konter et al. 2015a). Ring widths were measured and crossdated using a LinTab device and COFECHA software (Holmes 1983, Rinn 2007). Power transformation was applied to the raw TRW series to remove biological/age-induced spread-versus-level relationships (Cook & Peters 1997). Non-climatic juvenile growth trends, due to adjoining new rings to an increasing stem girth, were removed by fitting negative exponential functions or linear curve fits with negative slopes using the software ARSTAN and calculating residuals between the power transformed values and the smoothing curves (Fritts 1976, Cook 1985, Cook et al. 1990). Chronologies were compiled using robust bi-weight mean, while stabilization of temporal variance

changes was achieved with contemplating sample size and varying interseries correlations ( $r_{bar}$ ) (Frank et al. 2007b).

#### *Meteorological data and age-related calibration setups*

TRW data were calibrated against monthly-resolved meteorological observations from nearby instrumental stations in both regions. The station 'Gr. St. Bernhard' (45.80N, 6.10E, 2070 m asl) provides temperature measurements for the southern Swiss Alps over the period 1850-2011, while the nearby station in the Tatra region 'Poprad' (49.07N, 20.25E, 695.0m asl) only reaches back to 1951. Due to this rather short period we additionally used the a gridded temperature product from CRUTEM 4 (Jones et al. 2012) extending back to 1901, and accessible via the KNMI Climate Explorer (<http://climexp.knmi.nl>) from 47.5N/7.5E in the Alps and 47.5N/22.5E in the Tatras.

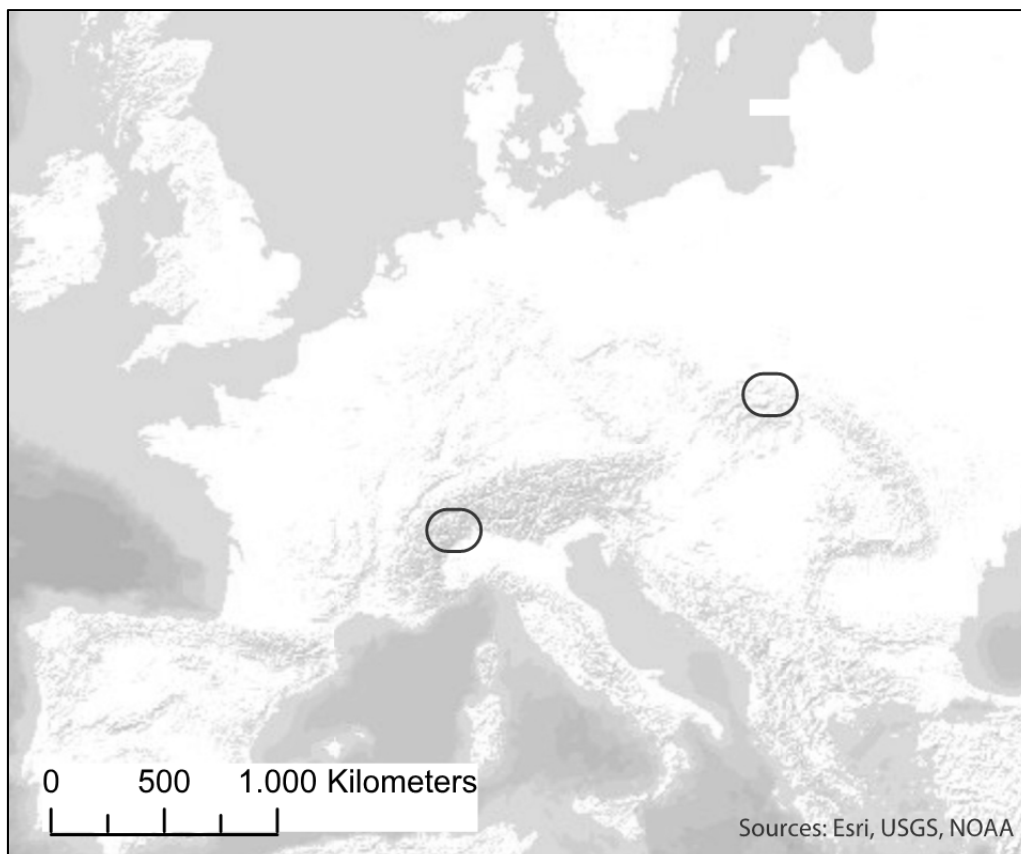


Figure 1: Sampling sites in the Alps and Tatra Mountains (ovals).

Growth-climate relationships were assessed using *Pearson's* correlation coefficients ( $r$ ) between the TRW chronologies and individual core samples from both regions and the corresponding temperature means (Konter et al. 2015a, Konter et al. 2015b, Hartl-Meier et al. 2016). Correlations with seasonal temperatures of the individual cores were aligned by cambial age (Esper et al. 2003) and linear regression functions were applied to these age-aligned climate correlations using R 3.1.1 (R Development Core Team 2014), the package *dplR* (Bunn et al. 2016) and *treeclim* (Zang & Biondi 2015). Positive and negative slopes of the predicted linear regression functions indicate the presence and orientation of CSAE trends, while associated p-values denote significance levels of these trends. Gradient 'g' signifies the slope of the linear regression functions over 100 years. Temporal robustness of growth-climate relationships and CSAE trends are assessed by splitting the centennial period 1901-2010/11/12 into an early split period (1901-1958), a late split period (1959-2010/11/12) and a station/grid overlap period (1951-2010/11/12).

## Results and discussion

Larch and pine TRW chronologies reflect distinct mean summer/growing season temperature signals in their respective habitats (Fig. 2). The detrended larch chronology from the Alps is well in agreement with June-August temperatures, which is detected with significant correlation values at  $p < 0.001$  during all calibration periods (Table 1). The same behaviour is found for pine from the Alps, except that the seasonality of the signal is extended from May-August. Similarly, the pines from the Tatras respond best to May-July, while larch TRW is most sensitive to a shorter May-June interval.

Correlation values of larch and pine TRW from the Tatras are positively significant, but fall below the corresponding values from the Alps (Table 1) (Büntgen et al. 2007, Büntgen et al. 2010, Büntgen et al. 2013). The signals are generally weaker in the early calibration periods (1901-1959), particularly in the Tatras ( $r_{Larix}=0.30$ ,  $p < 0.05$ ;  $r_{Pinus}=0.28$ ,  $p < 0.05$ ). This effect might also refer to the reduced quality of early instrumental measurements systematically impacting the calibration exercise (Parker 1994, Frank et al. 2007a, Böhm et al. 2009).

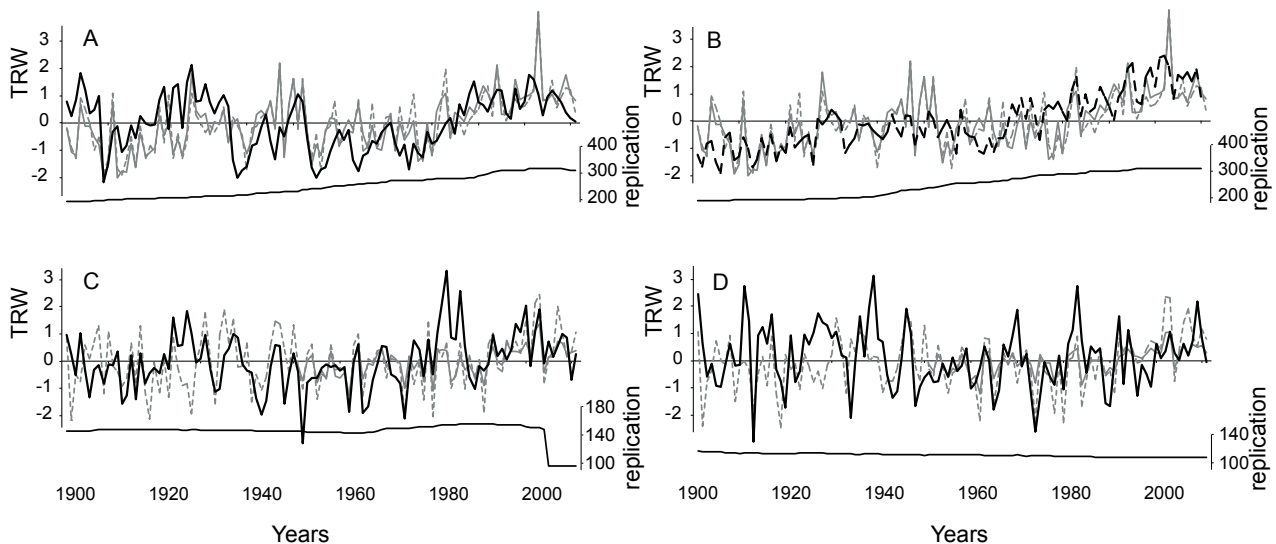


Figure 2: Larch and pine TRW chronologies (black) and seasonal temperatures (grey) from station (solid) and gridded data (dashed) in the Alps and the Tatra Mountains. A: *Larix decidua* TRW from the Alps and JJA temperature, B: *Pinus cembra* TRW from the Alps and MJJA temperature, C: *Larix decidua* TRW from the Tatras and MJ temperature, D: *Pinus cembra* TRW from the Tatra and MJJ temperature.

Table 1: Chronology and calibration statistics. 'Temperature Signal' indicates seasonality of highest growth-climate relationships. Numbers in Centennial, Early split, and Late split periods refer to correlation values  $r$  (using station data / gridded data). Values denoted in black reach  $p < 0.001$ , values in grey  $p < 0.05$ . Station/Grid period specifies the overlapping period of instrumental with gridded data.

Region	Species	Chronology Length	Temperature Signal	Centennial Period	Early Split Period	Late Split Period	Station/Grid Overlap
Alps	<i>Larix decidua</i>	1474-2011	JJA	0.48 / 0.42	0.38 / 0.35	0.65 / 0.55	1901-2011 0.48 / 0.42
	<i>Pinus cembra</i>	1428-2010	MJJA	0.65 / 0.61	0.53 / 0.46	0.66 / 0.65	1901-2010 0.65 / 0.61
Tatras	<i>Larix decidua</i>	1612-2012	MJ	-- / 0.44	-- / 0.30	0.60 / 0.56	1951-2012 0.60 / 0.55
	<i>Pinus cembra</i>	1687-2012	MJJ	-- / 0.39	-- / 0.28	0.54 / 0.53	1951-2012 0.54 / 0.52

Most of the TRW correlation values against instrumental or gridded data are near similar, thereby enabling gridded data for analysing CSAE trends throughout the centennial calibration period in the Tatras, where instrumental data are shorter.

In the Alps, both larch and pine individual core climate correlations between larch and JJA-temperatures reveal significantly increasing trends with increasing age, which are also present considering pine cores (Fig. 3). Particularly larch tends to be more prone to CSAE and is more sensitive to temperature variations at higher cambial ages. These results highlight the importance of geographical location over tree species and support previously published evidence from the Eastern Italian Alps (Carrer & Urbinati 2004). The weaker sensitivity of younger trees in the region mostly refers to a higher between-tree competition in juvenile life stages, which can cause a prolonging of the vegetation period or higher assimilation at a greater risk of mortality (Bond 2000). Hence, the impact of temperature variations in a shorter period can be reduced, which culminates in lower temperature correlation values of several young individuals (Carrer & Urbinati 2004).

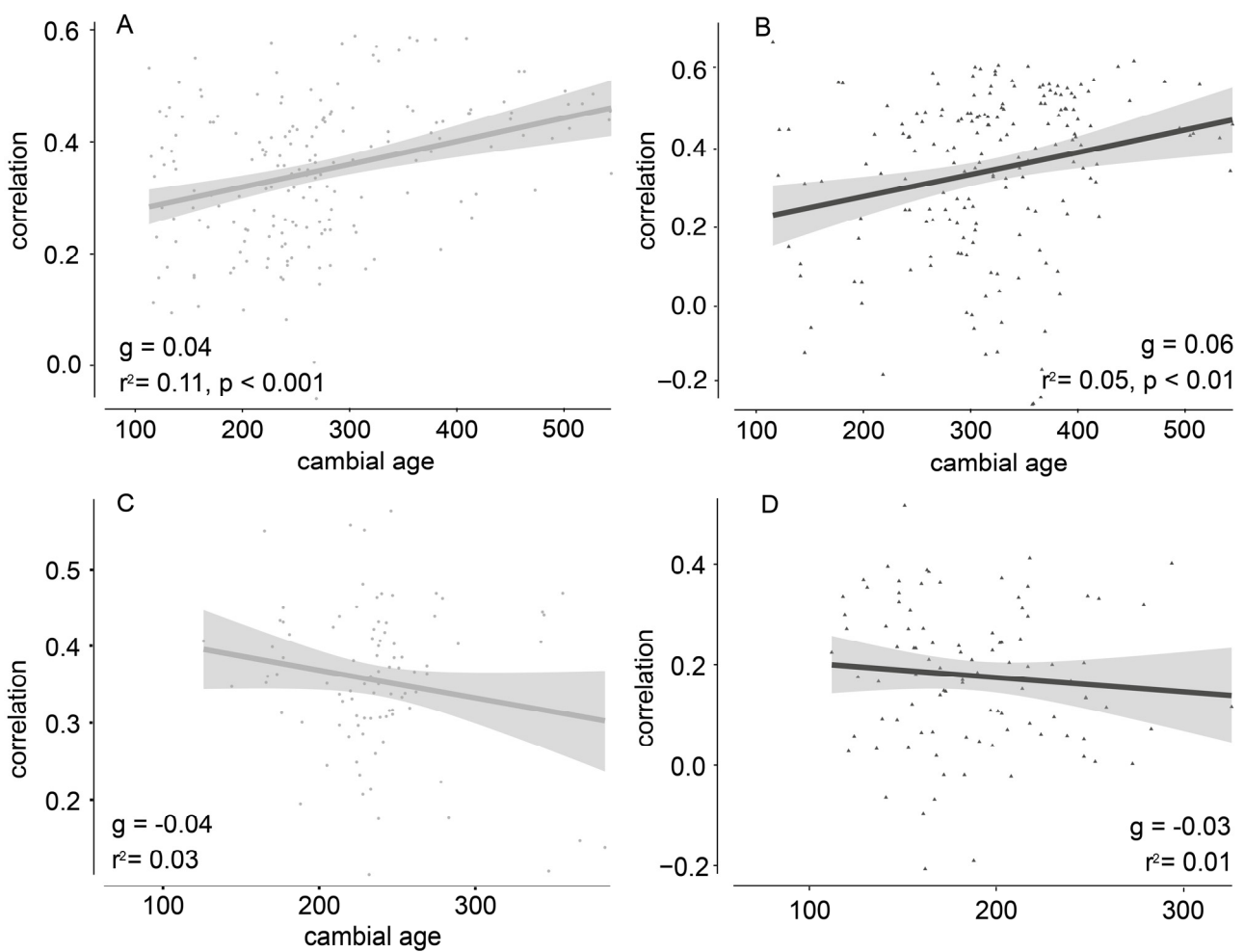


Figure 3: Correlations of individual cores aligned by cambial age with gridded temperatures data since 1901 and associated linear regressions. A: *Larix decidua* TRW from the Alps and JJA temperature, B: *Pinus cembra* TRW from the Alps and MJJA temperature, C: *Larix decidua* TRW from the Tatras and MJ temperature, D: *Pinus cembra* TRW from the Tatra and MJJ temperature. Shaded areas indicate 95% confidence limits of the predicted linear regression,  $g$  = regression slope over 100 years,  $r^2$  = adjusted coefficient of determination and  $p$  = significance level.

In contrast, both species from the Tatras show consistent negative trends with increasing age, though these trends lack significance and only a very small portion of the variance is explained by changing cambial ages ( $r^2_{Larix}=0.03$ ,  $r^2_{Pinus}=0.01$ ). So far, CSAE have not been analysed in this region, but negative CSAE trends in TRW data have also been reported for *Pinus sylvestris* from northern Fennoscandia (Konter et al. 2016), *Pinus nigra* and *Pinus uncinata* from eastern Spain

and the Pyrenees (Dorado Liñán et al. 2011), and *Juniperus thurifera* from central Spain (Rozas et al. 2009). Older trees tend to have shorter vegetation periods and produce fewer but larger cells per ring compared to young trees, which results in slower and shorter xylogenesis, making older trees more rigid to temperature variations (Rossi et al. 2008, Carrer et al. 2015, Konter et al. 2016). In addition, older trees can face hydraulic constraints due to tree height and long root-leaves path length, which can decrease temperature correlations of certain individuals, particularly under favourable conditions (Ryan & Yoder 1997).

These pronounced differences between the regions and, in contrast, consistency between the species at the same site become even more obvious when considering split calibration periods (Fig. 4). For all calibration periods the CSAE trends of larch individuals from Alps are increasing with age, with only the early split period (1901-1958) exhibiting non-significant results. CSAE trends of pines show comparable significant positive slopes in the linear regression functions, except for the non-significant trend in the late split period (1959-2011). Independent of the species, the growth-climate relationship of conifer trees in the Alps appears to be more distinct with tree individuals of older cambial ages.

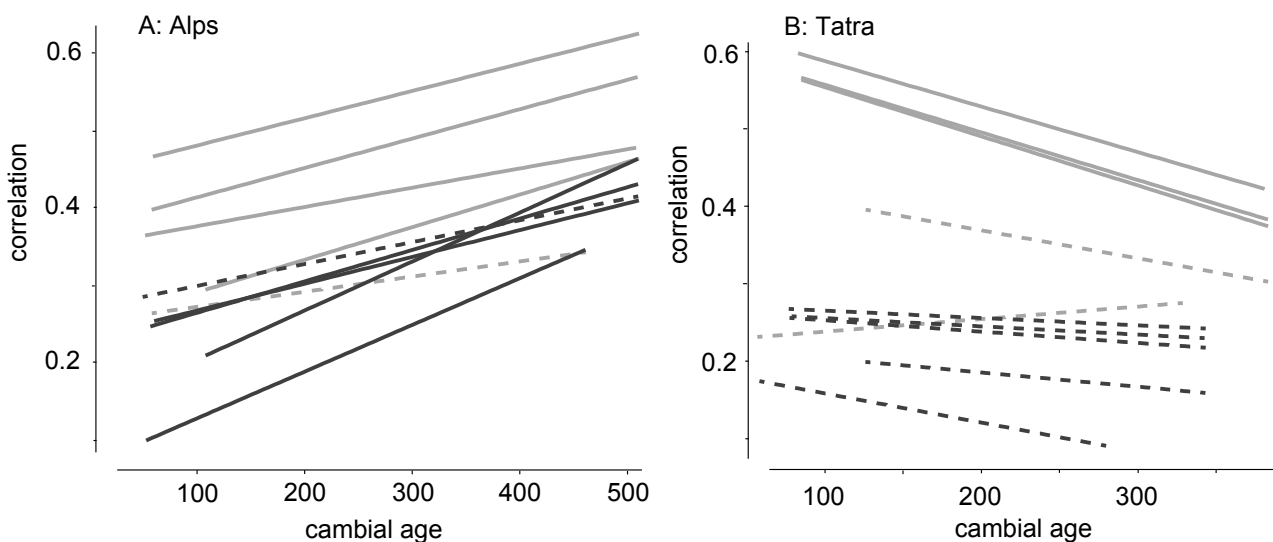


Figure 4: CSAE linear trends of *Larix decidua* (grey) and *Pinus cembra* (black) for correlations against corresponding best seasonal temperatures over variable calibration periods (see Table 1). Solid lines indicate significant linear regressions, dashed lines indicate insignificant linear regressions.

The larch CSAE trends from the Tatras are consistently negative with increasing age, however, one positive but insignificant trend ( $g=0.02$ ) is detectable in the larch data for the early calibration period 1901-1958. These findings are independent of trees species since the pine CSAE trends are also consistently negative, although insignificant for all calibration periods. Contrary to the Alps, the climate sensitivity of conifer trees in the Tatra Mountains decreases with age, proving the greater importance of geographical location compared to tree species.

It has to be noted, that the early calibration period 1901-1958 in almost all cases exhibits the lowest correlation values against the best-responding season and the weakest CSAE trends. This could be related to varying temperature trends over the 20<sup>th</sup> century (Konter et al. 2016) and contribute to the on-going discussion about the overall reliability of early meteorological measurements (Parker 1994, Frank et al. 2007a, Böhm et al. 2009).

## Conclusions

Age-related variations in the growth-climate relationships are present in many TRW datasets, but the magnitude of their impact and the orientation of trends seem to vary among species and geographical origins. The results from this study reveal the higher importance of geographical locations. Whereas the climate sensitivity of two species, *Larix decidua* and *Pinus cembra*, in the Alps increase with increasing age, it decreases in the Tatras with the trends being consistent in both species, but only significant for *Larix decidua*. More research is needed on this topic, since lack of clarity in physiological and climatological explanations for these opposed CSAE trends complicate the aggregation of larger networks including multiple species.

## Acknowledgements

We thank Tomas Kyncl, Dana Riechelmann, Stefan Reiffenberg, and Kolja König for sampling efforts and providing data. Ulf Büntgen was supported by the Ministry of Education, Youth and Sports of CR within the National Sustainability Program I (NPU I), grant number LO1415.

## References

- Böhm, R., Jones, P. D., Hiebl, J., Frank, D., Brunetti, M. and Maugeri, M. (2009): The early instrumental warm-bias: a solution for long central European temperature series 1760–2007. *Climatic Change* 101, 1-2: 41-67.
- Bond, B. (2000): Age-related changes in photosynthesis of woody plants. *Trends in Plant Science* 5: 349-353.
- Bunn, A., Mikko, K., Biondi, F., Campelo, F., Mérian, P., Qeadan, F. and Zang, C. (2016). dplR: Dendrochronology Program Library in R. R package version 1.6.4.
- Büntgen, U., Frank, D. C., J., K. R., Verstege, A., Zwijacz-Kozica, T. and Esper, J. (2007): Growth responses to climate in a multi-species tree-ring network in the Western Carpathian Tatra Mountains, Poland and Slovakia. *Tree Physiology* 27: 689-702.
- Büntgen, U., Brázdil, R., Frank, D. and Esper, J. (2010): Three centuries of Slovakian drought dynamics. *Climate Dynamics* 35, 2-3: 315-329.
- Büntgen, U., Kyncl, T., Ginzler, C., Jacks, D. S., Esper, J., Tegel, W., Heussner, K. U. and Kyncl, J. (2013): Filling the Eastern European gap in millennium-long temperature reconstructions. *Proceedings of the National Academy of Science USA* 110, 5: 1773-1778.
- Carrer, M. and Urbinati, C. (2004): Age-Dependent Tree-Ring Growth Responses To Climate In *Larix Decidua* And *Pinus Uncinata*. *Ecology* 85, 3: 730-740.
- Carrer, M., von Arx, G., Castagneri, D. and Petit, G. (2015): Distilling allometric and environmental information from time series of conduit size: the standardization issue and its relationship to tree hydraulic architecture. *Tree Physiology* 35, 1: 27-33.
- Cook, E., Briffa, K., Shiyatov, S. and Mazepa, V. (1990). Tree-ring standardization and growth-trend estimation. *Methods of Dendrochronology*. E. R. Cook and L. A. Kairiukstis. Dordrecht, The Netherlands, Kluwer Academic Publishers: 104-123.
- Cook, E. R. (1985). A Time Series Analysis Approach To Tree Ring Standardization. Ph.D. Thesis, University of Arizona.
- Cook, E. R. and Peters, K. (1997): Calculating unbiased tree-ring indices for the study of climatic and environmental change. *The Holocene* 7, 3: 361-370.
- Dorado Liñán, I., Gutiérrez, E., Heinrich, I., Andreu-Hayles, L., Muntán, E., Campelo, F. and Helle, G. (2011): Age effects and climate response in trees: a multi-proxy tree-ring test in old-growth life stages. *European Journal of Forest Research* 131, 4: 933-944.
- Esper, J., Cook, E. R., Krusic, P. J., Peters, K. and Schweingruber, F. H. (2003): Tests of the RCS method for preserving low-frequency variability in long tree-ring chronologies. *Tree-Ring Research* 59, 2: 81-98.
- Esper, J., Niederer, R., Bebi, P. and Frank, D. (2008): Climate signal age effects—Evidence from young and old trees in the Swiss Engadin. *Forest Ecology and Management* 255, 11: 3783-3789.

- Frank, D., Büntgen, U., Böhm, R., Maugeri, M. and Esper, J. (2007a): Warmer early instrumental measurements versus colder reconstructed temperatures: shooting at a moving target. *Quaternary Science Reviews* 26, 25-28: 3298-3310.
- Frank, D., Esper, J. and Cook, E. R. (2007b): Adjustment for proxy number and coherence in a large-scale temperature reconstruction. *Geophysical Research Letters* 34, 16: n/a-n/a.
- Fritts, H. C. (1976): *Tree Rings and Climate*. Academic Press, 567.
- Harti-Meier, C., Büntgen, U. and Esper, J. (2016): On the occurrence of cyclic larch budmoth outbreaks beyond its geographical hotspots. *TRACE* 14 14: 86-92.
- Holmes, R. L. (1983): Computer-assisted quality control in tree ring dating and measurement. *Tree Ring Bulletin* 43: 69-78.
- Jones, P. D., Lister, D. H., Osborne, T. J., Harpham, C., Salmon, M. and Morice, C. P. (2012): Hemispheric and large-scale land surface air temperature variations: An extensive revision and an update to 2010. *Journal of Geophysical Research* 117.
- Konter, O., Esper, J., Liebhold, A., Kyncl, T., Schneider, L., DÜthorn, E. and Büntgen, U. (2015a): Tree-ring evidence for the historical absence of cyclic larch budmoth outbreaks in the Tatra Mountains. *Trees* 29, 3: 809-814.
- Konter, O., Rosner, K., Kyncl, T., Esper, J. and Büntgen, U. (2015b): Spatiotemporal variations in the climatic response of *Larix decidua* from the Slovakian Tatra Mountains. *TRACE* 13.
- Konter, O., Büntgen, U., Carrer, M., Timonen, M. and Esper, J. (2016): Climate signal age effects in boreal tree-rings: Lessons to be learned for paleoclimatic reconstructions. *Quaternary Science Reviews* 142: 164-172.
- Linares, J. C., Tai'qui, L., Sangüesa-Barreda, G., Seco, J. I. and Camarero, J. J. (2013): Age-related drought sensitivity of Atlas cedar (*Cedrus atlantica*) in the Moroccan Middle Atlas forests. *Dendrochronologia* 31, 2: 88-96.
- Linderholm, H. W. and Linderholm, K. (2004): Age-dependent climate sensitivity of *Pinus sylvestris* L. in the central Scandinavian Mountains. *Boreal Environment Research* 9: 307-317.
- Parker, D. E. (1994): Effects Of Changing Exposure Of Thermometers At Land Station. *International Journal of Climatology* 14: 1-31.
- R Development Core Team (2014). R: A language and environment for statistical computing. R Foundation for Statistical Computing. Vienna, Austria.
- Rinn, F. (2007): TSAP Win Professional. Zeitreihenanalysen und Präsentation für Dendrochronologie und verwandte Anwendungen. Benutzerhandbuch. Rinntech, 91.
- Rossi, S., Deslauriers, A., Anfodillo, T. and Carrer, M. (2008): Age-dependent xylogenesis in timberline conifers. *New Phytologist* 177, 1: 199-208.
- Rozas, V., DeSoto, L. and Olano, J. M. (2009): Sex-specific, age-dependent sensitivity of tree-ring growth to climate in the dioecious tree *Juniperus thurifera*. *New Phytol* 182, 3: 687-697.
- Ryan, M. G. and Yoder, B. J. (1997): Hydraulic limits to tree height and tree growth. *BioScience* 47: 235-242.
- Yu, G., Liu, Y., Wang, X. and Ma, K. (2008): Age-dependent tree-ring growth responses to climate in Qilian juniper (*Sabina przewalskii* Kom.). *Trees* 22, 2: 197-204.
- Zang, C. and Biondi, F. (2015): treeclim: an R package for the numerical calibration of proxy-climate relationships. *Ecography* 38, 4: 431-436.



## **SECTION 2**

### **ECOLOGY**

# Frost rings in the service tree populations in Poland

A. Cedro<sup>1</sup> & B. Cedro<sup>2</sup>

<sup>1</sup>*Climatology and Meteorology Unit, Faculty of Geosciences, Szczecin University, Mickiewicza 16, 70-383 Szczecin, Poland*

<sup>2</sup>*Geology and Paleogeography Unit, Faculty of Geosciences, Szczecin University, Mickiewicza 16, 70-383 Szczecin, Poland*

*E-mail: anna.cedro@usz.edu.pl*

## Introduction

The emergence of frost rings (deformations) is associated with extreme weather conditions, mainly with the advection of cold water masses and temperature drop below 0°C during the growing period (particularly in late spring and summer, and also in early autumn) (Stone 1940). The temperature drop below the freezing point may occur during the night, whereas the temperature during the day is above zero. The low temperatures induce the formation of ice crystals in strongly hydrated xylem tissues, which results in tissue dehydration and deformation of vessels, tracheids and cells. Another mechanism of frost deformations has been reported from mountain areas: a temperature drop during the night may cause the water in the soil (frequently forming a thin cover only) to freeze, which renders the water unavailable to plants. Strong insolation and the associated intense transpiration during the day result in the “frost drought” resulting in tissue dehydration and the development of deformations (Schweingruber 2007).



Figure 1: Location of study plots (dots). The solid line marks the easternmost boundary of *Sorbus torminalis* range in Poland.

A frost ring may consist of layers of deformed tracheids and parenchymal cells (Schweingruber 1990, Gurskaya 2014). The site of a frost deformation in the annual ring indicates the timing of the deformation emergence; most frequently, this is a boundary between the late and early wood (the annual growth boundary), which dates the onset of frost to the beginning of cambial activity. Such deformation of tissue structure in the late wood will be associated with a rapid temperature drop in summer or early autumn (Payette et al. 2010, Brauning et al. 2016). Frost deformations affect part of the tree circumference only; in addition, they are more frequent in the lower part of the tree (Waito et al. 2013).

Frost rings are also used to reconstruct volcanic eruptions (La Marche & Hirschboeck 1984, Schweingruber 1989, Scuderi 1990, Banks 1992, Cedro 2004, Brauning et al. 2016). Volcanic dust transported to the stratosphere and spread there globally by strong winds restrict the amount of solar radiation reaching the surface of the Earth, thus resulting in temperature drop (Brunstein 1996).

This study was aimed at identification and dating of frost rings in populations of the service tree in Poland, relating their occurrence to unfavourable weather conditions, and exploring a possibility of using such deformations in dendroclimatological research.

## Material and Methods

The study involved samples collected with Pressler bores (1.3 m above the ground) from 612 specimens of the service tree (*Sorbus torminalis* L.) growing at 31 plots in Poland, at the north-eastern boundary of the species' geographic range in Europe (Fig. 1). A total of 984 samples were collected and a total of 81 043 annual growth rings were measured (Cedro 2016). The growth ring width was measured, to 0.01 mm, under a zoom-adjusted stereomicroscope. During sample examination, all irregularities in the ring structure were recorded: frost rings, missing rings, zones of strong growth reduction, traces of mechanical damage, callus, etc. Subsequently, the annual growth rings were dated using the classical dendrochronological cross-dating method, and 31 plot chronologies were developed using standard procedures (Cedro 2016). The data obtained served as a basis on which to study the abundance of frost rings and to date them.

## Results

Examination of annual growth rings of the service tree samples yielded 413 rings with frost deformations, which accounted for 0.51% of all the rings measured (81 043). The highest number of frost rings (44) was found in the specimens growing at Jamy (chronology JM1 from the eastern range boundary), the lowest number (1) being identified at Legnica (LE). Large numbers (more than 30) of frost rings were recorded at Smolarz (SM), Jarocin (JA) and Taczanów (TA). On the average, a plot chronology revealed 13 frost-deformed rings. The percentage contributions of frost rings were as follows: the lowest percentage (0.04%) was recorded at Legnica (LE), the highest percentage (2.27%) being typical of Taczanów (TA). Chronologies JM1, SM, TRZ and PI1 showed more than 1% of frost deformations (Fig. 2). As many as 84% deformations were found in the first 50 rings measured, which could be identified as the juvenile wood. On 13 plots (JM2, WZ, KZ, DPN, SM, PN1, WPN, PI2, LE, JW1, JW2, SO and SS), all the frost rings were found within the 50 rings closest to the pith (class 1-50); they were at their fewest (only 33%) at Gryfino (GR) (Fig. 3). The growth ring class 51-100 showed 14% of frost rings (13 specimens lacked such rings); the maximum proportion (67%) was recorded at GR. The fewest frost rings occurred in rings 100 and higher (class >100), as there were as little as 2% of such deformations, which were recorded at 4 sites only: Kwidzyn (KW), Jamy (JM1), Osie (OS) and Jarocin (JA) (Fig. 3).

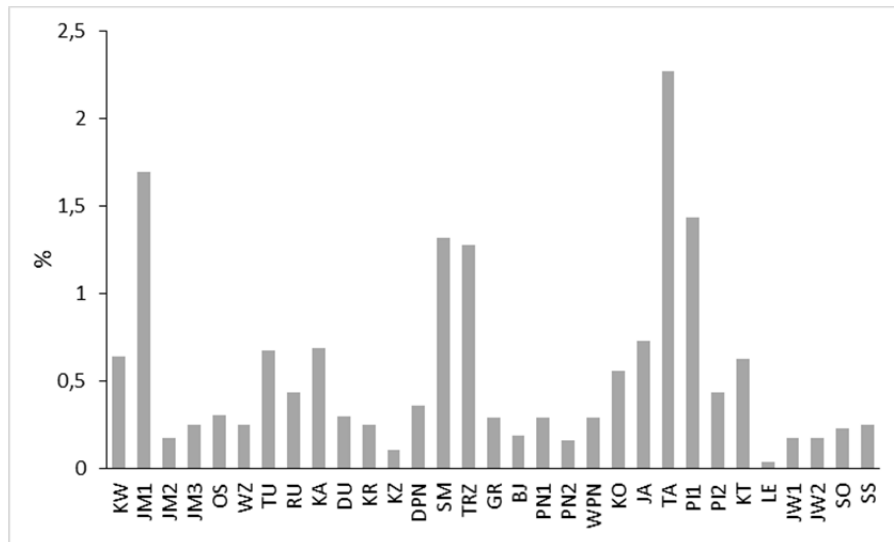


Figure 2: Percentages of frost rings in wild service tree populations.

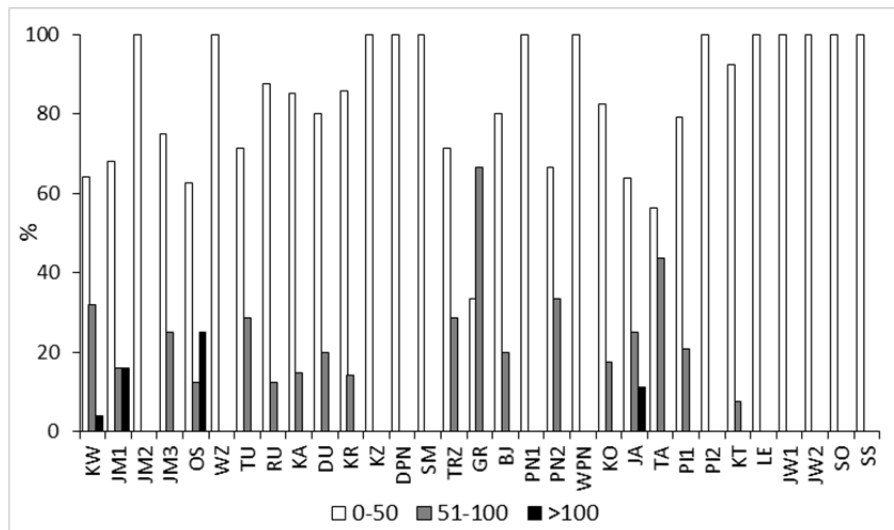


Figure 3: Percentages of frost rings in class: 0-50 (the first 50 tree rings measured), 51-100 and in rings 101 and above (>100) in wild service tree populations in Poland.

The service tree stand in Jarocin Forest District (JA) (Fig. 1) provides an example of a population with frost deformation. Among the 4962 annual growth rings measured, there were 36 (0.73%) frost rings. The first 50 rings (class 0-50) showed 64% (i.e. 23) deformed ones; rings 51-100 contained 25% (9 rings), rings 100 and above showing 11% (4 rings) (Fig. 3). A single year, 1875, showed four repetitions of frost deformations; three repetitions each were assigned to 1936 and 1941, two each – to 1869, 1872, 1939 and 1943, the remaining years showing frost deformation occurrence intermittently (Fig. 4). The full detailed set of meteorological data is available for Kalisz only, a site located 43 km away from the study plot, and only for a few last years showing the presence of frost rings. An example is furnished by the year 2011: the minimum temperature below 0°C was recorded on 4-5 May (Fig. 5).

## Discussion and Conclusions

The results obtained evidence poor applicability of the data on the abundance and temporal sequence of frost rings in the Polish wild service tree populations to dendroclimatological analyses. Virtually all the frost rings (except for 2-3 cases) were found at the borderline between the late

wood and the summer wood, which points to spring as the time of inclement weather conditions resulting in deformations. At the same time, frost rings were often associated with reduced annual growth. Deformations of this type results in poorer timber quality; the wood frequently breaks at the frost ring (Fig. 6). As many as 84% of frost rings were associated with juvenile wood and occurred in different years in the trees growing at a single plot, exposed to identical habitat conditions and inclement weather situations. Young small-diameter trees and with bark thinner than that of adult trees are more susceptible to temperature drops, as confirmed also by studies involving other species (Gurskaya & Shiyatov 2002, 2006, Cedro 2012, Gurskaya 2014, Brauning 2016). Insufficient isolation from external conditions results, during the cambial activity and a temperature drop below the freezing point, in the formation of ice crystals in interstitial spaces of the strongly hydrated tissue under the bark. This deforms the vessels and cells, the deformations being visible on each cross-section (Figs. 7, 8). Dendroclimatological studies, which usually do not rely on signals recorded in juvenile wood, may make use of frost rings developed in mature trees, but these feature frost deformations relatively seldom and, when found, the frost rings are difficult to correlate with time.

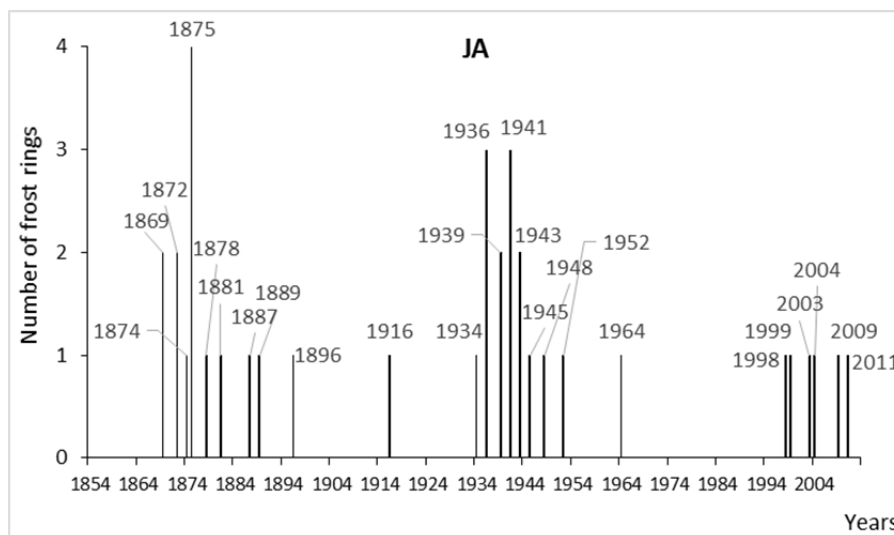


Figure 4: Years with frost deformations in wild service tree chronology JA.

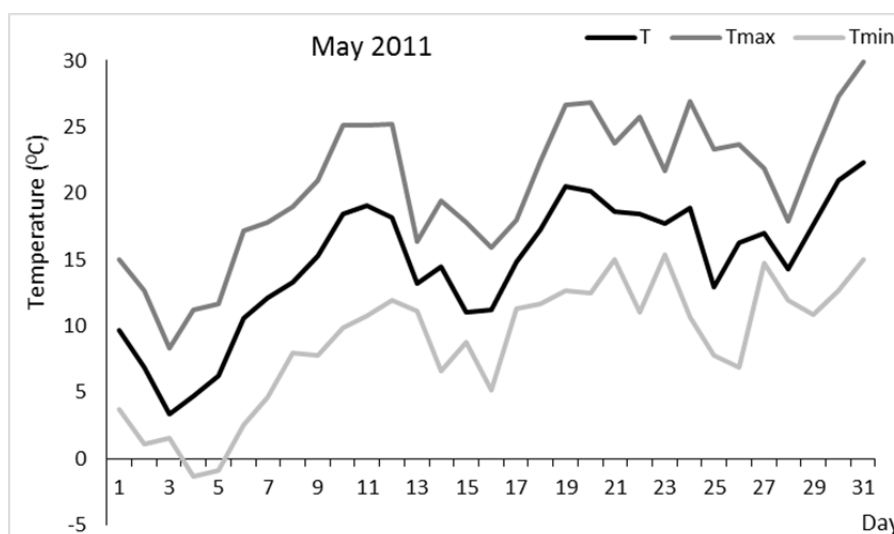


Figure 5: Air temperature in May 2011 in Kalisz.  $T$  – average temperature,  $T_{max}$  – maximum temperature,  $T_{min}$  – minimum temperature. Data source: [www.tutiempo.net](http://www.tutiempo.net).

Similar results on frost rings have been reported for the yew populations in Poland (Cedro 2012). A total of 803 frost rings (out of 102 606 growth rings measured) were identified, the frost rings accounting for 0.78% of all the rings. It was in 10 out of the 35 populations only that the percentage of frost rings exceeded 1%, the maximum share being 4.19% (Rokita Forest District). The first 50 rings contained 79% of all the frost-induced deformations; class 51-100 showed a little above 15% of the deformations which proved least numerous (around 6%) in the ring class >100. As the yew is dioecious, male and female specimens were analysed separately, male trees being found more sensitive to low temperatures in spring and early summer (Cedro 2012).

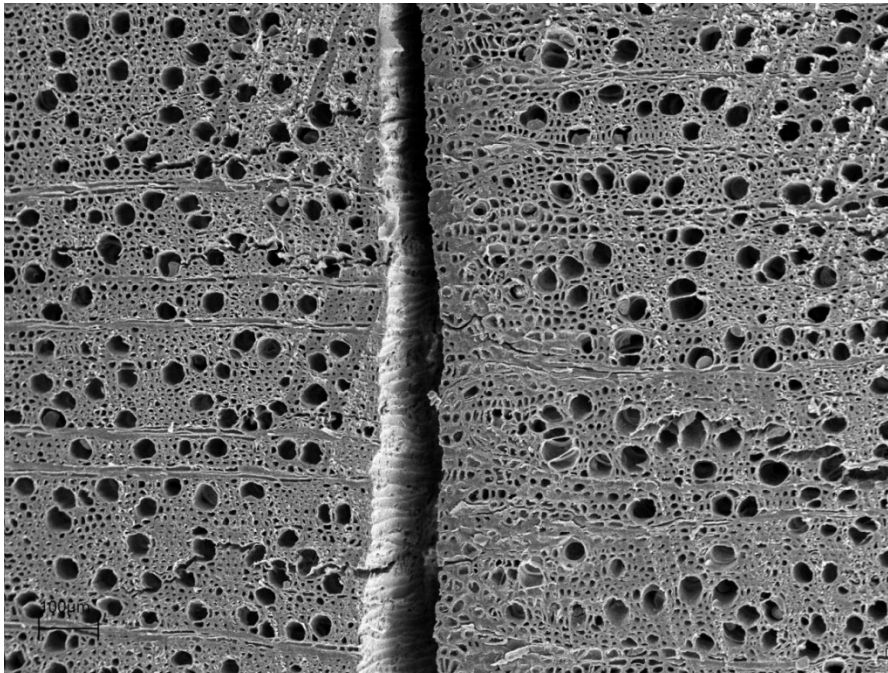


Figure 6: A frost ring weakens the wood and causes its breakage at the ring border (a wild service tree from Taczanów Forest District, TA7), transverse section, x200 magnification.

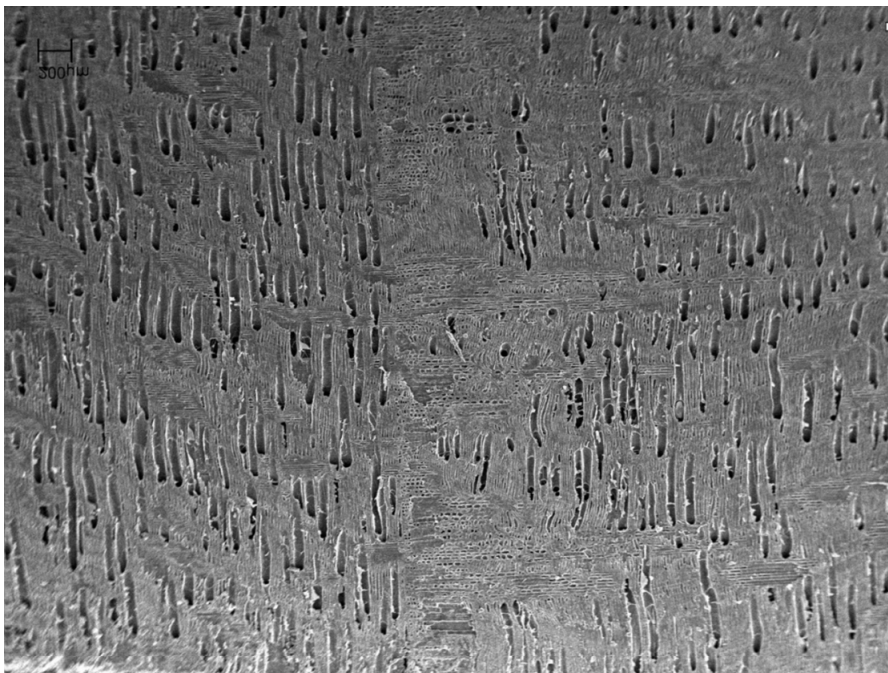


Figure 7: A frost ring in radial section, x70 magnification, tree no. TA12 from Taczanów Forest District (TA).

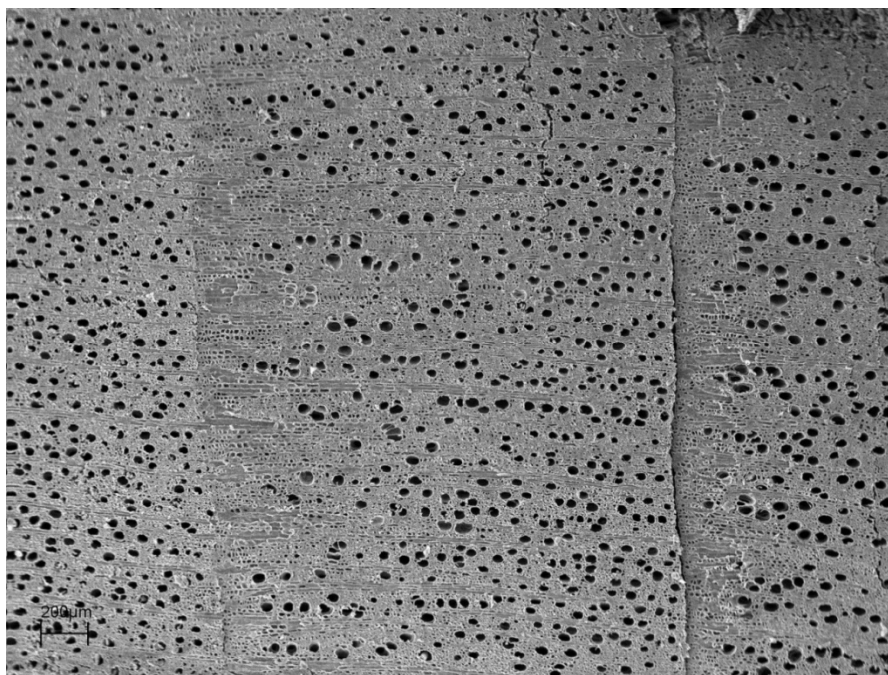


Figure 8: Frost rings in consecutive years in a transverse section, x100 magnification, tree no. TA16 from Taczanów Forest District (TA).

### Acknowledgements

The project was supported by the Polish National Science Centre grant No. DEC-2011/03/B/ST10/06157.

### References

- Banks, J.C.G. (1992): A review of the use of tree rings for the quantification of forest disturbances. Lundqua report. Tree rings and environment. Proceedings of the International Dendrochronological Symposium, Ystad, South Sweden, 3-9.09.1990. Lund, vol. 34: 3-13.
- Brauning, A., De Ridder, M., Zafirov, N., Garcia-Gonzalez, I., Dimitrov, D.P., Gartner H. (2016): Tree-ring features: indicators of extreme event impacts. *IAWA Journal* 37(2): 206-231.
- Brunstein, F.C. (1996): Climatic significance of the Bristlecone Pine latewood frost-ring record at Almagre Mountain, Colorado, U.S.A. *Arctic and Alpine Research*, vol. 28, no. 1: 65-76.
- Cedro, A. (2012): Dendrochronologia cisa pospolitego w Polsce i na zachodniej Ukrainie (Dendrochronology of yew in Poland and western Ukraine). Zapol, Szczecin: 1-230.
- Cedro, A. (2017): Dendrochronologia jarzęba brekinii (*Sorbus torminalis* L.) w Polsce. (Dendrochronology of wild service tree (*Sorbus torminalis* L.) in Poland). In press.
- Gurskaya, M.A. (2014) Temperature conditions of the formation of frost damages in conifer trees in the high latitudes of Western Siberia. *Biology Bulletin* 41/2: 185-195.
- Gurskaya, M.A., Shiyatov, S.G. (2002): Formation of two xylem frost injuries in one annual ring in Siberian spruce under conditions of Western Siberian forest – tundra. *Russian Journal of Ecology*, vol. 33, no. 2: 73-79.
- Gurskaya, M.A., Shiyatov, S.G. (2006): Distribution of frost injuries in the wood of conifers. *Russian Journal of Ecology*, vol. 37, no. 1: 7-12.
- La Marche, V.C. Jr., Hirschboeck, K.K. (1984): Frost rings in trees as record of major volcanic eruptions. *Nature* 307: 121-126.
- Payette, S., Delwaide, A., Simard, M. (2010): Frost-ring chronologies as dendroclimatic proxies of boreal environments. *Geophysical Research Letters*, vol. 37, L02711, doi:10.1029/2009GL041849.

- Scuderi, L.A. (1990): Tree-ring evidence for climatically effective volcanic eruptions. *Quaternary Research* 34: 67-85.
- Schweingruber, F.H. (1989): Tree rings. Basics and applications of dendrochronology. Kluwer Academic Publishers: 1-276.
- Schweingruber, F.H. (1990): Microscopic wood anatomy. Swiss Federal Institute for Forest, Snow and Landscape Research: 1-226.
- Schweingruber, F.H. (2007): Wood structure and environment. Springer series in wood science. Springer: 1-279.
- Stone, E.L. Jr. (1940): Frost rings in longleaf pine. *Science* 92/2395: 478.
- Waito, J., Conciatori, F., Tardif, J.C. (2013): Frost rings and white earlywood rings in *Picea mariana* trees from the boreal plains, Central Canada. *IAWA Journal* 34: 71-87.

# Tree-ring reductions among Norway spruce in relation to air pollution and a human morbidity – examples from southern Poland

P. Rutkiewicz, I. Malik, M. Wistuba & D. Gawior

Department of Reconstructing Environmental Change, University of Silesia in Katowice, ul. Będzińska 60,  
41-200 Sosnowiec, Poland  
E-mail: rutkiewiczpawel33@gmail.com

## Introduction

Air pollutants have an adverse impact on the tree health, that can even lead to its permanent damage. Different species of trees are characterized by varying degrees of sensitivity to air pollutants (Gawrońska 2000, Szychowska-Krąpiec & Wiśniowski 1996). Annual tree rings developed during high air pollution events are in general narrow (Borecki 1993). Such reaction of trees can be used as a source of information on the duration and strength of the impact of pollutants on tree stands and environment (Szychowska-Krąpiec 2009). There are numerous examples of studies on the influence of air pollution on coniferous trees growth suppression (Baes & McLaughlin in 1984, Danek 2007, Krąpiec & Szychowska-Krąpiec 2001, Malik et al. 2010). This effect was particularly clear in Central Europe in the 1970s and 1980s, when air pollution was on a very high level (Kandler & Innes 1995, Mazurski 2008). In the last decades emissions in Poland and in neighbouring countries have been significantly reduced and are no longer a significant threat (Duszyński 2014). However, since the beginning of the 21<sup>st</sup> century, the increase of air pollution has again been noticed, in particular, as a result of low emission from single-family detached houses with coal-based heating systems. This type of low emission determines the occurrence of abnormal events of air pollutant concentrations (Juda-Rezler & Manczarski 2010). Undoubtedly, the scale of contemporary emission is much smaller compared to industrial emissions in the second half of the 20<sup>th</sup> century, but at the local scale it may cause serious problems for environment and human health. Air pollution can cause increased incidence of morbidity and mortality among people. Even relatively low concentrations of very fine dust negatively affect human respiratory and cardiovascular system (Juda-Rezler & Kowalczyk 2010). The negative effects on human health increase with the increase of pollutant concentration and the length of contamination exposure (Malik et al. 2012). Previous studies show that the tree-ring reductions resulting from air pollution occurred earlier than the negative health effects among people (Malik et al. 2012). Therefore, they could possibly be used as an indicator of the future adverse health effects among humans.

The aim of the study was to determine periods of tree-ring reductions observed in trees (Norway spruce) growing near the centre of Zakopane and Nowy Targ, where the problem of air pollution is particularly burdensome. Moreover, potential relationships were sought between the time of reduction occurrence and changes in air pollution and morbidity among humans.

## Materials and methods

The preliminary study was carried out in southern Poland where we collected 36 cores from spruces (*Picea abies*) growing in the vicinity of Zakopane (16 cores) and Nowy Targ (20 cores) city centers. In our study we have selected Norway spruce among other coniferous tree species because it is sensitive to air pollution (Merkert et al. 2012). While selecting sampling sites we excluded areas located on slopes to eliminate the possible impact of mass movements on tree growth causing ring eccentricity and reaction wood development. Therefore we selected sites located on flat areas. Cores were collected using Pressler borer at the breast height. From each tree one core was taken from the same, south side of the stem, to ensure as far as possible,

uniform tree-ring pattern. We excluded tilted or injured trees, however, in our study we have included trees with damaged/reduced assimilation apparatus assuming that it may result from pollution. On each study site we have sampled all suitable trees which met above described criteria. Samples were glued into wooden holders and sanded to reveal wood anatomical structure. The first stage of the analysis was skeleton plot development, that was done for each core. These allowed quick dating of the radial growth reduction periods for each tree, which are present at the Fig. 1B and Fig. 2D as a beginnings of reductions. Then widths of annual tree rings were measured and local raw chronologies were developed. Tree ring patterns were unusual. It was not observed in the individual trees, characteristic tree ring growth pattern, which excludes the application of detrending (negative exponential curve). Tree-ring reduction periods were then determined for particular tree and divided into two categories: weak and strong reductions. Their values were calculated as the ratio between the sum of tree-ring widths of all rings in a reduction period and the sum of tree-ring widths of the same number of rings from the period before the reduction (Schweingruber et. al. 1985). Strong reductions were recognized when the average width of the series of at least three annual rings was lesser than 50% of the average width of the same number of tree rings preceding the reduction period. A similar rule was used for the weak (30-50%) reductions. Developed reduction graphs were compared with the data from the Regional Inspectorate for Environmental Protection in Krakow on air pollution in Zakopane and Nowy Targ, in the period 2000-2014. We analysed concentration of sulphur dioxide ( $\text{SO}_2$ ), nitrogen dioxide ( $\text{NO}_2$ ) and dust ( $\text{PM}_{10}$ ). Moreover, statistical data on the lung diseases morbidity for the same period, for the Małopolskie voivodeship were collected (Central Statistical Office of Poland (GUS)), as detailed epidemiological data for Zakopane and Nowy Targ were not available. We compared temporal patterns of data under study in search of common tendencies and relationships between the reduction of annual tree-ring widths, air pollution and the number of patients with lung diseases.

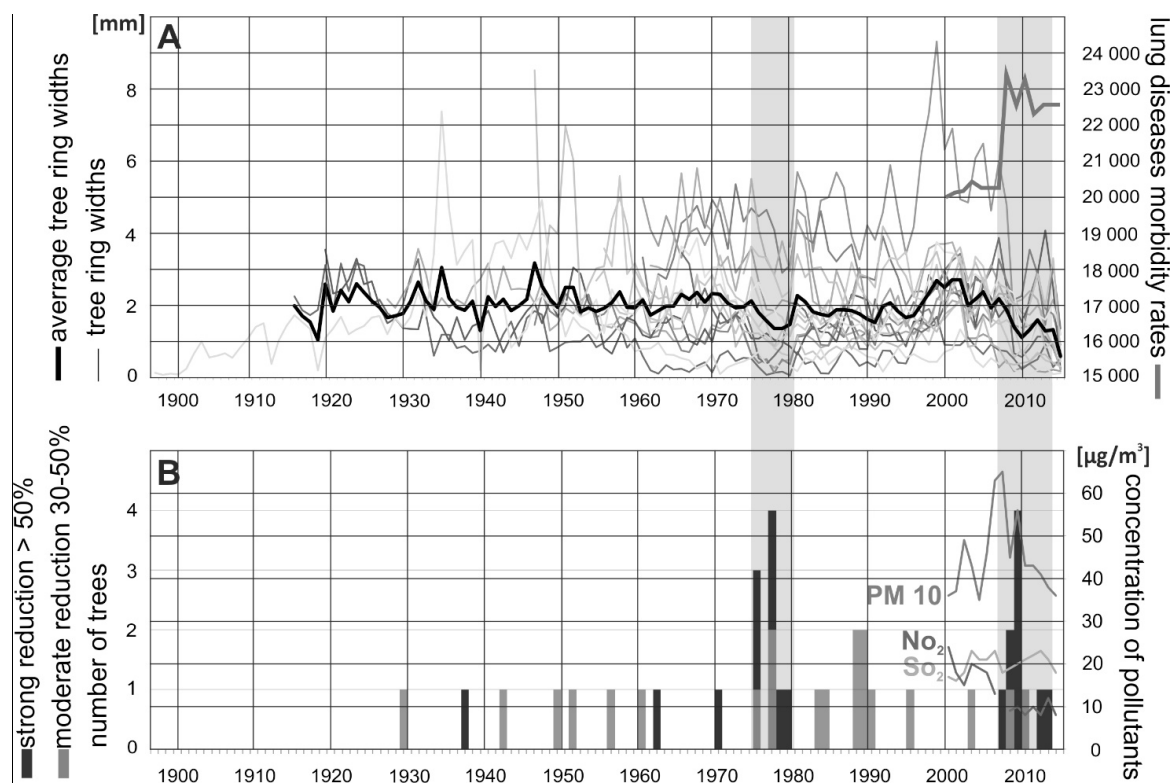


Figure 1: Dendrochronological data for the Zakopane study site: tree-ring widths (A) and number of trees showing the beginnings of ring reductions (B) compared to lung diseases morbidity rates and air pollution level in Zakopane..

## Results

Tree-ring data gathered in Zakopane show two reduction periods while in trees growing in Nowy Targ only one period was found. In Zakopane these are the 1970s (56 percent of all trees), which average lasted five years, with a strong and common reduction in 1977, and the period since 2007 (63 percent of all trees), which continues to the present. Particularly strong and common reduction was found in 2009 (Fig. 1). In Nowy Targ clear and common tree-ring width reductions (75 percent of all trees) started in 2003 and continue also to the present (Fig. 2). In all periods observed, both in Zakopane and in Nowy Targ, strong reductions predominate, while in other periods they are rare. The highest number of trees with strong ring reductions were identified in 2007, in case of Zakopane and in 2003, in case of Nowy Targ (Fig. 1, Fig. 2).

During the period 2000-2014, the concentrations of sulphur dioxide and nitrogen dioxide in Zakopane were more or less constant, even with a slight decreasing tendency. On the other hand, concentrations of dust (PM<sub>10</sub>) increased in both study sites, reaching particularly high values in 2007 (Zakopane) and in 2006 (Nowy Targ). The morbidity data for the whole Małopolskie voivodeship shows a slight increase in 2001-2007 period and significant raise since 2008 (Fig. 1, Fig. 2).

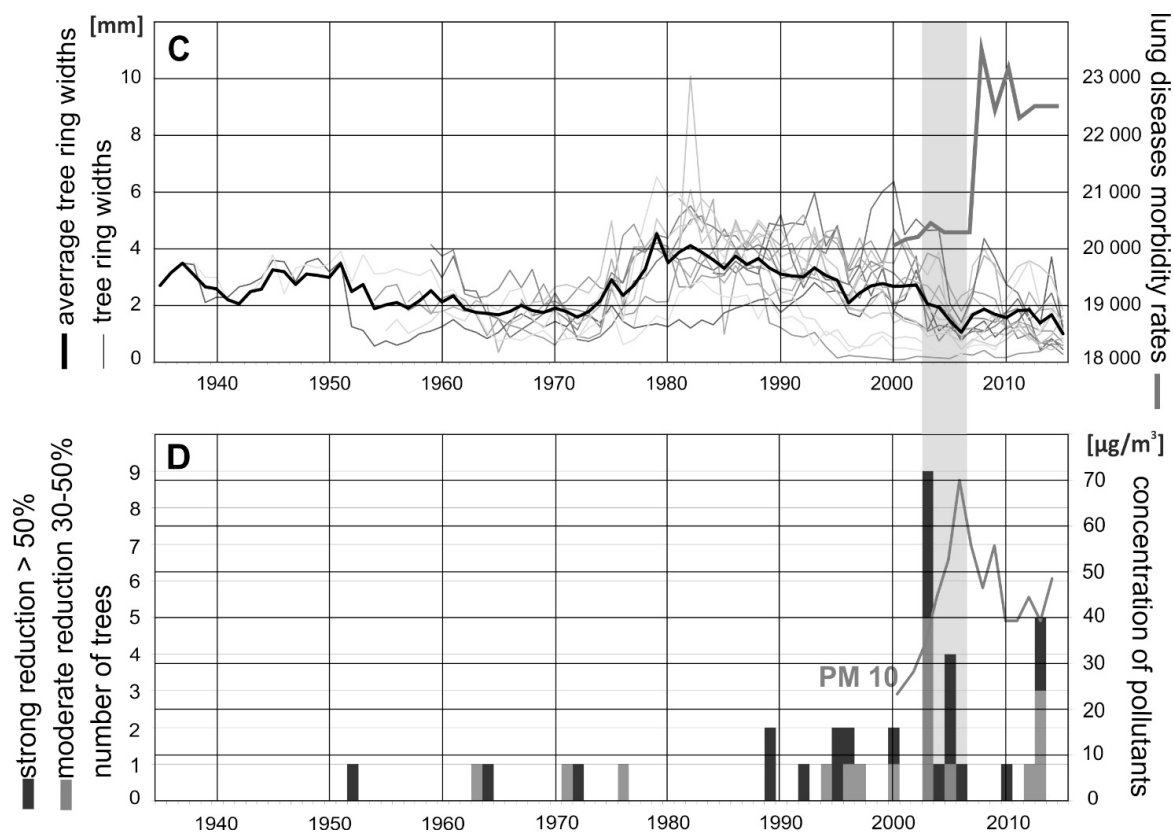


Figure 2: Dendrochronological data for the Nowy Targ study site: tree-ring widths (C) and number of trees showing the beginnings of ring reductions (D) compared to air pollution level in Nowy Targ and lung diseases morbidity rates.

## Discussion

The oldest among identified periods of tree-ring reductions – from the 1970s – is probably associated with the intensive development of industry in Poland and in Central Europe after the World War II. Numerous examples of deep reductions in annual tree rings were documented for that period, among all also local, massive tree mortality events (Danek 2007, Elling et al. 2009, Malik et al. 2012). The younger periods of reductions in tree-ring widths observed in Zakopane and

in Nowy Targ are probably associated with low emissions of air pollutants, responsible also for current poor air quality in vast parts of Poland (Dębski et al. 2015). With the Poland's accession to the European Union in 2004 quality standards for coal have been abolished and new regulations have not been established. Low quality, sulphur-contaminated coal started to be used for heating and as a result in many areas radial growth of conifers has been suppressed (Malik et al. 2012, Sensuła et al. 2015). The problem of low emission and thus the phenomena of contemporary tree-ring reductions is common in Poland. Trees in numerous forest stands, mainly coniferous, show signs of diseases and even increase tree mortality (Starzyk et al. 2005). Reductions of tree rings which occurred in the 21<sup>st</sup> century among trees growing in Zakopane and in Nowy Targ, affect more trees and are surprisingly stronger compared to tree-growth suppressions from the 1970s, although reductions in 1960-1980 are often considered as severe and caused by particularly strong industrial air pollution. The study conducted in Zakopane and Nowy Targ was preliminary and it covers a very short period of time, too short for extensive epidemiological conclusions. However, neither Zakopane, nor Nowy Targ are industrial cities. Industrial air pollution in the 1970s came only from long-distance transport and is not strongly recorded in tree rings. This explains why tree-ring reductions in 2003 and 2007, being a reaction to a local factor, are much stronger and more common among sampled trees.

Comparison of the tree-ring reductions in Zakopane and in Nowy Targ with pollution data suggests that PM10 dust is responsible for the recent tree health and radial growth deterioration. Michalik (2009) suggests that dust from the low emissions is often more toxic than the dust coming from industrial emissions. Although the increase in the dust pollution is synchronous with the appearance of the reduction in trees under study, it is difficult to directly connect the two phenomena. Reductions of annual tree rings that are started in 2003 and since 2007, an increase in dust pollution and increased lung disease morbidity occur almost at the same time or within few following years. This may mean that there is a cause-and-effect relationship between air pollution and growth suppression among spruces, as well as between air pollution and its adverse health effects on human population. The main issue is that morbidity data used in the analysis concern the entire Malopolskie voivodeship, while pollution data and tree-ring data were obtained only for the region of Zakopane and Nowy Targ. Still, the pilot study presented in the paper shows that adverse health effects among people in Zakopane are not delayed in relation to growth response of trees, while in the case of Nowy Targ the effect is delayed. Previous studies conducted in industrial areas of Poland indicated significant (a few-year long) delay of human reaction to pollution compared to effects observed in trees (Malik et al. 2012). It is worth noting that the results can be influenced by the fact that trees were not the same age (they could react differently to pollution). It is also necessary to take into consideration other factors that could cause the observed tree-ring reductions. Therefore in further studies factors such as climatic factors, site related factors or insect outbreaks will be incorporated.

## Conclusions

1. The investigated trees developed reduced annual rings in the two periods: in the 1970s, and recently, since 2003/2007. The first period of growth reductions is probably related to the high emission of industrial pollution. The second may be due to harmful, low emissions from single-family detached houses. Tree-ring reductions developed in the 21<sup>st</sup> century are more common among sampled trees and stronger than reductions recorded in the 1970s. This indicates severe impact of factor suppressing tree growth in recent years.
2. Recent reductions of annual rings in trees growing in Zakopane and Nowy Targ have appeared synchronously with the increasing dust pollution. This means that low emission of dust into the atmosphere is probably responsible for growth suppression among Norway spruce.
3. Both dust pollution, reductions of annual tree rings and the lung disease morbidity among people have increased in the recent years. Perhaps the increased emission of pollutants contributes not only to the decline of tree health but also to the alarming increase of adverse health effects among

human population. However, to confirm the preliminary results, there is a need for extending research: collecting tree-ring data in other locations and obtaining more accurate epidemiological data.

### Acknowledgements

Studies were supported by the Polish National Science Centre through grant no. 2011/01/B/ST10/07096.

### References

- Baes III, C.F., & McLaughlin, S.B. (1984): Trace elements in tree rings: evidence of recent and historical air pollution. *Science*, 224(4648): 494-497.
- Borecki, T. (1993): Metodyczne podstawy wielkoobszarowej inwentaryzacji zdrowotnego stanu lasu dla leśnictwa. *Prace Instytutu Badań Leśnictwa, Ser. B*, 18: 7-11.
- Danek, M. (2007): The influence of industry on Scots pine stands in the south-eastern part of the Silesia-Krakow Upland (Poland) on the basis of dendrochronological analysis. *Water, Air, and Soil Pollution*, 185(1-4): 265-277.
- Dębski, B., Olecka, A., Bebkiewicz, K., Kargulewicz, I., Rutkowski, J., Zasina, D., Zimakowska – Laskowska, M., Żaczek, M. (2015): Krajowy Bilans Emisji SO<sub>2</sub>, NO<sub>x</sub>, CO, NH<sub>3</sub>, NMLZO, pyłów, metali ciężkich i TZO. Krajowy Ośrodek Bilansowania i Zarządzania Emisjami (KOBiZE), *Instytut Ochrony Środowiska – Państwowy Instytut Badawczy*. Warszawa.
- Duszyński, F. (2014): Zapis zanieczyszczenia powietrza w przyrostach rocznych drzew= The record of air pollution in tree rings. *Przegląd Geograficzny*, 86(3): 317-338.
- Elling, W., Dittmar, C., Pfaffelmoser, K., Rötzer, T. (2009): Dendroecological assessment of the complex causes of decline and recovery of the growth of silver fir (*Abies alba* Mill.) in Southern Germany. *Forest Ecology and management*, 257(4): 1175-1187.
- Gawrońska, G. (2000): Wpływ zanieczyszczenia atmosfery na lasy Krainy Karpackiej. *Rocznik Ochrona Środowiska*, (Tom 2): 195-204.
- Juda-Rezler, K., Kowalczyk, D. (2013): Size distribution and trace elements contents of coal fly ash from pulverized boilers. *Pol. J. Environ. Stud*, 22(1): 25.
- Juda-Rezler, K., Manczarski, P. (2010): Zagrożenia związane z zanieczyszczeniem powietrza atmosferycznego i gospodarką odpadami komunalnymi. *Nauka*, 4: 97-106.
- Kandler, O., Innes, J.L. (1995): Air pollution and forest decline in Central Europe. *Environmental pollution*, 90(2): 171-180.
- Krapiec, M., Szychowska-Krapiec, E. (2001). Tree-ring estimation of the effect of industrial pollution on pine (*Pinus sylvestris*) and fir (*Abies alba*) in the Ojcow National Park (southern Poland). *Nature Conservation*, 58: 33-42.
- Krok, K. (2004): Zmiany zanieczyszczenia środowiska na obszarach ekologicznego zagrożenia w Polsce. *Studia Regionalne i Lokalne*, 5(17): 119-141.
- Malik, I., Danek, M., Krąpiec, M. (2010): Air pollution recorded in Scots pine growing near a chemical plant, preliminary results and perspective (Upper Silesia, southern Poland). *TRACE—Tree Rings in Archaeology Climatology and Ecology*, 8: 41-45.
- Malik, I., Danek, M., Marchwińska-Wyrwał, E., Danek, T., Wistuba, M., Krąpiec, M., Woskowicz-Ślęzak, B. (2012): Czasowe relacje pomiędzy redukcjami przyrostów rocznych sosny zwyczajnej (*Pinus sylvestris* L.) oraz śmiertelnością niemowląt pod wpływem zanieczyszczeń atmosferycznych – przykład z województwa śląskiego. *Ochrona Środowiska i Zasobów Naturalnych* 54: 248–260.
- Malik, I., Danek, M., Marchwińska-Wyrwał, E., Danek, T., Wistuba, M., Krąpiec, M. (2012): Scots pine (*Pinus sylvestris* L.) growth suppression and adverse effects on human health due to air pollution in the Upper Silesian Industrial District (USID), Southern Poland. *Water, Air, & Soil Pollution*, 223(6): 3345-3364.
- Marchwinska-Wyrwal, E., Dziubanek, G., Skrzypek, M., Hajok, I. (2010): Study of the health effects of long-term exposure to cadmium and lead in a region of Poland. *International journal of environmental health research*, 20(2): 81-86.

- Mazurski, K.R. (2008): Destruction of forests in the Sudetes—thirty years later,[w:] Výroční konference ČGS, Sborník příspěvků, Liberec, 25–29.08. 2008.
- Merkert, B., Wünschmann, S., Diatta, J., Chudzińska, E. (2012): Innowacyjna obserwacja środowiska – bioindykatory i biomonitoring: definicje, strategie i zastosowania. *Ochrona Środowiska i Zasobów Naturalnych* (53): 115–152.
- Michalik, P. (2009): Niska emisja-świadomość zagrożenia z niej wynikających wśród różnych grup społecznych na przykładzie rolników z powiatu płockiego i sierpeckiego. *Ochrona Środowiska i Zasobów Naturalnych*, (40): 617–622.
- Sensuła, B., Wilczyński, S., Opała, M. (2015): Tree growth and climate relationship: dynamics of Scots pine (*Pinus sylvestris* L.) growing in the near-source region of the combined heat and power plant during the development of the pro-ecological strategy in Poland. *Water, Air, & Soil Pollution*, 226(7): 1-17.
- Schweingruber, F.H., Kontic, R., Niederer, M., Nippel, C.A., Winkler-Seifert, A. (1985): Diagnosis and distribution of conifer decay in the Swiss Rhone Valley a dendrochronological study. In: Turner, H., Tranquillini W. (ed.): *Establishment and Tending of Subalpine Forest*. Berno: 189–192.
- Starzyk, J.R., Grodzki, W., Capecki, Z. (2005): Występowanie kornika drukarza *Ips typographus* [L.] w lasach zagospodarowanych i objętych statusem ochronnym w Górcach. *Leśne Prace Badawcze*, (1): 7-30.
- Szychowska-Krapiec, E. (2009). Monitoring drzewostanów zagrożonych przez emisje przemysłowe,[w:] A. Zielski, M. Krapiec (red.): *Dendrochronologia*: 243-250.
- Szychowska-Krapiec, E., Wisniowski, Z. (1996): Zastosowanie analizy przyrostów rocznych sosny zwyczajnej (*Pinus sylvestris*) do oceny wpływu zanieczyszczeń przemysłowych na przykładzie zakładów chemicznych "Police" (woj. szczecińskie). *Geologia-Kraków*, 22: 281-299.

# High-elevation inter-site differences in Mount Smolikas tree-ring width data

L. Klippel<sup>1</sup>, P.J. Krusic<sup>2</sup>, C. Hartl-Meier<sup>1</sup>, V. Trouet<sup>3</sup> & J. Esper<sup>1</sup>

<sup>1</sup>Department of Geography, Johannes Gutenberg University, Mainz, Germany

<sup>2</sup>Stockholm University, Sweden

<sup>3</sup>University of Arizona, USA

E-mail: laklippe@uni-mainz.de

## Introduction

Tree-ring chronologies of maximum latewood density (MXD) of *Pinus heldreichii* CHRIST, an endemic species of the Balkan Peninsula, are most suitable to reconstruct annually resolved late summer temperatures and further our understanding of past climate variability in the Eastern Mediterranean (Klesse et al. 2015, Trouet et al. 2012, Trouet 2015). In contrast, studies of tree-ring width (TRW) of *P. heldreichii* reported relatively weak and temporarily unstable climate signals (Panayotov et al. 2010, Seim et al. 2012, Todaro et al. 2007) owing to a temporarily unstable drought signal or the complex interaction of high temperatures and low precipitation. To assess tree-ring/climate associations in this old-growth species, we here present TRW records from a northwest- and a south-facing *P. heldreichii* site located near treeline in the Pindus Mountains in Greece and explore the importance of changing slope aspect on growth and climate signal.

## Data and Methods

### Study area and data collection

Mt. Smolikas (2637m a.s.l., 40.1N, 20.9E), situated in northern Greece (Fig.1), is the highest peak of the Pindus range stretching from southern Albania to the Peloponnese. Geologically, the range is an extension of the Dinaric Alps and consists of serpentine (ophiolitic) rocks (Hughes et al. 2006, Stevanovic et al. 2003). One hundred and one samples from 51 living *P. heldreichii* trees were collected at two sites near treeline on NW- and S-exposed slopes of Mt. Boghdhani (2236m a.s.l.) (Fig. 1), an eastern foothill of Mt. Smolikas, using 5 mm increment corers. The mean number of rings per sample is 446 and 372 with a minimum of 229 and 215 years and a maximum of 866 and 553 years at the NW- and S-facing sites, respectively.

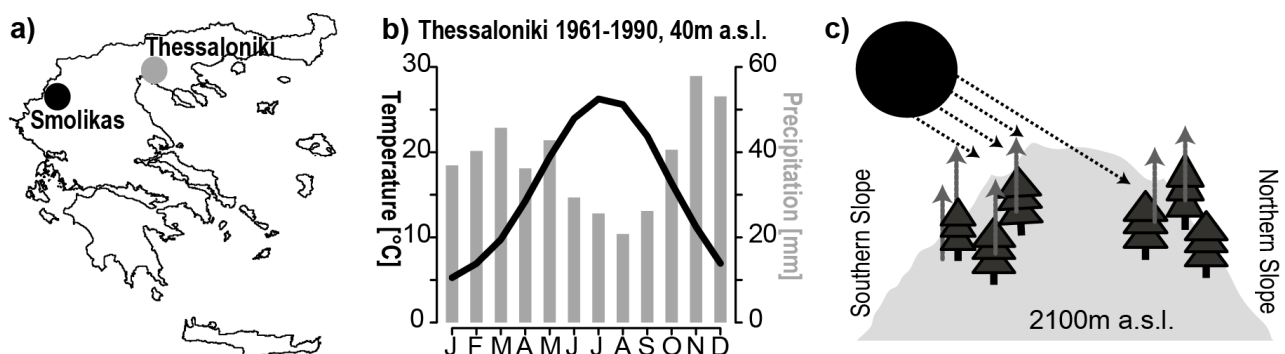


Figure 1: a) Map of Greece indicating the location of the investigation area (black circle) and the climate station (grey circle) and b) climate diagram of the meteorological station in Thessaloniki (40 m a.s.l., 1961-1990) and c) sampling design with sites according to slope exposure.

### Meteorological data

Due to limited availability and time-series length of nearby meteorological records (e.g. Ioannina, Metsovo), TRW chronologies were calibrated against temperature and precipitation data from the meteorological station in Thessaloniki (Fig.1) over the period 1931-2014. To estimate the influence of drought on tree growth, the 1- and 2- month standardized precipitation evaporation index (SPEI-1, SPEI-2), which integrates precipitation and temperature, was calculated and calibrated against the TRW chronologies (Vicente-Serrano et al. 2010).

### Chronology development and statistics

TRW was measured with an accuracy of 0.01mm using the TSAP-Win software (Rinn 2003) and a subsequent quality check of the crossdating was performed visually and with the help of the program COFECHA (Holmes 1983). Prior to standardization using a cubic smoothing spline with a 300-year low-pass filter (Fig.2, Cook 1985), the data were power-transformed to remove non-climatic differences in variance (Cook & Peters 1997). Variance stabilization was applied according to Frank et al. (2007) considering the number of samples and average correlation coefficients. The final chronology was calculated using a robust bi-weight mean (Cook 1985) and signal strength was estimated using the inter-series correlation and EPS statistics in a 30-year moving window with 15-year overlap (Wigley et al. 1984). High-frequency variability was assessed using the mean sensitivity (Cook 1990) and growth was compared using the series average growth rates of the first 300 years of the trees life as well as the means of the age-aligned individual series, the Regional Curves (Esper et al. 2003). Pith-offset estimates were considered for growth analysis. For the study of climate-growth relationships, the standardized chronologies, precipitation, and temperature data were additionally high-pass filtered by computing residuals between the original data and their corresponding 10-year cubic smoothing splines.

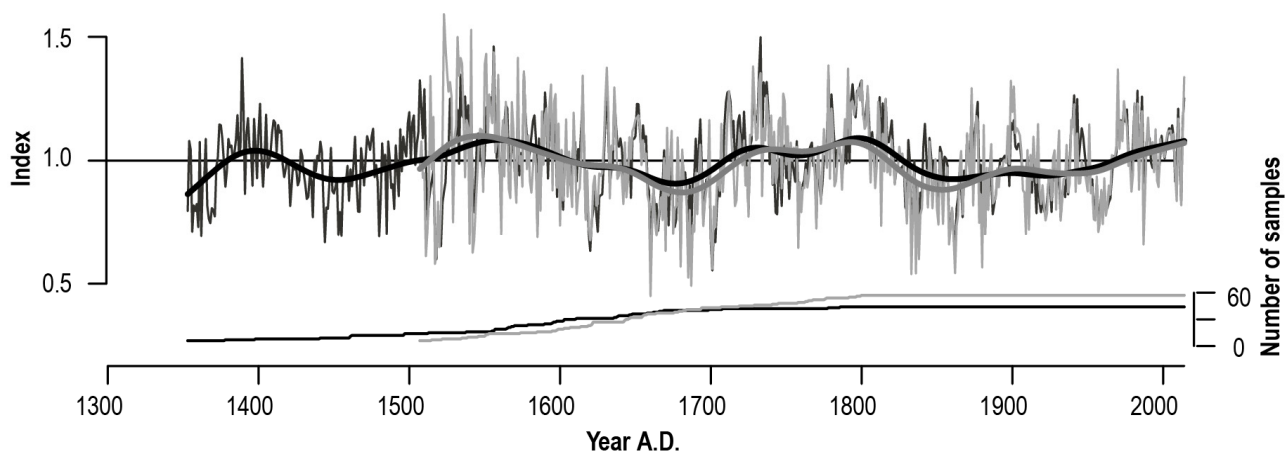


Figure 2: NW-facing (black) and S-facing (grey) power-transformed 300-year smoothing spline standardized tree-ring width chronologies (thin lines) and their corresponding 50-year smoothing splines (bold lines). Chronologies were truncated at  $n > 5$  series. The lower panel displays number of samples.

## Results and Discussion

### Intra- and inter-site (growth) coherence

The site chronologies date back to 1353 and 1507 ( $n > 5$ ) and are reliable after 1495 for the NW- and 1575 for the S-facing stand, respectively (Fig.2), when EPS increases above the widely-accepted threshold of 0.85. The raw chronologies correlate at  $r = 0.89$ , the 300-year spline-detrended chronologies at  $r = 0.86$  ( $p < 0.01$ , 1575-2014). A temporally stable and strong correspondence with *P. heldreichii* TRW chronologies from Albania (Seim et al. 2012, 968-2008)

and Greece (Mt. Olympus, Klesse et al. 2015, 1470-2008) with correlation coefficients ranging between 0.57 and 0.84 among 300-year spline detrended chronologies ( $p < 0.01$ , common period  $n > 5$  1515-2008, Schweingruber 1981, Klesse TRW not published) points to comparable environmental conditions and similar growth forcing. The correlation coefficients increase with decreasing distance indicating a coherent pattern of climate-growth signals over the Balkan Peninsula (Panayotov et al. 2010, Seim et al. 2012).

Tab. 1: Site chronology statistics.

Site	Chronology AD	n	MSL	AGR <sup>1</sup>	SD <sup>1,2</sup>	MS <sup>1,2</sup>	RBAR <sup>1,2</sup>	EPS <sup>1,2</sup>	AC1 <sup>1,2</sup>
NW	1353-2014	44	446	0.89	0.33	0.21	0.38	0.95	0.82
S	1507-2014	57	372	0.75	0.37	0.27	0.39	0.95	0.79

Chronology AD (truncation  $> 5$  series), MSL: mean segment length in years, AGR: average growth rate (mm) of the first 300 years of growth, SD: standard deviation, MS: mean sensitivity, Rbar: inter-series correlation, EPS: mean expressed population signal, AC1: first order auto correlation,<sup>1</sup> common period <sup>2</sup>1507-2014.

Despite a strong covariance between the site chronologies, we found significant growth differences. The S-facing stand shows higher mean sensitivity and lower growth rate denoting a higher degree of high-frequency climatic information (Table 1, Fritts 1976). Focusing on the first 300 years of growth, statistically significant differences between the average growth rates appear. Annual increment is significantly higher and variance more heterogeneous at the NW-facing site, whereas in the S-facing stand 75% of the individual growth rates appear below the median growth of the NW-facing site (Fig.3a). The means of the age-aligned individual series, the Regional Curves (RC; Esper et al. 2003), show opposing growth trends in the first 150 years of growth and the differences in absolute growth level are independent of tree age. The RC of the NW-facing stand initially increases and moderately decreases, whereas the RC of the S-facing stand decreases exponentially (Fig.3b). The growth increase over the first 150 years in the NW-facing site is likely related to ecological conditions, e.g. shading effects and competition for resources, masking the regular age trend (Chi et al. 2015, Muthuchelian et al. 1989). The significant differences in growth prove that differently exposed stands do not necessarily belong to the same biological growth population (Esper et al. 2003), thus perhaps also implying differences in the climatic response.

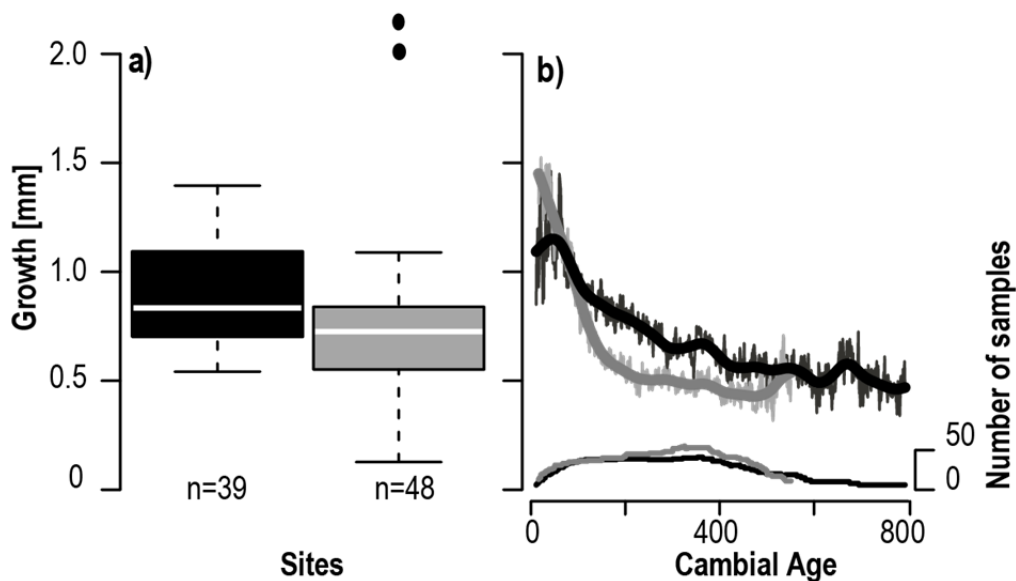


Figure 3: Growth characteristics of NW-facing (dark grey) and S-facing (light grey) sites. a) Mean growth rates over the first 300 years of cambial age, and b) regional curves and 100-year cubic smoothing splines truncated at  $n < 10$  series.

### Climate response

In the high-frequency domain, growth is significantly controlled by temperature, precipitation, and drought in April and June-July. This is the case at both sites. Positive correlations with April temperature ( $r_{1931-2014} = 0.39/\text{NW}$  and  $0.43/\text{S}$ ,  $p < 0.01$ ) and negative correlations with SPEI-1 ( $r_{1931-2014} = -0.36/\text{NW}$  and  $-0.35/\text{S}$ ,  $p < 0.01$ ) and precipitation ( $r_{1931-2014} = -0.34/\text{NW}$  and  $-0.33/\text{S}$ ,  $p < 0.01$ ) demonstrate that dry and warm spring conditions support growth. These conditions stimulate timely snowmelt and early cambial activity and elongate the vegetation period and time of cell formation (Vaganov et al. 1999, Moser et al. 2010). The negative response to June-July temperature ( $r_{1931-2014} = -0.34/\text{NW}$  and  $-0.18/\text{S}^*$ ,  $p < 0.01$ , \*not significant) and associated positive responses to precipitation ( $r_{1931-2014} = 0.34/\text{NW}$  and  $0.29/\text{S}$ ,  $p < 0.01$ ) and SPEI-2 ( $r_{1931-2014} = 0.34/\text{NW}$  and  $0.25/\text{S}$ ,  $p < 0.01$ ) synchronize with the beginning of the Mediterranean dry season that triggers increased water depletion, drought stress, and reduced metabolic activity (Vieira et al. 2013, Chaves 2002). The uniform seasonal response of differently exposed sites strongly suggests that the Mediterranean climate regime enforces growth synchronicity (Bolle 2003, Loukas et al. 2002, Luterbacher et al. 2012).

However, the absolute monthly climate signal strength appears to be associated with slope exposition. The S-facing site, receiving most insolation, is more sensitive to April temperatures and SPEI-1 as the trees benefit from warmer spring temperatures and an early growth onset (Rossi et al. 2007). The NW-facing site surprisingly shows a stronger response to June-July temperature, precipitation, and SPEI-2 (Fig.5). From a physiological point of view, S-facing trees were expected to suffer more from high temperatures and drought in June-July (Panayotov et al. 2010, Fritts 1976, Måren et al. 2015). The actual response is a product of biological memory effects, which artificially reduce the absolute strength of preserved climatic information. We hypothesize that potential biomass losses during high summer are masked by early season biomass gains and reduce the June-July climate sensitivity of S-facing trees. These findings highlight the importance of site selection even in high elevation environments (Frank & Esper 2005, D uthorn et al. 2016).

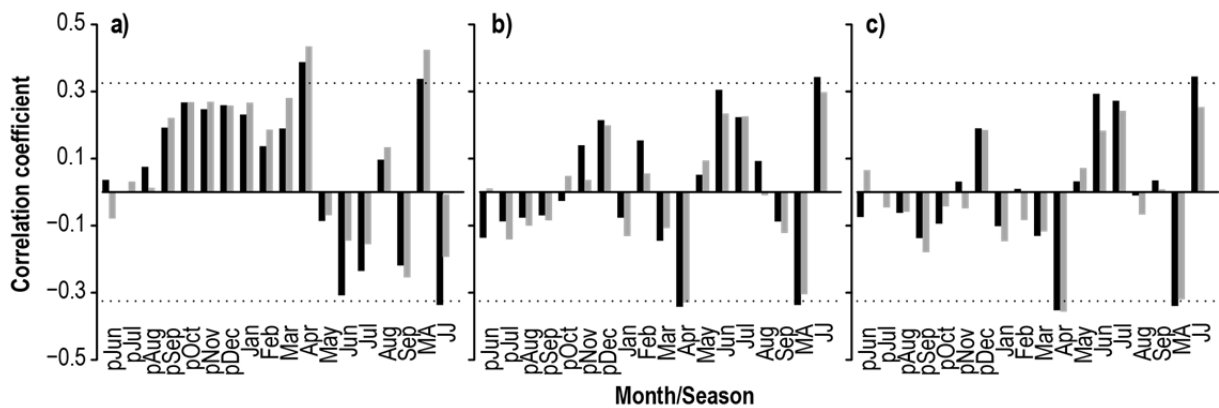


Figure 4: Correlation coefficients between site chronologies (NW-/black and S-/grey) and meteorological data (both 10-year high-pass filtered) using monthly and seasonal a) temperature, b) precipitation, and c) SPEI-1/-2 data from the station in Thessaloniki (40.52N, 23.00E, 40m) for the period 1931-2014. Dashed lines indicate 99% significance levels. p- indicates month of the previous year, MA= March-June and JJ= June-July.

In contrast to previous studies on *P. heldreichii* TRW data revealing variable climate signals (e.g. Todaro et al. 2007, Panayotov et al. 2010, Seim et al. 2012), we find temporally robust signals after 1950 (Fig.5). Post-1950 April temperature and SPEI-1 correlations are fairly stable, whereas June-July precipitation sensitivity gradually decreases. However, for all meteorological parameters and months, we find a shift in climate sensitivity in the 1950s, in both tree sites, pointing to potential biases in the early observational data. The scarcity of meteorological data prior to the Second

World War complicate testing this hypothesis, but we suggest to use post-1950 data for calibration trials in northern Greece.

The significant, site-independent, and temporally robust temperature and SPEI-1 correlations underscore the potential of *P. heldreichii* TRW data for climate reconstruction. We hypothesize that the notable signal strength in comparison to previous *P. heldreichii* studies is related to *i)* the standardization approach including the application of a high-pass filter, *ii)* slope exposition effects, and *c)* site elevation. Splitting the data according to slope exposition allows maximizing the seasonal climatic response, as signal differs in single months of the growing season. Panayotov et al. (2010) collected *P. heldreichii* on a S-facing slope and report a weak association with summer precipitation. This study shows that S-facing trees are least suitable to analyze summer drought and precipitation, as the influence of drought stress and growth cessation is likely masked by compensating growth gains earlier in the season. Further tests on the inter-dependency between spring warmth and summer drought need to be conducted to support this hypothesis. Seim et al. (2010) suggested that the absence of a robust climate signal in Albania is associated with site elevation as the natural thermal tree line is 500 m above their sampling location resulting in a reduced climate growth control. The Smolikas sites analyzed here are located at the thermal treeline (Brandes 2006) and are therefore exposed to a harsher climate that likely supports the stronger climate signals.

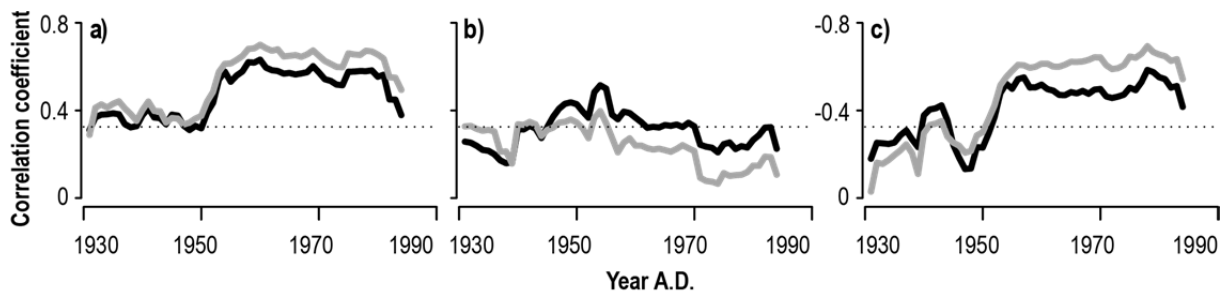


Figure 5: 31-year moving window correlation coefficients between high-pass filtered TRW chronologies of the NW- (black) and S-exposed (grey) sites and climate data displayed in Fig. 4 for **a)** April temperature, **b)** June-July precipitation, and **c)** April SPEI-1. Dashed lines indicate 99% significance levels.

## Conclusion

TRW data from NW- and S-exposed high-elevation sites in northern Greece are characterized by different growth rates, with the S-exposed trees being more growth limited. In addition, we found distinct aspect effects of the climate sensitivity of *P. heldreichii* associated with higher insolation rates on S-facing slopes. Due to the positive temperature and negative SPEI-1 and precipitation responses in April which stimulates early cell formation, a potential summer season signal cannot be properly resolved. The negative temperature and positive SPEI-2 and precipitation signal strength is strongly influenced by the previous month's cell productivity. Further work will focus on *(i)* including relict material to prolong the chronology back in time, *(ii)* extending the spatial scope including east- and west-facing sites, *(iii)* establishing a climate reconstruction using MXD measurements.

## References

- Bolle, H.J. (2003): Mediterranean Climate. Springer Berlin. 371p.
- Brandes, R. (2006): Waldgrenzen griechischer Hochgebirge: Unter besonderer Berücksichtigung des Taygetos, Südpeloponnes. (Walddynamik, Tannensterben, Dendrochronologie). PhD. Thesis. University of Erlangen. 316p.
- Chaves, M.M. (2002): How Plants Cope with Water Stress in the Field? Photosynthesis and Growth. *Annals of Botany* 89: 907-916.

- Chi, X., Tang, Z., Xie, Z., Guo, Q., Zhang, M., Ge, J., Xiong, G., Fang, J. (2015): Effects of size, neighbors, and site condition on tree growth in a subtropical evergreen and deciduous broad-leaved mixed forest, China. *Ecology and Evolution* 5: 5149-5161.
- Cook, E.R. (1985): A time series analysis approach to tree ring standardization.
- Cook, E.R. (ed) (1990): Methods of dendrochronology. Applications in the environmental sciences, Repr. Kluwer, Dordrecht
- Cook, E.R., Peters, K. (1997): Calculating unbiased tree-ring indices for the study of climatic and environmental change. *The Holocene* 7: 361-370.
- Düthorn, E., Schneider, L., Günther, B., Gläser, S., Esper, J. (2016): Ecological and climatological signals in tree-ring width and density chronologies along a latitudinal boreal transect. *Scandinavian Journal of Forest Research*, doi: 10.1080/02827581.2016.1181201.
- Esper, J., Cook, E.R., Krusic, P.J., Peters, K., Schweingruber, F.H. (2003): Tests of the RCS method for preserving low-frequency variability in long tree-ring chronologies. *Tree-Ring Research* 59: 81-98.
- Frank, D., Esper, J. (2005): Characterization and climate response patterns of a high-elevation, multi-species tree-ring Network in the European Alps. *Dendrochronologia* 22: 107-121.
- Frank, D., Esper, J., Cook, E.R. (2007): Adjustment for proxy number and coherence in a large-scale temperature reconstruction. *Geophysical Research Letters* 34, doi: 10.1029/2007GL030571.
- Fritts, H.C. (1976): Tree Rings and Climate. Academic Press, London, 567 p. □
- Holmes, R.L. (1983): Computer-assisted quality control in tree-ring dating and measurement. *Tree-Ring Bulletin* 43: 69-78.
- Hughes, P.D., Woodward, J.C., Gibbard, P.L. (2006): Late Pleistocene glaciers and climate in the Mediterranean. *Global and Planetary Change* 50: 83-98.
- Klesse, S., Ziehmer, M., Rousakis, G., Trouet, V., Frank, D. (2015): Synoptic drivers of 400 years of summer temperature and precipitation variability on Mt. Olympus, Greece. *Climate Dynamics* 45: 807-824.
- Loukas, A., Vasiliades, L., Dalezios, N.R. (2002): Hydroclimatic Variability of Regional Droughts in Greece Using the Palmer Moisture Anomaly Index. *Hydrology Research* 33: 425-442.
- Luterbacher, J., García-Herrera, R., Akcer-On, S., Allan, R., Alvarez-Castro, M., Benito, G., Booth, J., Büntgen, U., Cagatay, N., Colombaroli, D., Davis, B., Esper, J., Felis, T., Fleitmann, D., Frank, D., Gallego, D., Garcia-Bustamante, E., Glaser, R., Gonzalez-Rouco, F.J., Goosse, H., Kiefer, T., Macklin, M.G., Manning, S.W., Montagna, P., Newman, L., Power, M.J., Rath, V., Ribera, P., Riemann, D., Roberts, N., Sicre, M., Silenzi, S., Tinner, W., Tzedakis, P., Valero-Garcés, B., van der Schrier, G., Vannièrè, B., Vogt, S., Wanner, H., Werner, J.P., Willett, G., Williams, M.H., Xoplaki, E., Zerefos, C.S., Zorita, E. (2012)\_ A Review of 2000 Years of Paleoclimatic Evidence in the Mediterranean. In: Lionello P (ed) The climate of the Mediterranean region. From the past to the future, 1. ed. Elsevier Science, Amsterdam, 87-185.
- Måren, I.E., Karki, S., Prajapati, C., Yadav, R.K., Shrestha, B.B. (2015): Facing north or south: Does slope aspect impact forest stand characteristics and soil properties in a semiarid trans-Himalayan valley? *Journal of Arid Environments* 121: 112-123.
- Moser, L., Fonti, P., Büntgen, U., Esper, J., Luterbacher, J., Franzen, J., Frank, D. (2010): Timing and duration of European larch growing season along an altitudinal gradient in the Swiss Alps. *Tree Physiology* 30: 225-233.
- Muthuchelian, K., Paliwal, K., Gnanam A. (1989): Influence of shading on net photosynthetic and transpiration rates, stomatal diffusive resistance, nitrate reductase and biomass productivity of a woody legume tree species (*Erythrina variegata* Lam.). Proceedings: *Plant Sciences* 99: 539-546.
- Panayotov, M., Bebi, P., Trouet, V., Yurukov, S. (2010): Climate signal in tree-ring chronologies of *Pinus peuce* and *Pinus heldreichii* from the Pirin Mountains in Bulgaria. *Trees* 24: 479-490.

- Rinn, F. (2003) Time series analysis and presentation for dendrochronology and related applications. Heidelberg
- Rossi, S., Deslauriers, A., Anfodillo, T., Carraro, V. (2007): Evidence of threshold temperatures for xylogenesis in conifers at high altitudes. *Oecologia* 152: 1-12.
- Seim, A., Treydte, K., Büntgen, U., Esper, J., Fonti, P., Haska, H., Herzig, F., Tegel, W., Faust, D. (2010): Exploring the potential of *Pinus heldreichii* Christ for long-term climate reconstruction in Albania. In: Levanic, T., Gricar, J., Hafner, P., Krajnc, R., Jagodic, S., Gärtner, H., Heinrich, I., Helle, G. (eds) Tree rings in archaeology, climatology and ecology. TRACE 8: 75-82.
- Seim, A., Büntgen, U., Fonti, P., Haska, H., Herzig, F., Tegel, W., Trouet, V., Treydte, K. (2012): Climate sensitivity of a millennium-long pine chronology from Albania. *Climate Research* 51: 217-228.
- Stevanovic, V., Tan, K., Iatrou, G. (2003): Distribution of the endemic Balkan flora on serpentine I.- Obligate serpentine endemics. *Plant Systematics and Evolution* 242:149-170.
- Schweingruber, F.H. (1981): *Pinus leucodermis* chronologies—, Oros—Olympus Mountains (GR). World Data Center for Paleoclimatology Data Contribution Series, Boulder. □
- Todaro, L., Andreu, L., Dalessandro, C., Gutierrez, E., Cherubini, P., Saracino, A. (2007): Response of *Pinus leucodermis* to climate and anthropogenic activity in the National Park of Pollino (Basilicata, Southern Italy). *Biological Conservation* 137: 507-519.
- Trouet, V. (2015): A tree-ring based late summer temperature reconstruction (1675-1980) for the northeastern Mediterranean. *Tree-Ring Research/Radiocarbon* 56: 69-78.
- Trouet, V., Panayotov, M., Ivanova, A., Frank, D. (2012): A pan-European summer teleconnection mode recorded by a new temperature reconstruction from the northeastern Mediterranean (AD 1768-2008). *The Holocene* 22: 887-898.
- Vaganov, E.A., Hughes, M.K., Kirilyanov, A.V., Schweingruber, F.H., Silkin, P.P. (1999): Influence of snowfall and melt timing on tree growth in subarctic Eurasia. *Nature* 400: 149-151.
- Vicente-Serrano, S.M., Beguería, S., López-Moreno, J.I. (2010): A Multiscalar Drought Index Sensitive to Global Warming. The Standardized Precipitation Evapotranspiration Index. *Journal of Climate* 23: 1696-1718.
- Vieira, J., Rossi, S., Campelo, F., Freitas, H., Nabais, C. (2013): Seasonal and daily cycles of stem radial variation of *Pinus pinaster* in a drought-prone environment. *Agricultural and Forest Meteorology* 180: 173-181.
- Wigley, T., Briffa, K.R., Jones, P.D. (1984): On the average of correlated time series, with applications in dendroclimatology and hydrometeorology. *Journal of Climate and Applied Meteorology* 23: 201-213.

# Forward modeling of tree-ring growth process in north central China during the past sixty years

M.H. He<sup>1,2</sup>, B. Yang<sup>1</sup>, A. Bräuning<sup>2</sup> & S.Y. Kang<sup>1</sup>

<sup>1</sup>Key Laboratory of Desert and Desertification, Northwest Institute of Eco-Environment and Resources, Chinese Academy of Sciences, Lanzhou, China

<sup>2</sup>Institute of Geography, University of Erlangen-Nürnberg, 91054 Erlangen, Germany  
E-mail: hmh0503lb@163.com

## Introduction

A great progress of dendrochronology has been achieved in China during the past several years. Dendroclimatology as one of the main applications of dendrochronology has also been developed thoroughly (Liang et al. 2008, Liu et al. 2013, Gou et al. 2015, Yang et al. 2014, Zhang et al. 2015b, Bräuning et al. 2016, Liu et al. 2016). Temperature, precipitation, or moisture variability during the past hundreds to thousands of years was reconstructed for different study sites in different climate zones in China. Such information is of great importance to evaluate current climate change in a long-term context and to predict the response of forest ecosystems under future climate conditions. However, almost all dendroclimatological studies are based on statistical relationships between tree-ring width series and climate data on the monthly, seasonal, or annual scales, lacking tree-physiological based validation and explanation and making reliable forecasts about tree behavior under expected future climatic conditions difficult.

To overcome such constraints, the development of tree-physiological models needs to be strengthened. Meanwhile, process-based models developed for tree-ring width formation and isotope fractionation studies (for details, see Guiot et al. 2014) give us the opportunity to go further. Among the existing models, the Vaganov-Shashkin (VS) (Shashkin & Vaganov 1993, Vaganov et al. 2011) model is probably the most widely used one across the world. It has been successfully applied e.g. in the southeastern United States (Anchukaitis et al. 2006), North America and Russia (Evans et al. 2006), the Mediterranean region (Touchan et al. 2012), the northeastern Tibetan Plateau (Zhang et al. 2011), and northwestern China (Zhang et al. 2015a). The aim of our study was to extend the usage of the VS model and apply it, for the first time, to model tree-ring growth in north central China during the past sixty years.

## Material and Methods

### *Study site and climate condition*

Our study site is located at Hasi Mountain (104.5°E, 37.0° N) in Jingyuan County, Gansu Province, north central China (Fig.1). According to the records of the nearest meteorological station at Jingyuan (104.7°E, 36.6° N) during the period 1952–2011 the mean annual temperature was 9.1 °C. January was the coldest month with the mean temperature of -7.2 °C and July was the warmest one (22.6 °C on avg.). The mean annual precipitation was 231 mm, ~81% of which falls on May–September (Fig.2). The study site is characterized by a semi-arid continental climate.

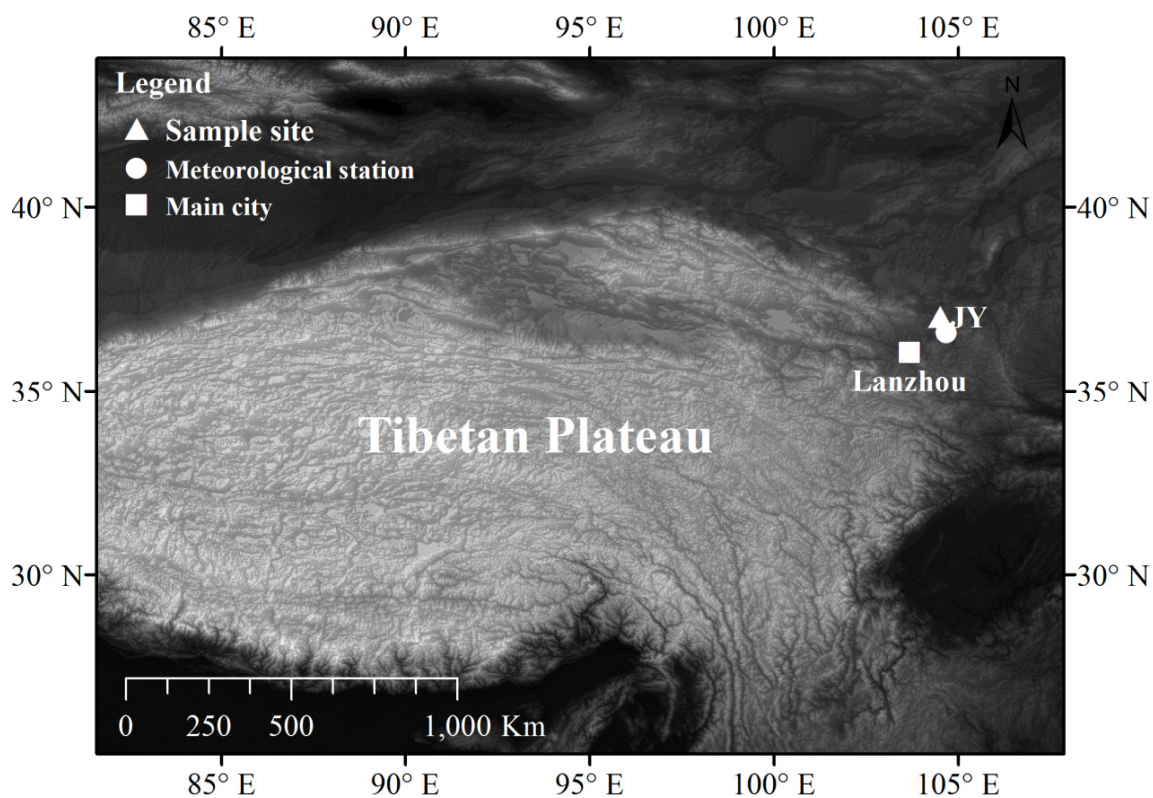


Figure 1: Locations of the study site (triangle), meteorological station at Jingyuan (circle) and the main city of Lanzhou (square).

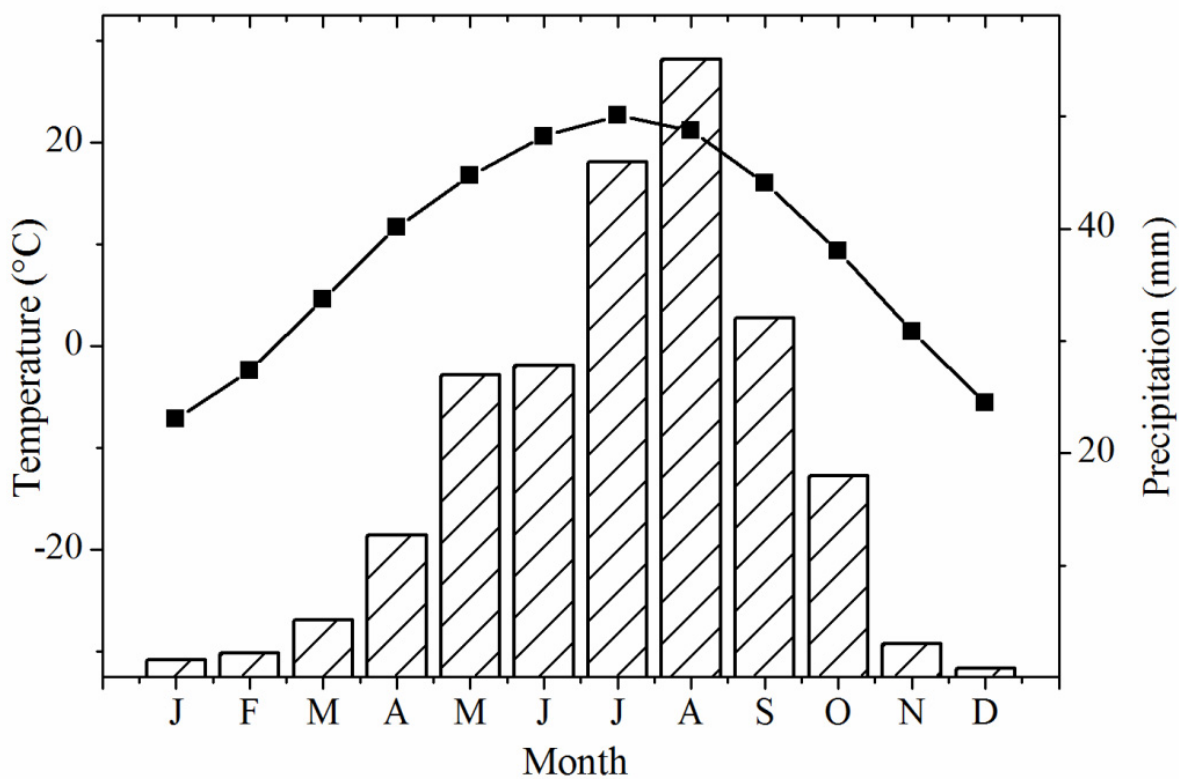


Figure 2: Mean monthly temperature (line with squares) and precipitation (hatched histogram) at the Jingyuan meteorological station 1952–2011.

### *Tree-ring width chronology*

Chinese pine (*Pinus tabulaeformis*) is the dominant tree species in the study region. It grows on north-facing slopes. A total of 187 cores from 110 living trees were extracted with increment borers at breast height. They were sampled along an altitudinal gradient of 2400–2740 m a.s.l. Based on statistical relationships the produced tree-ring width chronology has been used to reconstruct Palmer Drought Severity Index for the past three hundred years (Kang et al. 2012). Herein, we focused on the tree-ring width series during the period 1952–2011.

### *VS modelling*

The mechanism of Vaganov-Shashkin (VS) model is based on the assumption that climatic influences are associated nonlinearly with tree-ring width growth through controls on cell formation process in the developing wood (Shashkin & Vaganov 1993, Vaganov 1996). Simulated tree-ring width series is determined by comparing daily temperature and soil moisture budget to growth functions using the most limiting factor (Fritts 1976). The integral tree-ring growth rate  $Gr(t)$  is estimated based on the following equation:

$$Gr(t) = GrE(T) \times \min \{GrT(t), GrW(t)\}$$

where:  $GrE(t)$ ,  $GrT(t)$  and  $GrW(t)$  are the partial growth rates, calculated independently from solar irradiation, temperature, and soil moisture content.

Daily precipitation and temperature records from the Jingyuan meteorological station were used as model input data. To check the performance of the model in the study region, a split calibration and verification period is used. The model's parameters are tuned using daily climate data for 1985–2011 in the calibration period. The tuned model is applied to generate tree-ring indices for the verification period 1952–1984. The skill of the model is evaluated against their actual tree-ring width chronologies during their common interval periods. Model outputs of mean relative growth rates due to temperature ( $GrT$ ), soil moisture variability ( $GrW$ ), solar irradiance ( $GrE$ ), and the integral growth rate ( $Gr$ ) for each year were used for further analysis.

## **Results and Discussion**

The most appropriate physiological parameters were determined by iteratively debugging and comparing both the high- and low-frequency variabilities between the simulated and actual tree-ring width chronologies. During this process, we noticed that four parameter settings of the minimum soil moisture for tree growth ( $W_{min}$ ), lower range of optimal soil moisture for tree growth ( $W_{opt1}$ ), minimum temperature for tree growth ( $T_{min}$ ) and lower range of optimal temperature for tree growth ( $T_{opt1}$ ) were the most sensitive ones in the study region. Any increased or decreased change of the four parameters results in differences between the simulated and actual chronologies, demonstrating the four selected parameters determine tree-ring growth processes to a large extent.

Using the estimated optimal parameters, we obtained a highly significant ( $p < 0.01$ ) positive correlation ( $r = 0.64$ , 1985–2011) between the actual tree-ring width chronology and the simulated one during the calibration period. High similarity was also observed for the verification period 1952–1984 (Fig. 3). Such high consistency indicates that the VS model is suitable for the study region to simulating tree-ring width formation and analyzing their relationships with climate factors.

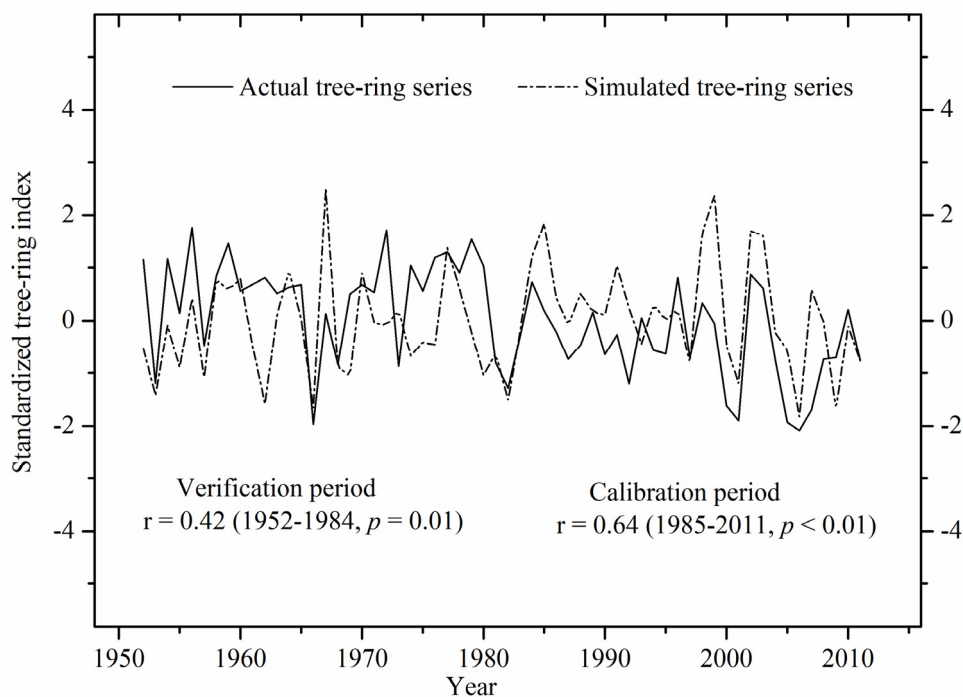


Figure 3: Comparison between the actual (straight line) and simulated (dash-dotted line) tree-ring width series during their calibration and verification periods. Both series are standardized for direct comparison.

According to the model output, the integral growth rate (Gr) is determined by low growth rates depending on soil moisture (GrW), temperature (GrT) or solar irradiance (GrE). As presented in Fig. 4, soil moisture affecting tree-ring formation from late April (Julian day 115) to late August (Julian day 238) because partial growth rate due to GrW was generally less than partial growth rate due to GrT, thereafter, temperature mainly influenced it until to the end of September (Julian day 274). Additionally, the model shows that the average duration of the growing season is 161 days, with considerable variation from year to year during 1952–2011. On average, soil moisture limits tree-ring growth for 124 days and temperature for 31 days, while solar irradiance affects that for 6 days during the Julian day of 239–244. Such growth patterns indicate soil moisture variability is the driving force for tree-ring width formation, because most of the ring width is formed during late April to late August under the influence of moisture variability. Overall, the relationships between tree-ring growth and climate factors derived from our model output are consistent with statistical analysis during the past sixty years (Kang et al. 2012). Such consistency indicates the VS model output is suitable for further analysis of tree-ring growth process on the daily scale in the study region. Our results herein provide evidence of moisture stress on tree-ring width growth from tree-physiological point of view.

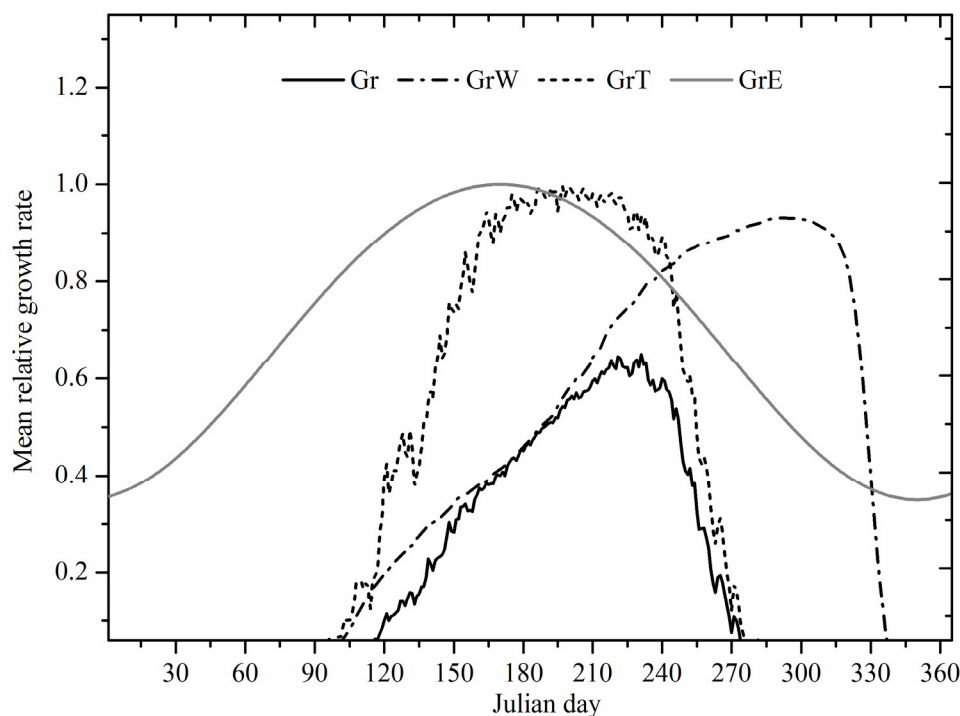


Figure 4: Simulated integral growth rate (*Gr*, black line) and mean relative growth rates due to soil moisture variability (*GrW*, dash-dotted line), temperature (*GrT*, short dash line) and solar irradiance (*GrE*, gray line) during the period 1952–2011.

## Conclusions

We used the process-based VS (Vaganov-Shashkin) model to simulate patterns of Chinese pine tree-ring growth and their relationships with climate data on the daily scale during the past sixty years (1952–2011) in north central China. Both calibration and verification periods yielded highly significant ( $p \leq 0.01$ ) positive correlations between the standard chronology and simulated tree-ring width series during their common interval periods. Model output showed that during the period 1952–2011, soil moisture limited tree-ring growth for 124 days on average and temperature for 31 days on averaged. Specifically, soil moisture affected tree-ring formation during late April to late August; thereafter temperature influence prevailed until the end of September. This is consistent with results from correlation functions, indicating that under semi-arid climate conditions, traditional statistical climate-growth analysis is a reliable indicator for tree growth under a wide range of precipitation change.

## Acknowledgements

This study was jointly funded by the National Natural Science Foundation of China (Grant No. 41325008, 41520104005, 41405085). Minhui He appreciates the support by the Alexander von Humboldt Foundation.

## References

- Anchukaitis, K.J., Evans, M.N., Kaplan, A., Vaganov, E.A., Hughes, M.K., Grissino-Mayer, H.D. & Cane, M.A. (2006) Forward modeling of regional scale tree-ring patterns in the southeastern United States and the recent influence of summer drought. *Geophysical Research Letters* 33: L04705.
- Bräuning, A., Griesinger, J., Hochreuther, P. & Wernicke, J. (2016) Dendroecological perspectives on climate change on the Southern Tibetan Plateau. In Singh, R.B. et al. (ed.): *Climate change, glacier response, and vegetation dynamics in the Himalaya*. Springer. 347-364.

- Evans, M.N., Reichert, B.K., Kaplan, A., Anchukaitis, K.J., Vaganov, E.A., Hughes, M.K. & Cane, M.A. (2006) A forward modeling approach to paleoclimatic interpretation of tree-ring data. *Journal of Geophysical Research* 111: G03008.
- Fritts, H.C. (1976) *Tree rings and climate*. Academic Press, London.
- Gou, X., Deng, Y., Gao, L., Chen, F., Cook, E., Yang, M. & Zhang, F. (2015) Millennium tree-ring reconstruction of drought variability in the eastern Qilian Mountains, northwest China. *Climate Dynamics* 45: 1761–1770.
- Guiot, J., Boucher, E. & Gea-Izquierdo, G. (2014) Process models and model-data fusion in dendroecology. *Frontiers in Ecology and Evolution* 2: 1-12.
- Kang, S., Yang, B. & Qin, C. (2012) Recent tree-growth reduction in north central China as a combined result of a weakened monsoon and atmospheric oscillations. *Climatic Change* 115: 519-536.
- Liang, E., Shao, X. & Qin, N. (2008) Tree-ring based summer temperature reconstruction for the source region of the Yangtze River on the Tibetan Plateau. *Global and Planetary Change* 61: 313-320.
- Liu, X., Zeng, X., Leavitt, S.W., Wang, W., An, W., Xu, G., Sun, W., Wang, Y., Qin, D. & Ren, J. (2013) A 400-year tree-ring  $\delta^{18}\text{O}$  chronology for the southeastern Tibetan Plateau: Implications for inferring variations of the regional hydroclimate. *Global and Planetary Change* 104: 23-33.
- Liu, Y., Zhang, X., Song, H., Cai, Q., Li, Q., Zhao, B., Liu, H. & Mei, R. (2016) Tree-ring-width-based PDSI reconstruction for central Inner Mongolia, China over the past 333 years. *Climate Dynamics*. doi:10.1007/s00382-016-3115-6.
- Shashkin, A.V. & Vaganov, E.A. (1993) Simulation model of climatically determined variability of conifers' annual increment (on the example of Scots pine in the steppe zone). *Russia Journal of Ecology* 24: 275-280.
- Touchan, R., Shishov, V.V., Meko, D.M., Nourri, I. & Grachev, A. (2012) Process based model sheds light on climate sensitivity of Mediterranean tree-ring width. *Biogeosciences* 9: 965-972.
- Vaganov, E.A. (1996) Mechanisms and simulation modeling of tree-ring formation for conifers. *Lesovedenie* 1: 3-17.
- Vaganov, E.A., Anchukaitis, K.J. & Evans, M.N. (2011) How well understood are the processes that create dendroclimatic records? A mechanistic model of the climatic control on conifer tree-ring growth dynamics. In: Hughes, M.K. et al. (ed): *Dendroclimatology, developments in paleoenvironmental research*. Springer. 37-75.
- Yang, B., Qin, C., Wang, J., He, M., Melvin, T.M., Osborn, T.J. & Briffa, K.R. (2014) A 3,500-year tree-ring record of annual precipitation on the northeastern Tibetan Plateau. *Proceedings of the National Academy of Sciences USA* 111: 2903-2908.
- Zhang, J., Gou, X., Zhang, Y., Lu, M., Xu, X., Zhang, F., Liu, W. & Gao, L. (2015a) Forward modeling analyses of Qilian Juniper (*Sabina przewalskii*) growth in response to climate factors in different regions of the Qilian Mountains, northwestern China. *Trees* 30: 175-188.
- Zhang, Q.B., Evans, M.N. & Lyu, L. (2015b) Moisture dipole over the Tibetan Plateau during the past five and a half centuries. *Nature Communications* 6: 8062.
- Zhang, Y., Shao, X., Xu, Y. & Wilmking, M. (2011) Process-based modeling analyses of *Sabina przewalskii* growth response to climate factors around the northeastern Qaidam Basin. *Chinese Science Bulletin* 56: 1518-1525.



## **SECTION 3**

### **GEOMORPHOLOGY**

# Dendrochronological record of terrain subsidence caused by underground mining (Silesian Upland)

M. Franek, M. Wistuba & I. Malik

University of Silesia, Department of Reconstructing Environmental Change  
E-mail: m.franek@onet.eu

## Introduction

Underground mining can affect terrain relief in two main ways. During continuous deformations bedrock layers bend without disturbing their continuity. During discontinuous deformations bedrock layers are disturbed and broken. In the former deep exploitation causes slow terrain subsidence. In the second type shallow exploitation (usually less than 80-100 m) causes rapid collapse of the mining caverns (Dulias 2013). Both types of underground deformations produce multiple landforms on the surface e. g. hollows, cracks or fractures and terrain faults (Gabzdyl & Gorol 2008).

There are numerous methods of subsidence detection, including neuron networks (Pawluś 2007), satellite radar interferometry InSAR/DInSAR (Yue et al. 2011) and digital terrain model based on data from air scanning LIDAR (Konagai et al. 2013). In recent years dendrochronology has been more and more often used in detecting and dating geomorphic processes. However, this mainly concerns rapid processes such as: landslides (e.g. Wistuba et al. 2013), fluvial erosion (e.g. Gärtner et al. 2001) and accumulation (e.g. Rzepecka et al. 2012), and debris flows (e.g. Malik et al. 2013). Gradual terrain subsidence has not been analysed with the use of tree rings. The aim of our study is to check if slow terrain subsidence caused by underground mining affects radial growth of trees and thus can be dated and reconstructed from tree rings. The basic assumption of the study is that anthropogenic subsidence affect tree growth in a way similar to natural geomorphological processes: it can cause tree tilting (recorded in reaction wood and growth eccentricity) (a) and it can change water conditions in the soil (recorded as ring reductions), as subsidence basins are often flooded by groundwater) (b).

## Materials and methods

### *Study and reference site*

Study site is located in the Silesian Upland, in the Katowice City, Poland (50°10'33.07"N, 19°1'12.17"E) (Fig. 1 I). On Silesian Upland about 1000 km<sup>2</sup> is affected by subsidence related to underground exploitation of hard coal (Machowski 2010). The Murcki-Staszic Coal Mine, one of the oldest in the region, works below the study site at two depths: 416 m and 600 m. Study site is an anthropogenic, subsidence basin located in a valley of a small stream (Fig. 1 II). The site under study is partly flooded. Channel of the stream flows at higher elevation than the bottom of subsidence basin (Fig. 1 III: A-B). The terrain profile of the stream channel (Fig. 1 III: C-D) shows a clear step at the edge of subsidence depression. The study site is covered with planted, even-aged Scots pine (*Pinus sylvestris*) forest (Fig. 2 I) with an admixture of Pedunculate oak (*Quercus robur*), silver birch (*Betula pendula*) and European beech (*Fagus sylvatica*).

Reference site is located on the flat surface in the Oświęcim Basin, c 14 km south from the study site (50°2'58.63"N, 19°0'26.63"E). No underground coal exploitation and human-induced subsidence occur there. Forest on the reference site is similar to observed on the study site: mixed, with predominance of Scots pine.

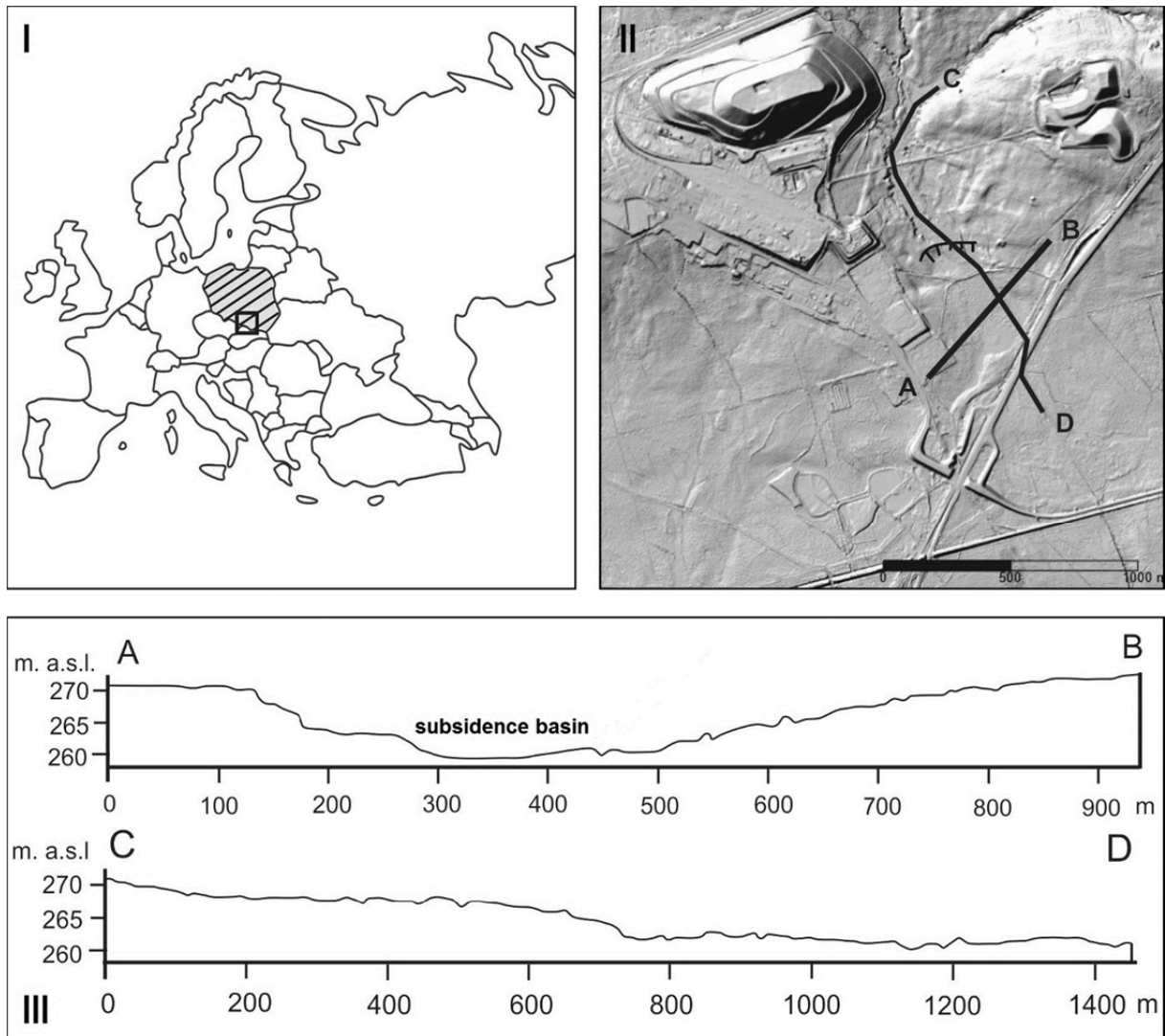


Figure 1: I – location of the Silesian upland. II – relief of the study site with the location of cross-sections through subsidence depression under analysis. The upper edge of the subsidence depression is marked. III – cross-sections through the subsidence depression under study (II and III: Digital Terrain Model based on airborne LiDAR).

#### Methods of the tree-ring study

The direction of tilting of 43 trees growing on the study site was measured using geological compass. For the dendrochronological analysis we have sampled 18 Scots pines. Samples were taken using Pressler borer, at the breast height. Three cores were taken from each specimen: two in the direction of terrain surface inclination in the subsidence basin (upslope and downslope samples) and the third sample perpendicularly to terrain inclination (Fig. 2 I). Ten Scots pine specimens on the reference site were sampled in the same way. Tree-ring widths were measured using RINTECH LinTab 6 measuring system with TSAPWin Professional 4.65 software. Tree ring widths on upslope and downslope sides of stems were compared. Tree-ring eccentricity was analysed using percent index calculated after Wistuba et al. (2013). Eccentricity events were dated in years with eccentricity index exceeding  $\pm 50\%$  (for up- and downslope eccentricity separately). Up- and downslope samples were also checked under a stereomicroscope in reflected light, in search for compression wood. In samples taken perpendicularly to terrain inclination (Fig. 2 I) we have calculated tree-ring reductions (after: Schweingruber et al. 1985). Reductions were divided into 3 categories: medium strong (30-50%), strong (51-70%) and very strong (>70%).

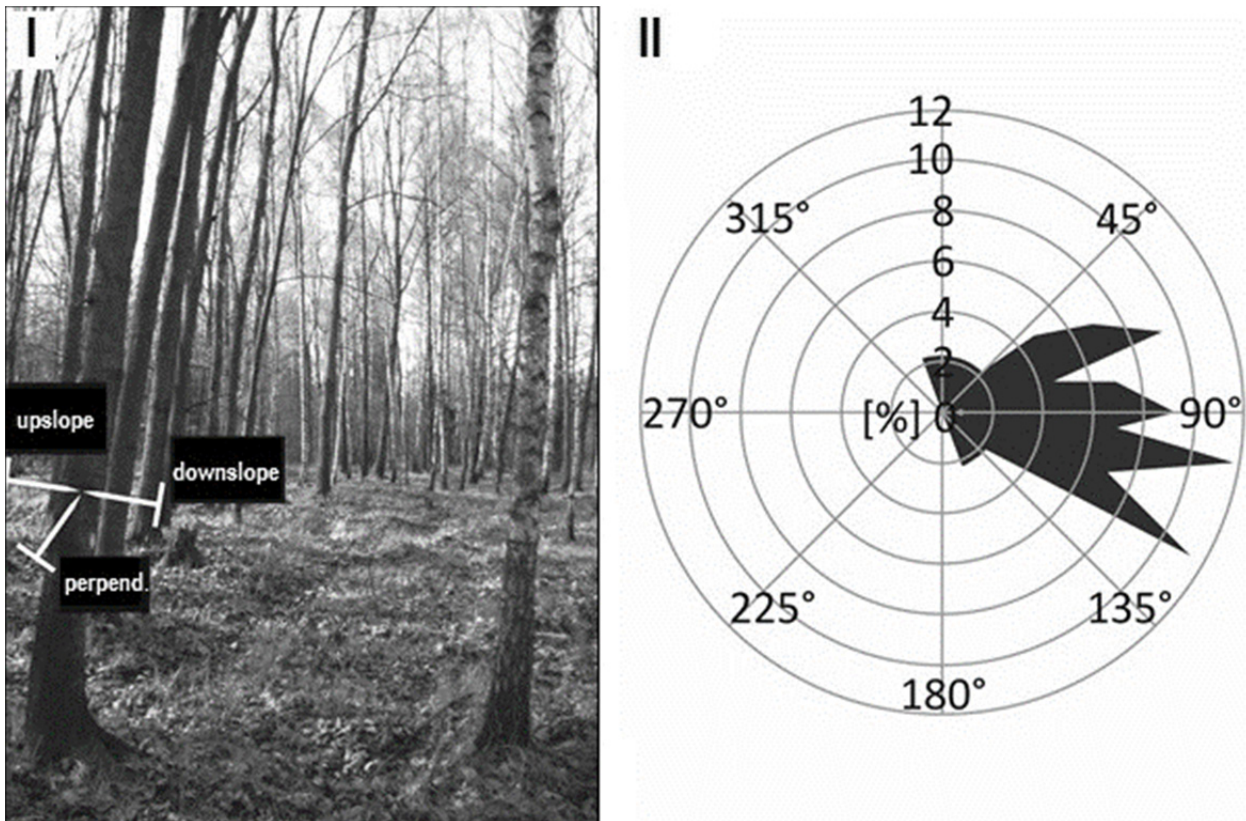


Figure 2: I – trees on the study site tilted along terrain inclination, towards the centre of subsidence depression. Directions of dendrochronological sampling are marked. II – directions of stem tilting measured for trees growing on the study site.

## Results and discussion

### *Tree tilting by terrain subsidence*

Trees growing on the western side of subsidence basin under study are clearly tilted eastwards, towards centre of the basin (Fig. 2). 97.7% of trees growing on the study site tilt N-SE direction (0-180°: Fig. 2 II). The direction of stem tilting is thus along the direction in which subsidence occurs (Figs. 1, 2). Beyond the edge of subsidence basin trees do not show any common direction of tilting. This indicates local character of tilting factor. Also trees growing on the reference site have mostly straight stems.

### *Results of dendrochronological dating*

The oldest event of eccentricity was dated in 1908 (Fig. 3 I). The highest amount of trees (57% of sampled trees) showing growth eccentricity was dated in 1968. Other eccentricity events are: 1961 (55% of sampled trees), 1924 and 1966 (35% each year), and 1978 (30%). There are also periods with smaller number of eccentricity events, e.g.: 1935-1947. However, trees on the study site show eccentricity events almost every year (Fig. 3 I). Up to 90% of trees sampled on the study site show growth eccentricity events at least once during their lifetime. The most trees growing on the reference site show eccentricity in 2007 (50% of the sampled trees), 2005 and 2008 (40% each year), 1952, 1954, 1966, 1970, 1994, 1997, and 2011-2014 (30%) (Fig. 3 II). However, on the reference site there are numerous years without any eccentricity event (40 compared to only 13 on the study site) (Fig. 3). In addition comparison of eccentricity record in single trees growing on reference and study site shows that trees growing on the former have low level of eccentricity with random distribution, typical for inactive slopes (e.g. Wistuba et al. 2013) (Fig. 4). At the same time eccentricity level in trees affected by subsidence are significantly higher with clear peaks (Fig. 4).

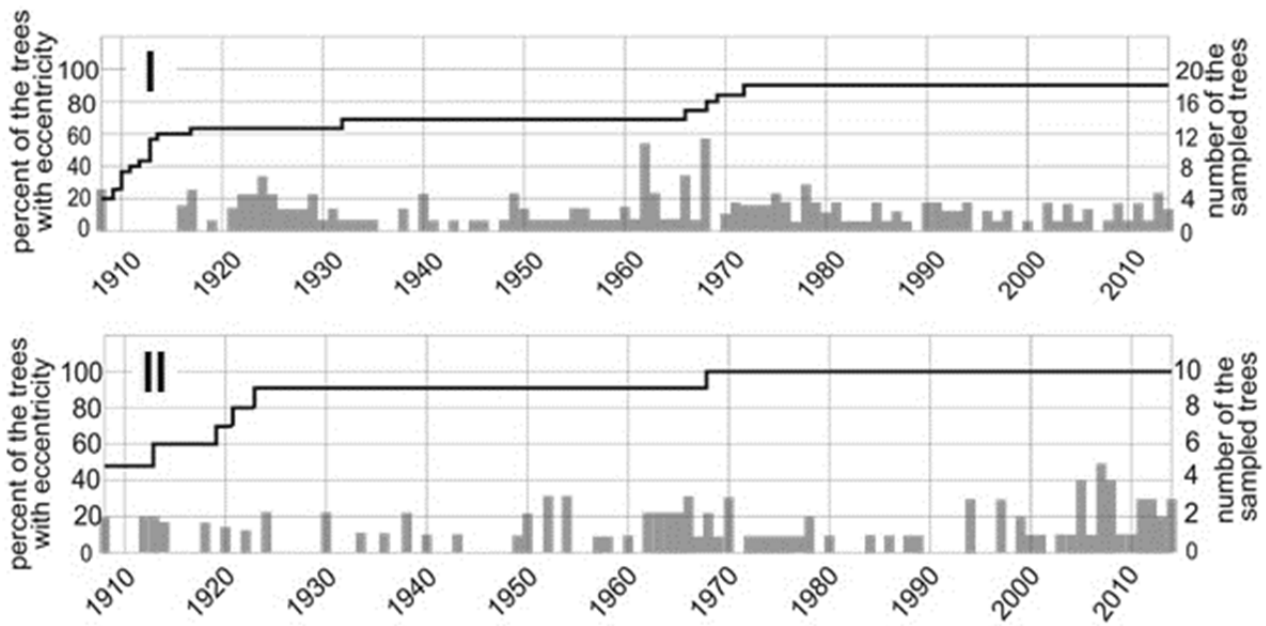


Figure 3: Percent of the trees showing eccentric growth: I – the study site influenced by subsidence, II – the reference site.

Compression wood occurs in 70% of trees sampled on the study site. The oldest event was dated in 1915 (Fig. 5 I). In 46.4% of samples compression wood occurs only on the downslope side faced to the centre of subsidence basin. In 28.6% of studied trees it was found only on downslope. In 25% compression wood occurs on both sides of stems. The highest amount of trees show compression wood in 1930, 1945-1946 (30% each year) and 2000-2001 (22%). On the reference site trees developed compression wood only in 1918 (15%), 1937, 2000-2002 and 2009 (10% each year) (Fig. 5 II). Eccentricity and compression wood events dated on the study site concentrate in two main periods with increased number of wood anatomy disturbances: 1921-1932 and 1962-1983 (Figs. 3 I, 5 I).

The earliest event of tree-ring reductions was dated in 1908 (Fig. 6 I). Reductions were found in all trees sampled on the study site. 55% of sampled trees show medium strong tree-ring reductions (30-50%) in 1910, and half of sampled trees in both 1911 and 2014. 40% and 30% of sampled trees show strong tree-ring reductions (51-70%) in 1909 and 1964, respectively. 22% of the sampled trees show very strong reductions (>70%) in 1925. 1913-1914, 1916, 1937-1938, 1985, 1988 and 1991 (Fig. 6 I) are reduction-free. Concentrations of tree-ring reductions on the study site occur in: 1919-1930, 1950-1976 and 1999-2014.

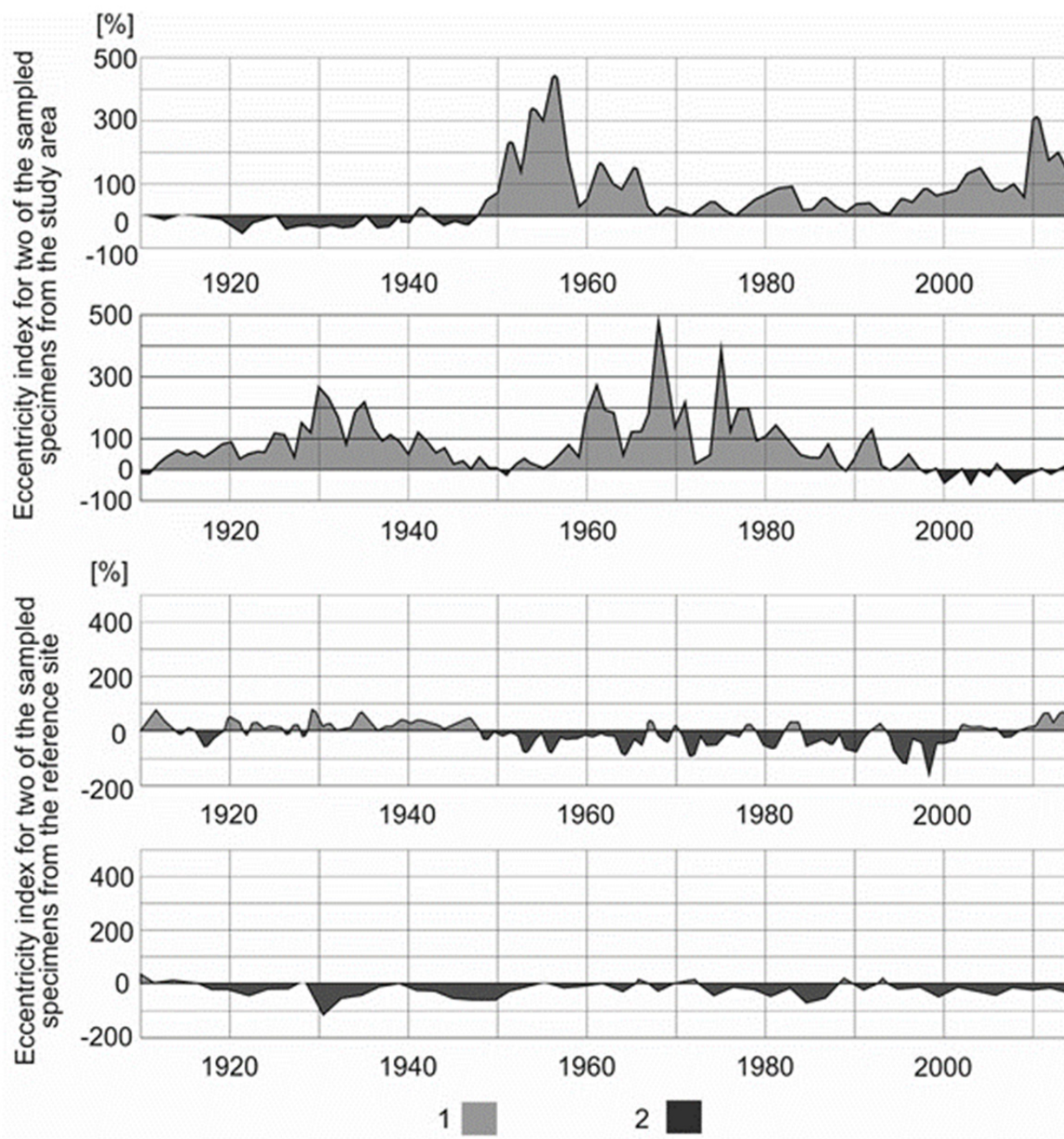


Figure 4: A comparison of eccentricity index values calculated for two pine trees growing under the impact of subsidence and two pine trees from the reference site: 1 – upslope eccentricity, 2 – downslope eccentricity.

On the reference site the peaks in medium strong (30-50%) reductions were found 1976 and 2005 (60% of the sampled trees each year), 2004 and 2013 (50% each year). Among strong reductions (51-70%) peaks were found in: 1967 (65% of sampled trees), 1911 (40%), 1940 and 1996 (30%). 35% of trees sampled on the reference site show very strong reductions (>70%) in 1923 (Fig. 6 II). On the reference site there are numerous years in which none of sampled trees developed reduced rings (25 compared to 8 on the study site). Concentrations of tree-ring reductions among trees in the reference site were found in: 1909-1911, 1920-1932, 1937-1943, 1947-1970, 1976-1980 and 1995-2006 (Fig. 6 II).

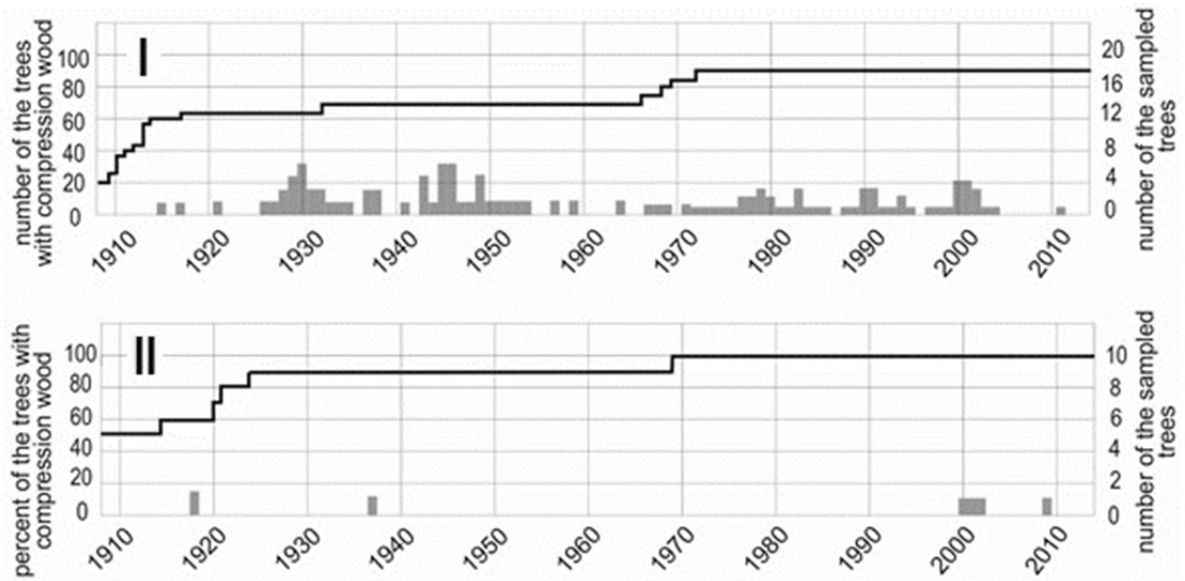


Figure 5: Percent of the trees with compression wood: I – the study site influenced by subsidence, II – the reference site.

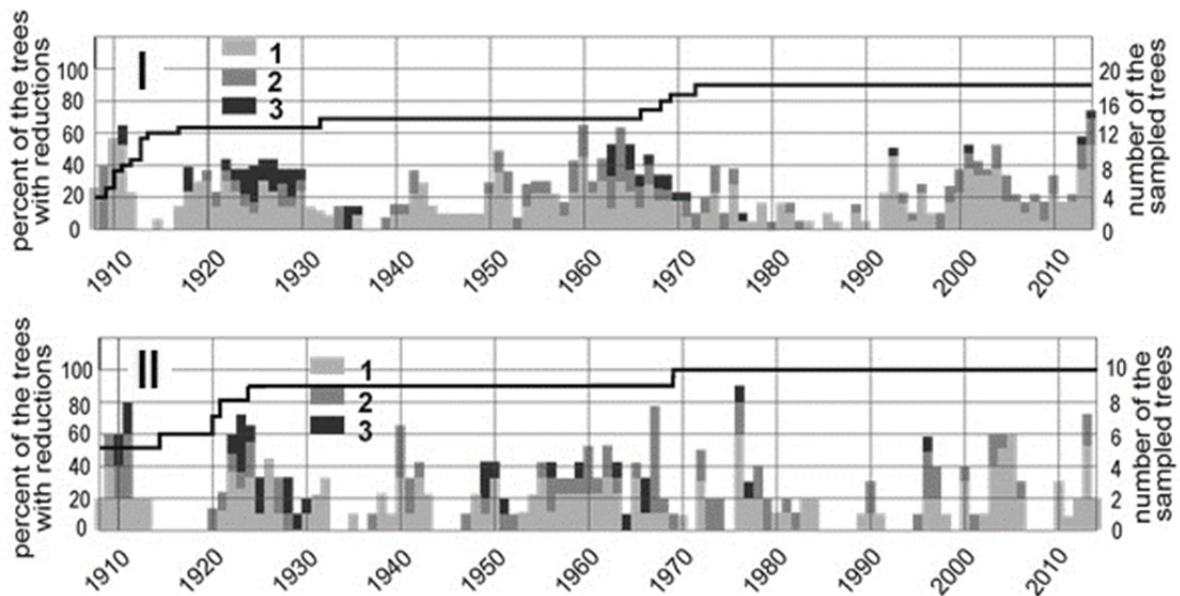


Figure 6: Percent of the trees with ring reductions: I – the study site influenced by subsidence, II – the reference site; strength of tree-ring reductions: 1 – 30-50%, 2 – 51-70%, 3 – over 70%.

*The potential of dendrochronology in dating mining-related terrain subsidence*

The results suggest that wood-anatomy features such as growth eccentricity and reaction wood can be interpreted as evidences of tree tilting caused by terrain subsidence. Comparison of the results from the study site and reference site shows different character of eccentric growth (Fig. 4) and significant disproportion in case of compression wood occurrence (Fig. 5). Dendrochronological analysis allowed to determine two periods with increased frequency of above mentioned wood anatomical features: 1921-1932 and 1962-1983. The older period is probably related to hard coal exploitation since the end of I World War till Great Depression at the turn of 1920's and 1930's when mining activity decreased significantly in the study area. According to Dulas (2013) first subsidence depressions in USID probably formed at the beginning of the 20<sup>th</sup> century. The younger period dated from tree rings is connected with intensive hard coal

exploitation in 1960-1990 when the subsidence was the most intensive in the history of the region (Dulias 2013). Both growth eccentricity and compression wood among Scots pines are good indicators for terrain deformations caused by underground mining.

Dated tree-ring reductions are less clearly related to terrain subsidence. They could have been caused with changes of the groundwater level (Perez-Valdivia & Sauchyn 2011). A significant habitat humidity changes can result in worsening growth conditions and in reduction of tree-rings widths. In the other hand, Laanelaid and Eckstein (2010) found that subsidence in some cases can cause better trees growth (various trees species). Also after a subsidence period trees can regenerate well. Such situation in this research can be observed after second subsidence period (1962-1983) when tree growth increases. In the study area tree-ring reductions can also have another cause: air pollution emitted by heavy industry. According to Danek (2007) and Malik et al. (2012) Scots pines growing on the Silesian Upland developed pollution-related strong reductions in the period from 1960s, 1970s and 1980s. Reductions developed due to harmful emission of sulphur compounds. Tree-ring reductions in trees under study can also be connected mostly to industrial air pollution, as they appear in similar periods, both on the study site and on reference site.

## Conclusions

Dendrochronological tools, in particular those involving wood anatomical features caused directly by stem tilting seem promising for future studies on terrain subsidence. Eccentricity and reaction wood can be applied in detecting and reconstructing the intensity of mining-related subsidence. The phenomenon is a danger to people infrastructure but data on its past activity are often limited and imprecise. Remote sensing methods can only be applied for short, recent periods. For the period after World War II only comparative analyses of maps is available. This, however, represent diverse scales and accuracy. Data from before World War II are even more scarce and inaccurate. Results of our study show that dendrochronology can be applied to provide the lacking information.

## References

- Danek M. 2007: The influence of industry on Scots pine stands in the south-eastern part of the Silesia–Kraków Upland (Poland) on the basis of dendrochronological analysis. *Water, Air, & Soil Pollution* 185(1–4): 265–277.
- Dulias R. 2013: Denudacja antropogeniczna na obszarach górniczych na przykładzie Górnosląskiego Zagłębia Węglowego. Uniwersytet Śląski.
- Gabzdyl W., Gorol M. 2008: Geologia i bogactwa mineralne Górnego Śląska i obszarów przyległych. Wydawnictwo Politechniki Śląskiej.
- Gärtner H., Schweingruber F. H., Dikau R. 2001: Determination of erosion rates by analyzing structural changes in the growth pattern of exposed roots. *Dendrochronologia* 19: 81-91.
- Konagai K., Kiyota T., Suyama S., Asakura T., Shibuya K., Eto C. 2013: Maps of soil subsidence for Tokyo bay shore areas liquefied in the March 11th, 2011 off the Pacific Coast of Tohoku Earthquake. *Soil Dynamics and Earthquake Engineering* 53: 240-253.
- Laanelaid A., Eckstein E. 2010: Tree growth in an area subsided due to mining activities in Northeast Estonia. *Baltic Forestry* 16 (1): 180-186.
- Machowski R. 2010: Przemiany geosystemów zbiorników wodnych powstałych w nieckach osiadania na Wyżynie Katowickiej. Wydawnictwo Uniwersytetu Śląskiego.
- Malik I., Danek M., Marchwińska-Wyrwał E., Danek T., Wistuba M., Krąpiec M., Woskowicz-Ślęzak B. 2012: Czasowe relacje pomiędzy redukcjami przyrostów rocznych sosny zwyczajnej (*Pinus sylvestris* L.) oraz śmiertelnością niemowląt pod wpływem zanieczyszczeń atmosferycznych – przykład z województwa śląskiego. *Ochrona Środowiska i Zasobów Naturalnych* 54: 248-260.

- Malik I., Tie Y., Owczarek P., Wistuba M., Pilorz W., Woskowicz-Ślęzak B. 2013: Human-planted alder trees as a protection against debris flows (a dendrochronological study from the Moxi Basin, Southwestern China). *Geochronometria* 3 (30): 208-216.
- Pawluś D. 2007: Prognozowanie osiadań powierzchni terenu przy użyciu sieci neuronowych. *Górnictwo i Geoinżynieria* 3 (31): 329-335.
- Perez-Valdivia C., Sauchyn D. 2011: Tree-ring reconstruction of groundwater levels in Alberta, Canada: Long term hydroclimatic variability. Original Research Article. *Dendrochronologia* 29 (1): 41-47.
- Rzepecka A., Czajka B., Mikuś P., Kaczka R. J., Wyżga B. 2012: Rozwój kępy o złożonej strukturze w żwirowej rzece górskiej. Wyniki analiz dendrochronologicznych i kartograficznych. *Stud. i Mat. CEPL* 1 (30): 105-110.
- Schweingruber F. H., Albrecht H., Beck M., Hessel J., Joos K., Keller D. 1985: Diagnosis and distribution of conifer decay in the Swiss Rhone Valley, a dendrological study. *Eidgenössische Anstalt für das Fortliche Versuchswesen* 270: 189-192.
- Wistuba M., Malik I., Gärtner H., Kojs P., Owczarek P. 2013: Application of eccentric growth of trees as a tool for landslide analyses: The example of *Picea abies* Karst. in the Carpathian and Sudeten Mountains (Central Europe). *Catena* 111: 41-55.
- Yue H., Liu G., Perski Z., Guo H. 2011: Satellite radar reveals land subsidence over coal mines. <http://spie.org/newsroom/technical-articles-archive/3898-satellite-radar-reveals-land-subsidence-over-coal-mines>.

# The impact of earthquakes on radial growth and wood anatomy, examples from Western Carpathians, Poland and Wenchuan, China

D. Gawior<sup>1</sup>, I. Malik<sup>1</sup>, M. Wistuba<sup>1</sup>, Y. Tie<sup>2</sup>, P. Michałowicz<sup>1</sup>, J. Jiang<sup>2</sup> & P. Rutkiewicz<sup>1</sup>

<sup>1</sup> Department of Reconstructing Environmental Change, Faculty of Earth Sciences, University of Silesia, Katowice

<sup>2</sup> Chengdu Centre of China Geological Survey, Chengdu University of Technology, China

E-mail: danielgawior@gmail.com

## Introduction

Earthquakes are phenomena associated with rapid stresses relaxation in the earth's crust, when part of the released energy reaches the Earth's surface. The main parameters describing earthquakes are magnitude and intensity. The magnitude is the value calculated on the basis of the data recorded by the measuring equipment (seismographs). The intensity is determined on the basis of damage or measurement of the acceleration of land in given place (Musson and Cécic 2012). In depopulated areas or in areas without an adequate network of seismographs, possibilities of direct observation are often limited or the data is incomplete. At the same time the trees growing in earthquake epicentres or in the immediate vicinity are frequently destroyed or heavily damaged (Jacoby et al., 1997, Nepop et al. 2013). Injuries disturb radial growth what causes that trees develop certain wood anatomy features recorded in the following tree rings, such as: resin ducts, callus tissue (scar tissue), reaction wood and eccentricity (both developed due to stem tilting), tree-ring reductions and missing rings (e.g. Schweingruber et al. 1990, Allen et al., 1999, Schneuwly et al. 2009, Genova 2012). On the other hand, trees which survived an episode of seismic shaking without serious damage can take abrupt increase in tree-ring widths as a result of the elimination of neighbouring specimens (Jacoby et al., 1997; Bekker, 2004). The aim of the study was to compare reaction of trees to two earthquakes of different magnitude and intensity recorded in tree rings and wood anatomy.

## Study area

The studies were conducted in the vicinity of the two epicentres of earthquakes: very strong earthquake in 2008, in the Sino-Tibetan Mts (Hengduan Shan, China, Sichuan Province, Wenchuan county) (Fig. 1A) and the epicentre of weak seismic shaking in 2004, in the Western Carpathian Mts (Podhale region, southern Poland) (Fig. 1B).

The main shock of 2008 Wenchuan earthquake occurred in the middle segment of a vast system of Longmenshan faults. Its magnitude was estimated at 7.9 Mw, and instrumental intensity X+ (the highest in a scale) (Hao et al. 2011). Based on the macroseismic intensity data, at the study site (Yingxiu village), the earthquake was estimated at XII degrees in EMS-98 scale. In 2008 the main shock was followed by 213 aftershocks with an average magnitude 4,3Mw (Lekkas 2010). The bedrock of the study area is composed of the Sinian shales, Cambrian sandstones and siltstones, Ordovician limestones, Silurian slates and phyllites, Devonian limestones and dolomites, Carboniferous limestones and shales, Permian limestones, Triassic sandstones and shales. Loose, Quaternary deposits cover the area in the form of river terraces and alluvial fans (Tang et al. 2011). This region has humid climate with annual precipitation exceeding 1200 mm.

The weak earthquake occurred in 2004 at the border of geological units of the Inner and the Outer Western Carpathians, Podhale, Poland. Its magnitude was estimated at 4.7 Mw. Records from seismographic station of the Institute of Geophysics Polish Academy of Sciences in Niedzica, the nearest to epicentre is defective because of distortion of recorded signals (the distance between the seismograph and the epicentre was too small). For this reason, it was not possible to estimate the maximum velocity and acceleration neither to determine the intensity of tremors near the

epicentre (Zembaty et al. 2007). Based on macroseismic data the epicentral intensity of the main shock at the study site (Czerwienne village) was estimated at VI degrees in EMS-98 scale (Zembaty et al. 2005). The bedrock is composed of the Podhale flysch sandstones, mudstones and claystones (Watycha, 1972). Average annual precipitation totals in the study area slightly exceed 900 mm with annual totals varying from 600 to 1100 mm.

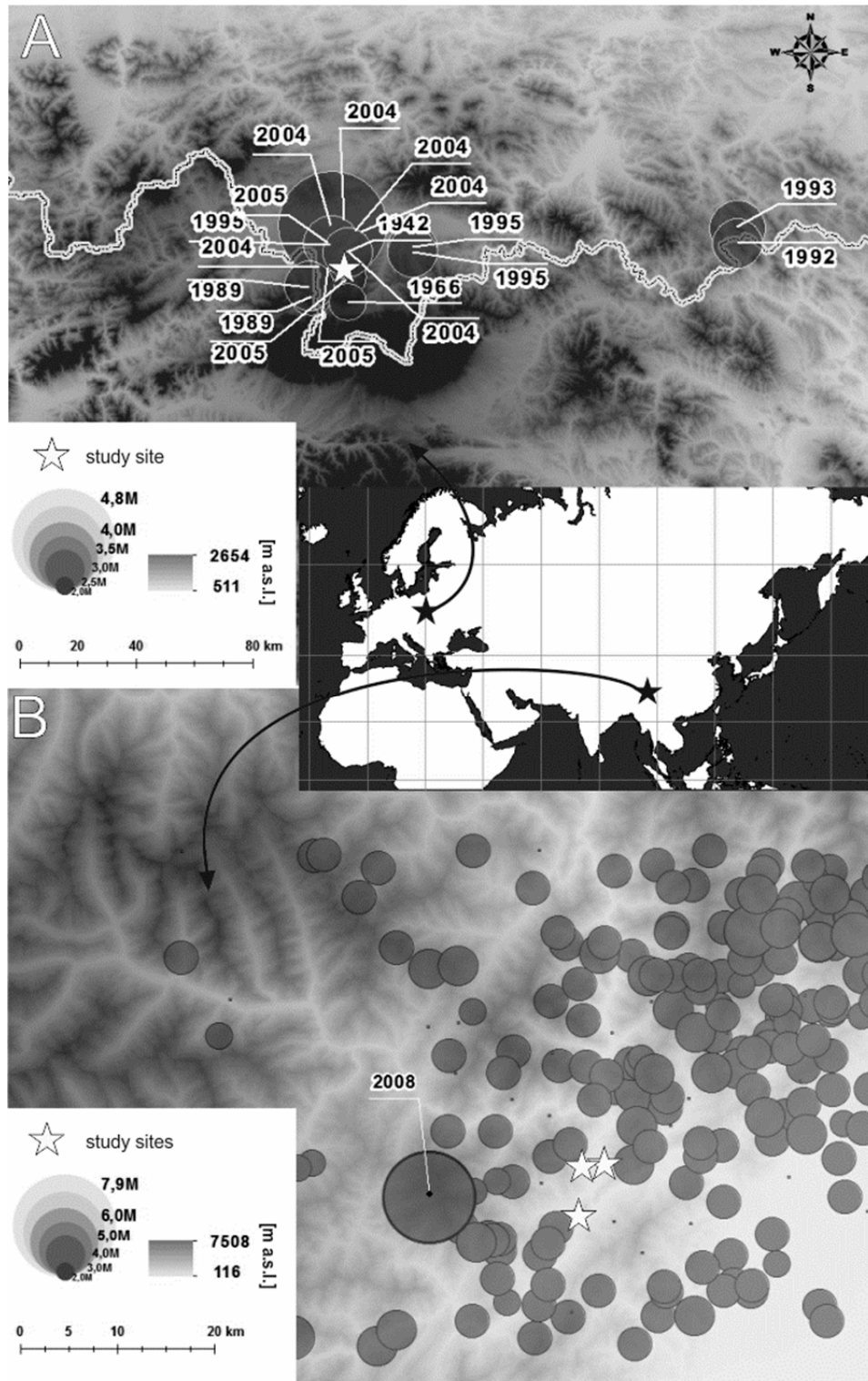


Figure 1: A – location of the sampling site near earthquake epicentres, Podhale, Poland, B – location of the sampling site near 2008 earthquake epicentre and aftershock epicentres, Wenchuan, China.

## Material and methods

For both epicentres of earthquakes we have selected sampling sites located on flat surface or slightly inclined slope. This allowed to exclude the impact of geomorphological processes, such as mass movements, from further analysis.

In China, we have sampled 12 firs (*Abies chensiensis*) growing in three locations, 11 km from the epicentre of 2008 Wenchuan earthquake (Fig. 1A). In Poland we have sampled 20 spruces (*Picea abies*) growing 1,5 km from the epicentre of 2004 earthquake (Fig. 1B). In both cases samples were collected at the breast height in two perpendicular axes: 2 cores were taken along the direction of stem tilting (one from upper and one from lower side of a stem) and 2 cores perpendicularly to tilting direction (left and right sides of stem).

The samples were subjected to a standard preparation for further analyses (sanding to reveal wood structure). Next, widths of annual tree rings were measured with 0.02 mm accuracy. Collected samples were analysed in terms of presence of the following features of wood anatomy (Fig. 2):

- (a) sudden changes in the width of annual growth rings: growth reductions and releases calculated according to the method by Schweingruber (1990) and divided by severity into two classes: 30-70% and > 70%; reductions and releases weaker than 30% were not taken into account,
- (b) traumatic resin ducts,
- (c) intra-annual disturbances of wood density (within single growth rings),
- (d) eccentric growth analysed using percent index by Wistuba et al. (2013) allowing to compare ring widths on opposite sides of tilted stems; events of eccentricity were determined when index yearly variation exceeded the range -50% to +50%.

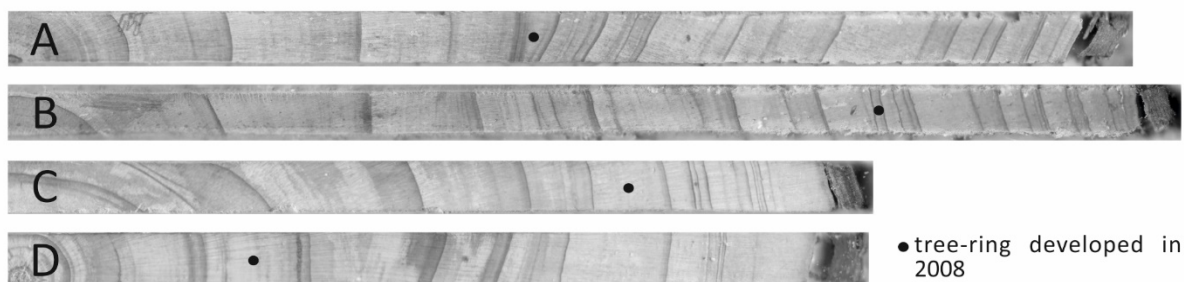


Figure 2: Examples of analysed wood anatomy features developed after the 2008 Wenchuan earthquake: A – disturbances of wood density after 2008, B – ring reduction since 2008, C – ring reduction after 2008, D – growth release after 2008.

## Results and discussion

The trees sampled in Poland, near the epicentre of weak earthquake were at least 25 years old during seismic event. During the earthquake they had 55 tree rings at the breast height, on average. Tree sampled in China, near the epicentre of very strong shocks are very young. During the earthquake they had 4 tree rings at the breast height, on average. During sampling, in 2015, we have not found any older specimens in the study area. Only small, young trees survived the earthquake. Besides the age of sampled trees, there is a clear difference in sampling site distance from earthquake epicentres. Sampling site in Poland is located only 1.5 km from the epicentre, and sampling area in China is located 11 km from the epicentre. These factors, along with the fundamental differences in the strength of shock (earthquake in Poland was 27 000 times weaker than the Wenchuan earthquake), should be considered in the interpretation of tree-ring data. In addition, weak earthquake in Podhale took place after the end of the growing season, and very strong earthquake in China occurred during the growing season.

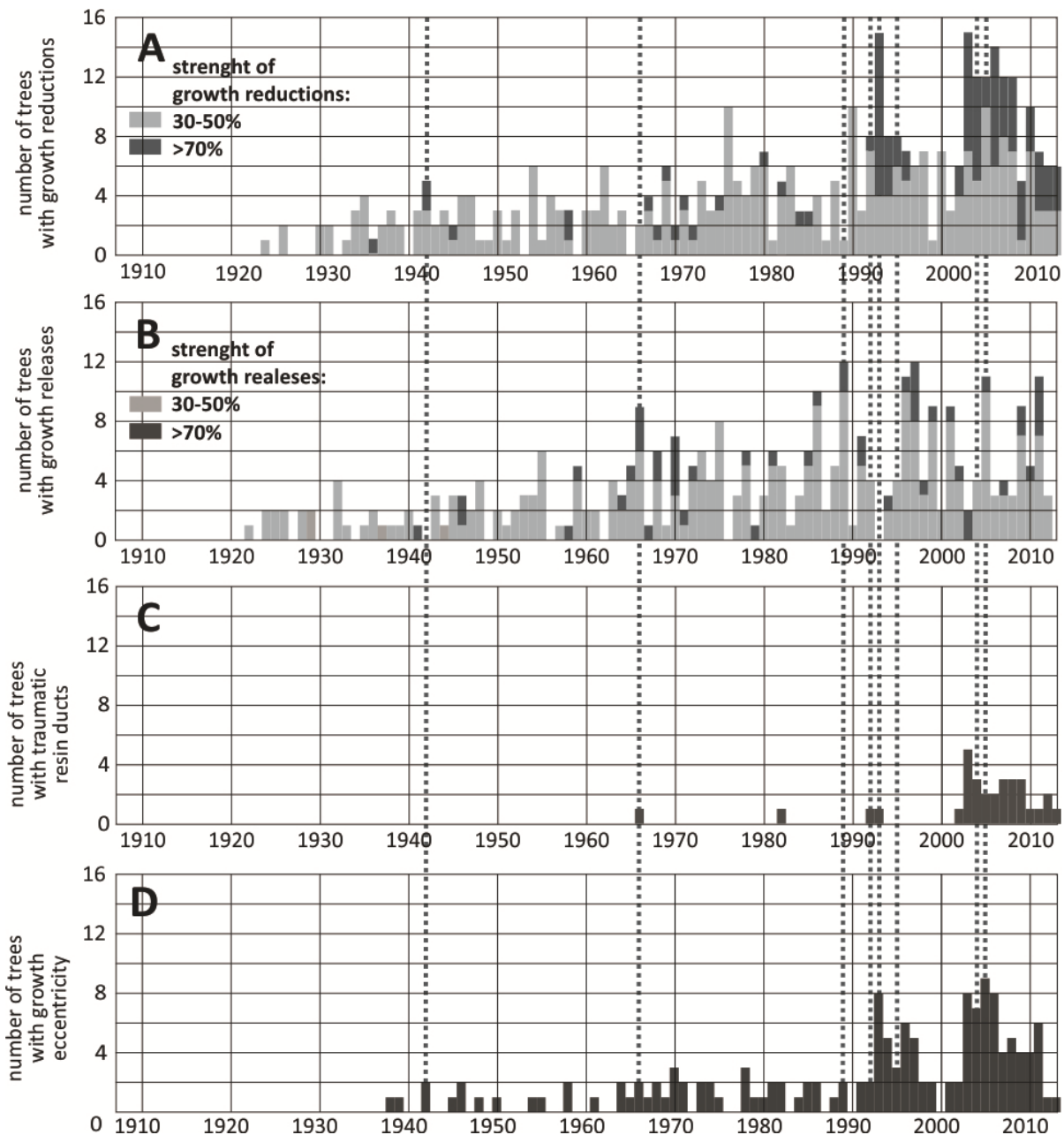


Figure 3: Disturbances of radial growth dated among trees sampled in Podhale, Poland 1.5 km from 2004 earthquake epicentre: A – tree-ring reductions, B – growth release, C – traumatic resin ducts, D – growth eccentricity. Dotted lines mark events of weak earthquakes observed in Polish part of the Western Carpathians.

#### Wood anatomy features in trees growing near epicentre of weak 2004 earthquake in Poland

Among trees sampled in Podhale, Poland we found reductions of annual tree rings in 1992-1999 and 2003-2013, with the largest number of trees showing growth suppression in 1993, 2003 and 2007 (Fig. 3A). Increased number of trees showing growth release was, on the other hand, recorded in 1966, 1986, 1989, 1996-1997, 2005, 2011 (Fig. 3B). Traumatic resin ducts are rare among studied trees and occur mainly in 2003-2009 (Fig. 3C). In the periods: 1993-1997 and 2003-2009 (Fig. 3D) we found increased incidence of eccentricity growth events. No intra-annual disturbances of wood density were found in studied samples.

The weak earthquake in Poland occurred in November 2004, after the end of growing season. Therefore, any wood anatomy disturbances caused by seismic tremors would be recorded in tree

rings developed in next years, from 2005 onwards. Also, between November 2004 and June 2005 6 earthquakes in total (including studied earthquake, the strongest of them) were recorded in the study area (Guterch 2009).

In 2005 we have found a high number of trees with eccentric growth. In 2006 this number was only slightly lower. However, eccentric growth appeared among trees under study since 2003. Similarly, tree-ring reductions are also numerous both before and after the 2004 earthquake. The maximum number of traumatic resin ducts and growth reductions in the trees under study was found in 2003, before the earthquake. At the same time, we have found that in 2005 the number of trees with growth release increases significantly (Fig. 3B).

Sampling site is located 5-15 km from the epicentres of some older earthquakes with epicentres in Podhale region, Poland (Guterch 2009) (Fig. 3). Their magnitudes ranged from 2.9 to 3.5 and they were weaker than this one in 2004. After one of the earthquakes, which occurred in 1995, we found increased number of incidents of the eccentricity and the growth releases (Fig. 3). At the same time there were no resin ducts and significant growth suppression among studied trees.

Within the distance of 100 km from sampling site the earthquakes occurred in March 1942, March 1966, October and November 1989, June 1992 and March 1993 (Guterch 2009) (Fig. 3). Magnitudes of these shocks were between 2.3 and 4.4. Upon the occurrence of stronger shocks in 1989, 1992 and 1993 we found numerous events of eccentricity (1993) and growth reductions (1989 and 1993) in studied trees (Fig. 3). In 1966, after a weak earthquake (M 2.3), we found increased number of trees with growth release among sampled population (Fig. 3).

In the case of weak earthquake, at the sampling site located 1.5 km from the epicentre we found that the best diagnostic feature in wood anatomy was a growth release with accompanying growth eccentricity. This is indicated by both the results obtained for 2004 earthquake and for 1995 earthquake. Development of eccentric rings in trees which have been influenced by weak earthquake is a result of tilting trunks during seismic shocks. Trees inclined from the vertical position are influenced by gravity: stresses in a stem become to be distributed unevenly. The upper side of a stem is subjected to tension and the lower is compressed. Conifers, such as spruce and fir, increase their radial growth rates on the compressed side of stems, developing eccentric tree rings (Wistuba et al. 2013). The results indicate that even earthquakes as weak as tested may cause a change in the position of tree stems. Due to the low power of earthquake studied in Podhale, Poland it is difficult to explain the occurrence of growth releases after the earthquake as results of the elimination of neighboring trees. In addition, we have not found any remains of trees destroyed by the earthquake.

#### *Wood anatomy features in trees growing near epicentre of very strong earthquake in 2008 in China*

Among trees sampled in China we found ring reductions in 2007-2015 with the largest number of trees with growth suppression in 2010, 2011 and 2013 (Fig. 4A). Growth release was recorded in 2012, 2013 and 2015 (Fig. 4B). Intra-annual wood density changes were common during whole lifetime of examined trees with the highest number of incidents in 2006, 2010-2011 and 2013-2015 (Fig. 4C). The greatest number of trees with eccentricity was observed between 2010 and 2015 (Fig. 4D).

The earthquake under analysis took place in May 2008, during vegetation period. Therefore, any disturbances in wood anatomy could have been recorded in 2008 and younger tree rings. The results (Fig. 4) show that in 2008 only two trees developed reduced rings, but these were strong reductions (>70%). In contrast, before 2008 reductions were almost absent among sampled trees.

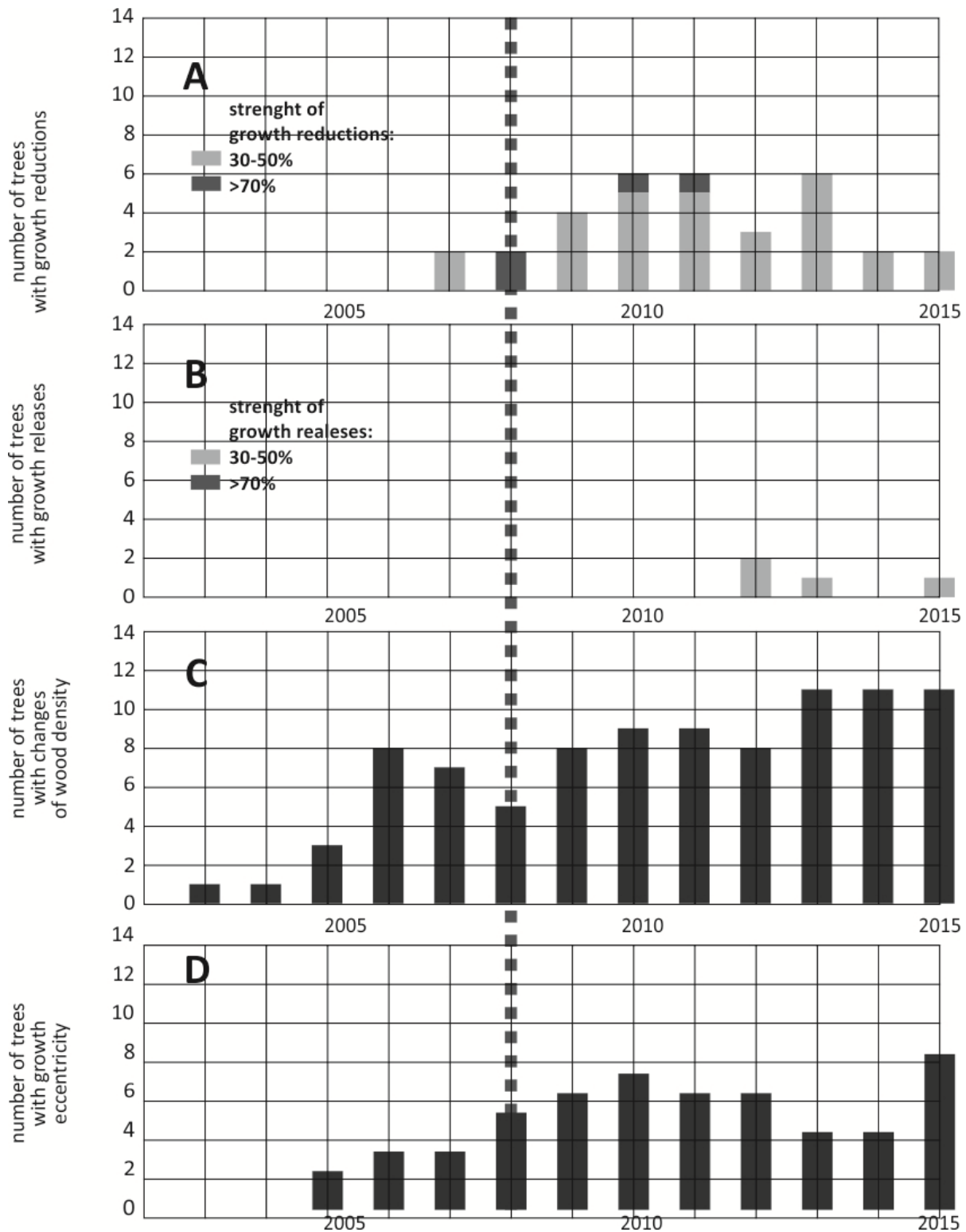


Figure 4: Disturbances of radial growth dated among trees sampled in Wenchuan, China 11 km from 2008 earthquake epicentre: A – tree-ring reductions, B – growth release, C – intra-annual changes of wood density, D – growth eccentricity.

After 2008 we found an increased incidence of tree-ring reductions, intra-annual changes of wood density and eccentricity among studied trees. The strongest disturbance of tree growth was found in 2010-2011. Growth eccentricity and intra-annual changes of wood density occurred also before 2008 but they were less severe (Fig. 4).

## Conclusion

Dendrochronology can be used in palaeoseismological analyses on the condition that the following factors are considered: species of sampled trees (a), age of sampled trees (b), the part of growing season in which an earthquake occurred (c), if possible the nature of earthquake itself, its magnitude, intensity, number of foreshocks and aftershocks (d), and distance between sampling site and earthquake epicentre (e).

Dendrochronology is a potential tool that could significantly supplement the other methods used for the reconstruction of the past seismic events, especially in the areas where observations and measurements are lacking or data is incomplete.

The results indicate that trees of large size are more sensitive to earthquakes. Trees sampled in Poland recorded earthquakes with magnitudes 3.0-4.0. However, the observations made in the epicentral area of 7.9 Wenchuan earthquake indicate that such trees are not able to survive very strong seismic events. The survival is possible for young trees due to flexibility of their stems and poorly developed root systems. Such young specimens are still able to provide dendrochronological record of the occurrence of the earthquake.

Further research on the development of standard anatomical features of wood in relation to varied intensity of earthquakes should allow a more precise palaeoseismic reconstruction. It should however be considered that for both studied earthquakes the tree reaction to seismic event is delayed by at least one year. In the case of weak shocks in Poland the delay is a result of earthquake occurrence after the end of 2004 growing season. In the case of Wenchuan earthquake, China which occurred during the growing season, the strongest reaction of trees was found 2-3 years after the earthquake. This may be due to the extensive character of injuries among sampled tree and due to the time necessary for their regeneration.

## Acknowledgements

A study conducted in China have been funded by the Centre for Studies Polar, University of Silesia - the National Centre for Scientific Lead (KNOW) 2014-2018. Studies in Podhale, Poland were supported by the Polish National Science Centre through grant no. 2011/01/B/ST10/07096.

## References

- Allen, R.B., Bellingham, P.J., Wiser, S.K. (1999): Immediate damage by an earthquake to a temperate montane forest. *Ecology* 80: 708-71.
- Bekker, M.F. (2004): Spatial variation in the response of tree rings to normal faulting during the Hebgen Lake Earthquake, Southwestern Montana, USA. *Dendrochronologia* 22: 53-59.
- Genova, M. (2012): Extreme pointer years in tree-ring records of Central Spain as evidence of volcanic eruptions (Huaynaputina, Peru, 1600AC) and other climatic events. *Climate of the Past* 7: 4223-4259.
- Guterch, B. (2009): Sejsmiczność Polski w świetle danych historycznych. *Przegląd Geologiczny*, vol. 57, nr 6, 513-520. (In Polish)
- Hao, X., Hu, X., Tian, L. (2011): Anomalous tremor before 2008 Ms 8.0 Wenchuan earthquake: a review. *Geodesy and Geodynamics* 2, 3: 56-60.
- Jacoby, G.C. (1997): Application of tree ring analysis to paleoseismology. *Reviews of Geophysics*: 109-124.
- Jacoby, G.C., Bunker, D.E., Benson, B.E. (1997): Tree-ring evidence for an A.D. 1700 Cascadia earthquake in Washington and northern Oregon. *Oregon Geology* 25: 999-1002.
- Lekkas, E.L. (2010): The 12 May 2008 Mw 7.9 Wenchuan, China, Earthquake; Macroscopic Intensity Assessment Using the EMS-98 and ESI 2007 scales and their correlation with the geological structure. *Bulletin of the Society of America* 100, 5B: 2791-2804.

- Musson, R.M., Cčić, I. (2012): Intensity and Intensity Scales. W: Bormann P. (red.). New Manual of Seismological Observatory Practice 2 (NMSOP-2). Deutsches GeoForschungs Zentrum GFZ, Potsdam: 1-41.
- Nepop, R., Agatova, A., Myglan, V., Barinov, V., Nazarov, A. (2013): New methodological aspects of using dendrochronological analysis for dating strong paleoearthquakes (by the example of SE Altai, Russia). *Geophysical Research Abstracts* 15: 177.
- Schneuwly, D.M., Stoffel, M., Bollschweiler, M. (2009): Formation and spread of callus tissue and tangential rows of resin ducts in *Larix decidua* and *Picea abies* following rockfall impacts. *Tree Physiology* 29: 281-289.
- Schweingruber, F.H., Eckstein, D., Serre-Bachet, F., Bräker, O.U. (1990): Identification, presentation and interpretation of event years and pointer years in dendrochronology. *Dendrochronologia* 8: 9-38.
- Tang, C., Li, W.L., Ding, J., Huang, X.C. (2011): Field investigation and research on giant debris flow on August 14, 2014 in Yingxiu Town, epicentre of Wenchuan Earthquake. *Earth Sci. J. Geosci.* 35 (1), 172–180.
- Wistuba, M., Malik, I., Gärtner, H., Kojs, P., Owczarek, P. (2013): Application of eccentric growth of trees as a tool for landslide analyses: The example of *Picea abies* Karst. in the Carpathian and Sudeten Mountains (Central Europe). *Catena* 111: 41-55.
- Zembaty, Z., Jankowski, R., Cholewicki, A., Szulc, J. (2005): Trzęsienie ziemi 30 listopada 2004 r. na Podhalu oraz jego wpływ na obiekty budowlane. *Inżynieria i Budownictwo* LXI, 9: 507-511. (In Polish)
- Zembaty, Z., Jankowski, R., Cholewicki, A., Szulc, J. (2007): Trzęsienia ziemi w Polsce w 2004 roku. *Czasopismo Techniczne. Budownictwo* 104, 2B: 115-126. (In Polish)

# Landslide activity and its triggering factors reconstructed from tree-ring eccentricity in Norway spruce (Western Carpathians, Czech Republic)

K. Łuszczynska, M. Wistuba & I. Malik

University of Silesia in Katowice, ul. Będzińska 60, 41-200 Sosnowiec, Poland  
E-mail: katarzyna\_luszczynska@o2.pl

## Introduction

Mountain areas, including the Western Carpathians, are shaped by mass movements, commonly by landslides (e.g. Šilhán 2012, Wistuba et al. 2013). Slope failures often endanger infrastructure, therefore identifying and monitoring landslide activity is an important issue. Among other methods, dendrochronology has been successfully applied in studies of various types of mass movements: rockfalls (e.g. Stoffel et al. 2005), debris flows (e.g. Hupp 1984) and landslides (e.g. Malik et al. 2016).

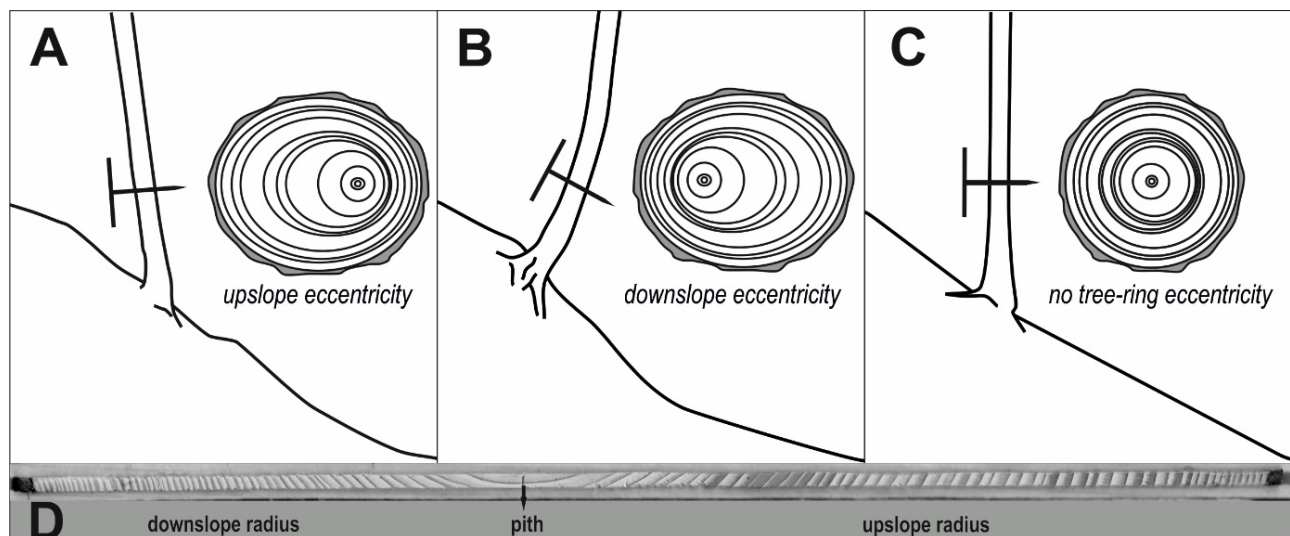


Figure 1: Schematic view of eccentric growth in stems of coniferous trees tilted upslope (A) and downslope (B). Concentric growth of wood in vertical stems (C). An example of an eccentric core collected from a spruce tree tilted upslope on a landslide (D).

Trees growing on active landslide slopes tend to be tilted (Wistuba et al. 2013). Mechanical stress affects also the structure of wood and width of tree-rings. The direction of the deformation produced depends on the direction of tilting: upslope or downslope (Fig. 1). Coniferous trees, such as Norway spruce, produce wider rings with compression wood on the lower side of a tilted stem, that is: upslope side, if tilted upslope (Fig. 1A,D) and downslope side, if tilted downslope (Fig. 1B). Trees growing on stable slopes have straight stems (Fig. 1C). Through analysing sequences of tree-rings on up- and downslope sides of stems we can reconstruct the activity of landslides in the past.

The objective of this study is to analyse the past activity of a selected landslide (Skalka landslide, Western Carpathians, Czech Republic) and to compare results of dendrochronological disturbance dating with the occurrence of precipitation, as especially rainfall is often considered as the main triggering factor of mass-movement activities in Western Carpathians.

## Material and methods

### Study area

The Skalka landslide (834.5 m a.s.l.) is located in the south-eastern part of the Moravian-Silesian Beskids range (Western Carpathians) in the Czech Republic (Fig. 2). The bedrock is of Cretaceous age, composed of sedimentary flysch rocks with extensive colluvial cover (Interactive Geological Maps of the Czech Republic). The landslide has one main scarp and four secondary scarps. Below the main scarp, the main body of the landslide has distinctly separated colluvial blocks dissected by numerous fluvial incisions.

The study area has comparatively cool, mountainous climate. It is located in a zone with a humid temperate climate, transitional between maritime and continental conditions. It has the highest frequency of extreme daily precipitation totals ( $\geq 150$  mm per day) in the Czech Republic (Štekl et al. 2001). Average annual precipitation equals 1423.8 mm (Lysá hora, 1324 m a.s.l.). The landslide area is entirely forested and belongs to the lower montane vegetation belt where deciduous beech forests with common beech (*Fagus sylvatica* L.) and silver fir (*Abies alba* Mill.) occur. However, the study site is covered with a planted, monoculture forest consisting of Norway spruce (*Picea abies* Karst.).

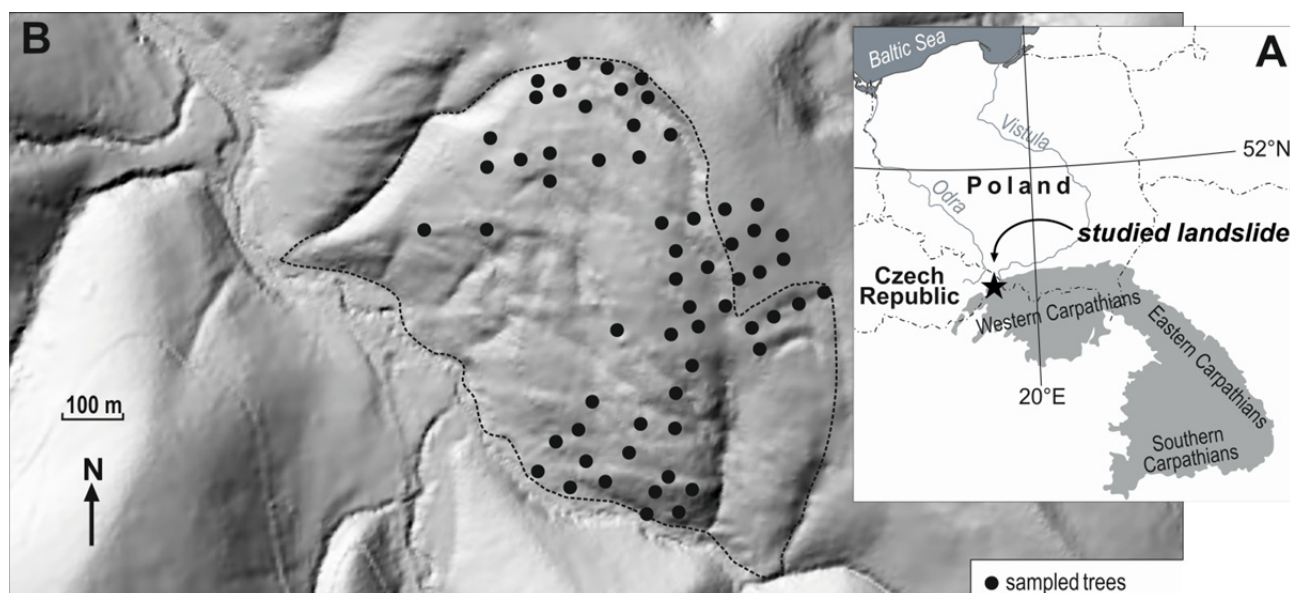


Figure 2: Location of the landslide in Western Carpathians (A) and on the slope of Skalka Mt. (B).

### Methods

On the Skalka landslide we have sampled 60 Norway spruce specimens. Using Pressler borer we took two cores from each tree: one from the upslope side of each stem and the second from the downslope side. To avoid dating other, non-geomorphic phenomena (e.g. growth disturbances caused by insect outbreaks, air pollution, injuries caused by logging of neighbouring trees, etc.), only trees visually assessed as healthy, without injuries and mechanical damages, and without visible losses of assimilation apparatus were sampled. Samples were taken mainly in the highest and lowest parts of landslide and to a lesser extent, in the central part (Fig. 2B). The distribution of sampled trees depends on the availability of healthy spruce trees in a suitably old age (we excluded young trees with a circumference of less than 50 cm). Next, cores were glued in the wooden holders and sanded to reveal the structure of wood and enable measuring tree-ring width (with 0.01 mm accuracy).

In the samples taken we have analysed tree-ring eccentricity. For dating landslide activity we applied the tree-ring eccentricity index of Wistuba et al. (2013). Dating landslide events was done by using reference thresholds. We applied average level of eccentricity on a stable slope located 500 m SE of the studied landslide, previously studied by Wistuba et al. (2013), who established reference thresholds for the study area as: 53.37% for upslope eccentricity and -56.05% for downslope eccentricity. Reference slope has bedrock, elevation, aspect and inclination similar to the studied landslide. It has, however, smooth surface and no signs of landsliding in the relief. Obtained dating results were compared with the precipitation records for summer and winter half-years on the Lysá hora Mt. (11 km W of the studied landslide, data source: Czech Hydro-Meteorological Institute, Ostrava), for 1949-2013. Precipitation was analysed as a potential triggering factor for landsliding on the studied slope.

## Results and discussion

### *Tree-ring record of landslide activity on the study site and its temporal variability*

Tree-ring record of landsliding on the studied slope dates back to 1940 (Fig. 3A). The oldest landsliding event was dated in 1949. For the period under study we have dated a total of 259 signs of eccentricity indicating instability of bedrock. Dendrochronological analysis shows that the most dynamic landsliding occurred in: 1975, 1993, 1985, 1968-1969 and 1995 (Fig. 3A).

For most of the period under study (1940-2013) the percentage of trees showing reaction to mass movements does not exceed 10%. This suggests that although the analysed landslide was almost constantly active over the past 75 years, the movement of colluvium was most likely slow and gradual. We assume that single landsliding events affected only small parts of studied slope. The highest amount of eccentricity signals was found in 1975 (20.3% of sampled trees were affected), 1993 (16.7%) and 1985 (15%) (Fig. 3B).

### *Precipitation as a triggering factor for landslide activity*

We have compared landslide events on the studied slope with precipitation totals for summer half-years (IV-IX, 901 mm on average) and preceding winter half-years (X-III, 522,7 mm on average) recorded on the Lysá hora Mt. in 1955–2011. The number of growth disturbances recording landsliding in particular years matches well with precipitation totals for summer half-years (e.g. landsliding and precipitation in: 1965, 1968, 1970, 1972, 1975, 1977, 1985, 1995-1997, 2010) (Fig. 3B). Similarly, Pánek et al. (2011) and Šilhán et al. (2012) found good correlation between the landslide activity and precipitation, in particular with precipitation totals >100 mm and 20/100 mm per day and precipitation totals during summer half-years. Examples of landslides triggered by summer precipitation were also provided by Gorczyca (2010) and Klimeš et al. (2009). However, the impact of precipitation on slope stability also depends on local relief, vegetation cover, soil type and groundwater level in the period directly before precipitation and landslide event (Margielewski et al. 2008). Krąpiec et al. (2008) dendrochronologically dated landslide activity in other parts of Polish Western Carpathians in years: 1971, 1975, 1985 and 1997. 1975 and 1985 are also years with the highest level of landslide activity on the Skalka site. Results described by Krąpiec et al. (2008) were obtained 200 km east from the site under study. This suggests that landsliding in 1975 and 1985 was of regional scale and affected vast area of the Western Carpathians.

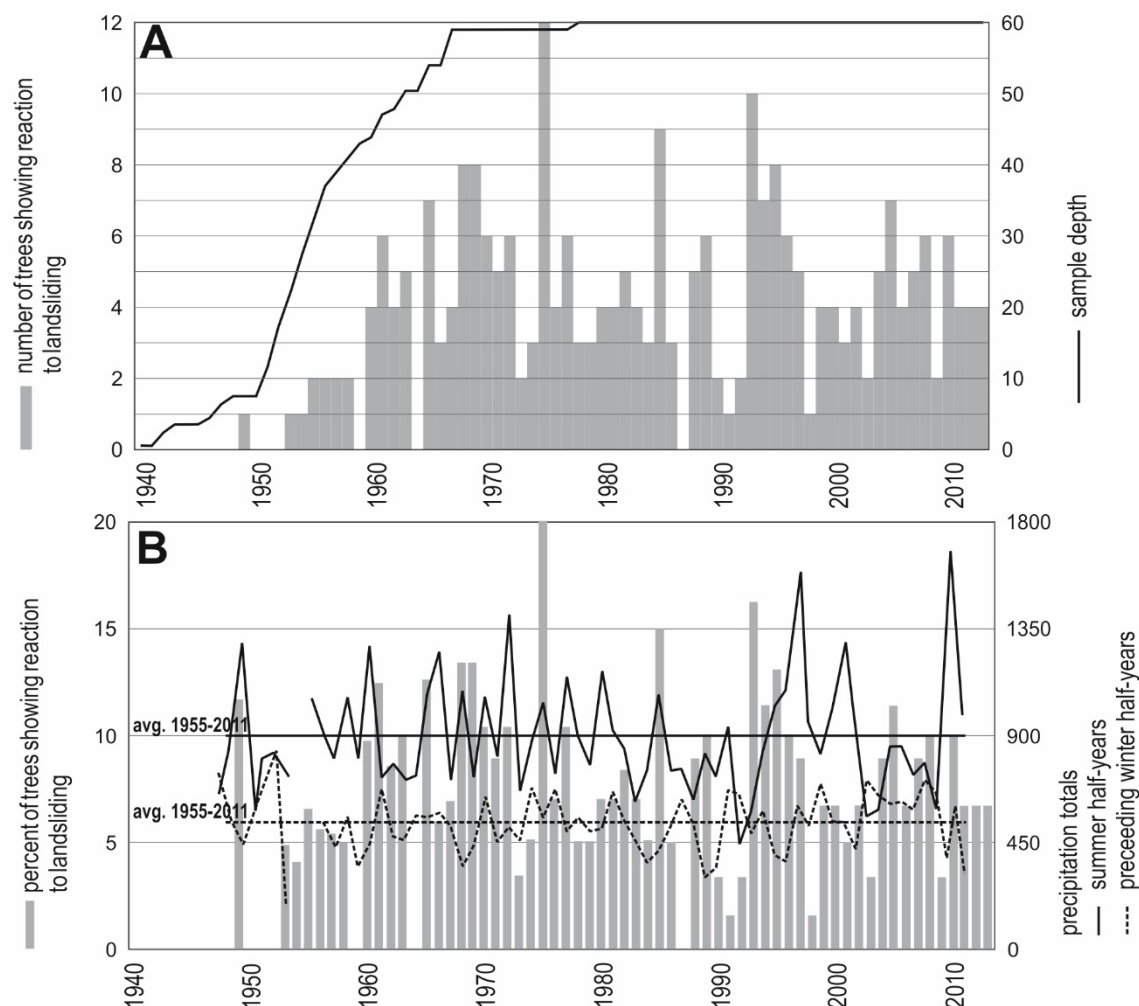


Figure 3: Number of dendrochronological events of landsliding on the study site (A). Percent of sampled trees affected by landsliding compared to precipitation totals on Lysá hora Mt. (B).

Papciak et al. (2015) indicated the relation between landslide events dated from tree rings and precipitation of preceding winters. However, dendrochronological results obtained for the Skalka study site indicate much fewer landslide events occurring in the same years as high precipitation totals of preceding winter half-years, e.g.: 1961, 1970, 2008 (Fig. 3B). At the same time among landsliding events dated on the studied slope there are years with particularly low precipitation totals (1992-1993), both for summer and preceding winter half-years. An example is 1993 event (Fig. 3), when landslide activity was probably caused by 1992 and 1993 earthquakes with epicentres in Western Carpathians (Guterch 2009). The strongest of the earthquakes was M 4.4 (Guterch 2009). The importance of earthquakes as triggering factor of landslide activity in the Polish Carpathians was also noticed Papciak et al. (2015) who, by using tree rings, recorded activity of a landslide in relation to earthquake in 1957.

*Spatial variability of tree-ring record of landsliding during selected events*

We have analysed spatial variability of the tree-ring record of landsliding during three selected strong events: 1975, 1996 (both with high precipitation totals of the summer half-years) and 1993 (with earthquake-triggered landsliding) (Figs. 3,4). Results (Fig. 4) show that single events do not involve whole landslide body, but rather that selected parts of the landslide are active during each event. The main scarp and upper part of landslide body seem to be the most active (Fig. 4). The extent of precipitation-triggered 1975 event and earthquake-triggered 1993 event was similar. However, in 1996 the lowest part of the landslide body was active (Fig. 4). It is possible that in 1996 the precipitation itself was not a trigger for landsliding but rather that precipitation caused

flood on the river at the foot of slope under study (Figs. 2,4). River erosion undermined the balance of slope under study and caused landsliding in its lower part, like it has been described in other parts of the Carpathians, e.g. by Gorczyca (2008).

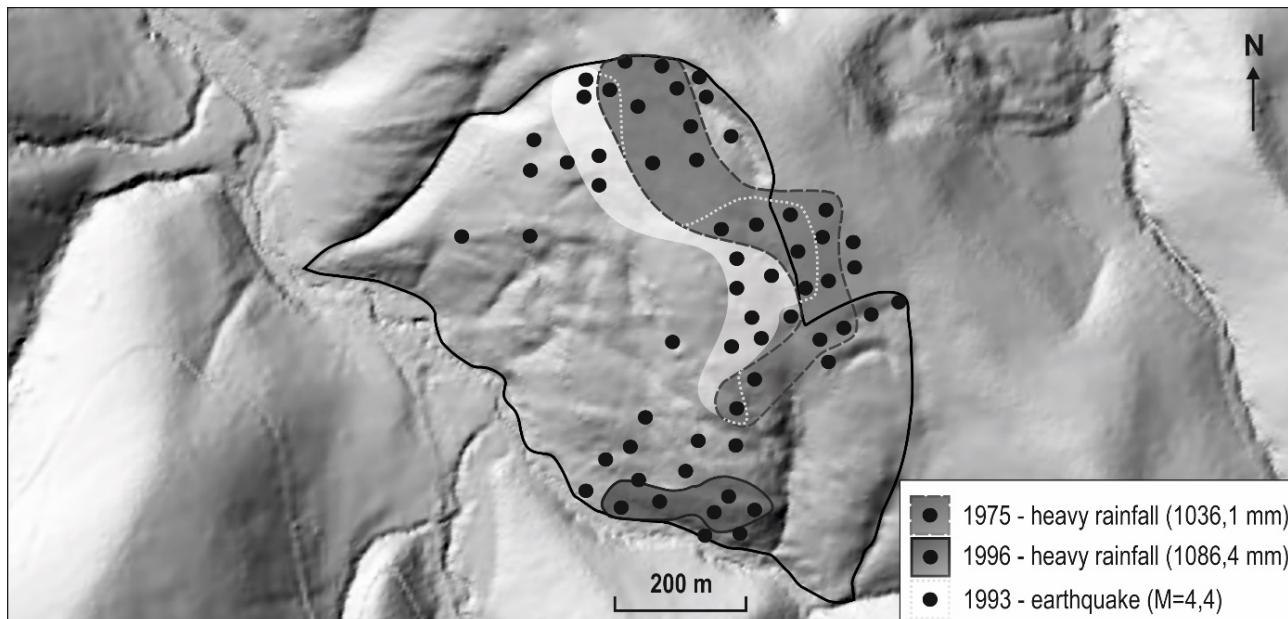


Figure 4: Spatial distribution of tree reaction to landsliding during three selected events related to the occurrence of high summer precipitation totals and earthquakes.

## Conclusions

1. Tree-ring eccentricity has been proved useful in determining temporal and spatial variability of landsliding and in determining triggering factors of landslide activity.
2. Results obtained for the landslide under study indicate low level of mass-movement activity. Tree-ring data show that during the last 75 years events of landsliding have only involved selected parts of the landslide. Upper part of the landslide body and the main scarp are the most active.
3. Different events of landsliding were triggered by different factors like: high precipitation during summer half-year (e.g. 1975), high precipitation during preceding winter half-year (e.g. 1961, 2008), earthquakes (1993), river erosion (1996). However, summer precipitation seems to be the main factor controlling landslide activity on the slope under study.

## Acknowledgements

Studies were supported by the Polish National Science Centre through grant no. 2011/01/B/ST10/07096.

## References

- Gorczyca, E. (2008): Rola płytkich ruchów osuwiskowych w kształtowaniu stoków fliszowych (na przykładzie Beskidu Wyspowego i Bieszczadów). *Przegląd Geograficzny* 80 (1): 105-126.
- Guterch, B. (2009): Sejsmiczność Polski w świetle danych historycznych. *Przegląd Geograficzny* 57: 513-520.
- Hupp C.R. (1984): Dendrogeomorphic evidence of debris flow frequency and magnitude at Mount Shasta, California. *Environ Geol Water Sci* 6, 2: 121-128.
- Interactive Geological Maps of the Czech Republic, 1:25 000, DVD-ROM. Czech Geological Survey, Prague.

- Klimeš, J., Baroň, I., Pánek, T., Kosačík, T., Burda, J., Kresta, F., Hradecký, J. (2009): Investigation of recent catastrophic landslides in the flysch belt of Outer Western Carpathians (Czech Republic): progress towards better hazard assessment. *Natural Hazards Earth System Sciences*. 9: 119–128.
- Krapiec, M., Rączkowski, W., Danek, M., Kłusek, M., Gil, E., Zabuski, L. (2008): Monitoring dendrogeomorfologiczny osuwisk w Beskidzie Niskim, *Prace Komisji Paleogeografii i Czwartorzędu PAU* 6: 173–184.
- Malik, I., Wistuba, M., Migoń, P., Fajer, M. (2016): Activity of slow-moving landslides recorded in eccentric tree rings of Norway spruce trees (*Picea abies* Karst.) – an example from the Kamienne Mts. (Sudetes Mts., Central Europe). *Geochronometria*: 43 (1): 24–37.
- Margielewski, M., Święchowicz, J., Starkel, L., Łajczak, A., Pietrzak, M. (2008): Współczesna ewolucja rzeźby Karpat fliszowych. In: Starkel, L. (ed.): *Współczesne przemiany rzeźby Polski*. Instytut Geografii i Gospodarki Przestrzennej UJ. 57–133.
- Papciak, T., Malik, I., Krzemień, K., Wistuba, M., Gorczyca, E., Wrońska-Wałach, D., Sobucki, M. (2015): Precipitation as a factor triggering landslide activity in the Kamień massif (Beskid Niski Mts, Western Carpathians). *Bulletin of Geography. Physical Geography Series* 8: 5–17.
- Pánek, T., Šilhán, K., Tábořík, P., Hradecký, J., Smolková, V., Lenart, J., Brázdil, R., Kašičková, L., Pazduri, A. (2011): Catastrophic slope failure and its origins: Case of the May 2010 Girová Mountain long-runout rockslide (Czech Republic). *Geomorphology* 130: 352–364.
- Šilhán, K., Pánek, T., Hradecký, J. (2012): Tree-ring analysis in the reconstruction of slope instabilities associated with earthquakes and precipitation (the Crimean Mountains, Ukraine), *Geomorphology* 173-174: 174–184.
- Štekl, I., Brázdil, R., Kakos, V., Jež, J., Tolasz, R., Sokol, Z. (2001): Extrémní denní stážkové úhrny na území ČR v období 1879–2000 a jejich synoptické příčiny. *Národní klimatický program České republiky* 31, Praha.
- Stoffel, M., Lièvre, I., Monbaron, M., Perret, S. (2005): Seasonal timing of rockfall activity on a forested slope at Täschgufer (Swiss Alps) - a dendrochronological approach, *Z. Geomorphol.* 49 (1): 89–106.
- Wistuba, M., Malik, I., Gärtner, H., Kojs, P., Owczarek, P. (2013): Application of eccentric growth of trees as a tool for landslide analyses: The example of *Picea abies* Karst. in the Carpathian and Sudeten Mountains (Central Europe). *Catena* 111: 41–55.



## **SECTION 4**

### **ISOTOPES**

# Stable oxygen isotope series in tropical trees – how much is enough to represent a robust signal?

A. Bräuning<sup>1</sup>, F. Volland<sup>1</sup> & A.D. Pucha<sup>2</sup>

<sup>1</sup>*Institute of Geography, Friedrich-Alexander-University of Erlangen-Nürnberg, Wetterkreuz 15, 91058 Erlangen, Germany*

<sup>2</sup>*Carrera de Ingeniería Forestal, Universidad Nacional de Loja, Ciudadela Universitaria Guillermo Falconí Espinosa “La Argelia”, EC-110101 Loja, Ecuador  
E-mail: achim.braeuning@fau.de*

## Introduction

Stable oxygen isotopes in tropical tree rings have been frequently used to prove the annual nature of wood anatomical tree-ring boundaries in tropical regions (Evans and Schrag, 2004; Anchukaitis et al., 2008) and to relate inter-annual and long-term variations of  $\delta^{18}\text{O}$  variations in tree rings to changes in hydroclimate, even over larger areas and across different climatic archives (e.g., Brienen et al., 2012; Schollaen et al. 2013). Especially, in tropical dendrochronology in very humid environments where tree-ring width chronologies may not contain strong climate signals (e.g. Bräuning 2009; Bräuning et al. 2009),  $\delta^{18}\text{O}$  variations show higher between-tree correlations and provide stronger environmental signals than ring width data (Volland et al., 2016).

Due to labour intensive and costly laboratory analyses on the one hand, and due to high inter-correlation between individual stable isotope series on the other hand, isotope chronologies are often generated by pooling samples of identical years to a mixed sample, whereupon a replication of 4 to 5 trees is usually regarded sufficient (e.g. Leavitt, 2010). However, to serve as reliable proxy for environmental reconstructions, stable isotope chronologies require adequate replication to ensure that they carry a representative signal for a tree population, resulting in reliable palaeoclimate reconstructions (Dorado Liñán et al., 2011). Hence, it has to be assured that the few selected trees also represent the tree population as good as possible. Nevertheless, several studies have demonstrated that stable isotope series from individual trees show considerable differences in their inter-correlations (e.g. Dorado Liñán et al., 2011), and it has not been systematically tested if tree-ring samples showing high correlations among their ring-width variations also concomitantly show highest co-variations among their stable isotope contents. In the present study, we analyse a  $\delta^{18}\text{O}$  data set of *Cedrela montana* (Meliaceae) trees collected in a tropical mountain rainforest in southern Ecuador to test how the number and selection of individual trees for stable isotope analysis influences the robustness of a site chronology established for climate reconstruction purposes (Volland et al. 2016). Specifically, we tested i) how many individual isotope series have to be measured to represent a robust mean isotope chronology; ii) if  $\delta^{18}\text{O}$  series from trees showing high ring-width covariation also exhibit highest similarities in stable isotope signals.

## Materials and methods

### *Study material and stable isotope analysis*

The study site, “Reserva Biológica San Francisco” (RBSF 1800-3180m a.s.l, 3.58°S, 79.04°W) is located at the northern slope of the Podocarpus National Park (PNP) in southern Ecuador (Fig. 1). Local climate data within a distance of 1 km from the sampling sites are available for the period since 1998 – 2011. Mean annual air temperature is 15.3°C and mean annual relative humidity amounts to 83%. Annual precipitation amounts circa 2100mm and varies only slightly between the years (Rollenbeck and Bendix 2011).

We selected the common and valuable tree species *Cedrela montana* that has been shown to have annual and cross-datable tree rings (Bräuning et al. 2009; Volland et al. 2016). The species

shows clear wood anatomical annual tree-ring boundaries that are marked by marginal parenchyma bands (Fig. 1). Wood samples of *C. montana* were collected as increment cores (5mm diameter) from the stands located at an elevation of ca. 2000 m a.s.l.

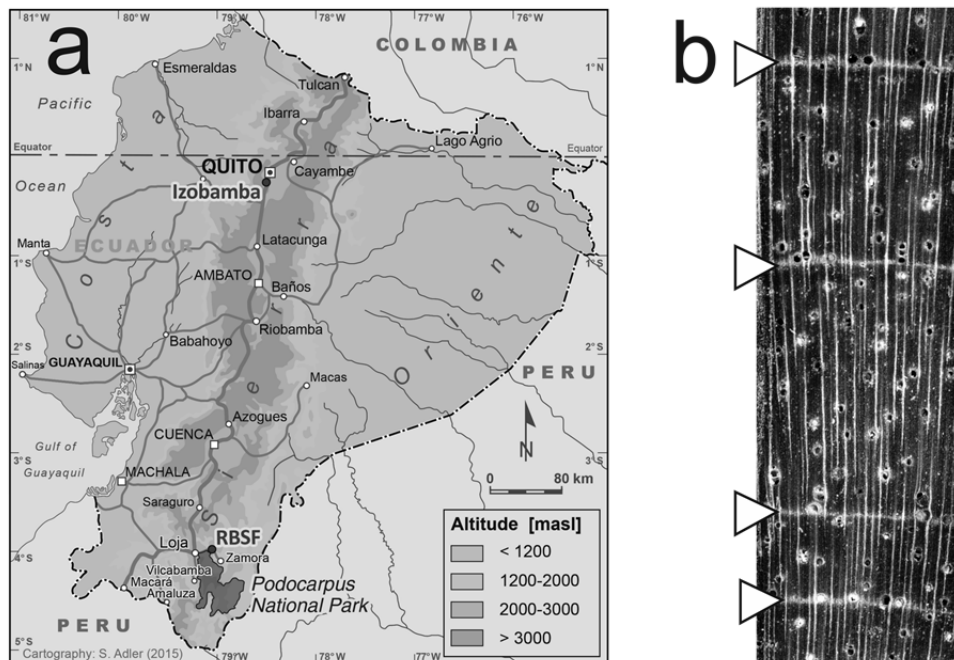


Figure 1: Location of the study area Reserva Biológica San Francisco (RBSF) in southern Ecuador (a) and wood anatomy of *Cedrela montana*. Anatomical ring boundaries are marked by arrows (b).

Tree cores for oxygen isotope analysis came from two nearby sites (ca. 1 km horizontal distance) located in two hydrological microcatchments called Q2 and Q5 and were selected considering the following criteria: (i) occurrence of no or only few missing or false rings, (ii) annual rings with straight borders to enable precise separation of annual rings with a razor blade under a binocular microscope and (iii) the ring-width curves of the sampled trees show high correlations to the master chronology, ensuring correct dating of each individual ring. Hence, the selected trees give a good representation of the total sample population. In total, 15 trees, aged up to 120 years, were selected.

To avoid a possible influence of wood chemicals on the oxygen isotope signal we extracted cellulose from the whole tree rings following the chemical treatment described by Wieloch et al. (2011). Afterwards, we homogenized cellulose with an ultrasonic unit and ca. 300µg of the freeze dried material was loaded into silver capsules (Laumer et al. 2009). The tree-ring cellulose was pyrolyzed in an high temperature HT- oven (Hekatech, Germany) and subsequently transferred to an IRMS (Isotope-ratio mass spectrometer, Delta V Advantage, Thermo Scientific) to detect the  $^{18}\text{O}/^{16}\text{O}$  ratio.

To test the quality of created  $\delta^{18}\text{O}$  chronologies out of the set of 15 individual stable isotope series, Pearson's correlation coefficients over the period 1962-2011 (50 years) that was covered by most samples and Expressed Population Signal (EPS; Wigley et al. 1984) were computed.

## Results

### Correlation of $\delta^{18}\text{O}$ variations among different individuals

Correlation coefficients between the  $\delta^{18}\text{O}$  series are shown in Table 1. Most isotope series show significant correlations among each other, however, some trees only show low correlations to other series. We selected four trees with highest mean correlations (Q5\_169, Q5\_789, Q5\_258, and

Q5\_179) and four trees showing lowest mean correlations (Q2\_1974, Q5\_268, Q5\_754, and Q5\_385) and calculated three isotope chronologies, a mean chronology including all 15 measured series ( $\delta^{18}\text{O}_{\text{mean}}$ ; mean correlation  $\bar{r}=0.467$ ;  $\text{EPS}=0.93$ ), one chronology containing the four series with highest correlation coefficients ( $\delta^{18}\text{O}_{\text{good}}$ ; mean correlation  $\bar{r}=0.694$ ;  $\text{EPS}=0.90$ ), and one chronology from the trees with lowest mean correlations ( $\delta^{18}\text{O}_{\text{poor}}$ ; mean correlation  $\bar{r}=0.297$ ;  $\text{EPS}=0.63$ ).

Table 1: Correlation coefficients between  $\delta^{18}\text{O}$  series of different individuals of *Cedrela montana*.  
\*  $p < 0.05$ ; \*\*  $p < 0.01$

	Q5_789	Q5_258	Q5_769	Q5_765	Q5_268	Q5_754	Q2_1974	Q5_385	Q2_1842a	Q2_1842b	Q2_1874	Q2_2003	Q2_1989	Q2_1842
Q5_169	0.62**	0.62**	0.73**	0.29*	0.59**	0.48**	0.35**	0.36**	0.40**	0.58**	0.46**	0.60**	0.612**	0.77**
Q5_789		0.77**	0.75**	0.41**	0.65**	0.56**	0.40**	0.57**	0.61**	0.62**	0.68**	0.64**	0.74**	0.77**
Q5_258			0.70**	0.39**	0.54**	0.60**	0.25	0.55**	0.31*	0.40**	0.58**	0.64**	0.49**	0.52**
Q5_769				0.38**	0.48**	0.60**	0.20	0.36**	0.40**	0.45**	0.55**	0.58**	0.63**	0.52**
Q5_765					0.03	0.23*	0.14	0.49**	0.04	0.27	0.10	0.20	0.45**	0.37*
Q5_268						0.18	0.28*	0.62**	0.39**	0.43**	0.76**	0.58**	0.62**	0.53**
Q5_754							0.40**	0.25	0.47**	0.29*	0.58**	0.50**	0.44**	0.37*
Q2_1974								0.28*	0.12	0.52**	0.41**	0.22	0.35*	0.40*
Q5_385									0.26*	0.26	0.53**	0.36*	0.31*	0.47**
Q2_1842a										0.48**	0.57**	0.32*	0.26*	0.69**
Q2_1842b											0.35*	0.41**	0.56**	0.68**
Q2_1874												0.50**	0.54**	0.66**
Q2_2003													0.61**	0.61**
Q2_1989														0.58**

Figure 2 shows the three developed isotope chronologies, their characteristics and correlations are indicated in table 2.

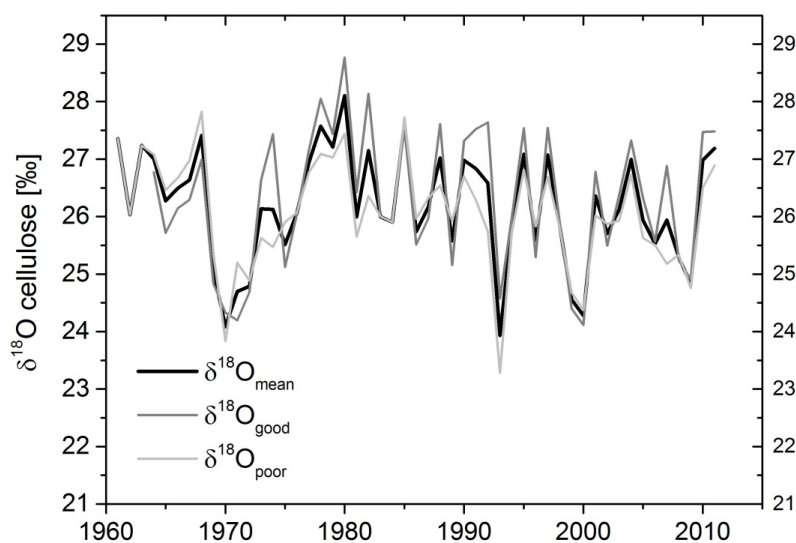


Figure 2: Stable oxygen isotope raw chronologies of 15 averaged individual series ( $\delta^{18}\text{O}_{\text{mean}}$ ), and chronologies of the four best ( $\delta^{18}\text{O}_{\text{good}}$ ) and least good ( $\delta^{18}\text{O}_{\text{poor}}$ ) fitting individual series.

The mean chronology correlates equally strong with  $\delta^{18}\text{O}_{\text{good}}$  and  $\delta^{18}\text{O}_{\text{poor}}$  ( $r=0.935$ ). Still,  $\delta^{18}\text{O}_{\text{good}}$  and  $\delta^{18}\text{O}_{\text{poor}}$  are significantly correlated among each other ( $r=0.751$ ). Although the average  $\delta^{18}\text{O}$  values of all chronologies are not significantly different,  $\delta^{18}\text{O}_{\text{poor}}$  has the smallest amplitude of all chronologies which is evident from the smallest standard deviation.  $\delta^{18}\text{O}_{\text{good}}$  shows the highest standard deviations and maximum/minimum values, and  $\delta^{18}\text{O}_{\text{mean}}$  has intermediate properties. From these numbers and figure 2 it becomes evident that the  $\delta^{18}\text{O}_{\text{poor}}$  chronology shows a dampened signal and hence does only capture a part of the inter-annual variability represented in the two other chronologies.

*Table 2: Correlation coefficients between  $\delta^{18}\text{O}$  raw chronologies composed of different individuals of *Cedrela montana*, and chronology characteristics (mean, minimum, and maximum individual isotope values, and their standard deviation SD). All correlations are significant at  $p<0.01$ .*

	$\delta^{18}\text{O}_{\text{mean}}$	$\delta^{18}\text{O}_{\text{good}}$	$\delta^{18}\text{O}_{\text{poor}}$
Mean [‰]	26.16	26.30	26.03
Min [‰]	23.93	24.12	23.28
Max [‰]	28.10	28.76	27.83
SD	0.97	1.18	0.92
Corr with $\delta^{18}\text{O}_{\text{good}}$	0.935	-	0.751
Corr with $\delta^{18}\text{O}_{\text{poor}}$	0.935	0.751	-

## Discussion and conclusions

We studied inter-annual variations of  $\delta^{18}\text{O}$  in tree-ring cellulose of 15 *Cedrela montana* individuals growing in a tropical mountain rainforest in Southern Ecuador. This is to our knowledge the largest sampling set of stable isotope chronologies from one study region in the tropics. The mean isotope chronology is significantly correlated with seasonal precipitation (January to April), frequency of wet days, and also contains a strong regional signal which is common to other stable isotope series from the Amazon lowland and Andean ice cores (Volland et al. 2016). According to the correlation matrix between individual trees, we found that several trees did not fit to the common population signal, probably to individual microsite conditions due to the highly complex topography and strongly varying soil conditions (Günter et al. 2009).

As it is evident from the EPS signals and statistics of the different isotope chronologies, a sample depth of four individual trees may be enough to reach an acceptable chronology strength as indicated by an EPS exceeding the recommended threshold of 0.85 (Wigley et al., 1984). However, it may also be possible that stable isotope series from four trees are not sufficiently well correlated to create a reliable isotope chronology passing statistical requirements and representing the full inter-annual variability of environmental changes. Finding an optimal balance between scientific requirements and cost and time-efficient study design by minimizing the number of analysed samples needs to be evaluated for each study site and is also dependent on arbitrary factors of microsite conditions which cannot be determined by *a priori* theoretical considerations. Hence, it is not clear without empirical tests if a selection of five trees represents a characteristic site signal or not. In our worst-case scenario ( $r_{\text{bar}}=0.297$ ), a sample depth of 15 individual isotope series would be required to obtain a robust isotope chronology with  $\text{EPS}>0.85$ , which is a requirement that can hardly be fulfilled due to time and resource constraints. However, as seen

from figure 1, even our  $\delta^{18}\text{O}_{\text{poor}}$  chronology was able to capture most of the high-frequency and mid-frequency variations of the other isotope chronologies, however failing to capture the full amplitude of climatic extremes. Hence, we recommend that the quality signal of a stable isotope chronology should be tested, before cost-saving approaches like pooling of tree rings from different tree individuals is considered. In most cases, including material from ca. six trees may probably be sufficient to obtain a chronology signal sufficiently robust to capture a suitable amount of inter-annual variability for environmental reconstructions.

### Acknowledgements

We thank Susanne Spannll, Wolfgang Pfautsch, Roswitha Höfner-Stich, and Dr. Christoph Mayr for technical assistance and helpful comments. This study was supported by the German Research Foundation (DFG) by funding the projects BR 1895/14-1/2 (FOR 816) and BR 1895/23-1 (PAK 823). A.D.P. was supported by a grant of the German Academic Exchange Service (DAAD).

### References

- Anchukaitis, K.J., Evans, M.N., Wheelwright, N.T., Schrag, D.P. (2008): Stable isotope chronology and climate signal calibration in neotropical montane cloud forest trees. In: *Journal of Geophysical Research* 113, G03030, doi:10.1029/2007JG000613.
- Bräuning, A. (2009): Climate variability of the tropical Andes since the Pleistocene. *Progress in Geosciences* 22: 13-25.
- Bräuning, A., Volland-Voigt, F., Burchardt, I., Ganzhi, O., Nauss, T., Peters, T. (2009): Climatic control of radial growth of *Cedrela montana* in a humid mountain rain forest in southern Ecuador. *Erdkunde* 63 (4): 337-345.
- Brienen, R.J.W., Helle, G., Pons, T.L., Guyot, J.L., Gloor, M. (2012): Oxygen isotopes in tree rings are a good proxy for Amazon precipitation and El Niño-Southern Oscillation variability. *PNAS* 109:16957-16962.
- Dorado Liñán, I., Gutiérrez, E., Helle, G., Heinrich, I., Andreu-Hayles, L., Planells, O., Leuenberger, M., Bürger, C., Schleser, G. (2011): Pooled versus separate measurements of tree-ring stable isotopes. *Science of the Total Environment* 409:2244-2251.
- Evans, M.N., Schrag, D.P. (2004): A stable isotope-based approach to tropical dendroclimatology. *Geochimica et Cosmochimica Acta* 68: 3295–3305.
- Günter, S., Gonzales, P., Álvarez, G., Aguirre, N., Palomeque, X., Haubrich, F., Weber, M. (2009): Determinants for successful reforestation of abandoned pastures in the Andes: Soil conditions and vegetation cover. In: *Forest Ecology and Management* 258, 81-91.
- Laumer, W., Andreu, L., Helle, G., Schleser, G.H., Wieloch, T., Wissel, H. (2009): A novel approach for the homogenization of cellulose to use micro-amounts for stable isotope analyses. *Rapid Communications in Mass Spectrometry* 23 (13): 1934–1940.
- Leavitt, S. W. (2010): Tree-ring C-H-O isotope variability and sampling. *Science of the Total Environment* 408: 5244-5253.
- McCarroll, D., Loader, N.J. (2004): Stable isotopes in tree rings. *Quaternary Science Reviews* 23: 771–801.
- Rollenbeck, R., Bendix, J. (2011): Rainfall distribution in the Andes of southern Ecuador derived from blending weather radar data and meteorological field observations. *Atmospheric Research* 99: 277-289.
- Schollaen, K., Heinrich, I., Neuwirth, B., Krusic, P.J., D'Arrigo, R.D., Karyanto, O., Helle, G. (2013): Multiple tree-ring chronologies (ring width,  $\delta^{13}\text{C}$  and  $\delta^{18}\text{O}$ ) reveal dry and rainy season signals of rainfall in Indonesia. *Quaternary Science Reviews* 73: 170–181.
- Volland, F., Pucha, D., Bräuning, A. (2016): Hydro-climatic variability in Southern Ecuador from tree-ring oxygen isotopes. *Erdkunde* 70: 69-82.

- 
- Wieloch, T., Helle, G., Heinrich, I., Voigt, M., Schyma, Ph. (2011): A novel device for batch-wise isolation of  $\alpha$ -cellulose from small-amount wholewood samples. *Dendrochronologia*. 29,2: 115-117.
- Wigley, T., Briffa, K.R., Jones, P.D. (1984): On the average value of correlated time series, with applications in dendroclimatology and hydrometeorology. *Journal of Applied Meteorology and Climatology* 23: 201-213.

# Climatic signals in stable carbon isotope ratios of juniper tree rings in northern Iran

Z. Foroozan<sup>1</sup>, K. Pourtahmasi<sup>2</sup> & A. Bräuning<sup>1</sup>

<sup>1</sup> Institute of Geography, Friedrich-Alexander-University of Erlangen-Nurnberg, Erlangen, Germany

<sup>2</sup> Department of Wood and Paper Science & Technology, Faculty of Natural Resources, University of Tehran, Karaj, Iran  
E-mail: parisa.foroozan@gmail.com

## Introduction

Trees are considered to be one of the most important proxies for paleoenvironmental and paleoclimatic studies. This results from their high living age and broad geographical distribution. Trees provide the greatest potential for reconstructions of past climates with annual or even sub-annual resolution and statistically defined confidence limits (e.g., Esper et al., 2002; Esper et al., 2007; Büntgen et al., 2011). Among all tree-ring parameters, stable isotopes have been proven as reliable recorders of former climate conditions (e.g., McCarroll and Loader 2004). Climatic and environmental conditions at the time of tree-ring formation affect the width of tree rings, wood density, and the isotopic composition of the cellulose in the xylem cell walls. In contrast to ring width, stable isotopes in  $\alpha$ -cellulose potentially record climate signal even when there is no dominant climatic control on tree growth, which is often the case in regions with temperate or tropical climate, where no single climate factor limits tree growth (Loader et al., 2008; Young et al., 2012).

The  $\delta^{13}\text{C}$  of tree-ring cellulose has been widely studied to reconstruct past environmental changes. A number of environmental parameters, including soil moisture, air temperature, precipitation, relative humidity, and solar irradiation can influence the fractionation of the carbon isotopes incorporated into plant material and hence may be potential aims for paleoclimate reconstructions (Francy and Farquhar 1982, Feng 1998, Bonal et al., 2000). The interplay between various factors involved in the carbon isotope fractionation in trees can be described in terms of the following equation (Farquhar et al. 1982):

$$\delta^{13}\text{C}_{\text{plant}} = \delta^{13}\text{C}_{\text{air}} - a - (b - a) \cdot (C_i / C_a)$$

With regard to this equation,  $\delta^{13}\text{C}$  values in tree rings record changes in the concentration of  $\text{CO}_2$  in the stomatal chambers ( $C_i / C_a$ ), reflecting the balance between diffusion of  $\text{CO}_2$  from the atmosphere into the intercellular spaces by the stomata (stomatal conductance), and carbon fixation. Previous studies found a correlation between tree-ring  $\delta^{13}\text{C}$  and temperature (Saurer et al. 1995, Liu et al. 2004, Szczepanek et al. 2006, Liu et al. 2007, Young et al. 2012) or precipitation (McCarroll and Pawellek, 2001, Liu et al. 2003, Ferrio and Voltas 2004, Liu et al. 2004). Negative correlations between tree-ring  $\delta^{13}\text{C}$  and precipitation were reported for deciduous species and evergreen tropical tree species (Gebrekristos et al., 2009). Results of Xu et al. (2014) confirmed that temperature has a positive effect on tree-ring  $\delta^{18}\text{O}$  and  $\delta^{13}\text{C}$  of spruce (*Picea schrenkiana*) in the central Tianshan Mountains of northwestern China, while precipitation and relative humidity have negative effects.

Juniper forests form the high-elevation forest belt in the Alborz Mountain (Sageb-Talebi et al. 2014) in north Iran. Junipers are drought and cold-tolerant species growing on south-facing slopes which are located in the rain shadow of moist Caspian air masses. Juniper (*J. polycarpus*) differs from moisture-demanding tree species like e.g. deciduous oak trees growing in their water use strategies and, hence, in their capacity to cope with drought. Evergreen juniper has a shallow root system and uses internally stored and superficial soil water supplies (Tranquillini, 1976; Valentini et al., 1994). Preliminary analyses of climate-tree growth relationships revealed that tree growth of high-elevation juniper trees growing on south-facing slopes is significantly ( $p > 0.05$ ) positively influenced by precipitation in spring. However, the correlations of chronology with monthly precipitation is rather weak (Pourtahmasi et al., 2012). While initial studies examined the climatic

signal contained in stable oxygen isotope ratios of different tree species in north Iran (Foroozan et al. 2015), no studies have yet analyzed the climatic signals retained in stable carbon isotope variations in annual tree rings in Iran. Hence, in this study, we examined the potential of stable carbon isotope ratios in juniper tree rings for climate reconstructions in northern Iran. The aim of this study was to determine the strength of the common signal shared among individual stable carbon isotope series of individual trees of one site, and to characterize the climatic signal retained in stable carbon isotope ratios of juniper (*Juniperus polycarpus*) trees.

## Materials and methods

### *Study site and climate conditions*

The Alborz Mountain range stretches along the entire southern coast of the Caspian Sea, the largest inland water body in the world (Fig. 1). The Alborz mountain range forms a climatological barrier for humid air masses from northerly directions moving into the dry central Iranian plateau. The juniper forests are located on the southern slopes of the Alborz Mountains, where arid conditions prevail with irregular and low precipitation during autumn to spring (Sagheb-Talebi et al., 2014).

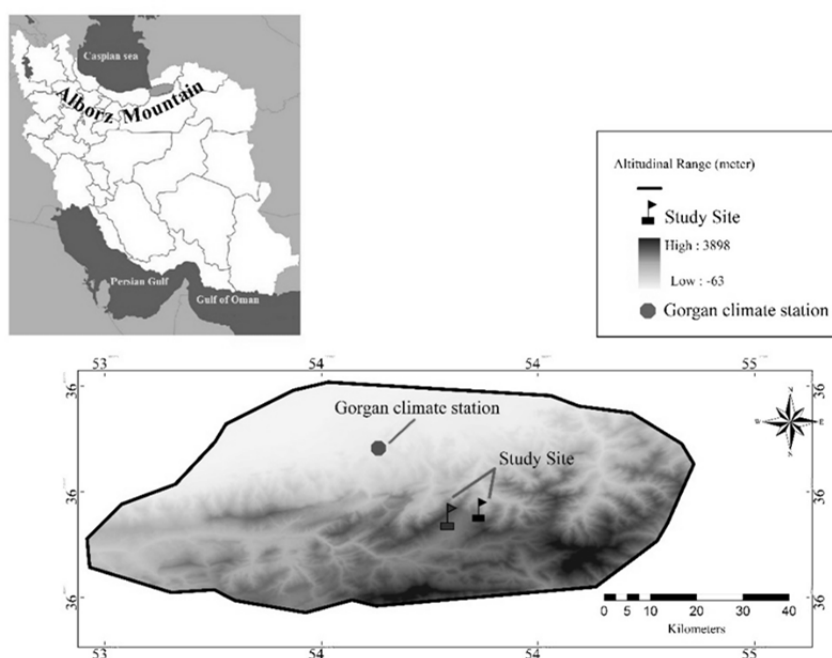


Figure 1: Location of the study sites and climate stations

In order to study tree-ring  $\delta^{13}\text{C}$ -climate relationships, meteorological data were taken from Gorgan meteorological station (36°85'N; 54°27'E; 1300 m a.s.l., 1958-2007), which is the closest climate station to the study site (Fig. 1). Gorgan has a mean annual temperature of 18.3°C and a mean annual precipitation of 616.5 mm (Fig. 2). The region experiences dry conditions during summer from the beginning of May until mid-September. Highest precipitation occurs in March and lowest precipitation in July when temperature is at a maximum. To evaluate the influence of climate parameters on tree-ring  $\delta^{13}\text{C}$ , we calculated Pearson correlation coefficients between the juniper  $\delta^{13}\text{C}$  chronologies and monthly and seasonally averaged data of temperature and precipitation.

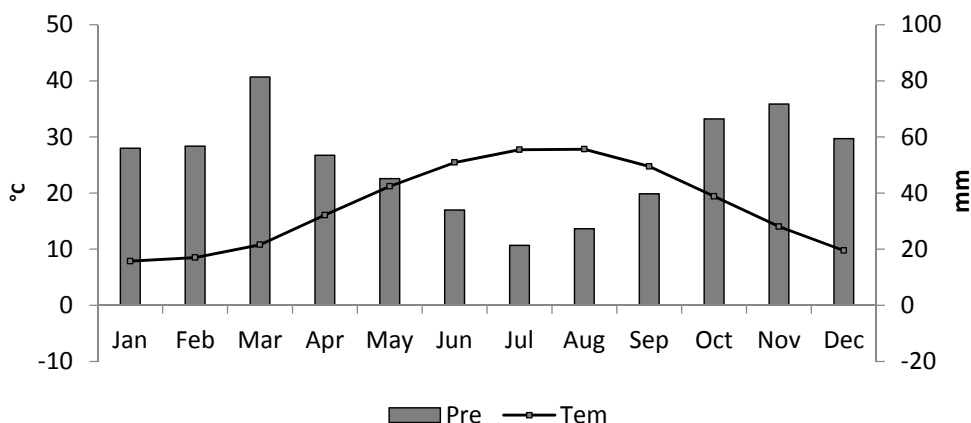


Figure 2: Climate diagram of Gorgan meteorological station

#### Tree-ring sampling and sample preparation

We sampled two increment cores per tree of long living juniper (*J. polycarpus*) trees growing on the south-facing slopes of Alborz Mountain range (36°39'54.4"N; 54°31'53.7"E) at an elevation of 2540 m a.s.l. Stable isotope analysis was conducted on 5 trees from each site that had no missing rings but showed high correlations of their ring-width series to the mean local tree-ring chronology. Potential juvenile effects of the stable isotope series (Esper et al. 2010) were eliminated by focusing on the past 50 tree rings. Individual rings of each core for the 50-year period from 1958 to 2007 were cut carefully and processed for cellulose extraction (Wieloch et al. 2011).

#### Measurement of stable isotope of cellulose

Cellulose was homogenized by ultrasonic homogenization (Laumer et al. 2009) and this is followed by freeze drying. The stable carbon isotopes ratios of  $\alpha$ -cellulose samples were analyzed (analytical precision  $\pm 0.25\%$ ) with a continuous-flow isotope ratio mass spectrometer. The  $\delta^{13}\text{C}$  values for carbon are calculated using the following equation:

$$\delta^{13}\text{C} = \left[ \frac{(^{13}\text{C}/^{12}\text{C})_{\text{sample}}}{(^{13}\text{C}/^{12}\text{C})_{\text{standard}}} - 1 \right] \cdot 1000\%$$

$\delta^{13}\text{C}$  values are reported with respect to either the PDB (Pee Dee Belemnite) or the equivalent (VPDB)Vienna-PDB) standard. In order to clarify the effects of climate factors on the inter-annual variations in  $\delta^{13}\text{C}$  of tree-ring cellulose, we investigated the linear correlations between  $\delta^{13}\text{C}$  values in tree-ring cellulose and temperature and precipitation amounts recorded in the Gorgan climate data.

## Results

#### Correlation of $\delta^{13}\text{C}$ variations among different individuals

In figure 3, the inter-annual variations of raw  $\delta^{13}\text{C}$  values of tree-ring cellulose of junipers are shown. The individual  $\delta^{13}\text{C}$  series correlated significantly (mean inter-tree correlation  $r = 0.49$ ;  $p < 0.01$ ), except for juniper no. 3 which was therefore excluded from further analyses.

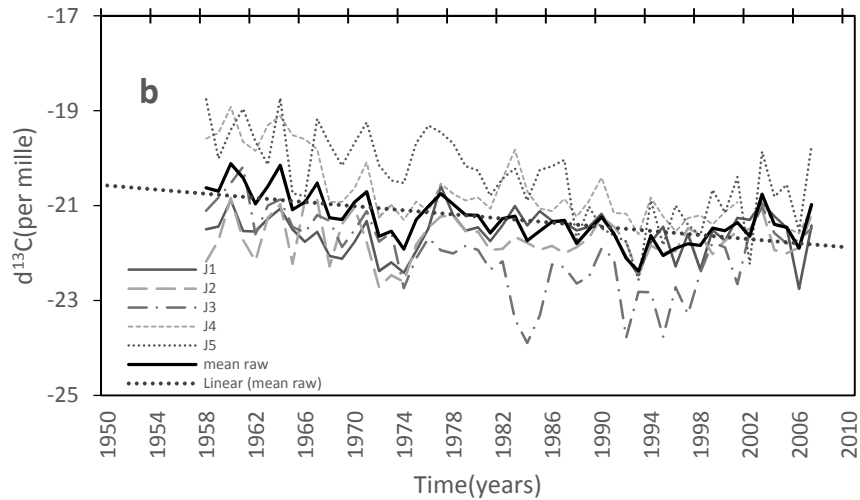


Figure 3. 50-year inter-annual pattern of raw  $\delta^{13}\text{C}$  of tree-ring cellulose collected from five trees of *J. polycarpus*.

A long-term declining trend in  $\delta^{13}\text{C}$  was observed in all studied trees (Fig. 3), which is related to changes in the concentration and isotopic ratio of atmospheric  $\text{CO}_2$  since industrialization (Freyer and Belacy, 1983; Leavitt and Long, 1989; Leavitt and Lara, 1994). This trend was removed following the method described in McCarroll and Loader (2004).

However, even after correcting the measured values for changes of  $\delta^{13}\text{C}$  in atmospheric  $\text{CO}_2$ , a declining long-term trend in mean  $\delta^{13}\text{C}$  values of *J. polycarpus* persisted. All series were therefore de-trended in a second step by taking first differences of the corrected values (Saurer et al., 1997; McCarroll and Pawellek, 1998). This simple method removed all low-frequency trends while retaining inter-annual variations in the de-trended series (Fig. 4) (McCarroll et al. 2009).

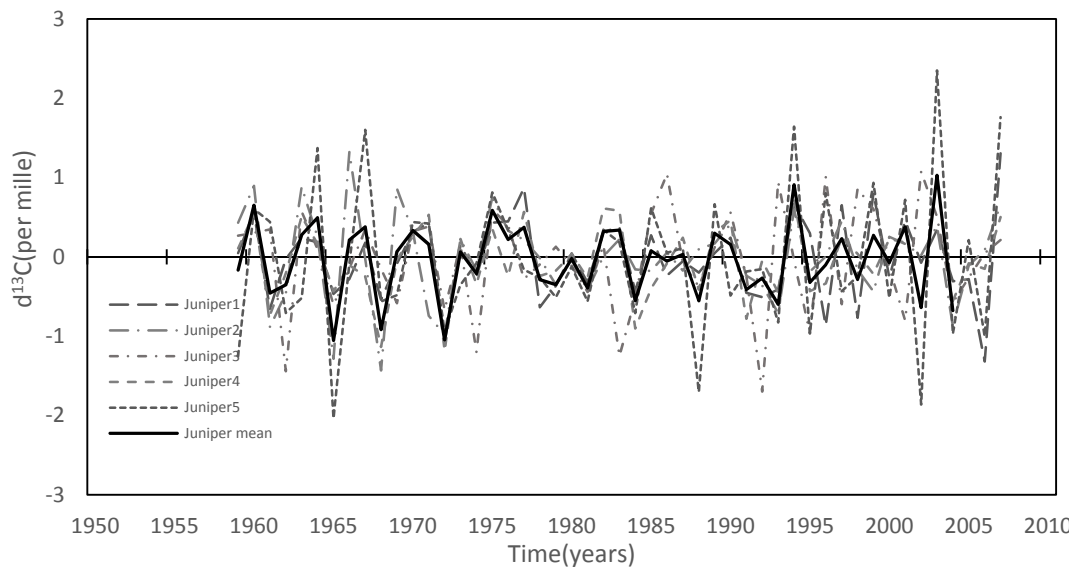


Figure 4: First differences of the 50-year inter-annual variation corrected  $\delta^{13}\text{C}$  of tree-ring cellulose in *J. polycarpus* (1958-2007). Juniper no. 3 which showed highly individual  $\delta^{13}\text{C}$  patterns, probably caused by disturbance or microsite conditions, was excluded from calculating the mean  $\delta^{13}\text{C}_{\text{cor}}$  series.

### Correlation between average $\delta^{13}\text{C}$ and climate

Correlation coefficients between stable carbon isotope ratios in tree rings of junipers and average monthly and seasonal climate data (precipitation and temperature) are shown in figure 5.

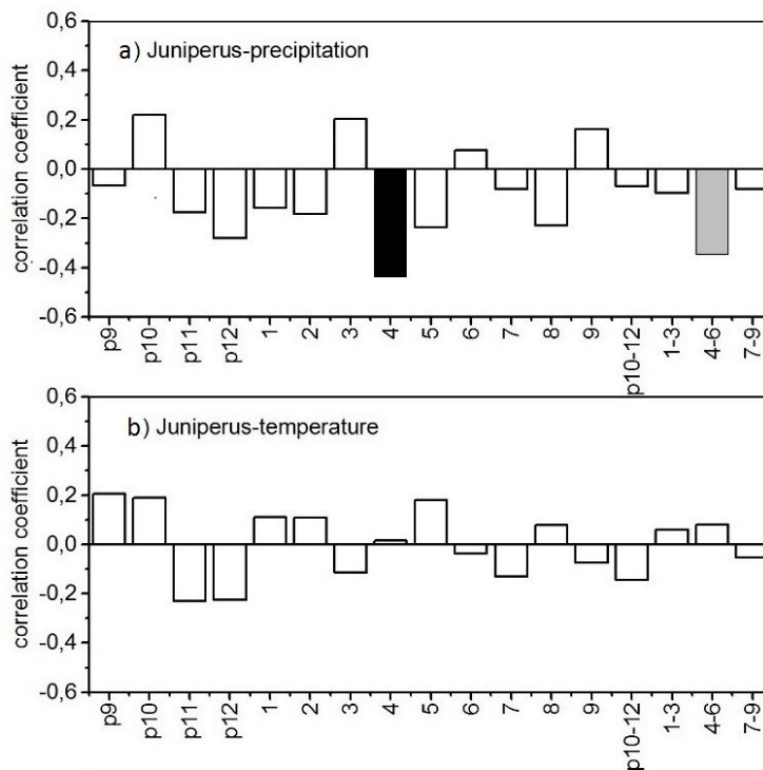


Figure 5: Correlations between *J. polycarpus*  $\delta^{13}\text{C}$  and precipitation (a), temperature (b) for a 13-month period from September of the previous growing season (p9) until September of the growth year (9) and seasonally averaged data (autumn: p10-p12, winter: 1-3; spring: 4-6; summer: 7-9). Correlations were calculated for the periods 1958 to 2007. Gray and black bars indicate significant correlations at the  $p < 0.05$  and  $p < 0.01$  levels, respectively.

We found a significant negative correlation between juniper  $\delta^{13}\text{C}$  and precipitation of April ( $r = -0.438$ ;  $p < 0.01$ ) and the entire spring season (Fig. 5a). No significant correlations between  $\delta^{13}\text{C}$  of junipers were found with temperatures of any month or seasonal average, neither in the current growing seasons nor in the previous year (Fig. 5b). All studied trees are photosynthetically active during spring (April – June), supporting that precipitation (moisture status) is the main environmental control of  $\delta^{13}\text{C}$  at our study site.

### Discussion

In this study, the juniper  $\delta^{13}\text{C}$  signals showed no significant correlation with temperature, indicating that temperature during the growing season does not constitute a limiting factor for carbon assimilation in the study site. No significant correlation between temperature and  $\delta^{13}\text{C}$  values in tree ring were reported also by McCarroll and Pawellek 2001, Liu et al., 2003, Gebrekirstos et al., 2009. In contrast, the results of Saurer et al. (1995), Liu et al. (2004), Szczepanek (2006), Liu et al. (2007), Seftigen et al. (2011), Young et al. (2012), and Xu et al. (2014) indicated significant correlations between  $\delta^{13}\text{C}$  values in tree rings and temperature. However, the significant negative relationship between precipitation and  $\delta^{13}\text{C}$  in this study underpins the importance of water availability for carbon isotope discrimination at the study site. Negative correlations with precipitation were found in many drought-limited deciduous and an evergreen species (Ferrio and Voltas, 2004, Liu et al. 2004, Gebrekirstos 2009, Seftigen et al. 2011, Schollaen et al. 2013, Xu et al. 2014).

Results of Roden et al. (2005) also indicated that  $\delta^{13}\text{C}$  values in organic matter of trees follow site water status (Bowling et al. 2002, McDowell et al. 2004). Other studies (Saurer et al. 1997, Treydte et al. 2001) showed an increase of carbon isotope ratios due to low air humidity or low soil moisture content as a result of reduced stomatal conductance.

## Conclusions

Studying stable carbon isotope variations in wood cellulose provides the opportunity to analyze tree physiological responses to environmental variations, which is important to understand tree responses to the past and present climate changes (McCarroll & Loader 2004, Ward *et al.* 2005, Gerhart et al. 2012, Gessler et al. 2014). We found that the interplay between climatic conditions and species behavior determines the inter-annual  $\delta^{13}\text{C}$  pattern of tree ring cellulose. Mean  $\delta^{13}\text{C}$  values in north Iranian juniper trees are the result of the combined influence of climate and local site conditions. This indicates that site specific factors, such as soil moisture availability and microclimatic conditions play an important role and determine whether stable carbon isotopes are an indicator of variations of temperature or precipitation, or a mixture of both.

The strong correlation between inter-annual isotopic patterns from tree rings of juniper with April and whole spring season precipitation indicates that  $\delta^{13}\text{C}$  is a good proxy to reconstruct local precipitation variations. It is obvious that the dominant climatic control on carbon isotopic values in Juniper is moisture stress (soil moisture and air relative humidity) which controls stomatal conductance.

## Acknowledgements

We express our deep appreciation to DAAD who supported Z. Foroozan.

## References

- Bonal, D., Sabatier, D., Montpied, P., Tremeaux, D., Guehl, J. M. (2000): Interspecific variability of  $\delta^{13}\text{C}$  among trees in rainforests of French Guiana: functional groups and canopy integration, *Oecologia*, 124 (3): 454-468.
- Bowling, D. R., McDowell, N. G., Bond, B. J., Law, B. E., Ehleringer, J. R. (2002):  $^{13}\text{C}$  content of ecosystem respiration is linked to precipitation and vapor pressure deficit. *Oecologia*, 131: 113–124.
- Büntgen, U., Tegel, W., Nicolussi, K., McCormick, M., Frank, D., Trouet, V., Kaplan, J.O., Herzig, F., Heussner, K.U., Wanner, H., Luterbacher, J., Esper, J. (2011): 2500 years of European climate variability and human susceptibility. *Science*, 331 (6017): 578–582.
- Esper, J., Cook, E.R., Schweingruber, F.H. (2002): Low frequency signals in long tree ring chronologies for reconstructing past temperature variability. *Science*, 295 (5563): 2250-2253.
- Esper, J., Frank, D., Buntgen, U., Verstege, A., and Luterbacher, J. (2007): Long-term drought severity variations in Morocco. *Geophysical Research Letters*, 34: L17702.
- Esper, J., Frank, D.C., Battipaglia, G., Büntgen, U., Holert, C., Treydte, K., Siegwolf, R.T.W., Saurer, M. (2010): Low-frequency noise in  $\delta^{13}\text{C}$  and  $\delta^{18}\text{O}$  tree ring data: a case study of *Pinus uncinata* in the Spanish pyrenees. *Glob Biogeochem Cycles*, 24: GB4018.
- Farquhar, G.D., O'Leary, M.H., Berry, J.A. (1982): On the relationship between carbon isotope discrimination and the intercellular carbon dioxide concentration in leaves. *Aust. J. Plant Physiol*, 9:121–137.
- Feng, X., 1998. Long-term ci/ca response of trees in western North America to atmospheric CO<sub>2</sub> concentrations derived from carbon isotope chronologies. *Oecologia* 117, 19–25.
- Ferrio, J.P., Voltas, J. (2005): Carbon and oxygen isotope ratios in wood constituents of *Pinus halepensis* as indicators of precipitation, temperature and vapour pressure deficit. *Tellus*, 57B: 164–173.

- Foroozan, Z., Pourtahmasi, K., Bräuning, A. (2015): Stable oxygen isotopes in juniper and oak tree rings from northern Iran as indicators for site-specific and season-specific moisture variations. *Dendrochronologia* 36: 33-39.
- Francy, R. J., Farquhar, G. D. (1982): An explanation of  $^{13}\text{C}/^{12}\text{C}$  variations in tree rings. *Nature*, 297: 28-31.
- Freyer, H.D., Belacy, N. (1983):  $^{13}\text{C}/^{12}\text{C}$  Records in Northern Hemispheric Trees During the Past 500 Years: anthropogenic impact and climatic superpositions. *Geophysical Research*, 88: 6844-6852.
- Gebrekirstos, A., Worbes, M., Teketay, M., Fetene, M., Mitlöhner, R. (2009): Stable carbon isotope ratios in tree rings of co-occurring species from semi-arid tropics in Africa: Patterns and climatic signals. *Global and Planetary Change*, 66: 253-260.
- Gerhart L. M., Harris J. M., Nippert J. B., Sandquist D. R., Ward J. K. (2012): Glacial trees from the La Brea tar pits show physiological constraints of low  $\text{CO}_2$ . *New Phytologist*, 194: 63–69.
- Gessler, A., Ferrio, J. P., Hommel, R., Treydte, K., Werner, R. A., Monson, R. K. (2014): Stable isotopes in tree rings: toward a mechanistic understanding of fractionation and mixing processes from the leaves to the wood. *Tree Physiol*, 34:796–818.
- Laumer, W., Andreu, L., Helle, G., Schleser, G.H., Wieloch, T., Wissel, H. (2009): A novel approach for the homogenization of cellulose to use micro-amounts for stable isotope analyses. *Rapid Communications in Mass Spectrometry*, 23 (13): 1934–1940.
- Leavitt, S.W., Long, A. (1989): Drought indicated in carbon12/carbon13 ratios in southwestern tree rings. *Water Res Bull*, 25: 341–347.
- Leavitt, S. W., Lara, A. (1994): South American tree rings show declining  $\delta^{13}\text{C}$  trend. *Tellus*, 46B: 152-157.
- Liu, X., Shao, X., Zhao, L., Qin, D., Chen, T., Ren, J. (2007): Dendroclimatic temperature record derived from tree-ring width and stable carbon isotope chronologies in the middle Qilian Mountains, China (Conference Paper).
- Liu, Y., Cai, Q. F., Park, W.K., An, Z. S., Ma, L. M. (2003): Tree-ring precipitation records from Baiyinaobao, Inner Mongolia, China since A.D. 1838. *Chinese Science Bulletin*, 48(11): 1140–1145.
- Liu, Y., Ma, L., Leavitt, S. W., Cai, Q., Liu, W. (2004): A preliminary seasonal precipitation reconstruction from tree-ring stable carbon isotopes at Mt. Helan, China, since AD 1804. *Global and Planetary Change*, 41(3-4): 229-239.
- Loader, N. J., Santillo, P. M., Woodman-Ralph, J. P., Rolfe, J. E., Hall, M. A., Gagen, M., Robertson, I., Wilson, R.; Froyd, C. A., McCarroll, D. (2008): Multiple stable isotopes from oak trees in southwestern Scotland and the potential for stable isotope dendroclimatology in maritime climatic regions, *Chemical Geology*, 252: 62 –71.
- McCarroll, D., Pawellek, F. (1998): Stable carbon isotope ratios of latewood cellulose in *Pinus sylvestris* from northern Finland: variability and signal strength. *The Holocene*, 8: 693–702.
- McCarroll, D., Pawellek, F. (2001): Stable carbon isotope ratios of *Pinus sylvestris* from northern Finland and the potential for extracting a climate signal from long Fennoscandian chronologies. *Holocene*, 11: 517–526.
- McCarroll, D., Loader, N.J. (2004): Stable isotopes in tree rings. *Quaternary Science Reviews*, 23: 771–801.
- McCarroll, D., Gagen, M.H., Loader, N.J., Robertson, I., Anchukaitis, K.J., Los, S., Young, G.H.F., Jalkanen, R., Kirchhefer, A., Waterhouse, J.S. (2009): Correction of tree ring stable carbon isotope chronologies for changes in the carbon dioxide content of the atmosphere. *Geochimica et Cosmochimica Acta*, 73: 1539-1547.
- McDowell, N. G., Bowling, D. B., Schauer, A., Irvine, J., Bond, B. J., Law, B. E., Ehleringer, J. R. (2004): Associations between carbon isotope ratios of ecosystem respiration, water availability and canopy conductance. *Global Change Biology*, 10: 1–18.

- Pourtahmasi, K., Bräuning, A., Poursartip, L., Burchardt, I. (2012): Growth-climate responses of oak and juniper trees in different exposures of the Alborz Mountains, northern Iran. *TRACE - Tree Rings in Archaeology, Climatology and Ecology*, 10: 49-53
- Roden, J. S., Bowling, D. R., McDowell, N. G., Bond, B. J., Ehleringer, J. R. (2005): Carbon and oxygen isotope ratios of tree ring cellulose along a precipitation transect in Oregon, United States. *Geophysical Research*, 110: 1-11.
- Sagheb Talebi, K., Sajedi, T., Pourhashemi, M. (2014): *Forests of Iran*. Springer Netherlands. 152.
- Saurer, M., Siegenthaler, U., Schweingruber, F. (1995): The climate-carbon isotope relationship in tree rings and the significance of site conditions. *Tellus*, 47B: 320–330.
- Saurer, M., Borella, S., Schweingruber, F., Siegwolf, R. (1997): Stable carbon isotopes in tree rings of beech: climatic versus site-related influences. *Trees*, 11: 291–297.
- Schollaen, K., Heinrich, I., Neuwirth, B., Krusic, P. J., D'Arrigo, R. D., Karyanto, O., Helle, G. (2013): Multiple tree-ring chronologies (ring width,  $\delta^{13}\text{C}$  and  $\delta^{18}\text{O}$ ) reveal dry and rainy season signals of rainfall in Indonesia. *Quaternary Science Reviews*, 73: 170–181.
- Seftigen, K., Linderholm, H.W., Loader, N.J., Liu, Y., Young, G.H.F. (2011): The influence of climate on C-13/C-12 and O-18/O-16 ratios in tree ring cellulose of *Pinus sylvestris* L. growing in the central Scandinavian Mountains. *Chemical Geology*, 286: 84–93.
- Szczepanek, M., Pazdur, A., Pawelczyk, S., Bottger, T., Haupt, M., Halas, S., Bednarz, Z., Krapiec, M., Szychowska-Krapiec, E. (2006): Hydrogen, carbon and oxygen isotopes in pine and oak tree rings from southern Poland as climatic indicators in years 1900–2003. *Methods and Applications of Absolute Chronology*, 25: 67-76.
- Tranquillini, W. (1976): Water relations and Alpine timberline. In: Lange, O.L., Kappen, L., Schulze, E.D. (Eds), *Water and plant life*. Springer, Berlin, Heidelberg, 473–491.
- Treydte, K., Schleser, G. H., Schweingruber, F. H., Winiger, M. (2001): The climatic significance of  $\delta^{13}\text{C}$  in subalpine spruces (Lötschental, Swiss Alps). *Tellus*, 53B: 593–611.
- Valentini, R., Anfodillo, T., Ehleringer, J.R. (1994): Water sources and carbon isotope composition ( $\delta^{13}\text{C}$ ) of selected tree species of the Italian Alps. *Canadian Journal of Forest Research*, 24(8): 1575–1578.
- Wieloch, T., Helle, G., Heinrich, I., Voigt, M., Schyma, P. h. (2011): A novel device for batch-wise isolation of  $\alpha$ -cellulose from small-amount wholewood samples. *Dendrochronologia*, 29, 2: 115-117.
- Xu, G., Liu, X., Qin, D., Chen, T., Sun, W., An, W., Wang, W., Wu, G., Zeng, X., Ren, J. (2014): Drought history inferred from tree ring  $\delta^{13}\text{C}$  and  $\delta^{18}\text{O}$  in the central Tianshan Mountains of China and linkage with the North Atlantic Oscillation. *Theoretical and Applied Climatology*, 116: 385–401.
- Young, G. H. F., Bale, R. J., Loader, N. J., Mccarroll, D., Nayling, N., Vousden, N. (2012): Central England temperature since AD 1850: the potential of stable carbon isotopes in British oak trees to reconstruct past summer temperatures. *Quaternary Science*, 27(6): 606–614.